Inflammasome activation and IL-1β secretion in human macrophages

A thesis submitted to the University of Manchester for the degree of Doctor of Philosophy in the Faculty of Biology, Medicine and Health

2021

Ines Diaz del Olmo

School of Biological Sciences
The University of Manchester

Contents

Word Count:

59,341 in total

47,342 excluding references

List of Figures

List of Tables

Abbreviations

Ab	Antibody
AF	Alexa Fluor
AIM-2	Absent In Melanoma 2
ALR	AIM2-like receptor
AmpR	Ampicillin resistance
ANOVA	Analysis of Variance
ATP	Adenosine triphosphate
ASC	Adapter protein apoptosis associated speck-like protein containing a CARD
BCA	Bicinchoninic Acid
BSA	Bovine Serum Albumin
CARD	Caspase recruitment domain
CD	Cluster of differentiation
CT	C-terminus
C3a	Complement component 3a
C3b	Complement component 3b
C3aR	C3a receptor
C5a	Complement component 5a
C5aR	C5a receptor
C5b6	Complex formed by complement component 5b and C6
C6	Complement component 6
C7	Complement component 7
C8	Complement component 8
C9	Complement component 9
Cyt	Cytochalasin D
DAI	DNA-dependent activator of IFN-regulatory factors
DAMP	Damage-associated molecular pattern
DC	Dendritic cell

DMEM	Dulbecco’s Modified Eagle Medium
DMSO	Dimethyl sulfoxide
DNA	Deoxyribonucleic acid
DOL	Degree of labelling
dsDNA	Double-stranded DNA
Dyn	Dynasore
ECL	Enhanced chemiluminescence
EEA1	Early endosome antigen 1
EGFP	Enhanced green fluorescent protein
ELISA	Enzyme-linked immunosorbent assay
ER	Endoplasmic reticulum
ERK	Extracellular signal-regulated kinase
ET	E-total
FACS	Fluorescence-activated single cell sorting
Fc	Fragment crystallisable region
FCS	Fetal calf serum
GBP	Guanylate-binding protein
GM-CSF	Granulocyte-macrophage colony-stimulating factor
gRNA	Guide ribonucleic acid
GSDM	Gasdermin
GSDMD	Gasdermin D
H	Hour
HEK	Human Embryonic Kidney
HeLa	Henrietta Lacks
HRP	Horseradish peroxidase
HS	Human serum
ICAM	Intercellular adhesion molecule
IFN	Interferon
Ig	Immunoglobulin

IκB	Inhibitor of nuclear factor kappa B
IKK	IκB kinase
IL-	Interleukin
IRAK	IL-1 receptor-associated kinases
JF	Janelia Fluor
JNK	C-Jun N-terminal Kinase
LC3	Microtubule-associated protein 1A/1B-light chain 3
LDH	Lactate dehydrogenase
LPS	Lipopolysaccharide
mAb	Monoclonal antibody
MAC	Membrane attack complex
MAMs	Mitochondria-associated ER membranes
MAPK	Mitogen-activated protein kinase
MBL	Mannose-binding lectin
M-CSF	Macrophage colony-stimulating factor
MDMs	Monocyte-derived macrophages
MFI	Mean Fluorescence Intensity
Min	Minutes
MLKL	Mixed lineage kinase domain like pseudokinase
MSU	Monosodium urate
MW	Molecular weight
MyD88	Myeloid differentiation primary response gene 88
NA	Numerical aperture
NEK7	NIMA-related kinase 7
NF-κB	Nuclear factor kappa light chain enhancer of activated B cells
Nig	Nigericin
NIK	NF-κB inducing kinase
NIK SMI-1	NIK small-molecule inhibitor-1
NK	Natural killer

NLR	NOD-like receptor
NLRP3	NOD-like receptor 3
NSA	Necrosulfonamide
NT	N-terminus
Nys	Nystatin
OA	Osteoarthritis
PAMP	Pathogen-associated molecular pattern
PBMCs	Peripheral blood mononuclear cells
PBS	Phosphate-buffered saline
PCN	Pericentrin
PCR	Polymerase chain reaction
PFA	Paraformaldehyde
PI3K	Phosphoinositide 3-kinase
PKD	Protein kinase D
PMA	Phorbol 12-myristate 13-acetate
PRR	Pattern recognition receptor
PSF	Point spread function
PYD	Pyrin domain
RA	Rheumatoid arthritis
RIPA	Radioimmunoprecipitation assay buffer
RIPK	Receptor-interacting protein kinase
RNA	Ribonucleic acid
ROI	Region of interest
ROS	Reactive oxygen species
RPMI	Roswell Park Memorial Institute 1640 media
SD	Standard deviation
ssRNA	Singe-stranded RNA
STORM	Stochastic optical reconstruction microscopy
TAB	TAK1-binding protein 2

TAK	Transforming growth factor-β-activated kinase
TBST	Tris Buffered Saline with Tween
TCC	Terminal complement complex
TGF	Transforming growth factor
TGN	Trans-Golgi network
TICAM-1	TRIF/TIR domain-containing adaptor molecule-1
TIR	Toll/IL-1 receptor
TIRF	Total internal reflection fluorescence
TBK	TANK-binding kinase
TLR	Toll-like receptor
TMB	3,3',5,5'-Tetramethylbenzidine
TNF	Tumour necrosis factor
TNFR	TNF receptor
TNFRSF	TNF receptor superfamily
TRAM	TRIF-related adaptor molecule
TRAF	TNF receptor-associated factor
TRIF	TIR domain-containing adaptor inducing IFNβ
VCAM	Vascular cell adhesion molecule
WGA	Wheat germ agglutinin
ZeoR	Zeocin resistance

Abstract

The inflammasome is an intracellular multi-protein complex, activated upon recognition of endogenous and exogenous danger signals. Assembly of the inflammasome triggers caspase 1 activation leading to gasdermin D (GSDMD) cleavage and pore formation in the cell membrane, and to IL-1β and IL-18 processing and secretion. These cytokines play major roles in inflammation, enhancing the immune response but promoting autoimmune and pro-inflammatory diseases when dysregulated. Thus, understanding how they are secreted is important to therapeutically target these cytokines. The role of GSDMD in the secretion of IL-1β and IL-18 have been shown using liposomes and in murine myeloid cells. However, whether GSDMD is involved in IL-1β and IL-18 released in human macrophages, one of the main sources of these cytokines, has not been addressed. This thesis establishes that in human macrophages stimulated with LPS and nigericin, GSDMD is processed to form pore-like structures in the cell membrane through which IL-1β and IL-18 could be released. This is supported by the fact that chemical inhibition of GSDMD pore formation in primary human macrophages, and depletion of this protein in the human macrophage-like THP1 cells impaired cytokine secretion upon NLRP3 inflammasome activation. During infection, danger signals that activate the inflammasome are also able to engage the complement system, a group of proteins that act in a cascade-like fashion, resulting in the formation of the complement component 5a (C5a) and the membrane attack complex (MAC). Although, the levels of C5a and the MAC are enhanced in IL-1β and IL-18-mediated pathologies, it is unknown whether these complement components can induce inflammasome activation in human myeloid cells. This thesis shows that sublytic concentrations of the MAC triggered dispersion of the trans-Golgi network upstream of NLRP3 inflammasome assembly, and IL-1β and IL-18 secretion in a NLRP3 and a GSDMD-dependent manner in human macrophages. Moreover, this thesis shows that to activate the NLRP3 inflammasome, the MAC needs to be internalized and that it colocalises with early endosomes at early time points and with the adapter protein ASC and NLRP3 at later time points. Overall, this shows how two major pathways of the innate immune system – the complement system and the inflammasome – are linked together, identifying a potentially druggable pathway for major diseases.

Declaration

No portion of the work referred to in this thesis has been submitted in support of an application for another degree or qualification of this or any other university or other institute of learning. The findings presented in this thesis are my own work, with the following exceptions:

- Dr. Kevin Stacey (Daniel Davis Lab, University of Manchester) isolated monocytes from blood cones used in most experiments.

- Shmuel Hanson (Daniel Davis Lab, University of Manchester) obtained the data of panels a and b in figure 3.8 and of panels a, b and c in figure 3.9. These experiments were performed for his final year undergraduate project. I was responsible for the supervision of this project and all the experiments he performed during his time in the Davis Lab.

- Dr. Ashley Ambrose (Daniel Davis Lab, University of Manchester) analysed the data represented in panel b of figure 5.8 as part of a publication.

Copyright statement

Publications

Diaz-del-Olmo I, Worboys J, Martin-Sanchez F, Gritsenko A, Ambrose AR, Tannahill GM, Nichols E-M, Lopez-Castejon G and Davis DM (2021) Internalization of the Membrane Attack Complex Triggers NLRP3 Inflammasome Activation and IL-1β Secretion in Human Macrophages. Front. Immunol. 12:720655. doi: 10.3389/fimmu.2021.720655

Gritsenko A, Yu S, Martin-Sanchez F, **Diaz-del-Olmo I**, Nichols E-M, Davis DM, Brough D and Lopez-Castejon G (2020) Priming Is Dispensable for NLRP3 Inflammasome Activation in Human Monocytes In Vitro. Front. Immunol. 11:565924. doi:10.3389/fimmu.2020.56592

Acknowledgements

First of all, I would like to thank my supervisors: Prof Daniel M. Davis for making me a part of his lab and teaching me how important basic research is to understand the 'big picture'; Dr. Gloria Lopez-Castejon for believing in me and welcoming me to her lab before I started this PhD, and for co-supervising me during the PhD itself; and to Dr. Eva-Maria Nichols for supervising this PhD project and for giving me a taster of what working in industry is like. I would also like to thank all three of them for their personal support throughout the whole PhD - finishing a PhD during a pandemic is not easy and having such great, supportive, and understanding supervisors has been key to the success of this project.

I also want to thank present and past members of the Davis and Lopez-Castejon Labs for your help during these years. Particularly, the climbing crew for sharing this great hobby with me, and to Anya and Fatima for all our discussions about the inflammasome. A special mention goes to Jonathan and Ashley who helped me day after day, taught me multiple techniques and 'infected' me with their passion for science. Thanks a lot for all your support and for always answering my endless questions without complaining.

Thanks to all the people who started as just work colleagues and ended up being great friends. Especially, Rajia 'pour m'avoir forcé à utiliser mon français et pour un peu de potins de temps en temps', and Alex for becoming my brother, for supporting me inside and outside the lab, for assuring me that everything was going to be ok when I panicked about stupid things, and for all the amazing moments we lived together.

I would like to acknowledge all the friends I made in Manchester. Tasa, thanks for our deep conversations about life, and all the free coffees. Karmele, thanks for our walks and our meetings when everyone abandoned us and escaped from Manchester. Thanks Cate and Marco (and Cami for introducing them to me) for the great time we spent together, and Ollie and Beth for our great climbing sessions.

Thanks a lot for the support from all my friends back home. Talking with you, meeting you (whether in person or by videocall) and having you visiting me in Manchester were great ways to escape from the PhD worries and stress. Thank you to the Pink Ladies and, especially, Esther. Thanks for being my best friend, for always supporting me and not letting the distance weaken our friendship. I wouldn't change all the time we have spent together during these years (even virtually) for anything in the world.

A big acknowledgment is for my science teachers and my university lecturers and professors. Especially, my biology teacher Maria Angeles and my professor of Microbiology Juani. Thanks for showing me the micro world and kindling my interest and passion for it. Without your classes and love for science, I would not have become a researcher.

I would also like to thank Hayley and Anthony for your love and support and for welcoming me into your home where I had the perfect environment to finish writing this thesis.

'El mayor agradecimiento de todos es para mi familia, especialmente para mis padres. Sin ellos no habría llegado hasta donde estoy y este PhD no hubiera sido posible. Gracias por quererme y apoyarme incondicionalmente y por enseñarme que el esfuerzo siempre tiene recompensa. Soy la persona más afortunada del mundo por tener unos padres como vosotros'

And last but not least, thank you very very much Josh. You have been my best supporter, been there in every single moment and helped me to disconnect and enjoy my free time when I really needed it. I feel so lucky to have you, and I am really impressed that you haven't killed me when I have been at my most stressed - having someone going through the same during this PhD definitely made things easier. Thanks for all the proof reading as well.

Chapter 1 Introduction

1.1 Inflammation and Innate Immunity

The immune system encompasses all the barriers and mechanisms established to defend the organism against danger, including tissue injury and pathogen infection[1]. Consequently, it is also responsible for the process of inflammation[2]. Inflammation, characterized by pain, redness, warmth, swelling and loss of function, is the first response to harmful stimuli in the organism[2,3]. This process recovers the organism's homeostasis by containing and eliminating the immunological challenge and by repairing the affected area[2,3].

Multiple stimuli can induce inflammation including pathogen infection, disruption of homeostasis and endogenous stress[2,3]. Following these signals, host cells release pro-inflammatory mediators to activate the immune response. Cytokines such as interleukin (IL)-1β and tumour necrosis factor (TNF) that activate macrophages and neutrophils, as well as chemokines which recruit immune cells to the affected site[2,4]. IL-1β and TNF are also responsible for general inflammatory symptoms such as fever, fatigue and anorexia[2]. Several cell types with different roles are involved in the immune responses that occur during inflammation. For example, during infection the main role of neutrophils is to phagocytose and kill pathogens, whilst macrophages and other myeloid cells recognize the infectious agent and activate other immune cells to drive the immune response forward[2,5,6].

The immune system has long been divided into two subsystems: the innate immune system and the adaptive immune system. Innate immunity recognizes antigens that are conserved among different pathogens providing a rapid response against infection and representing the first line of protection for the organism[3]. It plays a fundamental role in the activation of the resulting adaptive immune response that recognizes pathogen-specific molecules and represents a selective type of immunity[3].

The innate immune system initiates the immune response against microbial infection and tissue damage. It comprises humoral components such as antibodies (Abs)

and the complement system, and cellular components including neutrophils, eosinophils, natural killer (NK) cells, and myeloid cells such as dendritic cells, monocytes and macrophages[3].

Macrophages, the focus of this thesis, have important roles in inflammation and homeostasis maintenance, with dysregulation of their functions leading to several pathologies including inflammatory and autoimmune diseases[7].

1.2 Macrophages

Macrophages, first described as phagocytes by Metchnikoff[8], are multifunctional cells with essential roles in maintenance of homeostasis, tissue development and repair, host defence and promotion and resolution of inflammation[9]. They are considered ancient cells in the phylogeny of metazoans and in mammals they are present in every tissue[10]. Traditionally, macrophages have been defined as blood monocyte-derived cells. However, nowadays it is known that macrophages are a heterogeneous cell type and multiple populations, each with different origins, have been identified across the organism[11,12].

During embryogenesis macrophages originate from fetal progenitors in the yolk sac and, after liver formation, from monocytes produced during liver hematopoiesis[13]. This type of hematopoiesis is substituted for bone marrow hematopoiesis when bones are developed[13]. In the adult, macrophages were thought to be differentiated only from circulating monocytes, produced from bone marrow hematopoiesis[13]. Although this is the case for certain populations, research has shown that tissue resident macrophages have multiple origins. For example, Langerhans cells, which are epidermis-resident macrophages, have a mixed origin from yolk sac and fetal hematopoiesis progenitors, whereas brain microglia, which are a population of macrophages that reside in the central nervous system, are mainly derived from yolk sac progenitors[14,15].

1.2.1 Macrophage phenotypes

A simplistic and classical approach to classify macrophages is to divide them into two major groups: the classically activated or pro-inflammatory macrophages (M1) and

the alternatively activated or regulatory macrophages (M2)[13,16]. In response to interferon (IFN)γ and bacterial products recognized by toll-like receptors (TLRs), monocytes differentiate towards an M1 phenotype; whilst they differentiate towards an M2 phenotype when they sense cytokines such as IL-4, IL-13, and IL-10[13,16] (Fig 1.1). M1 and M2 macrophages have functional differences and are related to type I and a type II inflammation, respectively[16](Fig 1.1). However, this classification only reflects macrophages in specific conditions such as bactericidal or anti-parasite reponses[13,16,17]. Due to the large amount of diversity among populations, a phenotypic approach based on receptor expression is normally used to classify macrophages. Nonetheless, due to their heterogeneous morphology, transcriptional profile, function and location, it is difficult to establish a solid classification for subsets of this cell type[13,17].

Monocytes can also differentiate into different types of macrophages when they are exposed to specific growth factors. Indeed, in vitro studies have shown that macrophage colony stimulating factor (M-CSF or CSF-1) and granulocyte-macrophage colony stimulating factor (GM-CSF) drive the polarization and differentiation of monocytes towards an M2 or M1 response, respectively[13]. CSF-1 receptor is expressed in every monocyte-derived cell and targeted ablation of its gene *Csf1r* leads to severe macrophage depletion in various tissues, highlighting the importance of this factor for macrophage differentiation[18,19].

As previously mentioned, a commonly used approach to classify different types of macrophages is based on the receptors they express. For example, human monocytes stimulated with GM-CSF, calcium oxalate or IFNγ and LPS to generate pro-inflammatory macrophages express high levels of the receptor CD86[20,21]. On the other hand, human monocyte-derived macrophages stimulated with IL-4 to generate an M2 phenotype express high levels of the mannose receptor CD206[20]. Interestingly, M1 and M2 macrophages share expression of some receptors, though the level of expression can differ among them. For example, CD16 is expressed on human monocyte-derived macrophages that have been differentiated using GM-CSF or M-CSF[22]. However, CD16 expression is higher on macrophages treated with M-CSF[22], indicating that this receptor is more abundant in M2 macrophages.

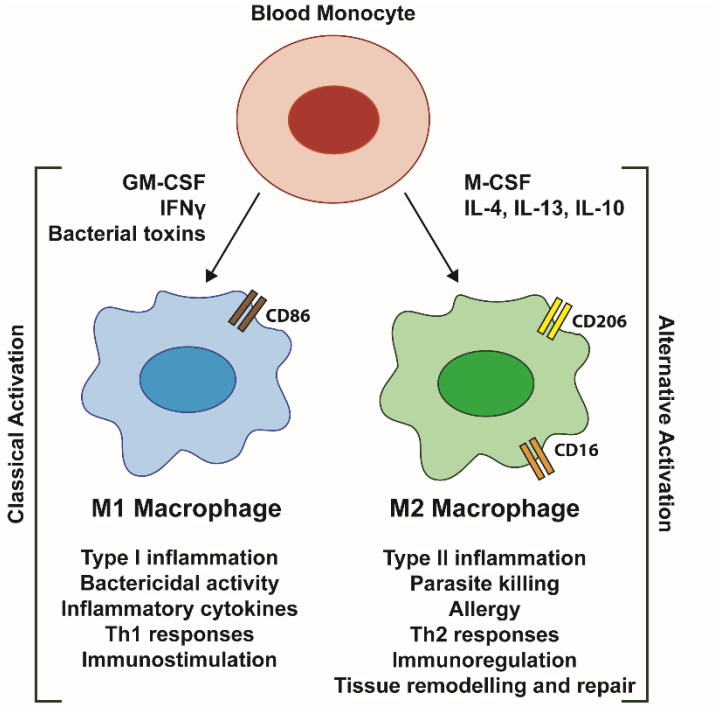

Figure 1.1 Classical and alternative macrophage activation and function. Classically activated or M1 macrophages, induced by IFNγ, bacterial toxins and GM-CSF, expressed receptors such as CD86 and have important roles in Th1 response activation, immunostimulation, and bacterial killing. On the other hand, alternatively activated or M2 macrophages, induced by IL-4, IL-13 and IL-10, immune complexes and M-CSF expressed receptors such as CD206 and higher levels of CD16. Moreover, they have important roles in Th2 response activation, immunoregulation, tissue remodelling and repair and killing of extracellular parasites[13,16,17,20–22].

1.2.2 Macrophages in inflammation

Macrophages have multiple membrane and cytosolic receptors including pattern recognition receptors (PRRs). These receptors recognize pathogen and damage associated patterns (PAMPs and DAMPS). PAMPs are microbial structures conserved among pathogens, whereas DAMPs refer to endogenous danger signals that appear during tissue damage and cell lysis[3,23]. The binding of PAMPs and DAMPs to PRRs in innate immune cells such as macrophages results in the stimulation of rapid immune responses[3,23,24].

1.2.2.1 Macrophage activation and signalling pathways

Pattern recognition receptors (PRRs) comprise various families of receptors including membrane receptors such as toll-like receptors (TLRs), cytosolic receptors such as NOD-like receptors (NLRs), AIM2-like receptors (ALRs), C-type lectin receptors (CLRs)

and retinoic acid-inducible gene (RIG)-I-like receptors (RLRs)[23]. TLRs are activated upon pathogen recognition, leading to the engagement of intracellular signalling pathways, as explained later in this section. CLRs are membrane receptors that recognize carbohydrates from different microorganisms and their activation can result in the production of proinflammatory cytokines and the modulation of TLR-mediated responses[25]. RLRs, ALRs and NLRs are intracellular receptors that detect dsRNA viruses, dsDNA from pathogens or disrupted cells and changes of the intracellular homeostasis, respectively[23,26,27]. Importantly, NLRs and ALRs are sensors involved in inflammasome activation[23], a process which is described later in this chapter.

TLRs comprise several receptors that recognize different PAMPs (Fig 1.2). TLR1, 2, 5 and 6 are found in the plasma membrane whereas TLR 3, 7, 8 and 9 are found in endosomes[23]. Interestingly, TLR4 is found both in the cell membrane and in endosomes[23]. Upon ligand binding, TLRs signalling pathway is activated by dimerization of monomeric TLRs[23]. TLR1/2 and TLR1/6 recognise diacyl and triacyl lipoproteins, TLR3 targets double-stranded RNA, TLR4 binds to LPS, TLR5 to flagellin, TLR7/8 recognises singe-stranded RNA, and TLR9 interacts with unmethylated DNA[23] (Fig 1.2). TLRs share a conserved intracellular domain, the Toll/IL-1 receptor (TIR) that binds TIR-domain containing molecules such as myeloid differentiation primary response gene 88 (MyD88), TIR domain-containing adaptor inducing IFNβ (TRIF)/TIR domain-containing adaptor molecule-1 (TICAM-1), TIR domain-containing adaptor protein (TIRAP)/MyD88-adaptor-like (Mal) and TRIF-related adaptor molecule (TRAM)[28–30]. Following recognition of PAMPs and DAMPs, TLRs recruit TIR-domain-containing adaptors that initiate downstream signalling pathways[31].

The MyD88 pathway is one of the most studied signalling pathways engaged by PRRs (Fig 1.2). This molecule activates IL-1 receptor-associated kinases (IRAKs)[28–30]. IRAKs induce TNF receptor-associated factor (TRAF)-6 and TAK1-binding protein 2 (TAB2) translocation from the membrane to the cytosol where they associate and activate transforming growth factor (TGF)β-activated kinase (TAK)1[32]. TAK1 starts a signalling cascade that results in the activation of both nuclear factor (NF)-κB and mitogen-activated protein kinases (MAPKs) signalling pathways[33]. Active NF-κB migrates to the cell nucleus where it promotes the transcription of multiple inflammatory

proteins[34,35]. On the other hand, activated MAPKs phosphorylate downstream molecules to potentiate inflammatory events[34,35]. It is important to point out that the MyD88 pathway is only one example of cellular signalling upon pathogen recognition. In macrophages, multiple signalling cascades are activated at the same time. Moreover, they are interconnected and signalling factors such as NF-κB can be activated through different routes. For instance, canonical NF-κB activation is triggered by multiple PRRs and it is mediated by the activation of IκB kinase (IKK) through TAK1. Active IKK phosphorylates IκBα, a protein that is bound to the NF-κB complex p50/RelA, targeting it for degradation. This allows p50/RelA to translocate to the nucleus[36]. On the other hand, non-canonical NF-κB activation is triggered by members of the TNF receptor (TNFR) family, ligation of which results in the activation of NF-κB inducing kinase (NIK). NIK mediates the processing of NF-κB p100 into NF-κB p52 that together with RelB translocates to the cell nucleus. Nuclear translocation of p50/RelA or p52/RelB promotes the activation of different signalling pathways[36,37].

Macrophage activation through these signalling pathways results in the production of inflammatory mediators such as oxygen and nitrogen free radicals, lipid mediators, chemokines and cytokines with essential roles in the progression of inflammation[5,6,38]. Importantly, macrophages are also involved in inflammation resolution by production of anti-inflammatory mediators once the immunological challenge is eliminated such as TGFβ, IL-10 and TNF[32]. TGFβ activates extracellular matrix complex components, leading to wound healing; IL-10 regulates the inflammatory response by inhibiting the synthesis and performance of multiple pro-inflammatory cytokines; and TNF is involved in the activation of programmed cell death to eliminate damaged cells[39–41].

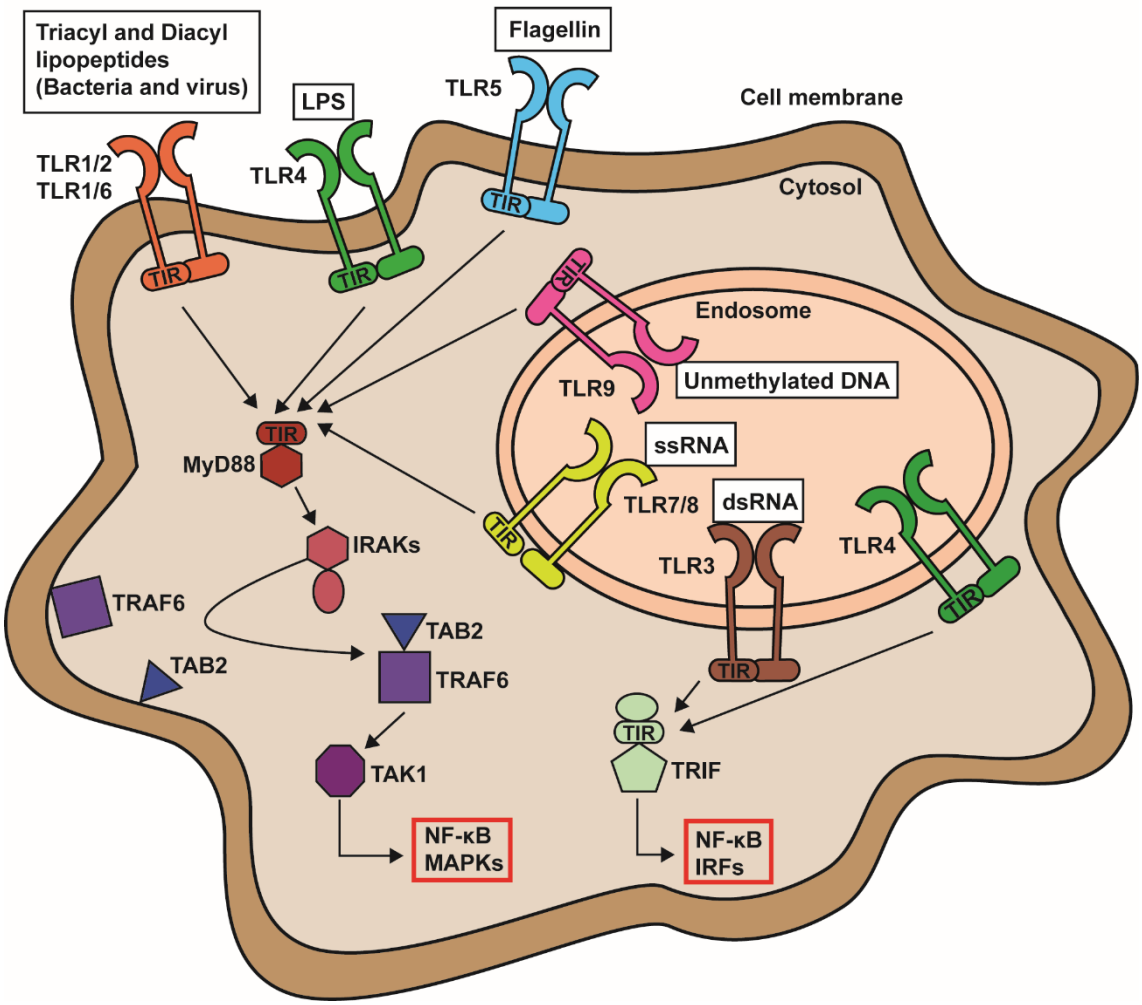

Figure 1.2 Toll-like Receptors (TLRs) signalling pathways. TLR5 and the heterodimers TLR1/TLR2 and TLR1/TLR6, placed in the cell membrane, bind to extracellular PAMPs (white boxes). TLR3, TLR9 and the heterodimer TLR7/TLR8, localized in endosomes, recognize intracellular PAMPs (white boxes). TLR4 is found in both endosomes and the cell membrane and detects PAMPs such as LPS. Upon ligand recognition, TLRs engage adaptor molecules such as TRIF and MyD88 through TIR interactions to activate downstream signalling pathways. For instance, MyD88 engages IRAKs leading to the recruitment of TRAF6 and TAB2 and resulting in the activation of TAK1. The activation of intracellular pathways downstream of MyD88 and TRIF ultimately results in the activation of NF-κB and interferon regulator factors (IRFs) translocation to the cell nucleus and activation of multiple enzymes including MAPKs. These signalling cascades trigger the production of inflammatory mediators. Adapted from O'Neill, Golenbock and Bowie, 2013[42].

1.2.3 Other roles of macrophages

Macrophages are involved not only in immune processes but also in tissue development and repair and have important roles during homeostasis. For instance, they contribute to ductal structure formation in the mammary gland and to tissue morphogenesis, with a lack of macrophages leading to structural abnormalities in organs such as the kidney and the pancreas[10,43]. Moreover, tissue resident macrophage

populations have very specific roles. For example, osteoclasts, a bone-resident population, play a major role in bone maintenance and remodelling[44], and microglia, the only macrophage population in the central nervous system parenchyma, remove synaptic terminals from injured neurons in damage tissue to promote remapping of the nervous network in a process known as synaptic stripping[45,46].

As previously mentioned, macrophages were first described as phagocytes. This property allows them to process apoptotic cells, not only after infection, but also during steady state conditions, clearing, among others, apoptotic neutrophils and erythrocytes in the spleen and liver, respectively[47]. Macrophages are also involved in metabolic homeostasis. They contribute to the adaptation of hepatocytes to caloric intake increases and they provide a trophic support to adipocytes, responsible for the regulation of systemic metabolism[10].

Macrophages are also implicated in disease. Upon tissue injury or infection, circulating monocytes migrate to the affected tissue and differentiate into pro-inflammatory macrophages that produce TNFα, IL-1, nitric oxide and reactive oxygen species (ROS), among other inflammatory mediators. These factors drive the inflammatory response forward, but also produce tissue damage if they are sustained over time[9]. Macrophage response is tightly regulated and ceases when the infection or injury is resolved. However, under pathological conditions, when macrophage performance is dysregulated, different subsets of this cell type are involved in chronic inflammation, autoimmune diseases, and tumour initiation, development and metastasis[48–51].

1.3 The Inflammasome

As previously indicated, upon recognition of pathogens and tissue stress, macrophages activate different signalling pathways that result in the activation and/or upregulation of multiple processes including the assembly of intracellular multiprotein complexes called inflammasomes[52]. Inflammasome activation triggers the processing and release of IL-1β and IL-18, contributing to the recruitment and the activation of other immune cells[53].

The canonical inflammasome is formed by a sensor molecule, connected to caspase 1 by the adaptor molecule apoptosis-associated speck-like protein containing a CARD (ASC), in most cases[53–55]. There are different inflammasome complexes that are named under the protein that constitutes their sensor molecule. To date, NLR protein 1 (NLRP1), NLR protein 3 (NLRP3), NLR C4 (NLRC4) and absent in melanoma 2 (AIM2) inflammasome complexes are the most studied[53–58]. These sensors are activated by various stimuli including lipopolysaccharide (LPS), ATP, crystals such as silica and alum, double-stranded DNA, and various pathogenic toxins[53–58].

Inflammasome activation also leads to an inflammatory type of programmed cell death called pyroptosis[53–58]. This type of cell death was thought to be dependent on caspase 1[59]. However, it has been shown that an alternative inflammasome, independent of caspase 1, can also be responsible for this process[60]. This non-canonical inflammasome activates pyroptosis, but it does not directly mediate IL-1β and IL-18 processing[61–63]. Nevertheless, under non-canonical inflammasome activation these cytokines are produced by indirect activation of the canonical inflammasome, although the mechanism of this route is not well-defined yet[61–63].

1.3.1 Structure of the canonical inflammasome

1.3.1.1 Sensor molecule

Numerous cytosolic PRRs have been described as sensor molecules for inflammasome complexes, with the NLRs and the ALRs being the most studied[53–58]. The structure of NLRs include a C-terminal domain with leucine-rich repeats (LRRs), a central NACHT nucleotide-binding domain, and an N-terminal death-fold domain that can be a caspase recruitment domain (CARD) or a pyrin domain (PYD)[56] (Fig 1.3). NLRP1 also contains a C-terminal CARD and a function-to-find domain (FIIND)[56] (Fig 1.3). On the other hand, ALRs consist of an N-terminal PYD domain and a C-terminal HIN200 domain that binds to double-stranded cytosolic DNA[64] (Fig 1.3).

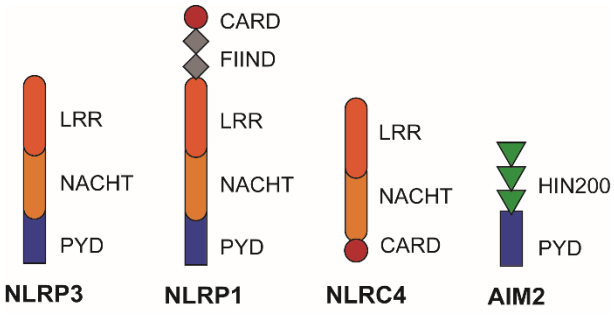

Figure 1.3 Sensor molecules of the NLRP3, NLRP1, NLRC4 and AIM2 inflammasomes. NLRP3, NLRP1 and AIM2 share an N-terminal pyrin domain (PYD), whereas NLRC4 has an N-terminal caspase recruitment domain (CARD). NLRP3, NLRP1 and NLRC4 contains a NACHT inter-domain and a C-terminal leucine-rich repeats (LRR) domain, whereas AIM2 contains a HIN200 C-terminal domain. NLRP1 also contains a function-to-find domain (FIIND) and a CARD in its C-terminal. Adapted from Vanaja, Rathinam and Fitzgerald, 2015[65].

1.3.1.2 Adaptor molecule

As previously mentioned, most inflammasome sensors need an adaptor molecule to bind to caspase 1. ASC is this adaptor molecule and it is a 22 KDa protein that is essential for inflammasome assembly[66]. ASC contains a C-terminal CARD and an N-terminal PYD that interact with caspase 1 and PYD-containing receptors including NLRs, respectively[67] (Fig 1.4). ASC also possesses an interdomain between CARD and PYD that has an important role in the assembly of the inflammasome complex. This interdomain facilitates binding of ASC to other proteins by avoiding chemical interactions between the CARD and the PYD of ASC, and providing a specific orientation for ASC[67].

Upon NLR activation, ASC migrates to bind these receptors through PYD-PYD homotypic interactions[67,68]. Following this event, ASC binds to caspase 1 through CARD-CARD interactions, constituting the inflammasome complex[69]. Importantly, the oligomerization of multiple ASC molecules with the NLR sensors leads to the formation of an ASC speck which is broadly considered a sign of inflammasome activation[68,70]. In this complex, caspase 1 is activated, leading to IL-1β and IL-18 processing[71–73]. Of note, LPS-primed ASC-depleted murine macrophages infected with *Salmonella* are unable to produce active IL-1β and lack the ability to activate caspase 1[74], highlighting the importance of this adaptor protein for canonical inflammasome function.

1.3.1.3 Caspase 1

Caspases (cysteinyl aspartic proteases) are enzymes generally associated with apoptosis, a non-inflammatory type of programmed cell death. However, caspase 1 is an inflammatory caspase that is not directly involved in apoptosis, but it has an important role in inflammasome activation and pyroptosis[53–59,75]. Active caspase 1 catalyses pro-IL-1β and pro-IL-18 processing into their mature forms[71–73], allowing them to be secreted to the extracellular milieu where they function as pro-inflammatory mediators[76,77]. As explained later in this chapter, active caspase 1 also cleaves gasdermin D (GSDMD), leading to the formation of membrane pores that are responsible for pyroptosis[78–81]. This makes caspase 1 an important mediator for this type of proinflammatory cell death. Indeed, before the discovery of GSDMD, caspase 1 was considered the effector of pyroptosis[59].

The structure of caspase 1 monomers comprises a catalytic domain that cleaves proteins downstream of the amino acid aspartate, and a CARD responsible for binding to several proteins through homotypic interactions[72,73,82]. Some of these proteins are ASC, NLRC4 and NLRP1[74,83].

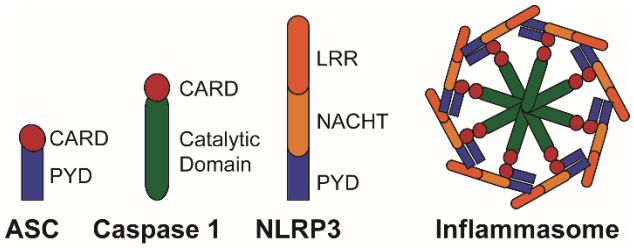

Figure 1.4 A simplified model for NLRP3 inflammasome structure. NLRP3 inflammasome is a multiprotein complex formed by multiple units of ASC, caspase 1 and NLRP3 sensor molecules. ASC C-terminal CARD binds to caspase 1 N-terminal CARD, whereas ASC N-terminal PYD binds to NLRP3 N-terminal PYD. The binding of multiple adaptor molecules (ASC) to multiple units of caspase 1 and NLRP3 results in the formation of the inflammasome complex[56,65,67–69,72,73,82].

Traditionally, caspase 1 has been seen as a proenzyme (pro-caspase 1) that is not catalytically active by itself. After activation of inflammasome sensors, pro-caspase 1 is recruited to the inflammasome complex by interaction with ASC through their CARDs (Fig 1.4). Once in the complex, pro-caspase 1 associates in dimers forming p46 complexes and undergoes auto-proteolytic cleavage leading to the formation of

p20/p10 dimers that constitute the active form of caspase 1[83,84]. However these observations mainly studied recombinant proteins, and it has been demonstrated more recently that p46 caspase 1 dimers are active and that, together with transient p33/p10 dimers of the enzyme, constitute the active form of caspase 1 in the cell[85]. Importantly, auto-proteolytic cleavage of p33/p10 fragments result in the formation of p20/p10 dimers that are released from the inflammasome complex and become inactive[85]. Therefore, detection of p20 and p10 caspase 1 fragments is still a sign of previous caspase 1 activation.

1.3.2 The canonical NLRP3 inflammasome: priming and activation

The NLRP3 inflammasome, the focus of this thesis, also known as NACHT, LRR and PYD domains-containing protein 3 (NALP3) or cryopyrin inflammasome, is one of the best characterised inflammasomes and plays an important role in inflammation, both during infection and in sterile immune responses[54].

Inflammasome activation is fundamental in the immune response against pathogens and inflammatory sterile processes. However, overstimulation of this complex has harmful consequences. For example, the NLRP3 inflammasome and NLRP3-mediated responses are enhanced in multiple diseases including sepsis, diabetes, gout and arthritis[86–88]. Moreover, specific gain of function mutations of the NLRP3 gene result in the cryopyrin-associated autoinflammatory syndrome (CAPS) that is characterized by chronic systemic inflammation[89], indicating that the correct function of this inflammasome is key for maintaining homeostasis in humans. Consequently, canonical activation of the NLRP3 inflammasome is tightly regulated and requires the detection of two consecutive stimuli: a first or priming signal and a second or activation signal[86,90]. The priming step induces pro-IL-1β and NLRP3 production and the activation step triggers the assembly of the inflammasome complex, resulting in caspase 1 activation, GSDMD cleavage and IL-1β and IL-18 processing and release[86,90].

1.3.2.1 Priming

Multiple molecules, including pathogenic virulence factors such as LPS and sterile stimuli such as amyloids or oxidized low-density lipoproteins, function as a signal for NLRP3 inflammasome priming[55,90,91]. In general, inflammasome priming is mediated

by engagement of PRRs leading to the activation of the transcription factor NF-κB[92] (Fig 1.5), which is suggested to be mediated through MyD88 and TRIF[93]. As previously explained, the activation of the NF-κB pathway results in the translocation of NF-κB complexes to the cell nucleus inducing downstream signalling events. During inflammasome priming, nuclear NF-κB triggers and upregulates the transcription of pro-IL-1β and NLRP3, respectively[93]. It is important to highlight that NLRP3 is constitutively transcribed in resting cells and that its expression differs among cell types, being higher in monocytes and dendritic cells than in macrophages and neutrophils[94]. However, this level of expression is not normally sufficient for the efficient assembly of the inflammasome[93]. On the other hand, pro-caspase 1, ASC and pro-IL-18 are constitutively expressed in myeloid cells and do not require a priming signal to be transcribed[95–99].

NLRP3 inflammasome priming is not a simple mechanism and multiple proteins participate in this process. Some of these proteins trigger post-transcriptional modifications of the NLRP3 sensor that enables NLRP3 oligomerization, including phosphorylation by c-Jun N-terminal Kinase 1 (JNK1) or protein kinase D (PKD) and deubiquitination by Lys-63-specific deubiquitinase BRCC3[100–102]. Other proteins such as TANK-binding kinase 1 (TBK1) and I-kappa-B kinase epsilon (IKKε) prevent NLRP3 activation during priming[103]. Moreover, molecules participating in the caspase 1 activation pathway, such as cellular inhibitor of apoptosis protein (cIAP) 1 and 2, and TRAF6, are also important for inflammasome priming[104,105].

1.3.2.2 Activation

The NLRP3 activation step leads to inflammasome assembly and caspase 1 activation resulting in GSDMD processing and IL-1β and IL-18 release[55,90]. The NLRP3 inflammasome is activated by a diverse range of stimuli, including endogenous and exogenous molecules such as extracellular ATP, infection with pathogens such as *Staphylococcus aureus,* particulate matter such as monosodium urate (MSU), aluminium salts or cholesterol crystals, and pore-forming drugs like nigericin – the last of which is used together with the priming stimuli LPS as a standard model of NLRP3 inflammasome activation[106–112]. A broad range of stimuli activate the NLRP3 inflammasome. However, a common cellular event upstream of inflammasome assembly has not been identified yet. Since structures and mechanisms of action of NLRP3 activators vary, a shared event

acting downstream in their pathways may be the main activator of this complex. Indeed, the NLRP3 sensor may not directly interact with their activators. Instead, NLRP3 senses changes in the cells homeostasis induced by these activators, resulting in inflammasome engagement. Some of the cellular events that have often been described to occur before NLRP3 activation are disturbance of the intracellular ion homeostasis, mitochondrial damage and production of reactive oxygen species, and lysosomal disruption[86,113] (Fig 1.5).

Cation fluxes, both to and from the extracellular space of the cell, have been shown to be important for NLRP3 inflammasome activation. Potassium (K^+) efflux is a common event triggered by most NLRP3 activators[114]. Specifically, ATP and nigericin, two of the most studied NLRP3 stimuli, trigger K^+ efflux, and high extracellular K^+ inhibits NLRP3-dependent caspase 1 activation and cytokine secretion in macrophages and monocytes[115,116]. Thus, for a long time, a decrease in intracellular K^+ was considered the universal trigger of the NLRP3 inflammasome. However, it is now known that certain stimuli, such as imiquimod, activate the NLRP3 inflammasome independently of K^+ efflux[117], indicating that this event may be common for multiple NLRP3 stimuli but not fundamental for NLRP3 activation. Another cation involved in NLRP3 inflammasome engagement is calcium (Ca^{2+})[86]. Multiple NLRP3 stimuli, including ATP, nigericin or MSU, induce an increase in intracellular calcium (Ca^{2+}) that is necessary for inflammasome activation[118,119]. This is evidenced by the fact that inhibition of plasma membrane Ca^{2+} channels or inhibition of Ca^{2+} release from ER stores impairs IL-1β secretion following treatment with different NLRP3 activators[118,119]. Various studies suggest that in the context of inflammasome activation, Ca^{2+} mobilization only occurs as a result of K^+ fluxes, and that an increase in cytosolic Ca^{2+} may not be required for NLRP3 activation[120]. However, whether mobilization of both cations is necessary for the activation step, or if only one of these ions is involved in the process, and the other one is needed to merely balance ion forces in the cell is not clear yet.

Other studies suggest that NLRP3 senses organelle dysfunction and therefore, damage of intracellular compartments is the trigger for the activation of this inflammasome[113]. Specifically, DAMPs with a mitochondrial origin such as mitochondrial DNA (mtDNA), ROS, ATP and cardiolipin can trigger NLRP3 inflammasome activation. In

LPS-primed macrophages, the induction of mitochondrial disruption results in an increase in ROS production that triggers caspase 1 activation and IL-1β release in an NLRP3-dependent manner[92]. Importantly, the release of mitochondrial cardiolipin and its direct binding to NLRP3 also induces inflammasome activation[121]. Moreover, the translocation of oxidized mtDNA to the cytosol and its interaction with NLRP3 contributes to IL-1β and IL-18 secretion in macrophages stimulated with LPS and ATP[121,122]. Overall, these findings indicate a role for mitochondrial disruption in NLRP3 inflammasome activation. Interestingly, in macrophages treated with LPS and ATP, it has been proposed an activation model for NLRP3 where Ca^{2+} influx, dependent on K^+ efflux, leads to mitochondrial ROS production and consequently to inflammasome activation[123].

As previously mentioned, particulate matter induces NLRP3 activation[108,124–128]. Internalization of particulate matter such as silica or cholesterol crystals triggers lysosomal disruption and release of lysosomal contents to the cytosol[124,126]. Moreover, direct induction of lysosomal rupture results in NLRP3 and ASC-dependent secretion of IL-1β in macrophages[124], suggesting that lysosomal damage may be the common mechanism triggering inflammasome activation by particulate stimuli. However, the specific mechanism for inflammasome activation following lysosomal disruption is not clear. Two of the proposed processes for inflammasome activation in this context are lysosome acidification leading to ion fluxes such as K^+ efflux, and the escape to the cytosol of lysosomal enzymes such as cathepsins[124,129]. In fact, the lysosomal escape of cathepsin B induces caspase 1 activation in macrophages stimulated with LPS and silica crystals and it is necessary for ASC speck formation, caspase 1 activation and the secretion of IL-1β in LPS-primed macrophages treated not only with particulate matter, but also with nigericin and ATP[93,109]. Moreover, following treatment with diverse inflammasome stimuli, cathepsin B is immunoprecipitated with NLRP3 and both proteins are found together in proximity ligation assays[93], indicating that cathepsin B may have a major role in NLRP3 inflammasome activation.

In conclusion, multiple cellular events occur downstream of NLPR3 stimuli, indicating that there may not be a unique event responsible for NLRP3 activation and

that the cellular events preceding inflammasome assembly described to date may not be mutually exclusive.

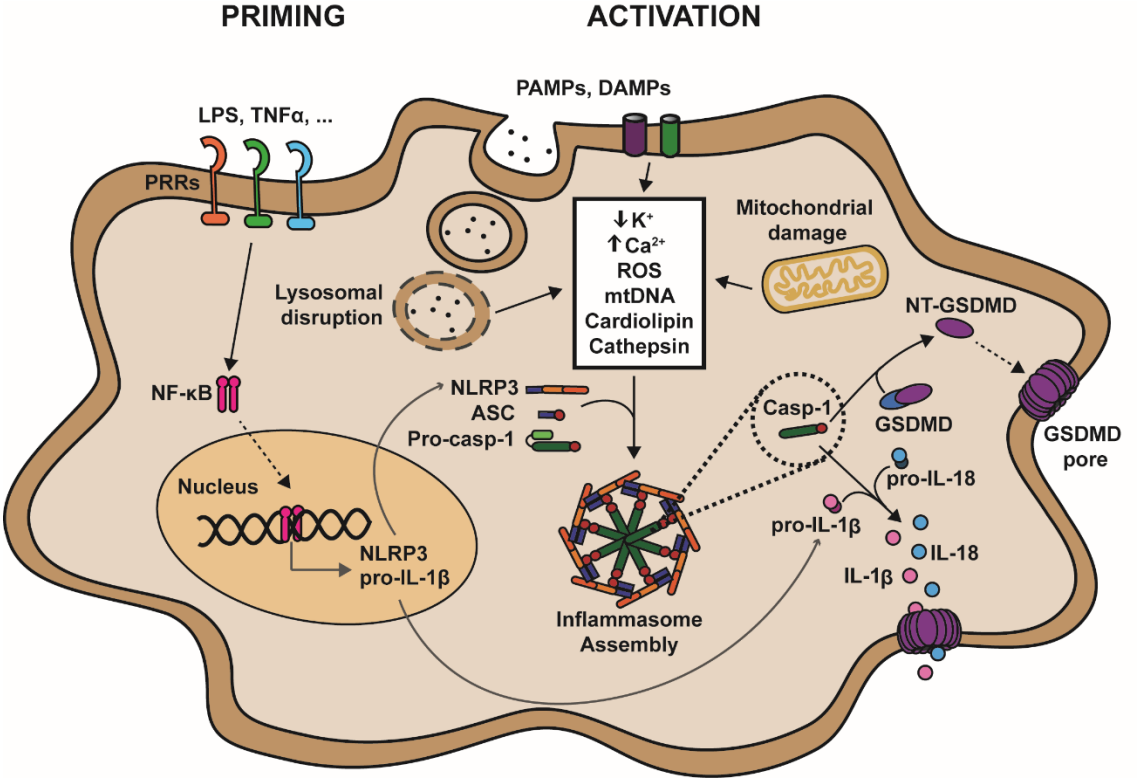

Figure 1.5 Canonical activation of the NLRP3 inflammasome. Two steps are required for canonical NLRP3 inflammasome assembly: a priming step and an activation step. First, a priming stimulus engages PRRs resulting in the activation of NF-κB. This induces and upregulates the production of pro-IL-1β and NLRP3, respectively. Second, an activation signal induces intracellular processes such as ion fluxes including K^+ efflux and increase in cytosolic Ca^{2+}, lysosomal disruption leading to cathepsin escape to the cytosol, or mitochondrial damage resulting in ROS production and release of mtDNA. These events trigger NLRP3 inflammasome assembly leading to caspase 1 activation, IL-1β and IL-18 maturation and release, and GSDMD pore formation. Adapted from Guo, Callaway and Ting, 2015 and Seoane *et al*, 2020[54,113].

1.3.3 Non-canonical NLRP3 inflammasome activation

The non-canonical NLRP3 inflammasome pathway was discovered whilst investigating the response to bacterial toxins that induce septic shock. Gram-negative bacteria that can induce sepsis also activate caspase 11 in *in-vitro* infection models, with depletion of caspase 11 but not ASC or NLRP3, protecting mice from LPS-induced toxic shock[61,130]. This indicates that caspase 11 mediates septic shock-induced mortality. Interestingly, caspase 11 depletion in murine macrophages impaired IL-1β release triggered by gram-negative bacteria or their toxins but did not affect IL-1β secretion

following treatment with canonical NLRP3 activators like ATP[61]. Moreover, depletion of caspase 1, ASC or NLRP3 in murine macrophages inhibited IL-1β secretion but not cell death following infection with gram-negative bacteria[61]. Altogether, these findings uncovered a non-canonical pathway for NLRP3 inflammasome activation.

One of the main components of the membrane of gram-negative bacteria is LPS and caspase 11 is now known to be a sensor for cytosolic LPS[131], explaining its role during sepsis. In fact, direct LPS binding to caspase 11 results in its oligomerization and activation[131]. Human caspases 4 and 5 are the homologs of murine caspase 11 and, as for caspase 11, LPS binding to caspase 4/5 triggers its oligomerization and activation[131]. Moreover, in human myeloid cells deletion of caspases 4/5 blocks IL-1β release and cell death in response to intracellular LPS[131–133], demonstrating their role as mediators for non-canonical inflammasome activation in humans. In addition, it has recently been discovered that guanylate-binding proteins (GBPs) play an important role in LPS recognition by caspases 4/5/11. GBPs mediate the disruption of pathogen-containing vacuoles and LPS-containing outer membrane vesicles secreted by bacteria, facilitating LPS recognition by these caspases[134–137]. In human macrophages infected with *Salmonella Typhimurium*, although not involved in the disassembling of Salmonella-containing vacuoles, GBP1 directly binds cytosolic bacteria and recruits caspase 4 to facilitate LPS detection[136], highlighting the importance of GBPs in the activation of the non-canonical inflammasome in human myeloid cells. Importantly, research has shown that activation of caspases-4/5/11 triggers indirect activation of the canonical NLRP3 pathway, and whereas caspases-4/5/11 are able to cleave GSDMD leading to pyroptosis, caspase 1 activation through the canonical pathway seems to be necessary for processing pro-IL-1β and pro-IL-18 into their active forms following non-canonical inflammasome activation[61,138].

1.3.4 Cellular localisation of NLRP3 inflammasome components

The NLRP3 inflammasome complex has been detected in multiple cellular compartments[113,139]. However, the exact subcellular localisation for NLRP3 inflammasome activation is yet to be uncovered. To date, NLRP3 localisation to multiple organelles including the endoplasmic reticulum (ER), the Golgi, the mitochondria, the

centrosome, and the autophagosome have been described following different stimuli and in different cell types[113,139]. Therefore, it is uncertain if there is a unique localisation for NLRP3 inflammasome assembly.

In resting conditions, NLRP3 is found in the ER in monocyte-like THP1 cells and in the cytosol in murine macrophages[92,140], whereas ASC can be found in the cytosol in macrophage-like THP1 cells, in the mitochondria or nucleus in murine macrophages and in the nucleus in human macrophages[70,141–143]. Importantly, the localisation of NLRP3 and other NLRP3 inflammasome components changes after stimulation with NLRP3 activators. In THP1 cells transfected with tagged NLRP3 and ASC, stimulation with nigericin or particulate matter triggers the relocation of NLRP3 and ASC to the mitochondria[92,143]. In THP1 cells and murine macrophages, stimulation with nigericin and MSU results in microtubule-mediated transport of mitochondria-associated ASC to the perinuclear region of the cell where NLRP3 and ASC localize to mitochondria-associated ER membranes (MAMs)[92,142]. In murine macrophages, treatment with different canonical NLRP3 stimuli results in the recruitment of NLRP3 to the mitochondrial outer membrane in a process mediated by the binding of NLRP3 to cardiolipin[144]. As previously mentioned, mitochondrial-derived stimuli such as ROS, mtDNA and cardiolipin are able to trigger or facilitate NLRP3 inflammasome activation[92,121,122]. Therefore, the association of NLRP3 with the mitochondria or MAMs may facilitate this process.

The Golgi may also be important for NLRP3 inflammasome activation. In murine macrophages, canonical stimulation of the NLRP3 inflammasome results in an increase in production of diacylglycerol in the Golgi membrane which in turn activates PKD leading to phosphorylation of NLRP3[102]. In this context, the Golgi and the MAMs, where NLRP3 is found, are suggested to be in close proximity, facilitating NLRP3 phosphorylation by PKD, and resulting in the release of NLRP3 from these membranes, allowing inflammasome assembly[102]. Moreover, multiple inflammasome stimuli trigger dispersion of the trans-Golgi network (TGN), and NLRP3 localizes to this dispersed TGN prior to inflammasome speck formation in Hela and HEK cells stably expressing NLRP3 and in murine macrophages[102]. Moreover, NLRP3 can directly bind to phosphatidylinositol 4-phosphate (PtdIns4P) which is exposed in the dispersed TGN

providing a hub for inflammasome assembly[102]. Thus, whilst it is perhaps unclear how the Golgi is involved in NLRP3 activation, the findings summarized above indicate that the Golgi could have a role in the inflammasome pathway.

Other subcellular locations where NLRP3 has been found are the centrosome and the autophagosome. NIMA-related kinase 7 (NEK7) is a kinase enriched in the centrosome that binds to NLRP3 and that has been shown to be required for inflammasome activation in LPS-primed murine macrophages and dendritic cells following activation with K^+ efflux-dependent and independent stimuli[117,145]. Moreover, when oligomerized into a speck, NLRP3, ASC and caspase 1 colocalised with NEK7 and the centrosomal protein ninein in murine macrophages and THP1 cells[146]. This indicates that the centrosome could operate as a platform for NLRP3 inflammasome assembly. On the other hand, NLRP3 and ASC have also been detected in the autophagosome in macrophage-like THP1 cells stimulated with LPS and ATP or particulate matter[146,147]. However, to regulate inflammasome activation, IL-1β, ASC and NLRP3 can be sequestered in the autophagosome to be targeted for degradation through the lysosomal pathway[146–148]. Thus, further investigation is needed to understand whether NLRP3 inflammasome assembly and activation can occur at the autophagosome or if localisation to this organelle is a consequence of the process of inflammasome degradation.

In conclusion, the observation of NLRP3 and NLRP3 inflammasome components in various intracellular compartments in different cells stimulated with a variety of stimuli indicate that NLRP3 inflammasome assembly is a dynamic process that may not have a unique cellular hub for activation.

1.3.5 Pyroptosis

Cell death is a powerful stimulus for inflammation that alerts the immune system to rapidly recognize and localize potential danger sites to limit the spreading of harmful agents[149,150]. During inflammation, different types of cell death activated by diverse cellular pathways and resulting in multiple processes occur simultaneously to boost the inflammatory signal[149,150].

Pyroptosis is a proinflammatory type of cell death that protects the organism against intracellular pathogens by eliminating their replication niche, and promotes immune responses by releasing intracellular DAMPs[59,75,151]. On the other hand, if overstimulated it can contribute to the pathology of various diseases including lethal toxic shock and sepsis[152–154]. This type of cell death is dependent on proinflammatory caspases being tightly related to the activation of the inflammasome[55,57,75]. Pyroptosis was first described as a 'caspase 1-dependent type of cell death'[155]. However, since it has recently been discovered that GSDMD is necessary for caspase 1-mediated pyroptosis, and that caspase 4 and 5 in humans and caspase 11 in mice are able to activate this process too, pyroptosis has been redefined as a 'GSDMD-dependent type of cell death'[78,156].

Pyroptosis shares characteristics with various types of cell death[57] (Table 1.1). As well as apoptosis, it is characterized by DNA fragmentation and membrane blebbing[57]. Nevertheless, unlike apoptosis, pyroptosis is a lytic process characterized by the formation of large membrane pores, leading to ion and water influx as well as cellular contents release - features that are similar to necroptosis[57]. As in other types of cell death, one of the main events that occurs during pyroptosis is the rupture of the plasma membrane. This results in the release of intracellular DAMPs inducing a potent pro-inflammatory response[59,75,151]. During pyroptosis, membrane rupture was thought to be a passive event that followed GSDMD pore formation in the cell membrane. However, it has recently been discovered that plasma membrane rupture is directly mediated, downstream of GSDMD, by the transmembrane protein ninjurin-1[157]. Specifically, treatment of HEK293T cells and murine macrophages with stimuli that induce not only pyroptosis but also other types of cell death like necrosis and apoptosis, results in the oligomerisation of ninjurin-1 in the cell membrane, leading to membrane rupture, with this event prevented by genetic ablation of ninjurin-1 ($Ninj1^{-/-}$)[157]. Nonetheless, treatment of $Ninj1^{-/-}$ cells with death stimuli still results in cell death, since no metabolic or mitochondrial activity is detected[157]. However, membrane rupture and the release of intracellular DAMPs are prevented[157]. In conclusion, pyroptosis is a potent immune system activator since it results in membrane rupture followed by the release of multiple DAMPs, including IL-1β and IL-18[57,151].

Type	Molecular and morphological features	Characteristic	Pathway	Effectors
Apoptosis	Membrane shrinkage and blebbing, mitochondrial outer membrane permeabilization, chromatin condensation, genomic DNA fragmentation, and translation inhibition	Non-inflammatory	Initiator and effector caspase activation	Effector caspases
Pyroptosis	Membrane blebbing, cell swelling, plasma membrane pore formation and rupture, DNA fragmentation, and release of proinflammatory intracellular contents	Inflammatory	Canonical and non-canonical inflammasome, inflammatory caspases activation	Inflammatory caspases GSDMD
Necrosis	Mitochondrial damage, membrane integrity loss, and release of intracellular contents	Inflammatory	Spontaneous	———
Necroptosis	Cell rounding up, cell swelling, membrane ion channel formation, release of cellular contents, and explosive membrane cell rupture	Inflammatory	TNFRSF-RIPK1/RIPK3, DAI-RIPK3, TLR-TRIF/RIPK3	MLKL

Table 1.1 Inflammatory and non-inflammatory types of cell death. TNFRSF: TNF receptor superfamily; RIPK: Receptor-interacting protein kinase; DAI: DNA-dependent activator of IFN-regulatory factors; TLR: Toll-like receptor; TRIF: TIR domain-containing adaptor inducing IFNβ; GSDMD: gasdermin D; MLKL: Mixed lineage kinase domain like pseudokinase. Table adapted from Liu and Lieberman, 2017[57].

1.3.6 NLRP3 activation in inflammatory diseases

As indicated before, NLRP3 activation is involved in the physiopathology of multiple infectious or sterile inflammatory diseases. During infection, the detection of PAMPs by PRRs and the presence of pathogen-derived toxins prime and activate the NLRP3 inflammasome. This results in the production and secretion of IL-1β and IL-18 and the released of intracellular DAMPs following pyroptosis that activate an immune response to eliminate the pathogen at the site of infection. This immune response is normally followed by restoration of homeostasis. However, when this inflammatory

process is not self-contained and there is an over-production of pro-inflammatory mediators, a systemic and prolonged immune response can be triggered, leading to sepsis[158].

NLRP3 inflammasome activation also occurs in sterile inflammatory diseases such as type II diabetes, gout and arthritis[86–88] . Type II diabetes is characterised by the development of insulin resistance triggered by constant high levels of glucose in the blood, also known as chronic hyperglycaemia. High levels of extracellular glucose activate the NLRP3 inflammasome, leading to IL-1β release in murine macrophages and pancreatic islets[159]. In this context, IL-1β antagonises insulin signalling, contributing to insulin resistance, and the destruction of β cells in the pancreas, dysregulating insulin secretion and worsening the disease[160]. Animal models and clinical trials have demonstrated that pharmaceutical inhibition or genetic blockade of the NLRP3 inflammasome or IL-1β reduces insulin resistance in type II diabetes[161,162].

Gout is produced in response to high levels of uric acid in blood, also known as hyperuricemia[163]. This results in deposition of MSU crystals in joints producing severe inflammation, arthropathy and pain[163]. As previously explained in this thesis, MSU is broadly known to activate the NLRP3 inflammasome, and several clinical trials have demonstrated that IL-1β antagonists can be used as a successful treatment for patients with gout[164–166], indicating that this cytokine is one of the main drivers of this inflammatory disease.

Arthritis is a disease characterised by the inflammation of the joint tissue. Patients with rheumatoid arthritis and osteoarthritis have high levels of IL-1β and IL-18 and NLRP3 inflammasome activation in blood and synovial fluid compared to healthy controls. Moreover, at the arthritic joint, increased levels of these cytokines mediates cartilage and bone degradation[167], the activation of proinflammatory responses at the joint, and tissue destruction[168]. Previous research has shown that NLRP3 activation occurs mainly in monocytes and macrophages that are infiltrating in the synovia of these patients[169–171], and treatment with the NLRP3 inflammasome inhibitor MCC950 significantly reduces inflammation and tissue destruction at the joint in murine models of these diseases[172,173], supporting an important role for the NLRP3 inflammasome in the development of arthritis.

The aforementioned diseases are examples that highlight the role of the NLRP3 inflammasome in inflammatory diseases. Importantly, an exacerbated activation of this inflammasome is also detrimental for many other acute, chronic and auto-immune diseases[174]. Therefore, studying the NLRP3 inflammasome is key to be able to therapeutically target a signalling pathway that is involved in a broad range of inflammatory diseases.

1.4 Interleukins 1β and 18

Inflammasome activation results in the secretion of IL-1β and IL-18 to the extracellular milieu[53–58]. These interleukins are proinflammatory cytokines with fundamental roles[175,176]. For instance, they induce antibody production in B cells and activate T cell-mediated immune responses[177]. Furthermore, their dysregulation potentiates infectious, autoimmune and degenerative diseases including diabetes, arthritis and lethal toxic shock[176,178,179].

These cytokines are produced by diverse cell types, including immune cells such as monocytes and macrophages[175,180]. Nevertheless, while IL-1β is mainly produced in hematopoietic cells, IL-18 is expressed in a wide range of cells including fibroblasts, endothelial cells and neuronal cells[175,180]. Both interleukins are closely related since they belong to the same family of proteins, the IL-1 family[77,175]. They are both produced as inactive precursors (pro-IL-1β and pro-IL-18) that are cleaved by caspase 1 into their active forms - IL-1β and IL-18[175]. Moreover, the precursors of these cytokines can be subject to extracellular cleavage by enzymes such as proteinase 3, and both cytokines have coreceptors and decoy receptors[181–183].

IL-1β was first described as an ‘endogenous pyrogen’ since it enhances corporal temperature[177]. It is known to be a potent thermal and mechanical hyperalgesic and it is dysregulated in multiple pathologies such as inflammatory bowel disease, rheumatoid arthritis, Alzheimer's disease and sclerosis[77]. It is involved in the activation of T cells, B cells, and neutrophils, as well as in T cell differentiation to a Th17 immune phenotype [77,184]. The IL-1β signalling pathway is similar to that of the NLRP3 inflammasome

activation. It starts when this cytokine binds to its receptor IL-1R. This allows for formation of a heterodimer with the coreceptor IL-1 receptor accessory protein (IL-1RAcP), forming a platform for MyD88 recruitment. Upon MyD88 binding, IRAK1 and IRAK4 are activated. This is followed by a downstream cascade of reactions that lead to NF-κB activation, inducing multiple inflammatory processes[185,186].

IL-18 was first described as 'IFNγ-inducing factor' since stimulation of spleen cells with this cytokine induced IFNγ production[187]. It is important for NK cell and macrophage activation, as well as for both Th1 and Th2 responses[76]. Like IL-1β, IL-18 dysregulation is involved in multiple pathologies including sepsis, arthritis and type I diabetes[76]. The IL-18 signalling pathway is similar to that of IL-1β, in that it binds to its receptor IL-18Rα/ IL-18Rβ heterodimer, which is followed by MyD88 binding and NF-κB activation. This results in the activation of multiple inflammatory pathways including IFNγ production. Furthermore, IL-18 is involved in both Th1 and Th2 immune responses; in the presence of IL-12, IL-18 promotes cell polarization to a Th1 immune response, while in the absence of IL-12 it induces natural killer (NK) cell protection against some viruses, promotes the interplay of NK cells with macrophages, and stimulates Th2 immune responses[76]. IL- 18 also promotes the expression of intercellular adhesion molecule 1 (ICAM- 1) on myeloid cells and vascular cell adhesion molecule 1 (VCAM-1) in fibroblasts and endothelial cells[188,189].

1.4.1 IL-1β and IL-18 Secretion Pathway

IL-1β and IL-18 are not released through the endoplasmic reticulum(ER)-Golgi-exocytosis 'conventional' protein pathway[190] (Fig 1.6). Proteins that are secreted through this pathway have an amino-terminal signal peptide for ER recognition that is absent in these cytokines[191,192]. Furthermore, IL-1β release is not affected when the ER and Golgi are impaired, as IL-1β and IL-18 are not associated with these organelles, and are instead translated onto cytoskeleton-associated polyribosomes[193–195]. From these facts, it is concluded that this family of cytokines has an alternative secretion pathway[190]. It is now clear that IL-1β and IL-18 secretion is regulated via the inflammasome pathway[190], making activators of this complex also stimuli for the secretion of these cytokines.

Different mechanisms have been proposed for IL-1β and IL-18 secretion, including release via vesicles, microvesicles shedding, exosomes and secretion through GSDMD pores, the last of which is the most accepted mechanism (Fig 1.7)[196,63]. It has been shown that endolysosomes, vesicles formed by the fusion of late endosomes and lysosomes, can contain IL-1β[197]. These IL-1β-containing vesicles are suggested to be autolysosomes that sequester this cytokine to be degraded when the cell is undergoing autophagy[197]. In monocytes, when activated by PAMPs or DAMPs, this fraction of IL-1β can be rescued and released through lysosomal exocytosis[197,198]. Furthermore, IL-1β-containing microvesicles have been found in astrocytes, microglia and dendritic cells (DCs)[199]. This fraction of IL-1β could be released when these cells recognize other cells expressing IL-1R, making this pathway a selective mechanism for IL-1β signalling[199]. IL-1β is also found in exosomes. It has been suggested that this fraction of the cytokine may be protected from degradation and may represent a 'long-lived' fraction of the interleukin since the half-life of free IL-1β in plasma is very short[200]. However, these mechanisms explain how small fractions of these cytokines could be released but do not constitute their main released pathway.

For a long time, various studies suggested that IL-1β and IL-18 could be released from the cell through plasma membrane transporters. In fact, as explained in the following section of the introduction, in 2015 the pore forming protein GSDMD was discovered to be involved in IL-1β and IL-18 release, making this protein an optimal candidate for IL-1β and IL-18 transport across the membrane[156,201–204].

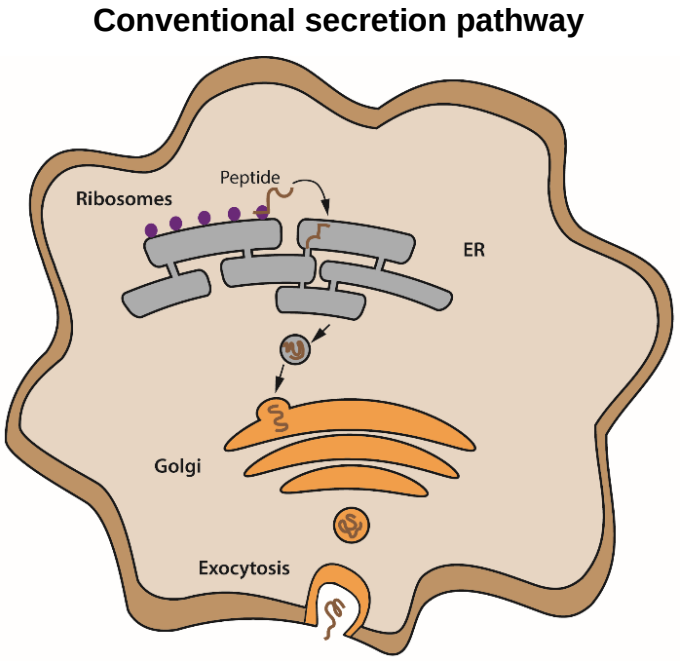

Figure 1.6 Conventional Protein secretion pathway. Conventionally secreted proteins are transported through the ER and Golgi, where they are post-translational modified before they are secreted to the extracellular space through exocytosis. Adapted from Lopez-Castejon and Brough, 2011[190].

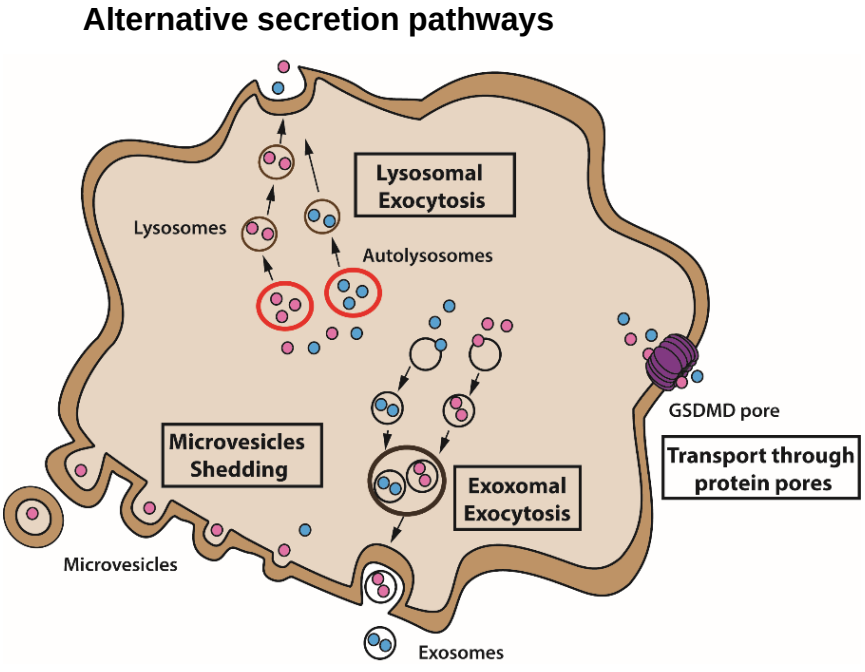

Figure 1.7 Alternative protein secretion pathways. IL-1β and IL-18 (pink and blue) follow alternative secretion pathways. These pathways include lysosomal exocytosis, exosomal exocytosis, microvesicles shedding and transport through membrane protein pores. Adapted from Lopez-Castejon and Brough, 2011[190].

1.5 Gasdermin D

Gasdermin D (GSDMD) is part of a recently discovered family of proteins that is conserved among vertebrates[205]. In humans, this group of proteins comprises six members: GSDMA, GSDMB, GSDMC, and GSDMD and the last added members DFNA5, also known as GSDME, and DFNB59, also known as PJVK. The first five proteins share two domains that are bound by a linker peptide, whereas DFNB59 only shares the N-terminus domain of the family[205,206 206–208].

The role of GSDMD in the inflammasome pathway was uncovered whilst investigating ways in which lethal toxic shock produced by bacteria could be prevented that resulted in the discovery of the non-canonical NLRP3 pathway. Caspase 1 had been considered the effector of pyroptosis. However, during non-canonical inflammasome activation, deletion of caspase 1 did not affect this process, and caspase 11 or caspase 4/5 were responsible for cell death[61,138]. Therefore, since both canonical and non-canonical inflammasome pathways lead to pyroptosis, a common event downstream of caspase 11/4/5 had to be the effector of this type of cell death. Recently, two groups identified GSDMD as the protein responsible for inflammasome-dependent cell death[63,156]. To do so, they used genome-wide CRISPR-Cas9 nuclease screens of caspase 11- and caspase 1-mediated pyroptosis in mouse bone marrow-derived macrophages (BMDMs), and a forward genetic screen with ethyl-N-nitrosourea (ENU)- mutagenized mice to study mediators of non-canonical inflammasome activation in response to intracellular LPS in peritoneal macrophages[63,156]. This was confirmed by the fact that impairment of the *gsdmd* gene blocked pyroptosis in murine BMDMs and peritoneal macrophages treated with multiple inflammasome stimuli, including LPS and nigericin, LPS electroporation and Pam3CSK4 and ATP[63,156]. Since then, multiple studies have confirmed the involvement of GSDMD in pyroptosis[78,79,201–203,209].

GSDMD is cleaved by inflammatory caspases into two fragments: a C-terminal p20 domain (CT-GSDMD) and an N-terminal p30 domain (NT-GSDMD). This p30 domain is able to bind to lipid membranes and oligomerize, forming pores[79–81,210]. While results among publications differ on the lipid-binding characteristics of this protein, probably due to experimental variability, they all agree that NT-GSDMD can only be inserted in

the inner leaflet of the cell membrane[79–81,210]. NT-GSDMD also binds cardiolipin, which is present in mitochondrial and bacterial membranes[203]. Recently, it has been reported that NT-GSDMD can form pores in the mitochondria of THP1 cells stimulated with LPS and Shiga toxin from *E. coli* and epithelial cells from mice treated with sublytic doses of LPS, suggesting that GSDMD pores mediate the release of mitochondrial DAMPs, inducing or enhancing inflammasome activation[211,212]. Moreover, extracellular NT-GSDMD cannot bind the outer cell membrane of human cells but it is able to disrupt bacterial integrity by forming pores in their membranes[79,213], opening a new field of study of this protein as a potential antibacterial drug.

While GSDMD or NT-GSDMD knock-out cells are viable, the lack of CT-GSDMD is lethal[79]. These studies, together with structural analysis of this protein, support the idea that GSDMD C-terminal domain inhibits NT-GSDMD membrane binding and oligomerization[79,214–216]. Altogether, this shows that the C-terminal domain of the protein has a regulatory role, preventing NT-GSDMD pore formation. In fact, only after inflammasome activation, when GSDMD domains are cleaved apart by inflammatory caspases, can NT-GSDMD pores be formed[79].

GSDMD pores may now be considered to be the ultimate downstream event leading to pyroptosis. However, it has been showed that in *gsdmd*$^{-/-}$ BMDMs, pyroptosis is blocked at early time points following canonical inflammasome activation. Interestingly, although hampered, this process is recovered at later time points[63]. Since there are multiple inflammasome activation pathways and this process is not fully understood, it has been suggested that GSDMD pores may be one but not the only effector of pyroptosis. Importantly, not only does the NT-GSDMD form pores that lead to cell death, the N-terminal domains of GSDMA, GSDMB, GSDMC and GSDME are also cytotoxic for the cell[79], and mutations in the C-terminal domain of GSDME result in cell death and diseases such as hearing loss[217,218]. These facts suggest a potential role for the Gasdermin family in cell death control and regulation.

It was recently shown that phagocytes are able to reach a hyperactivation state in which upon inflammasome activation, they secrete IL-18 and IL-1β and maintain their viability[201]. That is to say that these cytokines can be released independently of

pyroptosis. This discovery changed the idea of GSDMD as only a pyroptosis mediator, and gave a new role to GSDMD pores as potential channels for the secretion of intracellular cytokines when the cell is hyperactive[201].

GSDMD pores have been studied using both electron and atomic force microscopy[79,80]. However, super resolution images of the protein are still unavailable. Based on structural studies of other proteins of the family and the molecular weight of the complex, the pore was reported to be composed of 16-24 subunits and to have an inner diameter of 10-20 nm[79,80]. Recently, human GSDMD pore structure has been resolved using cryogenic electron microscopy, and it has been determined to have an inner diameter of 21.5 nm and an outer diameter of 31 nm[219]. It has also been shown that molecules smaller than 10 nm in diameter are able to pass through these pores[201]. Since inflammasome activation results in IL-1β and IL-18 secretion and these cytokines are 4.5 nm in size[220], these cytokines could be secreted through GSDMD pores. Moreover, both in liposomes and murine hyperactive macrophages or pyroptotic macrophages where membrane rupture is prevented with glycine, GSDMD is necessary for IL-1β and IL-18 secretion through intact lipid bilayers[201]. This strengthens the idea that IL-1β and IL-18 are secreted mainly through cell membrane GSDMD pores. However, whether this protein is responsible for cytokine release upon inflammasome activation in primary human macrophages has not been investigated.

1.6 The Complement system

The complement system is constituted by a large group of plasma proteins, cell receptors and regulatory proteins. Complement plasma proteins were first discovered for their ability to target pathogens, assisting or 'complementing' Ab-mediated opsonization of these pathogens[221]. However, it is now clear that the complement system is a very important part of the innate immune response and is able to modulate pro-inflammatory responses independently of Abs[222].

The complement proteins are activated through a cascade of enzymatic reactions from the first activated complement protein to the terminal pathway of this system. Certain complement proteins are zymogens (inactive precursors of an enzyme)

that are activated by proteolytic cleavage. The cleavage of a zymogen results in the formation of an active enzyme that will in turn cleave the next zymogen into an active enzyme that will continue this enzymatic cascade. Therefore, engagement of a small number of complement proteins triggers and amplifies the activation of multiple proteins in the complement cascade, driving a quick inflammatory response at the site of activation[221].

The complement cascade can be activated through three pathways: the classical pathway, the mannose-binding lectin (MBL) pathway and the alternative pathway (Fig 1.8). The classical pathway is triggered by the binding of complement component (C) 1 complex to Abs bound to the surface of pathogens and to damaged cells[221–224]. In this complex C1q binds to the Abs and C1s cleaves C2 and C4. This results in the formation of C4b2a, also known as C3 convertase[221,222]. The MBL pathway is initiated by the binding of MBL complexes, or complexes of similar proteins such as ficolins, to PAMPs. MBL-associated serine proteases 1 and 2 (MASP-1 and MASP-2) are part of these complexes and upon pathogen binding MASP-1 cleaves MASP-2, which in turn cleaves C2 and C4 resulting in the formation of the C3 convertase[221,222]. The alternative pathway is activated by spontaneous hydrolysis of C3 into C3b. C3b can bind Factor B, which undergoes a conformational change that allows Factor D, which is constitutively active, to cleave it. The result is the formation of the alternative pathway C3 convertase[221,222]. All C3 convertases cleave C3 into C3a and C3b, and the addition of C3b fragments to C3 convertases generates C5 convertases. C5a convertases cleave C5 into C5a and C5b. Together with C6, C7, C8 and C9, C5b will generate the terminal complement complex (TCC), also known as the Membrane Attack Complex (MAC)[221,222]. Importantly, the alternative pathway can also be engaged by membrane-bound C3b generated through the classical or MBL pathways leading to an “amplification loop” of the complement cascade[221,222].

The activation of the complement cascade is key for driving the immune response forward during infection. It results in the formation of multiple complement proteins that are able to bind pathogens and target them for opsonization by phagocytes[221]. Importantly, some complement components, such as C3a and C5a, have the ability to attract immune cells to the site of infection and activate them[225].

Furthermore, the MAC is able to form pores in the membrane of pathogens and damaged cells to clear them[226].

Although multiple components of the complement system have important roles in inflammation, this thesis will specifically study the terminal pathway of this system, focusing on C5a and the MAC and their ability to activate the inflammasome.

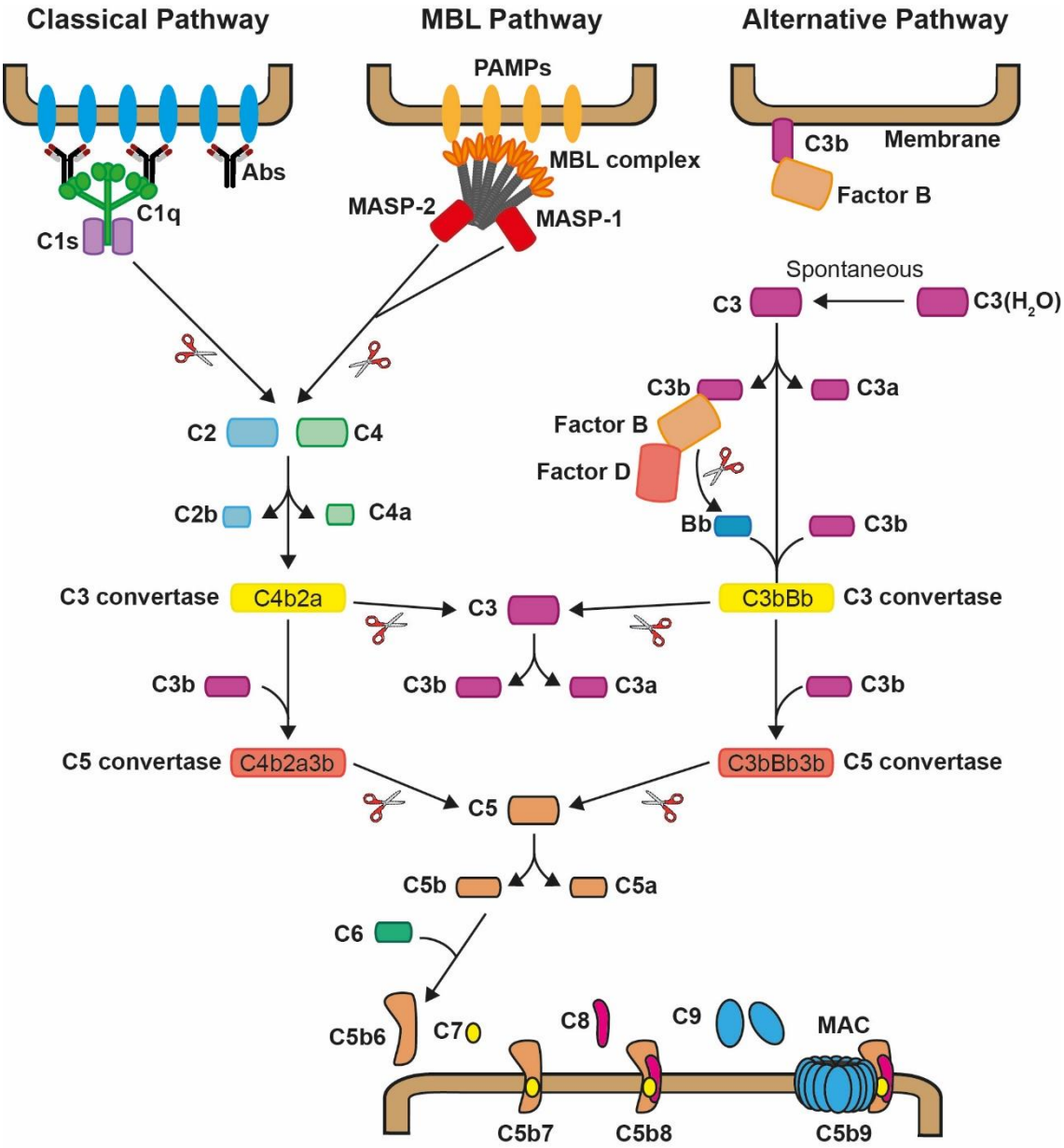

Figure 1.8 Activation of the complement system. The complement cascade can be activated through three different pathways: the classical pathway, the mannose-binding lectin (MBL) pathway, and the alternative pathway. The classical pathway is induced by Ab-mediated binding of C1 complexes to pathogens and damaged cells. Upon binding, the C1 complex is able to cleave C2 and C4 leading to the production of a C3 convertase (C4b2a). The MBL pathway is engaged by the binding of the MBL complex to PAMPs leading to the activation of MASP-1 and MASP-2 which cleave C2 and C4 to form a C3 convertase (C4b2a). The alternative pathway is initiated by spontaneous hydrolysis of C3, leading to the processing of C3 into C3a and C3b which binds Factor B, and to the recruitment of Factor D. Factor D cleaves Factor B into the Bb fragment which together with C3b forms a C3 convertase (C3bBb). All C3 convertases can cleave C3 into C3a and C3b, and addition of a C3b protein to C3 convertases results in the formation of C5 convertases (C4b2a3b or C3bBb3b) which cleave C5 into C5a and C5b. Finally, the sequential addition of C6, C7, C8 and multiple C9 proteins to C5b results in the formation of the MAC. C3b bound to the plasma membrane can also activate the alternative pathway leading to an "amplification loop" of the complement cascade. Adapted from Janeway Travers and Walport, 2001[221].

1.6.1 C5a

The activation of the complement cascade results in the formation of C5 convertases that cleave C5 into C5a and C5b[221,227]. Importantly, proteases such as thrombin and serine proteases secreted by neutrophils and macrophages can locally cleave C5, independently from the complement cascade, leading to the formation of C5a-like and C5b-like proteins[228–230]. Whilst C5b initiates the formation of the MAC, C5a is a potent inflammatory mediator with multiple functions[231].

The first discovered functions for C5a were its anaphylatoxic and chemotactic properties[230]. In fact, C5a is considered an anaphylatoxin for its ability to induce degranulation of granulocytes such as mast cells, eosinophils and neutrophils, what can result in anaphylactic shock[232–234]. Moreover, C5a is a potent chemoattractant for multiple cell types, including innate and adaptive immune cells. Specifically, C5a induces the migration of granulocytes and myeloid cells, with particularly high potency in neutrophils and macrophages[235–238]. Moreover, this complement protein enhances the expression of adhesion molecules and phagocytosis in neutrophils and macrophages, and it modulates the production of multiple cytokines, including IL-1β, in various immune cells[231,239]. C5a can also attract T cells, induce CD4+ T cell expansion and activate T cell immune responses, indirectly through modulation of multiple cytokines, and directly through engagement of C5a receptors in T cells[240–242].

C5a induces intracellular responses by binding to its receptors C5a receptor (C5aR) 1, also known as CD88, and C5aR2, also called C5L2[243,244]. Both receptors are part

of the seven transmembrane receptors family[244,245], and whilst C5aR1 is coupled to a G-protein and a β arrestin, C5aR2 is only coupled to a β arrestin but lacks a G-protein[245–247]. Both receptors are highly expressed in immune cells such as monocytes and neutrophils[247,248]. In these cells, C5aR1 is normally found in the cell membrane whereas C5aR2 is predominantly found intracellularly[246,247]. Binding of C5a to C5aR1 activates the couple G-protein, initiating downstream signalling pathways involving PI3K/Akt and MAPK/ERK [239,249–251]. Moreover, C5a is able to activate NF-κB in human myeloid cells[252]. Engagement of C5aR1 also induces the recruitment of β arrestin to the receptor which in turn desensitizes it and initiates its internalization to downregulate C5a-mediated cellular responses[253,254]. Due to the lack of a coupled G-protein[247], C5aR2 was originally believed to be a decoy receptor for C5a. However, it is now known that binding of C5a to C5aR2 also engage intracellular signalling in multiple cell types leading to both pro-inflammatory and anti-inflammatory responses[255].

1.6.2 The Membrane attack complex

The last event of the complement cascade is the formation of the MAC, a pore-forming complex that is able to oligomerize in lipid bilayers[221,226,227]. Upon cleavage of C5, C5b oligomerizes with C6, C7, C8 and multiple C9 proteins to form the MAC[256]. To do so, C5b, which is not very stable by itself, rapidly oligomerizes with C6 forming the C5b6 complex[257]. Then C7 is recruited to the complex leading to a change in conformation that makes the structure lipophilic[258]. Following this, the addition of C8 results in membrane insertion[256,258–260]. The C5b-8 complex functions as a self-oligomerized receptor for C9, and the sequential addition of 18 copies of C9 to this complex in a clockwise manner results in the formation of the transmembrane pore known as the MAC[256,258–260].

The MAC was first discovered as a lytic pore-forming complex, the assembly of which was induced by Abs, that had the ability to complement Ab-mediated lysis of pathogens[221]. The lytic function of the MAC is key in the defence against gram-negative bacteria, parasites and enveloped viruses since pore formation by the MAC in these pathogens triggers their osmolysis[261–263]. This is evidenced by the fact that human patients treated with therapies blocking the complement cascade or having genetic

abnormalities that result in impaired MAC function are more susceptible to recurrent infections[264–266].

Nucleated mammalian cells have mechanisms to resist cell lysis by self MAC. These include the inhibition of MAC insertion in the cell membrane by complement regulatory proteins such as the membrane proteins CD46, CD55, and CD59, and the elimination of already-formed MAC pores by endocytosis, exocytosis or membrane vesiculation. CD46 aids the cleaving of C3b and C4b deposited in the plasma membrane and therefore, inhibits the formation of complement convertases and the consequent downstream events of the complement cascade, including MAC formation, and inhibiting the "amplification loop" of the complement cascade triggered by membrane-bound C3b[267–269]. CD55 is involved in accelerating the decay of C3 convertases and, therefore, downregulating the complement cascade[270]. Finally, CD59 directly inhibits MAC formation in the cell membrane by interacting with C8 and the first C9 protein added to the complex to block the addition of more C9 proteins, and therefore preventing pore formation[271–273]. Of note, during prolonged inflammation these receptors can be depleted in the act of inhibition allowing formation of the MAC in host cells[274].

As previously mentioned, MAC pores that are already formed in the cell membrane of nucleated cells can be removed by endocytosis, exocytosis or outward vesiculation, also known as ectocytosis[275–278]. Removal of the MAC from the cell membrane through these processes attenuates its lytic effect, therefore, MAC formation does not imply cell death[278,279]. When this happens, the MAC is known as sublytic MAC. Importantly, although the MAC was traditionally studied for its lytic function, it is currently known that sublytic MAC can trigger multiple intracellular signalling pathways resulting in cell activation. For example, sublytic MAC can increase cell proliferation in fibroblasts and smooth muscle cells, upregulation of adhesion molecules in endothelial cells, and trigger secretion of proinflammatory cytokines in both immune and non-immune cells[280–292]. Moreover, sublytic MAC can induce responses in endothelial cells that result in the activation and recruitment of immune cells, including T cells[292–294].

Although the complement system is fundamental to fight harmful events during inflammation, overstimulation of complement components can contribute to the progression of multiple inflammatory diseases. In the context of the terminal pathway of the complement system, this is evidenced by the fact that the amount of C5a and soluble C5b-9 in plasma or serum from patients with sepsis or different types of arthritis is considerably increased when compared with samples from healthy patients[295–299]. Moreover, deletion or blockade of C5a or its receptors in animal models of diseases such as arthritis rescues pathology[300,301], and deletion of C9 reduces LPS-induced septic shock in mice[302], suggesting that these complement components are detrimental for these pathologies. Additionally, MAC-mediated immune cell recruitment can contribute to the development of certain inflammatory events including those associated with transplant rejection[303]. On the other hand, genetical alterations or deficiencies in C6, C7, C8 and C9 that impair the formation of the MAC pore are related to the development of certain diseases including macular degeneration and recurrent *Neisseria* infection[304–307]. Altogether, this indicates that both overstimulation and malfunction of the terminal pathway of the complement cascade can contribute to the development of disease.

1.7 The complement system and inflammasome activation

The innate immune system does not act as a group of isolated processes that occur individually in response to an immunological challenge. On the contrary, when a danger signal is detected, multiple cellular pathways are activated at the same time and interact with each other to modulate the immune response. Therefore, the complement system and the inflammasome, two of the most important pathways of the innate immune system, must also cooperate during inflammation. Indeed, there is evidence for the complement components C3a, C5a and the MAC to contribute to NLRP3 inflammasome priming or activation in different cell types[283,290,292,308–312].

1.7.1 C3a and C5a in inflammasome activation

As previously mentioned, NLRP3 priming induces the activation of the transcription factor of NF-κB, leading to the upregulation of pro-IL-1β and NLRP3 expression[56]. Both C3a and C5a are able to activate NF-κB[252,313–315], indicating that they

could potentially prime the NLRP3 inflammasome. Moreover, C3a and C5a can initiate calcium fluxes and the engagement of C3a receptor (C3aR) induces ATP release[252,308,313,314,316–319], two events that are associated with NLRP3 activation[121,320]. In fact, treatment with C3aR agonists enhances LPS-mediated IL-1β secretion in human monocytes via activation of ERK1/2 and secretion of ATP that engages the P2X7 receptor[308]. Moreover, C3aR agonists act synergistically with LPS to induce IL-1β release in human macrophages and dendritic cells[308]. C5a synergistically acts with TNF to prime the NLRP3 inflammasome in human PBMCs exposed to cholesterol crystals[309]. Moreover, C5a also has the ability to enhance inflammasome activation in murine monocytes treated with LPS and in LPS-primed murine macrophages treated with MSU, ATP or nigericin[310–312]. However, C5a reduces IL-1β secretion in murine macrophages treated only with LPS[310], indicating that the role of C5a in inflammasome activation may differ between cells types and depending on the inflammasome stimuli. In addition, autocrine secretion of C5a and engagement of C5aR results in NLRP3 inflammasome activation and IL-1β secretion in CD4+ T cells[309], demonstrating that the complement system can also activate adaptive immune cells.

1.7.2 The Membrane attack complex and the NLRP3 inflammasome

The MAC can also mediate inflammasome activation in various cell types. Particularly, treatment of human lung epithelial cells with human serum as a source of complement, results in the increase of cytosolic Ca^{2+}, attributed to MAC pore formation in the cell membrane, and the loss of mitochondrial transmembrane potential, triggering the activation of the NLRP3 inflammasome[290]. Depletion of C7 or C9 from serum impairs caspase 1 processing and IL-1β secretion in these cells indicating a role for the MAC in inflammasome engagement[290]. Treatment of LPS-primed murine dendritic cells with rabbit serum engages NLPR3 inflammasome activation leading to caspase 1 cleavage and IL-1β release in a C6 and C9-dependent manner suggesting that the MAC is responsible for inflammasome activation[283]. Moreover, in human endothelial cells primed with IFN-γ, treatment with human serum from transplant patients containing alloantibodies triggers NLRP3-dependent caspase 1 activation, GSDMD processing and IL-1β release. ASC speck formation is significantly reduced in these cells

when they are stimulated with C9-deficient serum suggesting that inflammasome activation is induced by the MAC[292]. Thus, serum containing the complement components needed for MAC assembly and potentially MAC pore formation can mediate inflammasome activation in both immune and non-immune cells. However, whether the MAC triggers inflammasome activation in human myeloid cells, or if formation of the MAC in the absence of other serum components can activate the inflammasome has not been determined yet. To answer these questions, this thesis will explore the link between the MAC and the inflammasome in human macrophages.

1.8 Fluorescent microscopy

Multiple biological processes and cellular functions, including intracellular interactions, subcellular localisation of proteins, and the dynamics of cellular events have been discovered through direct visualisation. As such, microscopy techniques, and the development of fluorescent probes to specifically visualize certain proteins or intracellular compartments, have played a fundamental role in building up our current knowledge of cellular biology. Thus, this thesis uses fluorescence microscopy techniques to broaden our understanding of the inflammasome pathway in human macrophages.

Fluorescence microscopy uses fluorophores to label specific structures in a sample. When a laser beam excites a fluorophore in its low-energy, one of its electrons is moved to an orbital further from the molecule nucleus. That transitory electron in a high-energy state returns to its original state emitting different forms of energy, including fluorescent light that is detected and forms the image seen with the microscope[321]. This type of microscopy constitutes an accessible technique that allows the study of cell protein organization and dynamics.

Fluorescence microscopy has physical, biological and technological limitations including equipment features like objective numerical aperture (NA), detector sensitivity and fluorophore properties. Apart from that, even under optimal conditions, light diffraction is the major limitation for fluorescence microscopy resolution. On the basis of Abbe's law (Fig 1.9), stating that the highest resolution (the smallest distance between two different points in a sample that can be differentiated as two distinct

entities) that a microscope can achieve is restricted by the diffraction limit of light, the maximum resolution that a fluorescent microscope can reach is approximately 250 nm along the x-y axis and 500 nm in the z axis[321–323]. As such, a whole range of subcellular organelles, proteins and molecules remain invisible for this conventional approach.

a $$d_{x,y} = \frac{\lambda}{2NA}$$

b $$d_z = \frac{2\lambda}{NA^2}$$

Figure 1.9 Abbe's law. a) $d_{x,y}$ represents the lateral resolution of a microscopy. **b)** d_z represents the axial resolution of a microscope. In both equations λ is the wavelength of the excitation beam and NA the numerical aperture of the microscope objective.

1.8.1 High-resolution techniques

High-resolution microscopy techniques such as confocal fluorescence microscopy and total internal reflection fluorescence (TIRF) microscopy represent an important step forward in fluorescence imaging. Nevertheless, these technical approaches are still limited by light diffraction, with the highest obtainable resolution with them being approximately 150 nm[324,325].

In conventional fluorescence microscopy, the whole sample is excited with light at the same time which leads to background fluorescence and out-of-focus images. Confocal microscopy eliminates this out-of-focus fluorescence glare using spatial filtering[325]. Laser scanning confocal microscopy limits the sample focal plane by using pinhole apertures to produce a restrict point of excitation. This point of excitation is moved along the sample to capture several consecutive images. Once the whole sample is scanned, it is reconstructed in a single image. Moreover, this technique is able to obtain 3D models of the sample by acquiring multiple images along the z axis. This type of microscopy is extremely valuable for biological research since it produces high-resolution images and permits live visualisation of cellular processes[325].

TIRF microscopy detects the energy emitted by the fluorophores of a sample after been excited with an evanescent laser beam reflected on a surface, normally the coverslip of the sample. Only the fluorophores next to the surface will be excited,

eliminating the background fluorescence. This technique is especially used to study cell adhesion, cell membrane structure and membrane-related processes such as cell synapsis, and membrane proteins and receptors. However, this technique has a major disadvanta–e - due to light reflection properties, the maximum depth that can be visualized in the sample is approximately 200 nm[324]. Nonetheless, this can be seen as an advantage when the interest of research is only the membrane fraction of a specific protein that also has a cytosolic portion, with an example of this being the study of membrane-bound GSDMD pores.

1.8.2 Super resolution microscopy

Super-resolution microscopy 'breaks' the light diffraction barrier by exciting the fluorophores of the sample at different times. With this approach, molecules that are closer to one another than the diffraction of light are able to be resolved[323,326,327]. This type of imaging, also known as fluorescence nanoscopy, is a powerful tool that improves image resolution up to ten times compared to that of traditional microscopy. Using such a high-resolution, scientists have been able to see nuclear pores, cytoskeletal components, cellular vesicles, mitochondrial structure, membrane proteins and other structures and processes that would not have been possible to image using conventional approaches[327].

Nowadays, multiple super-resolution techniques are used in biological research including stimulated emission depletion (STED) microscopy, stochastic optical reconstruction microscopy (STORM) and photoactivated localisation microscopy (PALM). This project uses STORM to visualize GSDMD in the cell membrane. STORM is based on the time-resolved localisation of single fluorescent molecules in a sample. This results in the point by point reconstruction of the image, which is achieved using fluorescent molecules that have on and off states. In these techniques, the microscope captures consecutive images of the same plane. Due to their photoswitchable properties, different fluorophores are detected in different frames which, after image reconstruction, permits visualisation of molecules closer than the diffraction limit of light. STORM uses immunolabelling with organic fluorophores conjugated to Abs that recognize the target of interest. With optimal conditions, this microscopy approach is

able to achieve resolutions of 10 nm and 20 nm in the axial and lateral axis in fixed samples, respectively, and of 30 nm and 50 nm during live-microscopy when all the parameters are optimal[323,326], meaning that GSDMD pores that are 31 nm in size could theoretically be observed using this technique. However, this size is very close to the resolution limit of this type of microscopy which may make it difficult to clearly visualise the structure of GSDMD pores.

1.9 Aims

Macrophages have key roles during inflammation, with one of their main roles being to rapidly respond to exogenous and endogenous danger agents by generating pro-inflammatory mediators that amplify the immune response to restore homeostasis. IL-1β and IL-18 are two of these proinflammatory mediators, and they are essential for the correct activation of innate and adaptive immune responses. However, when the production of these cytokines is prolonged overtime, they can contribute to the development of harmful pathologies. In humans, macrophages are one of the main sources of these cytokines. Therefore, understanding how they are released and what stimuli trigger their production and secretion in human macrophages is very important to develop strategies to manipulate the impact of these cytokines in IL-1β and IL-18-mediated diseases.

A growing body of evidence suggest that GSDMD is directly involved in IL-1β and IL-18 secretion. Thus, one of the foci of study of this thesis is this protein. Furthermore, the complement system is one of the first lines of defence against danger signals in the human body. However, a prolonged activation of the terminal pathway of this system plays a role in the development of pathologies mediated by IL-1β and IL-18. Nonetheless, whether there is a link between the terminal pathway of the complement system and the secretion of these cytokines in human myeloid cells is not clear. Therefore, the second focus of study of this thesis was to investigate if C5a and the MAC can engage IL-1β and IL-18 release in human macrophages.

The three main objectives of this thesis were:

1. To investigate whether GSDMD plays a role in IL-1β and IL-18 release upon canonical NLRP3 inflammasome activation in human macrophages. (Chapter 3)

2. To address whether the complement components C5a and the MAC can induce NLRP3 inflammasome priming and activation, respectively, leading to cytokine release in human macrophages. (Chapter 4)

3. To understand the mechanism by which the MAC activates the NLRP3 inflammasome in human macrophages. (Chapter 5)

Chapter 2 Materials and Methods

2.1 Cells

2.1.1 Monocyte-derived macrophages

Primary human macrophages were differentiated from monocytes isolated from blood acquired from the National Blood Transfusion Service (Manchester, UK) with full ethical approval from the Research Governance, Ethics, and Integrity Committee at the University of Manchester (REC 05/0401/108). For this, peripheral blood mononuclear cells (PBMCs) were isolated from leukocyte cones by ficoll gradient centrifugation for 40 min using soft acceleration and no break (Ficoll-Paque; GE Healthcare). PBMCs were collected, washed in RPMI media (Sigma-Aldrich), and resuspended in 10 mL of Red Blood Cell Lysing Buffer (Sigma-Aldrich) during 5 min to remove erythrocyte contamination. Then, CD14+ cells (monocytes) were obtained using the human CD14+ MACS separation kit (Miltenyi Biotec) following manufacturer's instructions. Monocytes were seeded onto 6, 12 or 24-well plates or into chambered coverglasses (Nunc™ Lab-Tek™ II, Thermo Scientific™) at a concentration of 5 x 10^5 cells/mL or 2 x 10^4 cells/mL, respectively, and culture for 6 days at 37 °C and 5% CO_2. To obtain macrophages, monocytes were incubated in complete RPMI media (10% FCS [Gibco], 1% L-glutamine [Gibco], 1% Penicillin/Streptomycin [Sigma-Aldrich]) with 50 ng/mL M-CSF (Prepotech). On day 3, half of the media was removed from each well and replaced with fresh complete RPMI media with 50 ng/mL M-CSF[328,329]. Alternatively, macrophages were obtained by culturing monocytes for 2 days in X-VIVO 10 media (Lonza) with 1% human serum (Sigma-Aldrich) following by 4 days of culture in Dubelcco's Modified Eagle's Medium (DMEM, Sigma-Aldrich) supplemented with 10% FCS, 1% L-glutamine, 1% Penicillin/Streptomycin, and 10 mM HEPES buffered saline (Sigma-Aldrich)[330].

2.1.2 Cell Lines

THP1 cell lines were cultured and maintained in complete RPMI media at 37 °C and 5% CO_2. All the experiments performed with THP1 cell lines in this thesis used cells differentiated towards a macrophage-like phenotype. To do so, THP1 cell lines were plated at a concentration of 5 x 10^5 cells/mL in 6 or 12-well plates or at a concentration

of 2 x 10^4 cells/mL into chambered coverglasses in RPMI media with 50 nM phorbol 12-myristate 13-acetate (PMA, Sigma) for 16 h. Then, PMA-containing media was removed, cells were washed with Dulbecco's phosphate-buffered saline (PBS, Sigma-Aldrich) and rested for 24 h in RPMI complete media.

Wild type THP1 cells were from ATCC (TIB-202), THP1$^{nlrp3-/-}$ were a gift from Prof. Veit Hornung (Gene Centre Munich)[133]. EGFP-NLRP3-THP1$^{nlrp3-/-}$ and THP1$^{gsdmd-/-}$ cells were generated from THP1$^{nlrp3-/-}$ and wild type THP1 cells, respectively, as indicated below.

Human Embryonic Kidney (HEK) 293T cells were cultured in high-glucose DMEM (Sigma-Aldrich) supplemented with 10% FCS, and 1% Penicillin/Streptomycin at a concentration of 5 x 10^4 cells/mL.

2.2 Molecular Biology

2.2.1 Plasmid generation

2.2.1.1 Gateway system: eGFP-*nlrp3* plasmid generation

A lentiviral construct containing the gene coding for NLRP3 (*nlrp3*) tagged with enhanced green fluorescent protein (eGFP) in its N terminus was created using the commercial Gateway cloning system (Invitrogen). This system mimics the recombination method used by the lambda phage when it infects bacteria. This phage uses complementary attachment sites, called att sites, to recombine and integrate into the bacterial genome[331,332].

First, sites for recombination were added to the gene *nlrp3* by Polymerase Chain Reaction (PCR). The PCR running conditions were 35 cycles of 10 sec at 98 °C, 30 sec at 65 °C and 30 sec at 72 °C and the primers used to amplify the *nlrp3* sequence were flanked by recombination sequences called attB sites (Table 2.1 and Fig 2.1). The PCR product was run in a 1% agarose gel in Tris-Acetate-EDTA buffer pH 7.6 (2.42 g Tris-Base, 1 mL EDTA 0.5M pH 8.0, and 0.57 mL Glacial Acetic Acid in 500 mL dH_2O) and extracted from the gel using a commercial kit (Isolate II PCR and Gel Kit, Bioline) according to manufacturer's instructions. Following this, an entry clone with the *nlrp3* sequence was generated (Fig 2.1). To this end, the *nlrp3* sequence was shuttled to the gateway donor

plasmid pDONR/Zeo using the BP Clonase Reaction kit (Invitrogen). This process was achieved by recombination of the attB sequences of the *nlrp3* PCR product with attP sequences expressed in the donor plasmid (Fig 2.1 a). The result of the BP Clonase Reaction is the generation of an entry clone containing *nlrp3* flanked with new recombination sequences called attL sites (Fig 2.1 a). AttL sites can recombine with plasmids containing attR sequences. Once *nlrp3* was expressed in the entry clone, it was transferred to the lentiviral eGFP-containing destination vector, pLNT-UbC-eGFP-# using the LR Clonase Reaction kit (Invitrogen). This process was achieved by recombination of the attL sequences in the *nlrp3* entry clone with the attR sites of the destination vector, and it resulted in the production of a lentiviral plasmid containing *nlrp3* tagged with eGFP that was referred to as pLNT-UbC-eGFP-nlrp3 (Fig 2.1 b).

Primer	**attB flanking sequence**	**Primer sequence**
Forward	5'-GGGGACAAGTTTGTACAAAAAA GCAGGCTTCACC-3'	5'-GGGGACAAGTTTGTACAAAAAAGCAGG CTTCACCATGAAGATGGCAAGCACCCGC-3'
Reverse	5'-GGGGACCACTTTGTACAAGAAA GCTGGGTC3'	5'-GGGGACCACTTTGTACAAGAAAGCTGGG TCCTACCAAGAAGGCTCAAAGACGAC-3'

Table 2.1 Primers used to generate an attB-flanked *nlrp3* fragment.

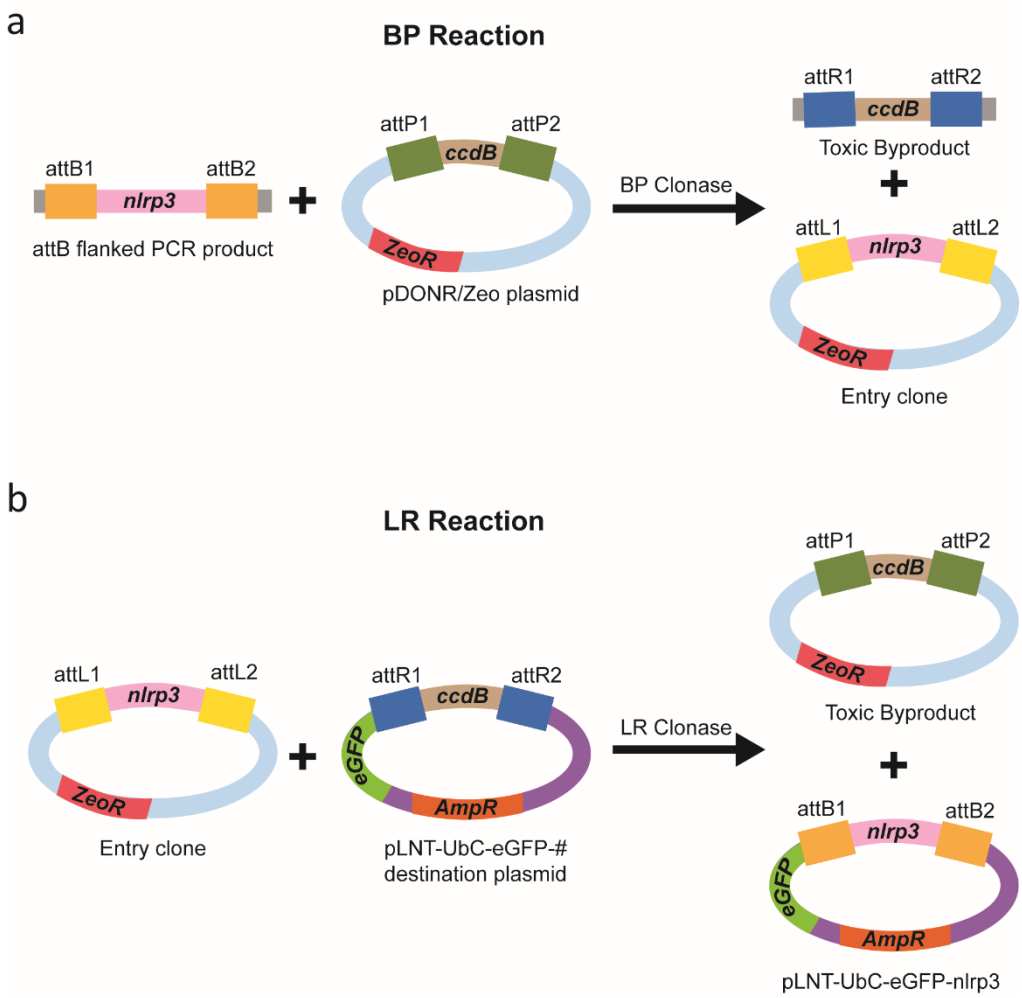

Figure 2.1 Gateway cloning system: BP and LR Clonase reactions. a) BP Clonase reaction: the attB-flanked *nlrp3* gene is inserted into the attP-containing donor plasmid by recombination of their attB and attP sites, resulting in the formation of a *nlrp3*-entry clone containing attL flanking sites. **b)** LR Clonase reaction: the attL-flanked *nlrp3* gene is shuttled to the attR-containing pLNT-UbC-eGFP-# destination plasmid by recombination of their attL and attR sites , leading to the production of pLNT-UbC-eGFP-nlrp3. Both, BP and LR clonase reactions lead to the formation of ccdB byproducts that are toxic when expressed in bacteria. Adapted from Addgene, 2017, accessed 18 May 2021, *https://blog.addgene.org/plasmids-101-gateway-cloning*

The used donor plasmid (Gateway pDONR/Zeo Vector) was purchased from Invitrogen and the destination vector pLNT-UbC-eGFP-# was generated by Dr Pawel Pazek[333] (University of Manchester).

For large-scale plasmid production, competent *Escherichia coli* DH5α (Invitrogen) were transformed with either the entry clone or pLNT-UbC-eGFP-nlrp3. These bacteria are sensitive to the gene ccdB, being incapable of growing when this gene is in their genome, meaning that the ccdB-containing byproducts of the BP and LP clonase

reactions are not produced. The donor plasmid and the pLNT-UbC-eGFP-# destination plasmid were grown into a ccdB-resistant *E. coli* strain (One Shot™ ccdB Survival™ 2 T1R Competent Cells, Invitrogen). It is important to highlight that the donor plasmid and entry clone have resistance genes to zeocin (ZeoR) and the pLNT-UbC-eGFP-# destination plasmid and eGFP-*nlrp3* plasmid to ampicillin (AmpR) (Fig 2. 1 a and b). Based on that, these antibiotics were used to select the bacteria producing these plasmids.

The plasmids were introduced into the bacteria by transformation. First, 2 µg of plasmid were mixed with 10^6 bacteria and kept on ice for 30 min. Bacteria were transformed at 42°C for 45 seconds and kept in ice for 2 min. Following this, they were cultured in 1 mL of SOC medium (Sigma-Aldrich) for 1 h at 32°C and 5% CO_2. After that, they were plated into Lysogeny Broth (LB) agar containing 50 ng/mL zeocin or 100 ng/mL ampicillin (UoM Media Stores) and cultured for 16 h at 32°C and 5% CO_2. Transformed *E. coli* colonies were cultured into 3 mL of liquid LB containing the same concentration of ampicillin or zeocin for 24 h. Following this, plasmids were isolated from bacteria using the QIAprep Spin Miniprep Kit (Qiagen).

2.2.1.2 CRISPR-Cas9: plasmid generation to knock out *gsdmd*

To knock out *gsdmd*, a CRISPR-Cas9 plasmid targeting *gsdmd* was generated using a protocol adapted from the one developed by Feng Zhang's lab[334]. The chosen RNA guides (gRNA) for *gsdmd* were previously used by Platnich *et al*[335].

First, 10 µM forward gsdmd gRNA and reverse gsdmd gRNA (Table 2.2) were annealed in 1X T4 Ligation Buffer (New England Biolabs or NEB) using 0.5 µL T4 PNK (NEB) at 37 °C for 30 min and incubated at 95 °C for 4 min to deactivate T4 PNK. Next, the annealed gRNAs were inserted into the LentiCRISPrv2 plasmid (#52961, Addgene). This was achieved incubating the annealed gRNAs with the plasmid in the presence of 1 µl BsmB1 digestion enzyme (Thermo Fisher) and 1 µl T4 DNA ligase (Promega) in 1X T4 Ligation Buffer containing 0.5 mM dithiothreitol (DTT, Sigma). This mix underwent 15 cycles of 37 °C for 5 min followed by 16 °C for 5 min, and the result was the generation of a lentiviral plasmid containing Cas9 and gRNAs to target gsdmd (LentiCRISPrv2-gsdmd).

gRNA	gRNA sequence
Forward	5'-CACCGACCAGCCTGCAGAGCTCCAC-3'
Reverse	5'-AAACGTGGAGCTCTGCAGGCTGGTC-3'

Table 2.2 RNA guided for *gsdmd*.

For large-scale production of the LentiCRISPrv2-gsdmd plasmid, the competent *E. coli* strain Stbl3 (Invitrogen) was used. These bacteria were transformed with 50 ng of the plasmid using the same protocol as that used for pLNT-UbC-eGFP-nlrp3 (Section 2.1.1.1). The LentiCRISPrv2-gsdmd plasmid has an AmpR gene. Thus, transformed bacteria were cultured in LB containing ampicillin. Finally, the LentiCRISPrv2-gsdmd plasmids were isolated from bacteria using the QIAprep Spin Miniprep Kit.

2.2.2 Production of lentiviral particles

HEK 293T cells were transfected with pLNT-UbC-eGFP-nlrp3 or LentiCRISPrv2-gsdmd plasmids to generate lentiviral particles containing these constructs. To do this, 6 x 10^5 cells/well were plated in 6-well culture plates in DMEM media and incubated for 24 h at 37 °C and 5% CO_2. Following this, the cells in each well were transfected with 1.5 µg pLNT-UbC-eGFP-nlrp3 or LentiCRISPrv2-gsdmd plasmid, 1.2 µg of the virus envelope expressing plasmid pMD2.G (Addgene, #12259) and 0.4 µg of the lentivirus packaging plasmid pPAX2 (Addgene, #12260) previously incubated with 9 µg/mL polyethylenimine (PEI MAX 40K, Polysciences) for 15 min at room temperature. Transfected HEK cells were incubated for 16 h at 37 °C and 5% CO_2. After this, media was replaced, and cells were incubated under the same conditions for 48 h. Finally, cell supernatants, containing pLNT-UbC-eGFP-nlrp3 or LentiCRISPrv2-gsdmd lentiviral particles, were collected and filtered through a 0.45 µM filters to remove any floating cells.

2.2.3 THP1 transduction

To generate a THP1 cell line endogenously expressing eGFP-nlrp3 or a $THP1^{gsdmd-/-}$ cell line, $THP1^{nlrp3-/-}$ cells were transduced with pLNT-UbC-eGFP-nlrp3 lentiviral particles and wild type THP1 cells with LentiCRISPrv2-gsdmd lentiviral particles. To this end, 5 x 10^4 cells were transduced with 1 mL of lentiviral particle-containing cell supernatant and 8 µg/mL polybrene and centrifuged at 1000 g and 30 °C for 1 h. Then, transduced THP1 cells were resuspended in complete RPMI media and incubated at 37 °C for 72 h. Importantly, the LentiCRISPrv2-gsdmd has a puromycin resistance gene that confers resistance to this antibiotic to mammalian cells. Thus, THP1 cells transduced with LentiCRISPrv2-gsdmd lentiviral particles were selected using 100 ng/mL puromycin (Sigma). From this moment, $THP1^{nlrp3-/-}$ cells transduced with pLNT-UbC-eGFP-nlrp3 were referred to as eGFP-NLRP3-$THP1^{nlrp3-/-}$, and wild type THP1 cells transduced with LentiCRISPrv2-gsdmd lentiviral particles as to $THP1^{gsdmd-/-}$.

2.3 Antibodies, proteins, and other reagents

2.3.1 Antibodies

2.3.1.1 Flow cytometry

Antibodies (Abs) used to stain cells for flow cytometry are indicated in Table 2.3. All Abs used for flow cytometry were used at a concentration of 2 µg/mL.

Abs against	Clone	Isotype	Fluorophore	Supplier
CD16	3G8	Mouse IgG1	BV421	BioLegend
CD86	IT2.2	Mouse IgG2b	PE	BioLegend
CD206	19.2	Mouse IgG1	FITC	BD
Isotype control	MOPC-21	Mouse IgG1	BV421	BioLegend
Isotype control	MPC-11	Mouse IgG2b	PE	BioLegend
Isotype control	G18-145	Mouse IgG1	FITC	BD

Table 2.3 Flow cytometry antibodies.

2.3.1.2 Immunoblots

Primary Abs used for immunoblotting are listed below (Table 2.4).

Abs against	Clone	Isotype	Concentration	Supplier
Caspase 1	D7F10	Rabbit IgG	1:1000	Cell Signalling Technologies
Caspase 4	4B9	Mouse IgG1	0.4 µg/mL	SantaCruz Biotechnology
Caspase-5	D3G4W	Rabbit IgG	1:500	Cell Signalling Technologies
GSDMD (CT)	Polyclonal	Rabbit IgG	1 µg/mL	Proteintech
GSDMD (NT)	Polyclonal	Rabbit IgG	0.4 µg/mL	Novus Biologicals
IL-1β	Polyclonal	Goat IgG	0.1 µg/mL	R&D Systems
NLRP3	Cryo-2	Mouse IgG2b	1 µg/mL	Adipogen
B-actin (HRP-conjugated)	AC-15	Mouse IgG1	0.13 µg/mL	Sigma

Table 2.4 Primary antibodies used for immunoblots.

The secondary Abs used for immunoblotting were conjugated to HRP and are listed in Table 2.5.

Abs against	Clone	Isotype	Concentration	Supplier
Rabbit IgG	Polyclonal	Goat IgG	1:3000	Bio-Rad
Mouse IgG	Polyclonal	Goat IgG	1:3000	Bio-Rad
Goat IgG	Polyclonal	Rabbit IgG	0.13 µg/mL	Sigma

Table 2.5 Secondary antibodies used for immunoblots.

2.3.1.3 Microscopy

The primary Abs used to stain cells for imaging are indicated below (Table 2.6).

Abs against	Clone	Isotype	Concentration	Supplier
GSDMD (NT)	EPR20829-408	Rabbit IgG	4 µg/mL	Abcam
ASC	O93E9	Mouse IgG1	2 µg/mL	Biolegend
TCC	aE11	Mouse IgG2a	5 µg/mL	Abcam
EEA1	C45B10	Rabbit IgG	1:200	Cell Signalling Technology
NIK	Polyclonal	Rabbit IgG	1:200	Cell Signalling Technology
NF-κB p52	C-5	Mouse IgG2a	2 µg/mL	SantaCruz Biotechnology
RelB	D-4	Mouse IgG1	2 µg/mL	SantaCruz Biotechnology
TGN46	Polyclonal	Sheep IgG	1.25 µg/mL	Bio-Rad
LC3B	Polyclonal	Rabbit IgG	1:200	Cell Signalling Technology
PCN	Polyclonal	Rabbit IgG	1 µg/mL	Abcam

Table 2.6 Primary antibodies used for microscopy.

The secondary Abs used for microscopy in this thesis are listed in table 2.7.

Abs against	Clone	Isotype	Fluorophore	Concentration	Supplier
Mouse IgG1	Polyclonal	Goat IgG	AF 647	2 µg/mL	Invitrogen
Mouse IgG1	Polyclonal	Goat IgG	AF 568	2 µg/mL	Invitrogen
Mouse IgG1	Polyclonal	Goat IgG	AF 488	2 µg/mL	Invitrogen
Mouse IgG2a	Polyclonal	Goat IgG	AF 488	2 µg/mL	Invitrogen
Rabbit IgG	Polyclonal	Goat IgG	AF 488	2 µg/mL	Invitrogen
Sheep IgG	Polyclonal	Donkey IgG	AF 488	2 µg/mL	Abcam

Table 2.7 Secondary antibodies used for microscopy.

Additionally, in chapter 3, wheat germ agglutinin conjugated to Alexa Fluor 488 (WGA-AF488, Thermo Fisher Scientific) was used at a concentration of 2 µg/mL to stain the cell membrane in THP1 cells.

2.3.1.4 Human proteins

The human purified complement components listed below were used in this thesis (Table 2.8). All proteins were endotoxin-free.

Name	Concentration	Supplier
C5a	0.01-2 µg/mL	Complement Technologies
C5b6	1-20 µg/mL	Complement Technologies
C7	10 µg/mL	Complement Technologies
C8	10 µg/mL	Complement Technologies
C9	10 µg/mL	Complement Technologies

Table 2.8 Purified complement proteins

2.3.1.4.1. Fluorescent labelling of C9

For all imaging experiments C9 was labelled with Alexa Fluor 647 (AF647) or with Janelia Fluor 549 (JF549). This was achieved by conjugating C9 to AF647 N-hydroxysuccinimide (NHS) ester (Thermo Fisher Scientific) or to JF549 NHS ester (Tocris). To this end, 50 µl of C9 (1 mg/mL) were mixed with 5 µl of JF549 or AF 647 NHS ester (1 mg/mL) in 100 µM $NaHCO_3$ in PBS and incubated for 1 h on a rotator in the dark at room temperature. During this time, the dye binds to C9 by forming stable amino bonds between the NHS ester attached to the fluorophore and amine residues in C9. Then, the excess dye was removed using size-exclusion chromatography (7K MWCO Zeba™ Spin Desalting Column Thermo Scientific) by centrifugation at 1500 g for 2 min. The final protein concentration and degree of labelling (DOL) were measured by absorption using a NanoDrop 200 spectrophotometer (ThermoFisher Scientific) and calculated using the equation below (Fig 2.2).

$$\boldsymbol{Moles\ of\ dye\ per\ mole\ of\ protein} = \frac{\boldsymbol{A_{max}\ x\ \varepsilon_{protein}}}{\boldsymbol{\varepsilon_{max}\ (A_{280}\ -\ A_{max}\ x\ C_{280})}}$$

Figure 2.2 Degree of labelling (DOL).

In this equation, A_{max} is the absorption of the fluorophore at its maximum absorption wavelength (549 nm for JF549 and 651 nm for AF647), $\varepsilon_{protein}$ is the molar extinction coefficient of the conjugated protein at 280 nm (98800 $cm^{-1}M^{-1}$ for C9), ε_{max} is the molar extinction coefficient of the dye at its maximum wavelength (101000 $cm^{-1}M^{-1}$ for JF549 and 270000 $cm^{-1}M^{-1}$ for AF647), A_{280} is the absorbance of the protein at 280 nm, and C_{280} is a correction factor to account for the absorbance of the used fluorophore at 280 nm (0.169 for JF549 and 0.03 for AF647). All the conjugated C9-JF549 had a DOL between 1.2 and 2.3 and all the C9-AF647 had a DOL between 4.1 and 5.5.

2.4 Functional Assays

2.4.1 Membrane attack complex formation

To form the Membrane Attack Complex (MAC), cells were washed with PBS and treated with 10 µg/mL anti-CD59 mAb (BRIC 229, mouse IgG2b, IBGRL) and 10 µg/mL C5b6, unless otherwise specified, for 15 min in serum-free RPMI media. Then the media was removed, and cells were stimulated with 10 µg/mL C7, 10 µg/mL C8 and 10 µg/mL C9 for the indicated time in serum-free RPMI media. Alternatively, cells were treated with isotype control for anti-CD59 mAb, and vehicle controls for complement proteins.

2.4.2 Inflammasome activation

For inflammasome activation, MDMs or THP1 cells were primed with 1 µg/mL LPS in RPMI complete media for 3 h or 4 h, washed with serum free RPMI media, and treated with 10 µM nigericin for 45 min, unless otherwise specified, or with the MAC for the indicated time in serum free RPMI media. These concentrations were used unless otherwise specified.

The following reagents were used during inflammasome activation assays (Table 2.9). Alternatively, cells were treated with the indicated matched vehicle. All incubations were made at 37 °C and 5% CO_2, and all inhibitors were used 30 min before and during nigericin or MAC treatment, unless otherwise stated, in serum-free RPMI media.

Name	Function	Concentration	Vehicle	Supplier
Lipopolysaccharide from *E. coli* O26:B6 (LPS)	TLR4 activator	0.12-1 µg/mL	PBS	Sigma
Nigericin (Nig)	NLRP3 activator	1.25-20 µM	Ethanol	Sigma
Glycine	Membrane rupture blocker	10 µM	PBS	Sigma
Necrosulfonamide (NSA)	GSDMD inhibitor	10-20 µM	DMSO	Calbiochem
MCC950	NLRP3 inhibitor	10 µM	DMSO	Pepreotech
Nystatin (Nys)	Endocytosis inhibitor	0.1-10 µg/mL	DMSO	Merck
Cytochalasin D (Cyt)	Endocytosis inhibitor	5-20 µM	DMSO	Merck
Dynasore (Dyn)	Endocytosis inhibitor	10-160 µM	DMSO	Calbiochem
NIK SMI-1	NIK inhibitor	0.1-10 µM	DMSO	MedChemExpress

Table 2.9 Other reagents.

2.4.3 Flow cytometry

Cells were detached from the culture plates using Enzyme-free dissociation buffer (Gibco), washed with PBS and plated in 96 well V-bottom plates (Greiner CELLSTAR® 96 well plates, Sigma-Aldrich) at a concentration of 2.5 x 10^5 cells/well. They were spun down at 500 *g* for 5 min at 4°C and resuspended in 100 µl PBS containing 0.5 µl Zombie Aqua dye (Biolegend) for 30 min at 4°C. Plates were centrifuged under the same conditions, supernatants were removed, and cells were blocked in 50 µl Human AB serum (Invitrogen). The primary Ab mix or the isotype control mix (Table 2.3) was added in 100 µl FACS buffer (0.5% FCS in PBS), and cells were incubated for 30 min at 4°C. Cells were then washed with 200 µl FACS buffer and fixed in 100 µl 4% Paraformaldehyde (16% PFA, Thermo Fisher Scientific) in FACs buffer for 20 min. Plates were spun down as before, resuspended in 200 µl FACS buffer and transferred to tubes. Samples were studied using the BD FACS CANTO cytometer and cell markers expression was analysed using FlowJo V10.

2.4.4 Enzyme-linked immunosorbent assay (ELISA)

Cytokine release was measured in cell supernatants using the Human IL-1β or IL-18 DuoSet ELISA kit (R&D) following manufacturer's instructions. In brief, ELISA plates (Maxisorb, NUNC) were coated with capture Ab in PBS at room temperature overnight. Then, plates were washed with 0.05% Tween 20 (Sigma) in PBS three times and blocked for 1 h with blocking buffer (1% BSA in PBS). Plates were then washed as indicated before and incubated with the samples, previously diluted in blocking buffer, for 2 h. To generate a standard curve for protein concentration, recombinant protein provided in each ELISA kit was sequentially diluted and added to the plate. After 2 h, plates were washed as before and incubated with the detection Ab in blocking buffer for 2 h. Plates were washed again and incubated with Streptavidin-HRP Ab in blocking buffer for 20 min in the dark. Then, plates were washed as before, and TMB ELISA substrate solution (Sigma-Aldrich) was added for 20 min in the dark. To stop the reaction 1 N H_2SO_4 (Sigma-Aldrich) was added to the plates.

The amount of MAC, also known as terminal complement complex (TCC), was measured in cell lysates using a human TCC ELISA kit (HycultBiotech) following manufacturer's instructions. Briefly, cells were lysed in RIPA buffer (50mM Tris-HCl pH 7.4, 1% NP-40, 0.25%Na-deoxycholate, 150 mM NaCl and 1 mM EDTA in miliQ dH_2O) supplemented with protease inhibitors (Protease Inhibitor Cocktail Set 1, Calbiotech) for 30 min on ice. Lysates were centrifuge at 17000 g for 15 min at 4˚C to eliminate the insoluble fraction. Then, the ELISA assay was performed. The TCC ELISA kit provided all reagents necessary for the assay. First, cell lysates were transferred to the ELISA plate provided by the kit (pre-coated with capture Ab). A standard curve for protein concentration, prepared by serial dilution of recombinant protein provided in the ELISA kit, was also added to the plate. ELISA plates were incubated 1 h and washed with wash buffer 4 times. After this, diluted tracer was added to the wells and incubated for 1 h. Plates were washed as before and incubated with Streptavidin-HRP Ab in wash buffer for 1h in the dark. After a final wash, the last step was to add TMB to the plate, incubate for 30 min in the dark and stop the reaction with stop solution.

All incubations for ELISA assays were performed at room temperature. In the IL-1β and IL-18 ELISAs, 50 µl/well were used, and in the TCC ELISAs 100 µl/well were used in every step.

After stopping the TMB reaction, the absorbance of each well was measured with a plate reader at 450 nm with a reference line of 570 nm, and the concentration of each sample was calculated by interpolating from the generated standard curves.

2.4.5 Cell Death quantification

Lytic cell death was established by measuring lactate dehydrogenase (LDH) release in cell supernatants using the CytoTox96® Non-Radioactive Cytotoxicity Assay (Promega) following the manufacturer's instructions. In short, 50 µL of CytoTox96® reagent were incubated with 50 µl of sample in a transparent flat bottom 96-well plate and incubated in the dark until a change in colour appeared. Then, the reaction was stopped with CytoTox 96® stop solution, and plates were read at 490 nm using a plate reader. Results were expressed as cell death percentage (LDH release percentage) relative to total cells death or as fold increase relative to vehicle-only treated cells.

2.4.6 Caspase 1 activity assay

The activity of caspase 1 was assessed using a quantitative luminescence assay (Caspase-Glo® 1 Inflammasome kit, Promega). In brief, cell supernatants were combined with the aminoluciferin substrate Z-WEHD for 1 h at room temperature in the dark, and then luminescence was measured. Results were expressed as fold-increase relative to vehicle-only treated cells.

2.4.7 Immunoblots

2.4.7.1 Sample preparation and protein quantification

Cells were lysed in RIPA buffer supplemented with protease inhibitors and centrifuged to eliminate the insoluble fraction as previously described (Section 2.4.4). Supernatants were collected for protein quantification and further analysis. Protein concentration was determined using a Bicinchoninic Acid Protein Assay (Pierce™ BCA Protein Assay Kit, Life Technologies) following the manufacturer's instructions. In brief,

samples were diluted 5 times in RIPA buffer and added to a transparent flat bottom 96-well plate. A standard curve of Bovine Serum Albumin (BSA) was also generated and added to the plate. Then, BCA reagent mix was added, and the plate was incubated for 30 min at 37°C. After this, absorbance from each sample was read at 562 nm and sample concentration was calculated based on the standard curve. Finally, cell lysates were diluted to an equal protein amount of 30 µg per sample.

Cell supernatants were centrifuged at 500 g for 5 min to remove cell debris and concentrated using centrifugal cellulose filters (10 kDa MW Amicon centrifugal filter devices, Merck Millipore), as indicated by the manufacturer. Briefly, up to 500 µl of cell supernatants were loaded into the cellulose filters and spun down for 30 min at 14000 g and 4°C. Then the filters were inverted, inserted in a clean tube, and centrifuged at 1000 g for 2 min to collect the concentrated sample.

Cell lysates or cell supernatants were diluted to 1x reducing Laemmli buffer (6x Laemmli buffer: 1.2 g SDS, 6mg Bromophenol Blue, 4,7 mL Glycerol, 1.2 mL 0.5M Tris pH 6.8 in 2.1 mL MiliQ dH_2O) containing 10 mM 1,4-Dithiothreitol (Sigma) and heated at 95°C for 10 min.

2.4.7.2 Electrophoresis

Samples were loaded into 4-12% Bis-Tris NuPAGE gels (Invitrogen) and underwent electrophoresis in NuPAGE MES buffer (Invitrogen) at 165 V for 35 min. A protein size ladder (Colour Protein Standard P7712 or P7719S, NEB or Precision Plus Protein™ All Blue, Bio-Rad) was also loaded into the gel for molecular weight references.

2.4.7.3 Transfer and protein detection

Proteins were transfer to 0.2 µm PVDF membranes (GE Healthcare) at 15 V for 25 min using the Bolt Western Blot system (Bio-Rad). Membranes were blocked with 5% Bovine Serum Albumin (BSA, Sigma) in TBST (10mM Tris-HCl, 15mM NaCl, 0.05% Tween® 20 at pH 7.5) for 1 h at room temperature in a roller, washed three times with TBST and incubated with the appropriate primary Ab (Table 2.4) in 5% BSA overnight at 4°C. Then, membranes were washed as before and incubated for 1 h at room temperature with HRP-linked secondary Ab (Table 2.5). Finally, membranes were washed and developed

using the Clarity Western ECL Substrate (Bio-Rad) and protein bands were visualized using a ChemiDoc™ MP Imager (Bio-Rad).

To identify β-actin, membranes were washed and incubated with anti-β-actin-HRP Ab for 20 min at room temperature, washed, developed, and visualized as before.

2.5 Microscopy

2.5.1 Sample preparation

For microscopy studies, monocytes or THP1 cells were directly differentiated to macrophage-like cells into chambered coverglasses as previously explained (Section 2.1.1 and 2.1.2). After cell stimulation was finalized, samples were fixed with 4% PFA in PBS for 15 min and washed three times with PBS. When cell membrane was stained, cells were incubated with WGA-AF488 in PBS for 20 min and washed as before. Samples were blocked and permeabilized with 2% BSA and 0.1% Triton X-100 (Sigma-Aldrich) in PBS for 30 min. Samples were then stained with the appropriate primary antibody at the indicated concentration (Table 2.5) in 2% BSA in PBS overnight at 4˚C. After that, cells were washed as before, and matched secondary antibodies at the indicated concentration (Table 2.6) were added for 1 h in 2% BSA in PBS. Samples underwent a final washing step with PBS before being imaged using confocal microscopy, total internal reflection fluorescence (TIRF) microscopy or stochastic optical reconstruction microscopy (STORM). All incubations were performed in the dark and at room temperature, unless otherwise specified.

2.5.2 Confocal microscopy

Confocal imaging was carried out with the inverted confocal microscope Leica TCS SP8 (Leica Microsystems) using a 100X/1.40NA oil-immersion objective, a 63X/1.20NA oil-immersion objective or a 20X/0.75NA air-objective. Excitation was performed with a pulsed white-light laser and emission was detected using time-gated HyD detectors functioning in standard mode. All images were acquired at room temperature. Images were exported and analysed using ImageJ[336]. When required, nuclei and cell outlines were identified manually using brightfield images.

2.5.2.1 Co-localisation analysis

To determine the level of colocalisation between 2 images or the same region of interest (ROI) in 2 images, the ImageJ (FIJI version) plugin Coloc2 was used. This plugin was used to calculate the Pearson's correlation coefficient (Pearson's R) between the selected images or ROIs.

2.5.3 TIRF and STORM microscopy

TIRF and STORM imaging was performed with the inverted microscope TCS SP8 STED CW (Leica Microsystems) using a 160X/1.43NA oil-immersion objective and an Andor iXon Ultra 897 EMCCD camera. For TIRF imaging, at the beginning of every session TIRF auto-alignment was performed and this process was repeated every 2 h. TIRF illumination with a penetration depth of ≈150 nm was used, images were illuminated for 150 ms and the electron multiplying (EM) gain was set to 120. For STORM, freshly made STORM buffer (400 µg/mL glucose oxidase, 40 µg/mL catalase, 50 mM Tris-HCl, 10 mM NaCl, 10% glucose and 1% β-mercaptoethanol in dH_20, pH 8 and 0.22 µm sterile-filter) was added to the samples before acquisition. The 642 nm continuous wave laser (2.1 kW/cm^2) at a 35 % of its maximum power was used to illuminate the samples. For every picture, 1 x 10^4 frames were acquired with TIRF illumination and images were illuminated for 11 ms and an EM gain of 120 nm was used.

2.5.3.1 STORM data processing and analysis

Super-resolution images were reconstructed from the 1 x 10^4 frames per image acquired with STORM using the ImageJ plug-in ThunderSTORM[337]. First, to eliminate noise and ameliorate the quality of event recognition, raw images were filtered. For this, a wavelet transformation, applying a convolution kernel with B-spline basis function of the third order with a scaling factor of 2[337], was used. The local intensity maxima method was applied to obtain the approximate position of the detected events. To do so, the intensity of every pixel in the image is compared with an intensity threshold, set up to three times the standard deviation of the intensity values from the first wavelet level F1, and with the intensity of the values within its 8-connected neighbourhood.

A point spread function (PSF) integrated Gaussian method, which is been described as the most accurate method to give a good approximation of the real PSF of

a microscope taking into account the use of a digital camera[338–340], was used to determine the sub-pixel localisation of each detected molecule. A fitting radius of 5 pixels was used. To obtain the coordinates (x, y) of each molecule, the least squares fitting method was used with an initial sigma (standard deviation of the Gaussian distribution) of 1.6 pixels. Then, images were filtered to remove noise molecules. To do so, intensity was set to >1000 photons, sigma to >50 nm and <170 nm, and uncertainty (uncertainty of localisation resulting from photon counting and background noise) to <30 nm, meaning that molecules that did not fit into those parameters were removed from the image. Finally, events within a maximum distance of 50 nm and 20 off frames were considered to have been originated from the same fluorophore and, therefore, they were combined to generate the final image.

2.6 Statistical analysis

Every data set of this thesis was analysed and graphically represented using Graphpad Prism v9. First, the normality of the data was analysed by the Shapiro-Wilk normality test. Normally distributed results were analysed by parametrical tests. When one or more of the analysed groups in the dataset were non-normally distributed, non-parametrical tests were used. The statistical significance of differences between two groups was analysed by paired two-tailed t-test. Statistical significance between more than two groups was evaluated using one-way ANOVA in normally distributed data and using Friedman test for matched values or Kruskal-Wallis for non-matched values in non-normally distributed results. Results were expressed as the mean ± standard deviation (SD) and significant differences between samples were established as $p<0.05$ (*), $p<0.01$(**), $p<0.001$ (***), and $p<0.0001$ (****).

Chapter 3 Role of GSDMD in IL-1β and IL-18 secretion in human macrophages

3.1 Introduction

Blood monocytes differentiate into macrophages with different phenotypes depending on the tissue environment. Traditionally, blood monocyte-derived macrophages (MDMs) are classified using a simplistic approach into two major groups: the classically activated macrophages (M1) that promote Th1 immune responses by producing pro-inflammatory cytokines, reactive oxygen and nitrogen species, and by mediating resistance to pathogens and, the alternatively activated macrophages (M2), considered regulatory cells involved in tissue remodelling, immune regulation and phagocytosis[13,16,17]. M1 macrophages are known to express high levels of CD86, whereas M2 macrophages have higher expression of CD206. CD16 is known to be expressed in both phenotypes, however its expression is higher in M2 macrophages[22,42]. It is important to highlight that this classification reflects macrophage phenotypes specific of extreme conditions. Thus, multiple intermediate macrophage populations exist and due to their heterogeneous morphology, transcriptional profile, function, and location, it is difficult to establish a simple robust classification for this cell type [13,17].

Upon recognition of pathogens and tissue stress, macrophages activate different signalling pathways that result in the activation and/or upregulation of multiple processes including the assembly of multiprotein complexes called inflammasomes[52]. Inflammasome activation triggers the processing and release of interleukin (IL-)1β and IL-18, contributing to the recruitment and the activation of other immune cells[53]. IL-1β and IL-18 are pro-inflammatory cytokines with essential roles in inflammation. However, when dysregulated they are responsible for the pathology and worsening of several inflammatory diseases including toxic shock syndrome, rheumatoid arthritis, and type II diabetes[76,176]. For this reason, the production of the active forms of these cytokines is tightly regulated by inflammasomes[55].

One of the best studied inflammasomes is the NOD-like receptor pyrin domain-containing protein 3 (NLRP3) inflammasome that is canonically activated upon detection of two consecutive stimuli such as LPS followed by the pore forming toxin nigericin. This leads to oligomerization of the NLRP3 inflammasome. Within this complex, caspase 1 is activated and processes the pro-forms of IL-1β and IL-18 into their active, mature forms to be released from the cell[341]. Inflammasome activation also leads to pyroptosis, a specific type of programmed lytic cell death, resulting in membrane rupture and release of the cytoplasm content to drive the immune response forward[342].

While the processing of IL-1β and IL-18 has been widely studied, how these cytokines are secreted from the cell is not fully understood. It has long been known that these cytokines lack the amino-terminal signal peptide for endoplasmic reticulum (ER) recognition that is present in proteins that are released through the ER-Golgi-exocytosis 'conventional' protein pathway[192], indicating an alternative pathway for their release. In fact, IL-1β secretion in monocytes is not inhibited when the ER to Golgi transport is impaired[195]. Moreover, IL-1β and IL-18 are translated onto cytoskeleton-associated polyribosomes instead of those associated with the ER[193], further demonstrating that these proteins are not conventionally synthesised and secreted. As such, it is concluded that this family of cytokines has an alternative secretion pathway.

Gasdermin D (GSDMD) is a pore forming protein recognized and processed by inflammatory caspases. GSDMD pore formation is autoinhibited by the binding of its C-terminus (CT) subunit to its N-terminus (NT) pore-forming subunit. When GSDMD is cleaved by caspase 1, the NT-GSDMD is released from the CT-GSDMD. As a result, multiple NT-GSDMD proteins oligomerize in the cell membrane, forming lytic pores that are big enough for IL-1β and IL-18 to pass through[201]. The formation of GSDMD pores also results in membrane rupture and pyroptosis leading to the emptying of the cytoplasmic contect[81,156,201].

3.2 Aims and objectives

The production of active IL-1β and IL-18 following NLRP3 inflammasome activation has been studied widely. However, how these cytokines are released from the cell has just recently become a focus of study. GSDMD represents a potential candidate to mediate IL-1β and IL-18 secretion, since the same inflammatory caspases that cleave these cytokines into their mature forms are responsible for GSDMD processing to allow pore formation. It has been suggested that IL-1β and IL-18 may be released following membrane rupture due to pyroptosis. However, blockade of membrane rupture does not impair the secretion of these cytokines in murine macrophages or MDMs and ablation of GSDMD considerably reduces IL-1β release in mice[201,328], suggesting that GSDMD is involved in its secretion. In primary human macrophages, the role of GSDMD in the secretion of IL-1β and IL-18 has not been directly studied. Studying the role of GSDMD in this process in human macrophages is important since this cell type is one of the main sources of IL-1β and IL-18, and GSDMD could become a potential druggable target for diseases mediated by these cytokines. Thus, the main aim of this chapter was to determine whether or not GSDMD in involved in IL-1β and IL-18 secretion in human macrophages.

The specific objectives of this chapter were as follows:

1. To establish the optimal culture conditions of human monocyte-derived-macrophages for inflammasome activation.
2. To optimize the concentrations of LPS and nigericin needed for NLRP3 inflammasome activation and GSDMD processing in human macrophages.
3. To determine if cell membrane rupture is required for IL-1β and IL-18 secretion in human macrophages.
4. To study whether or not GSDMD is directly involved in IL-1β and IL-18 secretion in human macrophages.
5. To investigate whether GSDMD is trafficked to the cell membrane to form pores upon inflammasome activation in human macrophages.

3.3 Results

3.3.1 Establishing monocyte derived macrophages culture conditions for inflammasome activation

There are multiple phenotypes of macrophages, and various protocols for their differentiation from blood monocytes. Consequently, early experiments used two different methods to obtain MDMs and studied their differences in response to inflammasome activation. CD14+ monocytes were isolated using magnetic separation from blood PBMCs. CD14+ cells were cultured at a concentration of 5 x 10^5 cells/mL for 6 days in RPMI with 50 ng/mL macrophage colony-stimulating factor (referred to as M-CSF MDMs), or for 2 days in X-VIVO medium with 1 % human serum (HS) followed by 4 days in DMEM (referred to as HS MDMs). The resulting cells (MDMs) were detached from the culture plate using enzyme-free cell dissociation buffer and characterized using flow cytometry. MDMs were first gated on live and single cells (Fig 3.1 a), where cell survival was significantly higher in cells differentiated using M-CSF (Fig 3.1 b). Then, the surface receptors CD16, CD86 and CD206 were analysed to study the phenotype of M-CSF or HS MDMs (Fig 3.1 c). CD16 is an Fc receptor involved in Ab-mediated phagocytosis[343,344]. This marker was expressed by 55.5 ± 20.5 % of M-CSF MDMs whereas only 4.4 ± 2.9 % of HS MDMs expressed it (Fig 3.1 d). Furthermore, CD16 expression was higher in M-CSF MDMs (Fig 3.1 e) suggesting that these cells have a more regulatory phenotype than HS MDMs. CD86 is constitutively expressed in macrophages[22]. Indeed, more than 70 % of both M-CSF and HS MDMs expressed this marker (Fig 3.1 d), though its expression was significantly higher in HS MDMs (Fig 3.1 e). CD206 is a mannose receptor involved in phagocytosis and resolution of inflammation that is expressed in macrophages with a regulatory phenotype[345]. This receptor was present on 43.6 ± 13.1 % of M-CSF MDMs and 10.2 ± 12.2% in HS MDMs (Fig 3.1 d), and its expression was very low in both cases (Fig 3.1 e). Considering that the percentage of cells expressing CD206 and CD16 was higher in M-CSF MDMs, we established that the phenotype of these cells was more regulatory or anti-inflammatory than that of HS MDMs.

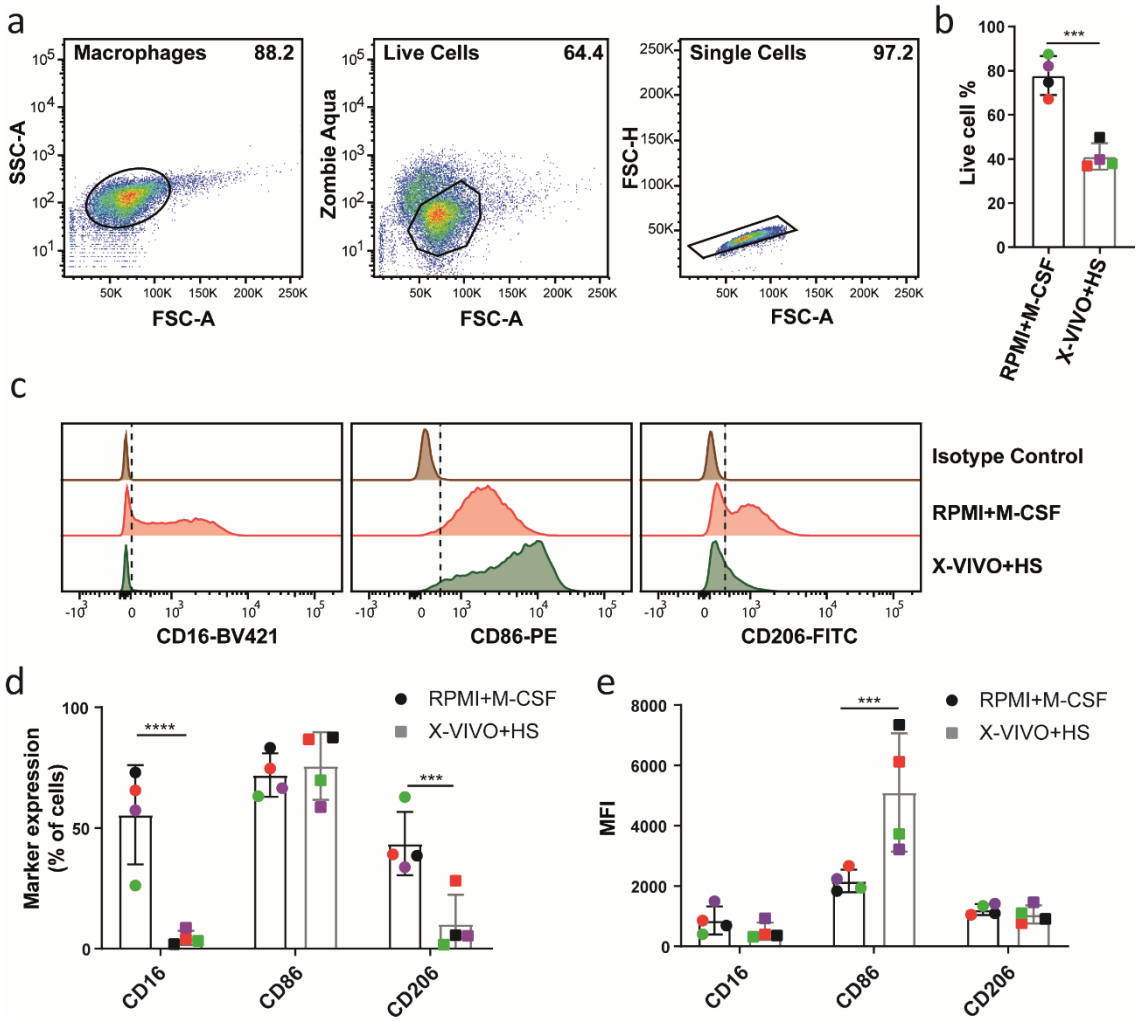

Figure 3.1 Flow cytometry analysis of human MDMs. Monocytes were differentiated with RPMI medium and 50 ng/mL of M-CSF (RPMI+M-CSF) for 6 days, or X-VIVO medium and 1% HS for 2 days followed by culture in DMEM medium for 4 days (X-VIVO+HS). **a)** Representative gating strategy for the selection of macrophages and exclusion of doublets. **b)** Percentage of live cells upon detachment from the culture plate. **c)** Representative histograms of the level of expression of CD16, CD86 and CD206. **d)** Percentage of macrophages expressing CD16, CD86 and CD206. **e)** Mean Fluorescence intensity (MFI) for CD16, CD86 and CD206 expression. In b, d and e data is plotted as mean ± SD, statistical significance was established by paired t-test (b) or one-way ANOVA (d, e) (***p<0.001, ****p<0.0001) and each colour represents a matched single donor. a-e) Data is representative of 4 independent experiments.

This project aimed to study different aspects of NLRP3 inflammasome activation in MDMs. Thus, we stimulated both M-CSF MDMs and HS MDMs for NLRP3 inflammasome activation using 1 μg/mL LPS for 4 h followed by 10 μM nigericin for 45 min (Fig 3.2), as previously described for NLRP3 inflammasome activation in human macrophages[329,346]. The secretion of IL-1β in supernatants was measured using an ELISA assay detecting mature IL-1β and cell death was quantified as a percentage of LDH release into the media. In both cases, we detected inflammasome activation, as evidenced by the release of IL-1β and LDH (Fig 3.2 a and b). However, despite the differences observed between donors due to biological variability[328,347], the amount of IL-1β secreted was increased in M-CSF MDMs, 3870 ± 1870 pg/mL vs 722 ± 772 pg/mL in HS MDMs. The focus of this chapter was to study the role that GSDMD plays in cytokine secretion. Therefore, GSDMD processing was examined in cell lysates by immunoblotting. Full GSDMD (GSDMD) was equally detected in both types of MDMs (Fig 3.2 c). However, GSDMD cleavage (CT-GSDMD) was only detected in samples from M-CSF MDMs (Fig 3.2 c) indicating a greater activation of the inflammasome in M-CSF MDMs. Altogether, the greater levels of IL-1β release and of GSDMD processing indicate a stronger activation of the inflammasome in M-CSF MDMs.

Given the fact that the phenotype of unstimulated M-CSF MDMs is less pro-inflammatory and that inflammasome activation is greater when MDMs are differentiated in this way, all further experiments were carried out with MDMs treated with 50 ng/mL M-CSF for 6 days in RPMI, which will now be referred to as MDMs.

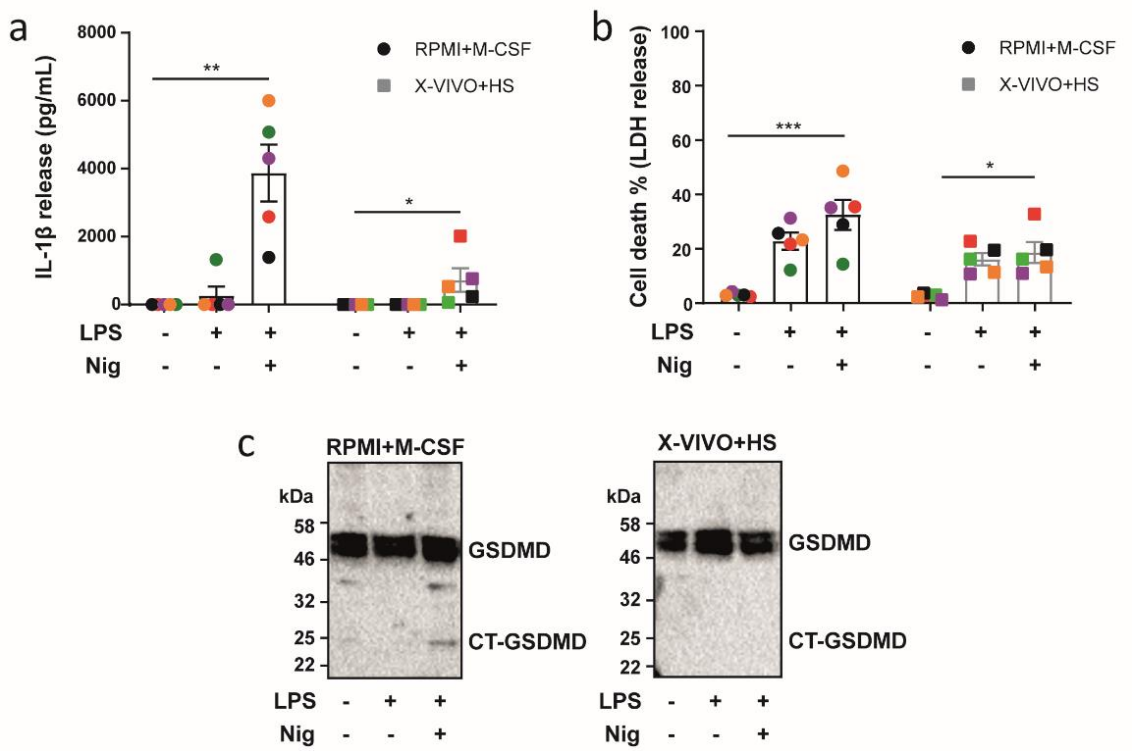

Figure 3.2 Optimization of human macrophage differentiation for the study of the NLRP3 inflammasome. Monocytes were differentiated to macrophages (MDMs) with RPMI media and 50 ng/mL of M-CSF (RPMI+M-CSF) for 6 days or X-VIVO media and 1% human serum for 2 days followed by culture in DMEM medium for 4 days (X-VIVO+HS). MDMs were treated with vehicle-only controls or with 1 µg/mL LPS for 4 h and 10 µM nigericin (Nig) for 45 min. **a)** IL-1β secretion was measured by ELISA. **b)** LDH release was measured as a proxy for cell death. **c)** GSDMD processing was analysed in cell lysates by immunoblot. In a and b data is plotted as mean ± SD, statistical significance was established by one-way ANOVA (*p<0.05 **p<0.01 ***p<0.001, ****p<0.0001), each colour represents a matched single donor and data is representative of 5 independent experiments. In c data is representative of 3 independent experiments.

Having established the culture conditions of MDMs, the following experiments sought to determine the optimal concentration of LPS and nigericin needed for NLRP3 inflammasome activation. Concentrations of LPS from 1 to 0.12 µg/mL and of nigericin from 20 to 1.25 µM were tested (Fig 3.3). MDMs were stimulated with LPS for 4 h in serum-containing media followed by nigericin in serum-free media for 45 min. Mature IL-1β and IL-18 release in supernatants was studied using ELISA assays, cell death was measured as a percentage of LDH release, and caspase 1 and GSDMD processing were analysed in cell lysates using immunoblotting. Inflammasome activation was achieved in every condition as evidenced by IL-1β and IL-18 secretion and increased cell death (Fig 3.3 a, b and c). However, cytokine secretion was significantly higher when cells were stimulated with 1 µg/mL LPS and 10 µM or 5 µM nigericin, and with 2 µg/mL LPS and 10

µM nigericin (Fig 3.3 a and b). Cell death was similar across conditions, though it was slightly higher with 1 µg/mL LPS and 5 µM nigericin (Fig 3.3 c). Caspase 1 and GSDMD processed forms (p20 and NT-GSDMD) were detected in every case apart from 1 µg/mL LPS and 20 µM nigericin (Fig 3.3 d). A p33 band of caspase 1, corresponding with its p33/p10 form, was detected when MDMs were stimulated with 2 µg/mL LPS and 20 µM nigericin. Although the three conditions of stimulation above mentioned showed similar levels of inflammasome activation, treatment with 1 µg/mL LPS and 10 µM nigericin was chosen for further experiments since in this condition inflammasome activation was achieved and cell death was lower than with other concentrations of LPS and nigericin.

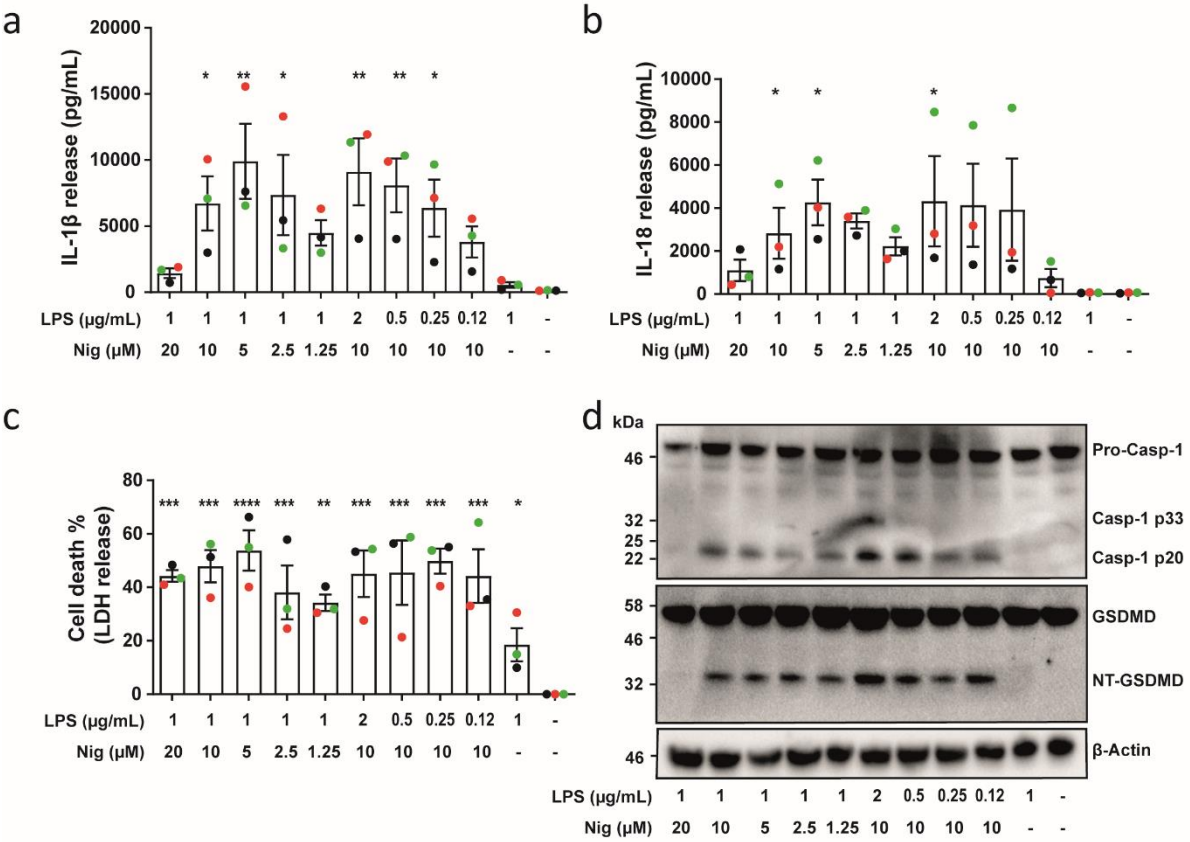

Figure 3.3 LPS and nigericin titration for optimal stimulation of the NLRP3 inflammasome in human MDMs. MDMs were treated with vehicle-only controls or primed with the indicated concentrations of LPS and nigericin (Nig) for 4 h and 45 min, respectively. **a)** IL-1β secretion was measured by ELISA. **b)** IL-18 secretion was measured by ELISA. **c)** LDH release was measured as a proxy for cell death. **d)** Caspase 1 (Casp-1) and GSDMD processing was analysed in cell lysates by immunoblot. In a-c data is plotted as mean ± SD, statistical significance to untreated cells was established by one-way ANOVA (*p<0.05 **p<0.01 ***p<0.001, ****p<0.0001) and each colour represents a matched single donor. In a-d data is representative of 3 independent experiments.

THP1 cells are one of the most used cell lines for studying the inflammasome in human monocytes and macrophages. Thus, we next sought to test whether similar concentration of LPS and nigericin stimulated inflammasome activation in these cells. THP1 cells were differentiated towards a macrophage-like phenotype using 50 nM PMA for 16 h. Cells were then rested for 24 h and treated with the indicated concentrations of LPS for 4 h and nigericin for 45min. IL-1β secretion (Fig 3.4 a) and cell death (Fig 3.4 b) were detected with every LPS and nigericin stimulation apart from 1µg/mL LPS and 1.25 µM nigericin, which was indicative of inflammasome activation in these conditions. IL-1β release was most significantly increased when cells were stimulated with 1µg/mL LPS and 10 µM nigericin. Although in this condition cell death was higher than 60%, this was the treatment selected for further experiments to match the stimulating conditions chosen for MDMs (Fig 3.3).

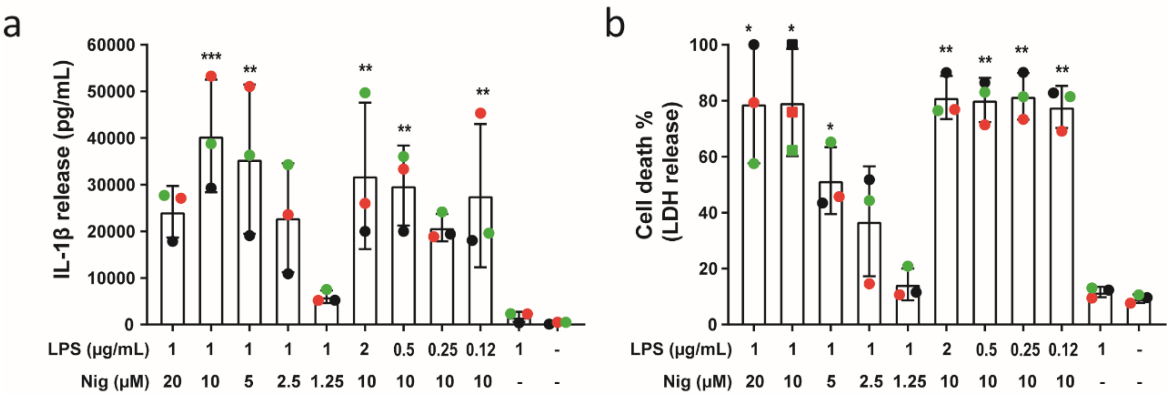

Figure 3.4 LPS and nigericin titration for optimal stimulation of the NLRP3 inflammasome in THP1 cells. THP1 cells were differentiated towards a macrophage-like phenotype using 50 nM PMA for 16 h. Cells were rested in fresh media for 24 h. Then, cells were treated with vehicle-only controls or treated with the indicated concentrations of LPS and nigericin (Nig) for 4 h and 45 min, respectively. **a)** IL-1β secretion was measured by ELISA. **b)** LDH release was measured as a proxy for cell death. In a and b data is plotted as mean ± SD, statistical significance to untreated cells was established by one-way ANOVA (*p<0.05 **p<0.01 ***p<0.001), each colour represents a matched experiment and data is representative of 3 independent experiments.

To investigate whether GSDMD processing is detected at different time points upon stimulation with nigericin, MDMs were stimulated with 1 µg/mL LPS for 4 h and 10 µM nigericin for the indicated time (Fig 3.5). The percentage of cell death increased over time, being significantly increased from 60 min of stimulation with nigericin (Fig 3.5 a).

IL-1β was detected in cell supernatants using an ELISA assay from 30 min of stimulation with nigericin (Fig 3.5 b). At this time point, GSDMD was cleaved into its p30 pore forming subunit (NT-GSDMD) and the amount of NT-GSDMD detected was higher than at 60 and 90 min of nigericin treatment (Fig 3.5 c). This could be explained due to the fact that at 60 and 90 min of nigericin stimulation, cell death was significantly increased leading to membrane rupture and loss of proteins that are in the cell membrane such as NT-GSDMD. Treatment with LPS alone did not trigger cell death (Fig 3.5 a), IL-1β secretion (Fig 3.5 b) or GSDMD cleavage (Fig 3.5 c), indicating that GSDMD processing only occurs after inflammasome activation.

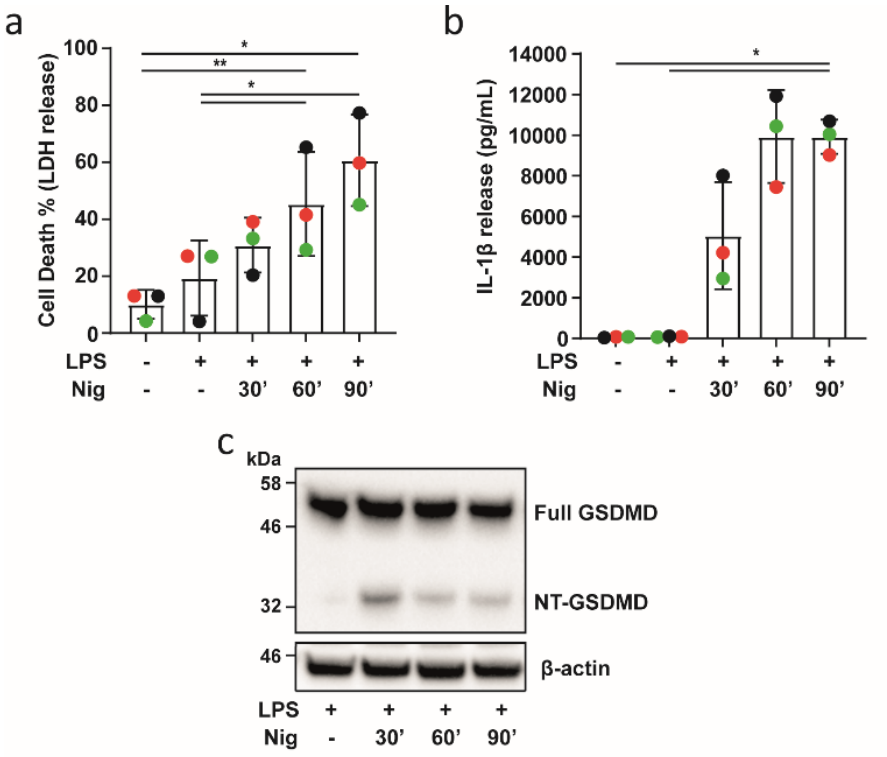

Figure 3.5 NLRP3 inflammasome activation increases overtime in human MDMs. MDMs were treated with vehicle-only controls or treated with 1µg/mL LPS for 4 h and 10 µM nigericin (Nig) for the indicated time. **a)** LDH release was measured as a proxy for cell death. **b)** IL-1β secretion was measured by ELISA. **c)** GSDMD processing was analysed in cell lysates by immunoblot. In a and b data is plotted as mean ± SD, statistical significance was established by Friedman test (*p<0.05 **p<0.01) and each colour represents a matched single donor. In a-c data is representative of 3 independent experiments.

3.3.2 Inflammasome-mediated cytokine secretion is independent of membrane rupture.

Inflammasome activation results not only in cytokine secretion but also in membrane rupture, which can cause the release of all the intracellular content[348]. Cytokine release could therefore just be a consequence of this membrane rupture, and not an active process. Thus, to understand whether membrane integrity loss is required for mature IL-1β and IL-18 to be secreted from the cell following inflammasome activation, MDMs where primed with LPS for 4 h and treated for 45 min with nigericin for inflammasome activation in the presence or absence of 10 mM of the osmoprotectant agent glycine, a concentration previously used in macrophages[349,350]. Glycine blocks membrane rupture while preserving membrane features[351]. Here, LDH release was significantly reduced upon inflammasome activation (Fig 3.6 a), whereas IL-1β and IL-18 secretion was consistently elevated irrespective of the addition of glycine (Fig 3.6 b and c). Moreover, following inflammasome activation in the presence of glycine, GSDMD was cleaved into its p30 pore forming subunit (NT-GSDMD) as evidenced by immunoblotting (Fig 3.6 d). Moreover, the amount of NT-GSDMD detected was higher in the presence of glycine (Fig 3.6 d) indicating that, as previously observed (Fig 3.5 a and c), higher cell death (Fig 3.6 a) may engage protein degradation pathways that reduce NT-GSDMD, or that membrane-bound GSDMD is lost in the cell supernatant due to membrane rupture. Altogether, these results indicate that glycine did not compromise inflammasome activation and suggest that IL-1β and IL-18 are released from MDMs independently of membrane rupture.

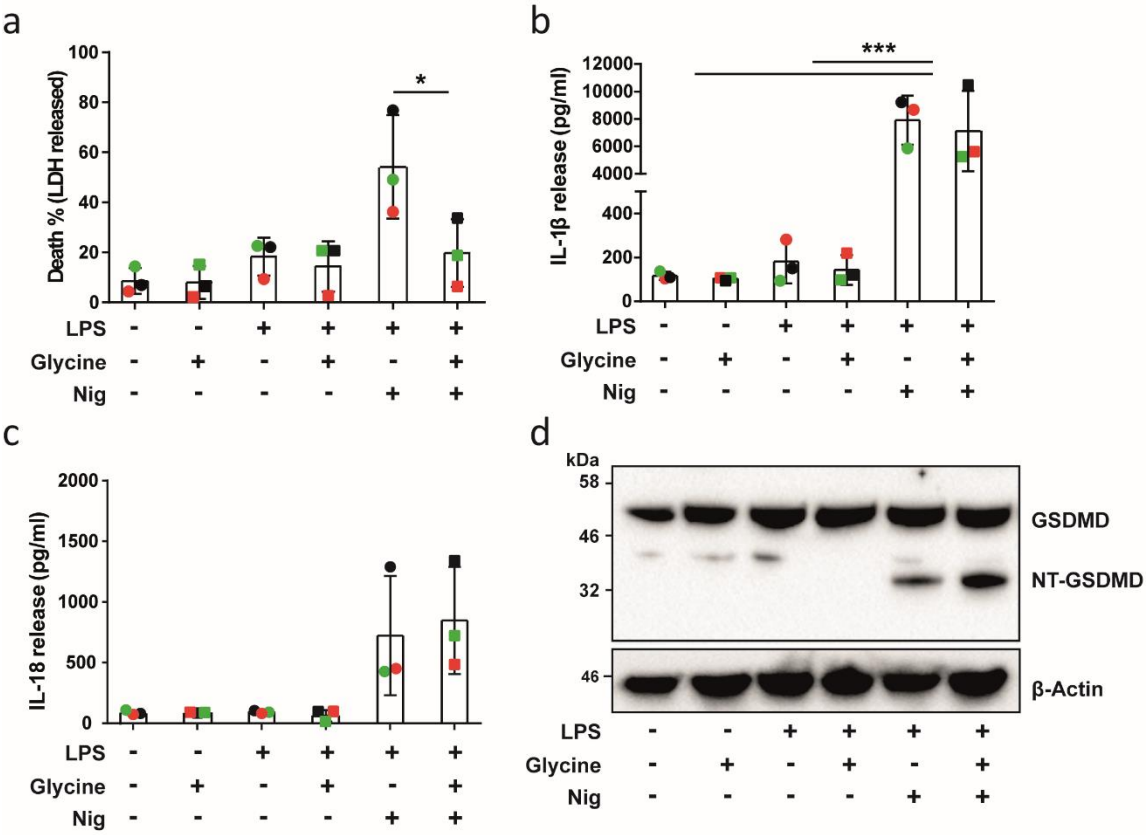

Figure 3.6 IL-1β and IL-18 secretion is independent on membrane rupture in human MDMs. MDMs were treated with vehicle-only controls or treated with 1µg/mL LPS for 4 h and 10 µM nigericin (Nig) for 45 min in the presence or absence of 10 mM glycine to prevent membrane rupture. **a)** LDH release was measured as a proxy for cell death. **b)** IL-1β secretion was measured by ELISA. **c)** IL-18 secretion was measured by ELISA. **d)** GSDMD processing was analysed in cell lysates by immunoblot. In a-c data is plotted as mean ± SD, statistical significance was established by one-way ANOVA (*p<0.05 **p<0.01 ***p<0.001) and each colour represents a matched single donor. In a-d data is representative of 3 independent experiments.

To address whether membrane rupture is necessary for IL-1β and IL-18 release at earlier and later time points, cells were primed with LPS for 4 h and treated with nigericin for inflammasome activation for 0, 30, 60, 90 or 120 min in the presence or absence of 10 mM glycine. Cytokine release increased overtime until 90 min of stimulation with nigericin, at which point it remained invariable (Fig3.7 a and b). On the other hand, the absence of glycine resulted in increased cell death overtime without reaching a plateau state (Fig 3.7 c). This suggests that after 90 min of nigericin stimulation, cytokine production reaches its peak regardless of an increase in cell death. As previously shown, cytokine release remained the same whether inflammasome activation took place in the presence or absence of glycine (Fig 3.7 a and b), whereas cell death percentage was

significantly reduced in the presence of the osmoprotectant agent at every time point (Fig 3.7 c). The amount of cytokine release was variable between donors. This has been previously described in human cells in the context of inflammasome activation[328,347], and it is likely the result of biological variability. Furthermore, GSDMD processing was detected from 30 min of stimulation with nigericin both in the presence and absence of glycine (Fig 3.7 d). As for NT-GSDMD, the amount of p20 caspase 1 detected in cell lysates was enhanced when membrane rupture was prevented (Fig 3.7 d), indicating that the release of this protease may be a consequence of pyroptosis. These findings show that IL-1β and IL-18 secretion and GSDMD processing are independent of membrane rupture both at early and later points of inflammasome stimulation, which suggests that these cytokines are actively released from the cell.

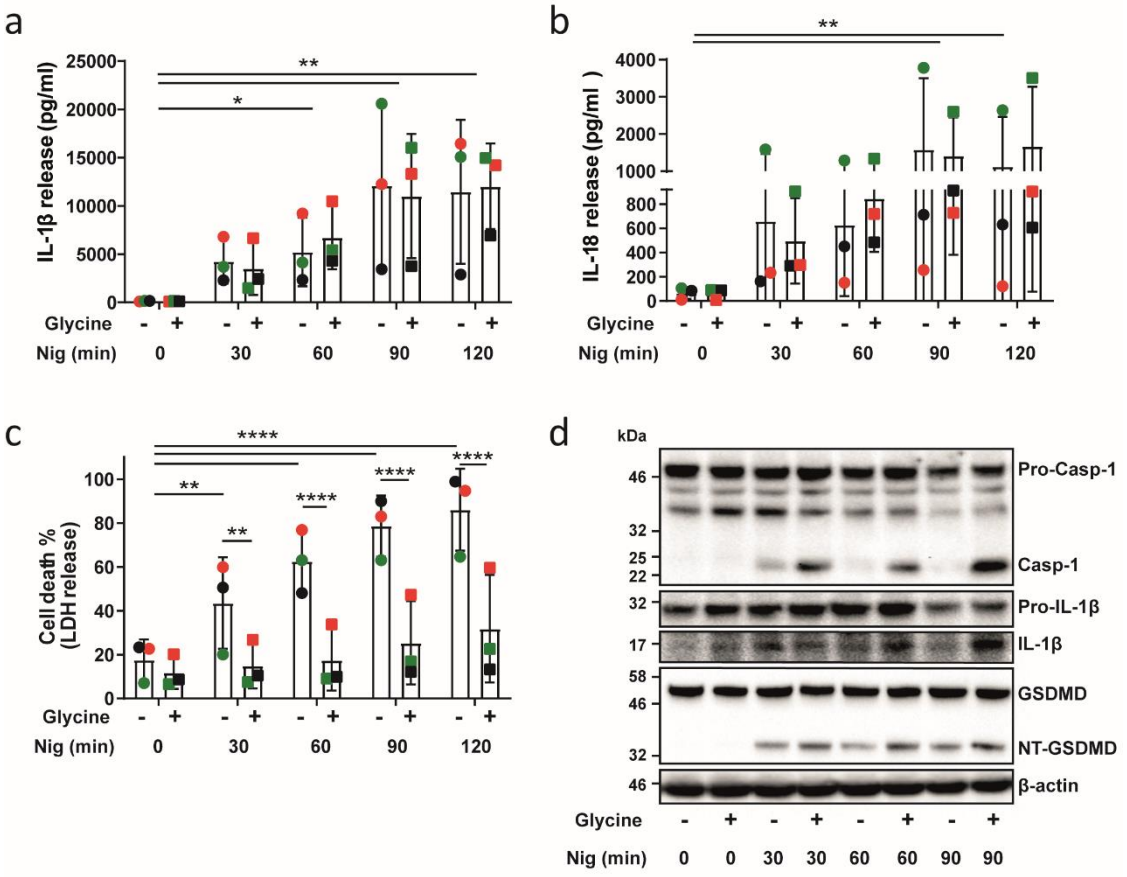

Figure 3.7 Inflammasome activation is independent of membrane rupture in human MDMs. MDMs were treated with vehicle-only controls or treated with 1µg/mL LPS for 4 h and 10 µM nigericin (Nig) for the indicated time in the presence or absence of 10 mM glycine to prevent membrane rupture. **a)** IL-1β secretion was measured by ELISA. **b)** IL-18 secretion was measured by ELISA. **c)** LDH release was measured as a proxy for cell death. **d)** Caspase 1 (Casp-1), IL-1β and GSDMD processing was analysed in cell lysates by immunoblot. In a-c data is plotted as mean ± SD, statistical significance was established by one-way ANOVA (*p<0.05 **p<0.01 ***p<0.001 ****p<0.0001) and each colour represents a matched single donor. In a-d data is representative of 3 independent experiments.

3.3.3 Inflammasome-mediated cytokine secretion is dependent on GSDMD.

GSDMD is a pore-forming protein cleaved by inflammatory caspases following inflammasome activation. The N-terminus cleaved form of GSDMD (NT-GSDMD) oligomerizes to form pores in the cell membrane. These pores have an inner diameter of 10-22 nm that is big enough for the cytokines IL-1β and IL-18 to pass through[79,81,219]. For this reason, the following experiments aimed to determine whether GSDMD pores are necessary for IL-1β and IL-18 secretion in human macrophages. To this aim, the GSDMD pore inhibitor necrosulfonamide (NSA) was used[352]. First, human MDMs were primed with LPS for 4 h, treated with 10-20 µM NSA for 30 min, as established by others[352], and activated with Nig for 45 min. Immunoblotting of cell lysates revealed that the use of NSA resulted in the inhibition of GSDMD cleavage into its pore-forming subunit NT-GSDMD (Fig 3.8 a). GSDMD's role in pyroptosis was also confirmed as inhibition of GSDMD pore formation blocked cell death (Fig 3.8 b). Moreover, IL-1β and IL-18 release was significantly decreased (Fig 3.8 a and b), suggesting that GSDMD pores are involved in the secretion of these cytokines in MDMs upon inflammasome activation.

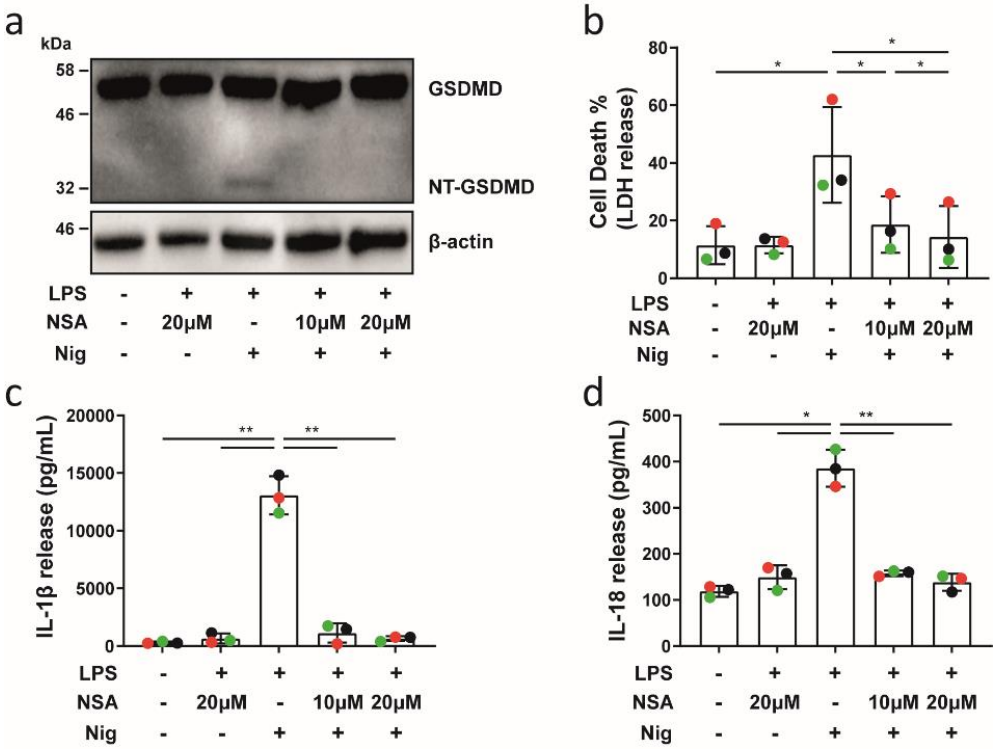

Figure 3.8 IL-1β and IL-18 release and pyroptosis are dependent on GSDMD processing in human MDMs. MDMs were treated with vehicle-only controls or stimulated with 1μg/mL LPS for 4 h and 10 μM nigericin (Nig) for 45 min in the presence or absence of 10 μM or 20 μM necrosulfonamide (NSA) to prevent GSDMD pore formation. **a)** GSDMD processing was analysed in cell lysates by immunoblot **b)** LDH release was measured as a proxy for cell death. **c)** IL-1β secretion was measured by ELISA. **d)** IL-18 secretion was measured by ELISA. In b-d data is plotted as mean ± SD, statistical significance was established by one-way ANOVA (*p<0.05 **p<0.01) and each colour represents a matched single donor. In a-d data is representative of 3 independent experiments.

As previously mentioned, THP1 cells are a commonly used model of study for inflammasome in human macrophage-like cells. For this reason, whether GSDMD plays a role in IL-1β and IL-18 in THP1 cells was investigated. First, THP1 cells were differentiated towards a macrophage-like phenotype using PMA as previously described. Inflammasome activation was achieved using LPS for 4 h and nigericin for 45 min and NSA was used to inhibit GSDMD pore formation. GSDMD cleavage was only partially inhibited by 10 μM NSA, as detection of NT-GSDMD was reduced in immunoblots when compared to fully activated conditions (Fig 3.9a). Importantly however, GSDMD cleavage was not completely impaired (Fig 3.9 a), as in primary macrophages (Fig 3.8 a). NT-GSDMD was not detected by immunoblotting when 20 μM NSA was used (Fig 3.8 a). Although cell death was reduced in this condition, it was not totally reverted (Fig 3.9 b). The use of 20 μM NSA slightly reduced IL-1β and IL-18 secretion (Fig 3.9 c and d). However, it did not prevent cytokine secretion as in primary cells (Fig 3.8 c and d).

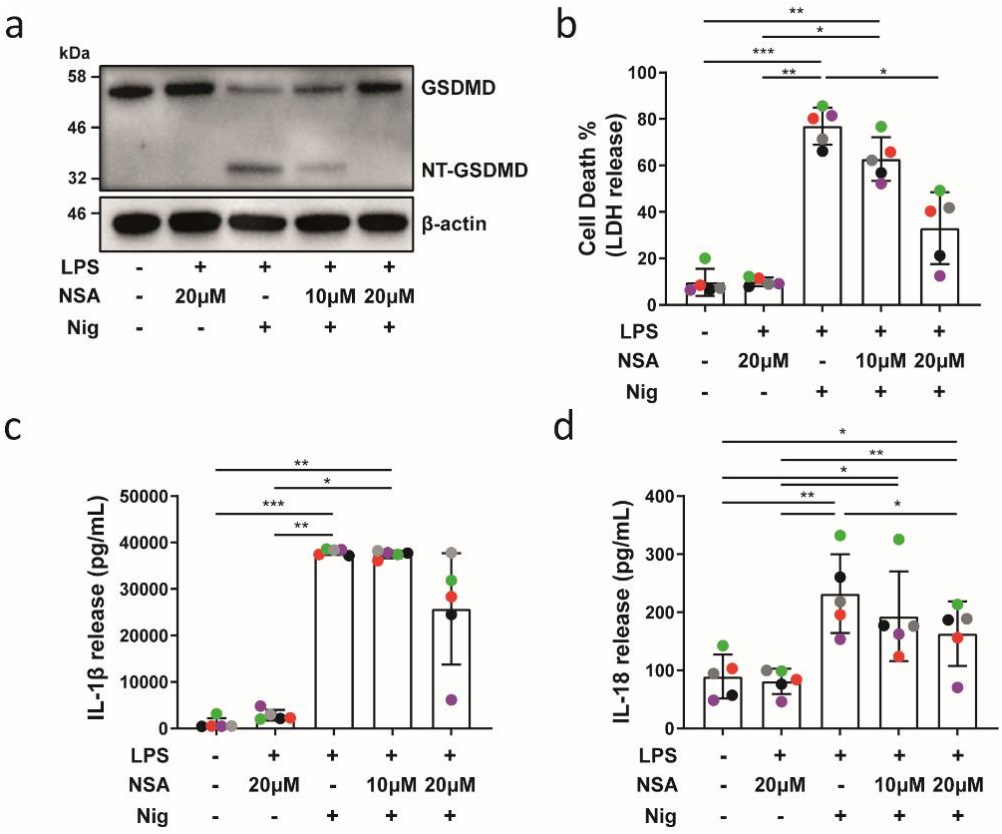

Figure 3.9 Inhibition of GSDMD pore formation diminishes IL-1β and IL-18 release and pyroptosis in THP1 cells. THP1 cells were differentiated with 50 nM PMA for 16 h. Cells were rested in fresh media for 24 h and treated with vehicle-only controls or treated with 1 μg/mL LPS for 4 h and 10 μM nigericin (Nig) for 45 min in the presence or absence of 10 μM or 20 μM necrosulfonamide (NSA) to prevent GSDMD pore formation. **a)** GSDMD processing was analysed in cell lysates by immunoblot **b)** LDH release was measured as a proxy for cell death. **c)** IL-1β secretion was measured by ELISA. **d)** IL-18 secretion was measured by ELISA. In b-d data is plotted as mean ± SD, statistical significance was established by one-way ANOVA (*p<0.05 **p<0.01 ***p<0.001) and each colour represents a matched single donor. Data is representative of 3 (a) or 5 (b-d) independent experiments.

The chemical inhibitor NSA did not completely block cytokine release and pyroptosis in THP1 cells. Thus, to determine whether GSDMD is fundamental for IL-1β and IL-18 secretion upon canonical inflammasome activation in these cells, a THP1$^{gsdmd-/-}$ cell line was used (Fig 3.10). THP1$^{gsdmd-/-}$ cells were generated from wild type THP1 cells by lentiviral transduction with a CRISPR-Cas9 plasmid targeting *gsdmd*, as indicated in chapter 2 (Section 2.2.1.2). The Lopez-Castejon laboratory (The University of Manchester) showed that the THP1$^{gsdmd-/-}$ cell line generated in this project could produce active caspase 1 and mature IL-18 upon stimulation with nigericin[346], indicating that depletion of GSDMD did not impair inflammasome function in THP1$^{gsdmd-/-}$ cells. To study the role of GSDMD, THP1 cells were differentiated towards a macrophage-like

phenotype using PMA as indicated before, and cells were treated with 1 µg/mL LPS for 4 h and 10 µM nigericin for 45 min to activate the inflammasome. Depletion of GSDMD in THP1$^{gsdmd-/-}$ cells was confirmed by immunoblotting, as both the band corresponding to full GSDMD (50 KDa) and the band corresponding to NT-GSDMD (31 kDa) were not detected in either steady state or inflammasome-activating conditions (Fig 3.10 a). GSDMD depletion also impaired cell death upon inflammasome activation (Fig 3.10 b), highlighting the requirement of GSDMD for pyroptosis. The lack of this protein also inhibited IL-1β and IL-18 secretion (Fig 3.10 c and d), indicating a direct role for GSDMD in cytokine secretions. Thus, genetic deletion of this protein robustly determined that GSDMD is directly involved in IL-1β and IL-18 secretion in human macrophage-like THP1 cells.

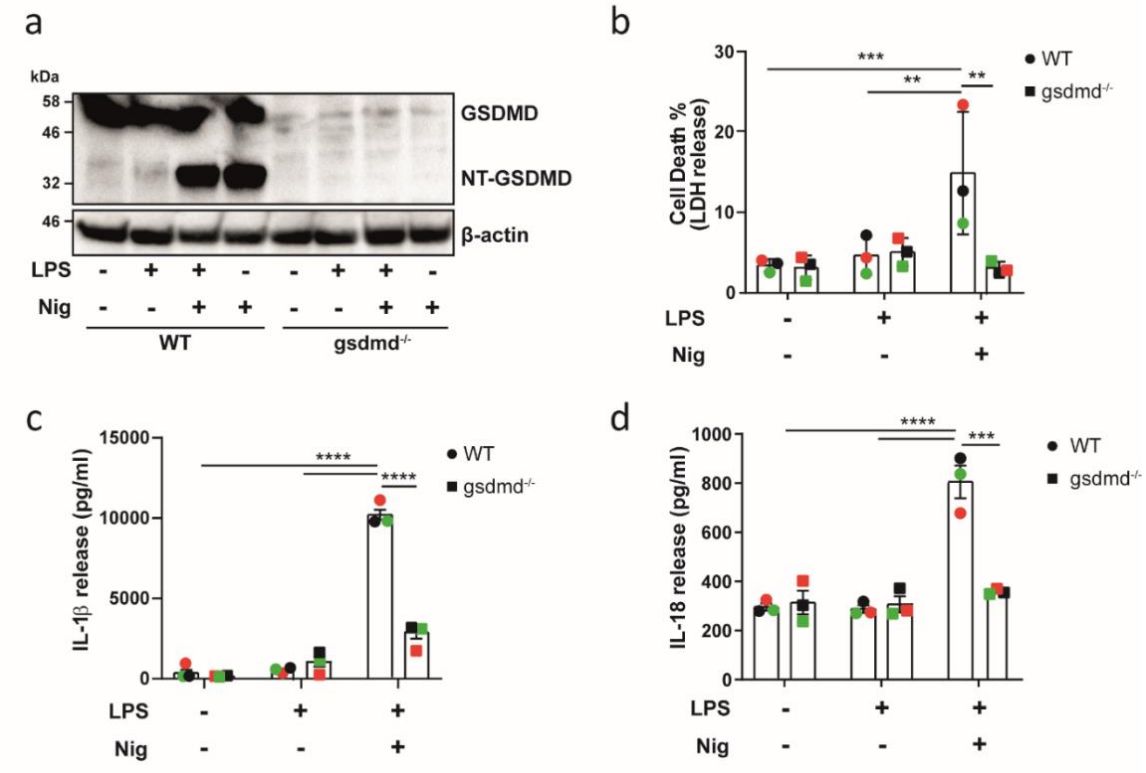

Figure 3.10 Depletion of GSDMD impairs IL-1β and IL-18 release and pyroptosis in THP1 cells. Wild type THP1 and THP1$^{gsdmd-/-}$ cells were differentiated towards a macrophage-like phenotype using 50 nM PMA for 16 h. Cells were rested in fresh media for 24 h. Then, cells were treated with vehicle-only controls or primed with 1µg/mL LPS for 4 h and activated with 10 µM nigericin (Nig) for 45 min. **a)** GSDMD processing was analysed in cell lysates by immunoblot. **b)** LDH release was measured as a proxy for cell death. **c)** IL-1β secretion was measured by ELISA. **d)** IL-18 secretion was measured by ELISA. In b-d data is plotted as mean ± SD, statistical significance was established by one-way ANOVA (**p<0.01 ***p<0.001 ****p<0.0001) and each colour represents a matched single donor. In a-d data is representative of 3 independent experiments.

3.3.4 NT-GSDMD localizes to the cell membrane upon inflammasome activation.

GSDMD processing does not necessary indicate traffic to the cell membrane and formation of pores. For this reason, we next investigated the localisation of NT-GSDMD in the cell upon inflammasome activation in THP1 cells using imaging approaches. To this end, THP1 cells were culture in chambered coverglasses and differentiated using PMA as previously described. Inflammasome activation was engaged using LPS for 4 h and nigericin for 30 or 45 min. Cells were fixed and stained with wheat-germ agglutinin (WGA) to mark the cell membrane and with an anti-NT-GSDMD mAb to study GSDMD localisation.

We first used confocal microscopy to globally assess the localisation of NT-GSDMD in the cell (Fig 3.11 a). Inflammasome activation resulted in an evident colocalisation of NT-GSDMD and WGA after stimulation with nigericin. This was especially evident after 45min of stimulation (Fig 3.11). This indicates that NT-GSDMD is localized to the cell membrane upon inflammasome activation. Although the anti-NT-GSDMD mAb used in these experiments specifically targets NT-GSDMD, under non-stimulatory conditions staining was observed (Fig 3.11 a). This suggests that this mAb is also able to bind to NT-GSDMD within the full GSDMD. Nonetheless, the localisation of this protein under non-stimulatory conditions was intracellular and did not match WGA localisation indicating that, unlike for LPS and nigericin-stimulated cells, NT-GSDMD was not localized to the cell membrane (Fig 3.11 a).

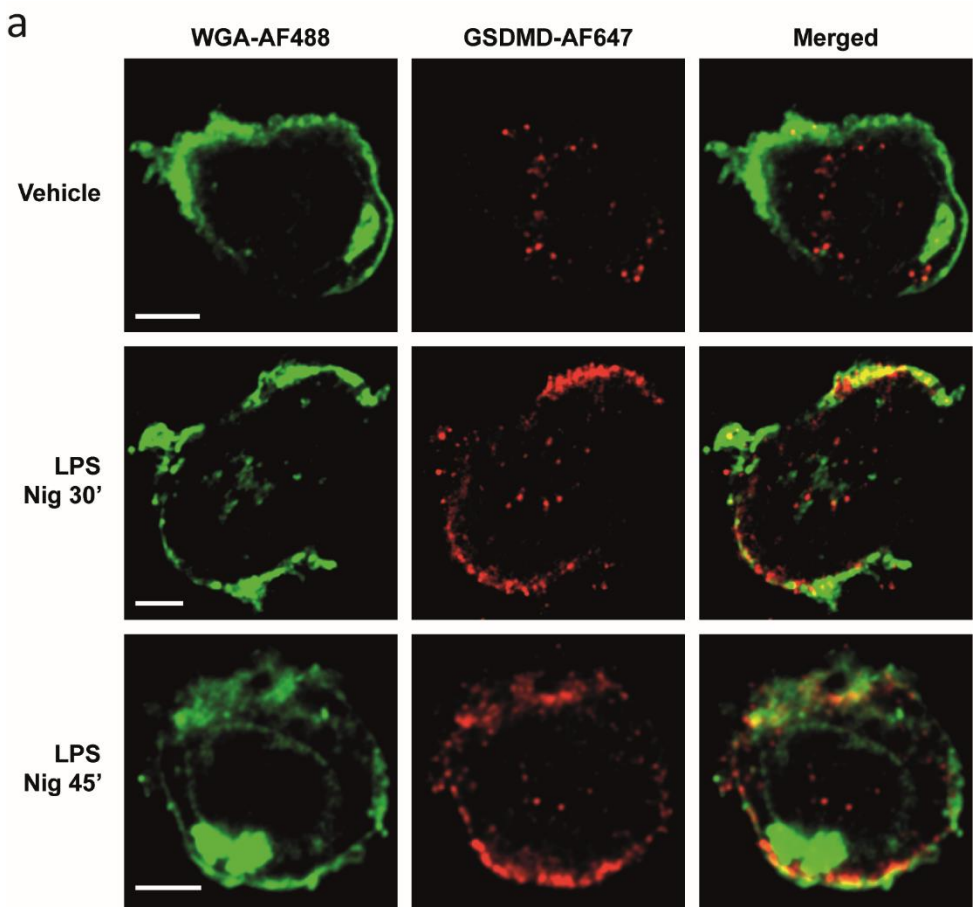

Figure 3.11 GSDMD is recruited to the cell membrane upon NLRP3 inflammasome activation in THP1 cells. THP1 cells were differentiated towards a macrophage-like phenotype using 50 nM PMA for 16 h. Cells were rested in fresh media for 24 h. Then, cells were treated with vehicle-only controls or primed with 1µg/mL LPS for 4 h and activated with 10 µM nigericin (Nig) for the indicated time, fixed and stain with 10µg/mL anti-GSDMD mAb and 10 µg/mL WGA to identify the cell membrane. **a)** Representative confocal images of WGA and GSDMD. Scale bars are 5µm, images are representative of 3 independent experiments, and ≥ 15 cells were imaged per condition in each experiment.

To further investigate NT-GSDMD distribution at the cell membrane, microscopy techniques with higher resolution were used. THP1 cells were stimulated and stained as in confocal microscopy experiments, and TIRF microscopy and the super-resolution technique STORM were performed (Fig 3.12). The cells were first analysed in TIRF mode, which constrains the imaging to molecules that are within ≈150 nm of the glass surface, therefore focusing on the cell membrane. This was confirmed by the detection of membrane-bound WGA (Fig 3.12 a). TIRF images revealed that GSDMD localisation to the membrane was restricted to LPS and nigericin-treated cells and was not observed under non-stimulatory conditions (Fig 3.12 a). Furthermore, the fluorescence intensity was significantly increased after inflammasome activation, and was more evident after

45 min of nigericin stimulation (Fig .3.12 b), indicating a continual recruitment of GSDMD to the cell membrane. Moreover, multiple particle-like structures, compatible with the structure of pores, were detected upon inflammasome activation (Fig 3.12 a and c). Although not statistically significant, the number of particles per region of interest (ROI) and per μm^2 detected after 45 min of stimulation with nigericin was increased compared with 30 min of nigericin treatment (particles/ROI were 92 ± 32 at 30 min and 118 ± 51 at 45 min, and particles/μm^2 were 5.1 ± 1.7 at 30 min and 6.5 ± 2.8 at 45 min) (Fig 3.12 c and d). This indicated an increase in the recruitment of NT-GSDMD to the cell membrane. We next measured the area of the GSDMD particles detected using TIRF microscopy. GSDMD pores are circular and symmetrical[219]. Therefore, although the particles detected using TIRF microscopy were not perfectly symmetrical, their diameter was inferred from their area by considering them to be circular. In stimulated cells, the area and the inferred diameter of the detected particles were significantly higher than in untreated cells (Fig 3.12 e and f), suggesting that NT-GSDMD was accumulating and oligomerizing at the cell membrane. Moreover, these measurements were significantly increased after 45 min of stimulation with nigericin (Fig 3.12 e and f), indicating an increased in GSDMD pore formation after longer exposure to inflammasome activators.

The same ROIs selected for TIRF microscopy were studied using super-resolution STORM (Fig 3.12 a). This revealed that the number of events per μm^2 was significantly increased upon inflammasome activation (Fig 3.12 g). Moreover, the number of events per μm^2 detected was significantly enhanced after 45 min of nigericin stimulation when compared to 30 min of stimulation (Fig 3.12 g). Altogether, high resolution imaging revealed that inflammasome activation results in the recruitment of NT-GSDMD to the cell membrane to form particulate structures that resemble pores.

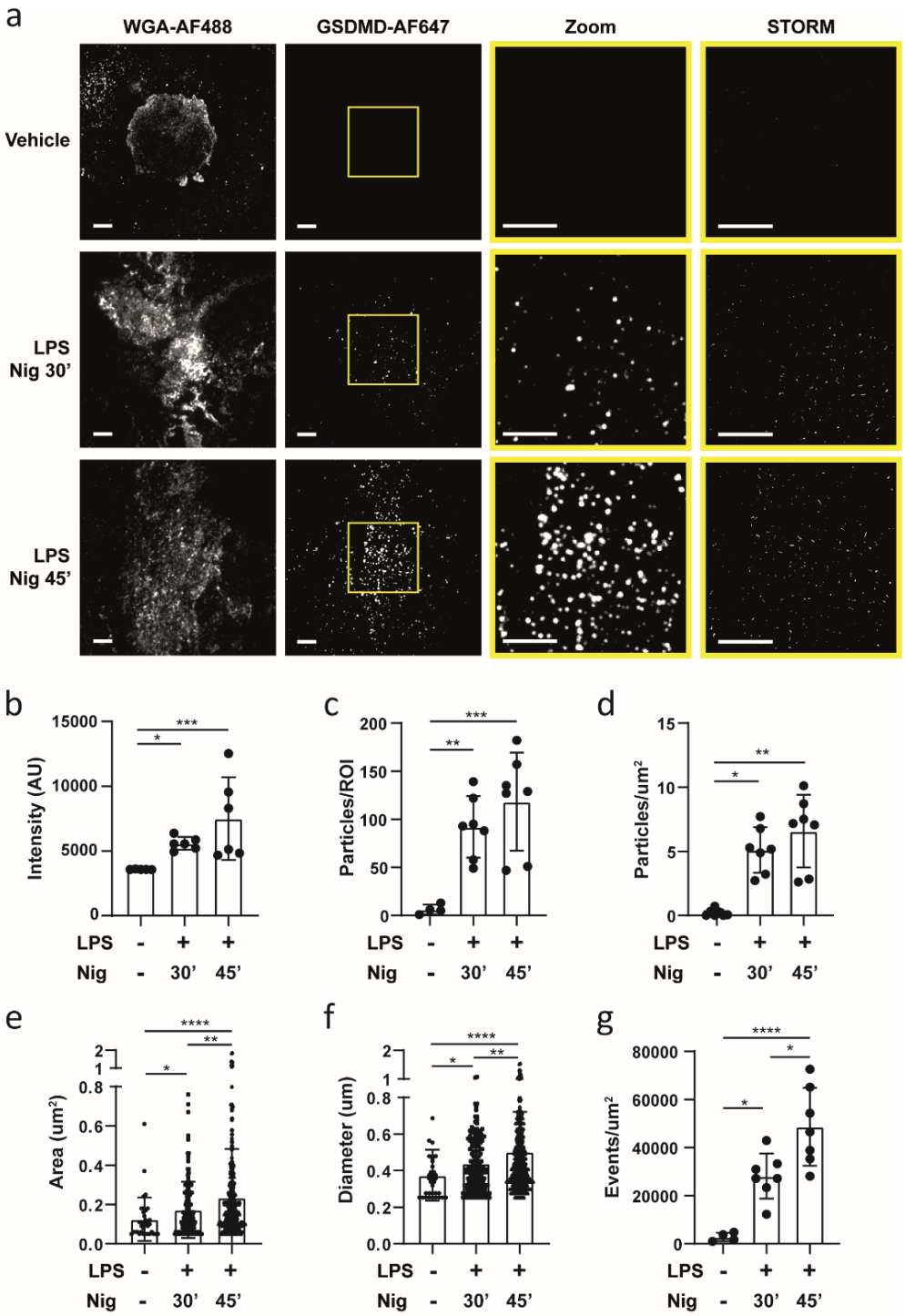

Figure 3.12 GSDMD localization in the cell membrane upon NLRP3 inflammasome activation in THP1 cells. THP1 cells were differentiated using 50 nM PMA for 16 h. Cells were rested in fresh media for 24 h and treated with vehicle-only controls or with 1µg/mL LPS for 4 h and 10 µM nigericin (Nig) for the indicated time. Cells were fixed and stain with 10 µg/mL anti-GSDMD Ab and 10 µg/mL WGA to identify the cell membrane. **a)** Representative TIRF images of WGA and GSDMD and STORM images of GSDMD. Scale bars are 5µm. **b)** Fluorescence intensity of GSDMD measured in the TIRF images. **c)** Number of particles detected in the zoom regions of the GSDMD TIRF images. **d)** Number of particles/µm^2 detected in the zoom regions of the GSDMD TIRF images. **e)** Area of the particles detected in the GSDMD TIRF images. **f)** Inferred diameter of the detected particles in GSDMD TIRF images. **g)** Number of events/µm^2 detected in the GSDMD STORM images. In b-e data is plotted as mean ± SD, statistical significance was established by one-way ANOVA (*p<0.05 **p<0.01 ***p<0.001 ****p<0.0001). In a-e data is representative of ≥ 4 independent experiments and ≥ 5 cells per condition were imaged in each experiment.

3.4 Discussion

3.4.1 Summary of results

The aim of this chapter was to evaluate the involvement of GSDMD in IL-1β and IL-18 secretion, as well as studying GSDMD localisation in the cell, upon inflammasome activation in human macrophages. The main results established in this chapter are summarised as follows:

1. Inflammasome activation of human MDMs and human macrophage-like THP1 cells results in GSDMD processing into its pore-forming subunit NT-GSDMD.
2. IL-1β and IL-18 secretion is independent of membrane rupture in MDMs.
3. Chemical inhibition of GSDMD impaired pyroptosis and cytokine secretion upon inflammasome activation in MDMs.
4. Genetic impairment of GSDMD inhibited cytokine secretion and cell death in THP1 cells following inflammasome activation.
5. Inflammasome activation results in NT-GSDMD recruitment to the cell membrane in THP1 cells.

Together these findings indicate that GSDMD plays a fundamental role in cytokine secretion following inflammasome activation in human macrophages. Moreover, this protein is also responsible for pyroptosis in these cells.

3.4.2 Significance of results

IL-1β and IL-18 are essential cytokines with fundamental roles in the process of inflammation[353]. Despite this, the mechanism of secretion for these cytokines is poorly understood. GSDMD is a pore-forming protein that plays an important role in IL-1β and IL-18 secretion, and is essential for the release of these cytokines in murine myeloid cells and human cell lines[78,201,354]. However, the role of this pore-forming protein in primary human macrophages is currently unknown. As macrophages are one of the main sources of these cytokines, the focus of this chapter was to study the role of GSDMD in human macrophages upon NLRP3 inflammasome activation.

3.4.2.1 Inflammasome activation in macrophages with different phenotypes

Human blood monocytes can be differentiated in vitro to obtain different types of primary human macrophages, and this is dependent upon the environment, in this case the culture conditions, in which they are differentiated[10,47]. In this chapter, we used two previously described methods to differentiate monocytes into macrophages, using M-CSF or human serum (HS) as the main drivers of differentiation[13,17,355]. Monocyte-derived macrophages (MDMs) obtained using human serum (HS MDMs) acquired a more pro-inflammatory phenotype, with high levels of the T cell co-stimulatory molecule CD86 and lower levels of the mannose receptor CD206 and the low affinity immunoglobulin G receptor CD16. Indeed, this phenotype is closer to what has traditionally been described as M1 or pro-inflammatory macrophages[20]. However, the non-responsiveness to inflammasome activators indicates a non-classical phenotype, suggesting that HS MDMs could instead resemble a non-activated or M0 macrophage[356]. On the other hand, those MDMs differentiated using M-CSF (M-CSF MDMs) exhibited a regulatory phenotype, expressing higher levels of CD206 and CD16, typically classified as M2 or anti-inflammatory macrophages[20,42]. Interestingly, stimulation with LPS and nigericin resulted in greater IL-1β release and cell death percentage in M-CSF MDMs than in HS MDMs, suggesting a greater activation of the inflammasome in M-CSF MDMs. Moreover, processing of GSDMD, the focus of study of this chapter, was only observed in M-CSF MDMs. LPS is a potent pro-inflammatory signal that is able to polarize anti-inflammatory macrophages towards a pro-inflammatory phenotype[357–359], which explains why inflammasome activation was achieved in M-CSF MDMs. Although not fully understood, the weak response of HS MDMs to inflammasome stimuli could be explained by the fact that M0 macrophages are known to express low levels of TLR4 - with this receptor being responsible for the detection of extracellular LPS[360]. Nonetheless, this thesis used a simplified method, analysing only extracellular receptors, to study the type of MDMs obtained upon treatment with M-CSF or HS. In order to fully understand the phenotype of M-CSF MDMs and HS MDMs, other approaches including the study of M1-like and M2-like genes such as iNos and Arg-I, respectively, and the secretion of pro-inflammatory cytokines like IFNγ or anti-inflammatory cytokines such as IL-10[16], could have been performed.

3.4.2.2 The role of GSDMD in IL-1β and IL-18 secretion in human macrophages

It is well established that inflammasome activation in the context of several stimuli results in the secretion of IL-1β and IL-18 from multiple immune and non-immune cells both *in vitro* and *in vivo*. However, how these cytokines are released from the cell is not entirely understood. It has long been known that these cytokines are not released through the ER-Golgi-exocytosis 'conventional' protein pathway[192]. Different mechanisms have been proposed for the secretion of IL-1β and IL-18, including release via vesicles[361], microvesicle shedding[199], exosomes[362], and secretion through membrane pores[201,354]. However, the amount of these cytokines detected within vesicles is very limited[361], suggesting that other mechanisms may play a more dominant role in cytokine release. In 2015, the protein GSDMD was proposed as the main driver for cytokine release upon canonical and non-canonical inflammasome activation in murine macrophage-like cells, HeLa and HEK cells[78,138,156]. These studies demonstrated that depletion of GSDMD diminished IL-1β release. Interestingly, GSDMD depletion also impaired cell death, suggesting that IL-1β release was linked to pyroptosis and therefore membrane rupture. Thus, GSDMD was initially studied as the effector of pyroptosis, and cytokine release was determined to be a consequence of cell death. In agreement with these studies, work in this thesis chapter showed that depletion, or chemical inhibition of GSDMD impaired both cell death and IL-1β and IL-18 secretion in human macrophages. As such, this suggests that GSDMD may play a similar role to that described for murine macrophages in human cells.

GSDMD is considered the effector of pyroptosis - meaning that the formation of GSDMD pores compromises membrane integrity, resulting in cell death and emptying of cytoplasmic content. This is a powerful stimulus that drives a pro-inflammatory immune response. Therefore, as it was first hypothesized, IL-1β and IL-18 could be released with the rest of the intracellular content due to pyroptosis. However, it has recently been shown that phagocytes are able to reach a state of hyperactivation in which, upon inflammasome activation, they secrete IL-1β and maintain their viability[201], indicative of pyroptosis-independent cytokine release. This discovery uncoupled pyroptosis and IL-1β secretion, indicating that the release of IL-1β and IL-18 upon inflammasome activation is an active process. In agreement with this, various studies have shown that IL-1β and

IL-18 release upon inflammasome activation still occurs when membrane rupture is actively blocked using the osmoprotectant agent glycine in murine and human macrophages[201,328], further indicating that the secretion of these cytokines is not linked to loss of membrane integrity. Our data not only confirmed that the release of these cytokines still happened in the presence of glycine, but also revealed that GSDMD processing still occurs when membrane rupture is inhibited.

More recently, it has been demonstrated that inflammatory caspases such as caspase 1 cleave GSDMD into two subunits[201,363]. Specifically, using a reductionist system in which recombinant human GSDMD and active caspase 1 or murine GSDMD and caspase 11 are placed inside liposomes, it has been shown that these caspases cleave GSDMD into a p20 C-terminus and a p30 N-terminus subunit[201,363]. Furthermore, these studies determined that the NT-GSDMD is able to oligomerize and form membrane pores. Based on structural analysis using electron and atomic force microscopy, GSDMD pores are known to have an inner diameter of 10-20 nm[79,80,219], a size that would permit IL-1β and IL-18 (4.5nm)[220] to pass through. This is evidenced by the fact that dextrans that are smaller than 10 nm in diameter were able to escape liposomes through GSDMD pores[201]. Moreover, the conduit formed in GSDMD pores is negatively charged, and has preference for the release of positively or neutrally charged molecules[219]. Thus, as mature IL-1β and IL-18 become positively charged upon cleavage by inflammatory caspases[219,364], this strengthens the idea that IL-1β and IL-18 are actively secreted from the cell through GSDMD pores. In agreement with this, we observed that in human macrophages inflammasome activation led to caspase 1 activation, resulting in the detection of the pore-forming subunit NT-GSDMD in cell lysates, and in the secretion of mature IL-1β and IL-18 even when membrane rupture was prevented. Importantly, p20 caspase 1 accumulated inside the cell when membrane rupture was blocked, suggesting that not every small protein can go through GSDMD pores and that these pores are selective to certain proteins. Moreover, in THP1 cells GSDMD localized to the cell membrane upon stimulation with LPS and nigericin, which could indicate pore formation. Furthermore, we detected that GSDMD accumulated in the cell membrane overtime, and that it was homogenously distributed, forming small structures that resembled membrane pores. Unfortunately, the resolution of these

techniques did not allow us to directly observe the structure of the GSDMD pore that has been previously shown in liposomes and mammalian cells lines using atomic force and electron microscopy[79,80]. Nevertheless, previous research has demonstrated that transfection of the breast cancer cell line MCF-7 with NT-GSDMD leads to pore formation in the cell membrane, with approximately 14 GSDMD pores detected in each 5 μm^2 region[365]. This means that approximately 3 GSDMD pores/μm^2 were formed in MCF-7 cells. Indeed, if the analysed particles in TIRF images from the data in this thesis are considered to be pores, this would indicate that GSDMD structures were present in the cell membrane, since we detected 5.1 ± 1.7 particles/μm^2 after 30 min of stimulation with nigericin.

3.4.3 Conclusion and future directions

In conclusion, this chapter showed that inflammasome activation in human macrophages resulted in processing of GSDMD into its p30 NT subunit and its localisation to the cell membrane, suggesting that membrane pores could be formed. Moreover, IL-1β and IL-18 release was not impaired when membrane rupture was prevented, but it was blocked in the absence of GSDMD or when GSDMD processing was chemically inhibited. Therefore, this data suggests that in human macrophages, NLRP3 inflammasome stimulation results in the formation of GSDMD pores in the cell membrane, and that IL-1β and IL-18 are most likely secreted through these pores (Fig 3.13). To further confirm this, cryo-EM could be used as previously done with GSDMD-containing liposomes[79,80].

As multiple stimuli activate the NLRP3 inflammasome, studying the influence of different stimuli on GSDMD distribution and IL-1β secretion in human macrophages would be very important. Of note, caspase 1 is also activated by other inflammasome complexes such as the AIM2, the NLRC4 and the NLRP1 inflammasomes that are engaged by double-stranded cytoplasmic DNA, gram-negative bacteria and muramyl dipeptide, respectively[366–368]. Thus, studying whether GSDMD is necessary for cytokine release upon stimulation of these inflammasomes or if the distribution and organisation of GSDMD pores varies upon stimulation with different inflammasome stimuli would help to uncover whether GSDMD pore function and cytokine secretion through GSDMD

pores is conserved among all caspase 1-mediated inflammasome pathways. Uncovering this would be fundamental for the development of new treatments for diseases mediated by IL-1β and IL-18, that are triggered by different inflammasome pathways.

Macrophages are one of the main sources of IL-1β and IL-18 and that is one of the main reasons why this thesis focuses on this cell type. However, inflammasome pathways can be engaged in multiple myeloid and non-myeloid cells[58]. Therefore, future research should study the role of GSDMD in inflammasome-dependent cytokine release and pyroptosis in other cell types. Moreover, considering the complex environment in which immune cells reside, a broader approach using animal models for NLRP3 inflammasome activation would also be useful, in order to gain a wider understanding of the role of GSDMD in IL-1β secretion following NLRP3 inflammasome activation. This approach would also permit the understanding of whether GSDMD is specifically needed for IL-1β and IL-18 secretion in macrophages, and if GSDMD pores are also necessary for cytokine release upon inflammasome activation in other cell types.

Overall, as the findings of this chapter establish that GSDMD is fundamental for the secretion of IL-1β and IL-18, successful modulation of this pathway may have major implications for the development of future therapies to control pathologies in which these cytokines are overproduced.

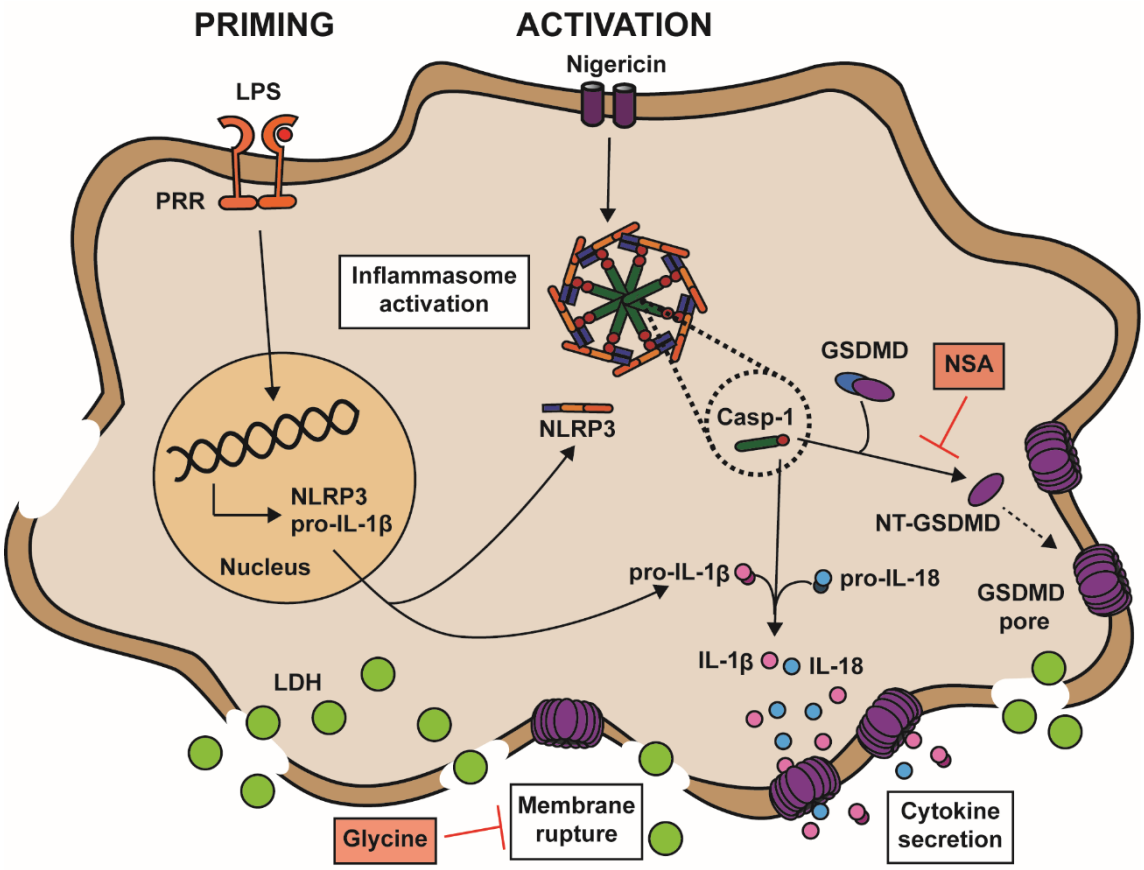

Figure 3.13 The role of GSDMD in IL-1β and IL-18 secretion upon canonical NLRP3 activation in human macrophages. Activation of the NLRP3 inflammasome with LPS and nigericin results in the formation of the NLRP3 inflammasome complex. Within this complex, caspase 1 is activated and processes pro-IL-1β and pro-IL-18 into their mature forms, and GSDMD into its pore forming subunit NT-GSDMD. Upon cleavage by caspase 1, multiple NT-GSDMD subunits assemble in the cell membrane to form pores through which mature IL-1β and IL-18 can be released. GSDMD pore formation also results in membrane rupture, characterized by LDH release, and in pyroptosis. Treatment with the GSDMD inhibitor NSA blocks both cytokine release and pyroptosis, whereas treatment with the osmoprotectant agent glycine blocks membrane rupture and cell death, but not cytokine release or GSDMD pore formation. Thus, this indicates that IL-1β and IL-18 secretion is independent of membrane rupture and cell death, but dependent on GSDMD pores.

Chapter 4 The Membrane Attack Complex activates the NLRP3 inflammasome in human macrophages

4.1 Introduction

The complement system is a group of proteins that acts in a cascade-like fashion that results in the formation of complement component 5a (C5a) and the membrane attack complex (MAC), also known as the terminal complement complex (TCC)[225,369]. This system is activated upon recognition of damage-associated and pathogen-associated molecular patterns (DAMPs and PAMPs), such as LPS, and it has traditionally been considered an adjuvant for the innate immune response[370].

C5a is an anaphylatoxin that mediates inflammation and immune regulation by attraction and activation of effector immune cells such as macrophages, dendritic cells and T cells[225]. The role of C5a as a chemoattractant is well studied. However, C5a can also induce intracellular signalling by binding C5a receptors (C5aR) 1 and 2. For instance, C5a can promote IL-1β secretion in monocytes and functions as a second signal for NLRP3 inflammasome activation in T cells[309,310].

The MAC is a multiprotein complex formed by the complement components C5b, C6, C7 and C8, and by multiple subunits of the complement protein C9. The MAC can form pores in the membrane of pathogens, as well as infected or dysfunctional host cells to lyse them[371]. Healthy host cells are able to prevent MAC lysis through various mechanisms. For example, they can remove the MAC from the cell membrane by exocytosis, endocytosis, or outward vesiculation[275–278]. In addition, the membrane receptor CD59 impairs MAC pore formation in the cell membrane by binding C8 and C9 and preventing the addition of more C9 subunits to the complex. Nevertheless, CD59 can become exhausted during persistent inflammation, permitting MAC insertion into the cell membrane[274]. For instance, the expression of CD59 is reduced in monocytes of patients infected with Dengue virus and in hepatocytes infected with Hepatitis B virus[372,373], and this receptor is downregulated in patients with Alzheimer's disease or

following lung transplantation[374,375]. Moreover, stimuli that activate the NLRP3 inflammasome can also downregulate CD59 expression. For example, treatment of endothelial and epithelial cells with shiga toxin from *E.coli* reduces the amount of membrane-bound CD59 and its mRNA levels[376]. This toxin also activates the NLRP3 inflammasome, leading to GSDMD processing and IL-1β secretion[211,376]. Furthermore, CD59 expression is downregulated in endothelial cells treated with IL-1β[173], suggesting that inflammasome activation could facilitate MAC insertion in the cell membrane. Although the levels of CD59 expression in myeloid cells have not been investigated during inflammation, these findings in endothelial cells could suggest that CD59 levels are reduced in inflammation, facilitating MAC insertion in the cell membrane of macrophages.

The MAC has predominantly been studied for its lytic function. However, it can also activate downstream signalling pathways in host cells. MAC pores can initiate ion fluxes that trigger cell cycle activation and cell proliferation in fibroblasts and smooth muscle cells, but also cell death pathways like necroptosis and apoptosis in other cell types[280,281,377–379]. The MAC can also induce intracellular signalling independently of ion fluxes. For instance, MAC assembly in the cell membrane can activate different metabolic pathways including the metabolism of arachidonate which, among others, results in the production of prostaglandin E2 and other inflammatory mediators from rat macrophages and human monocytes[289,380]. In addition, endocytosis of the MAC also initiates intracellular pathways such as the activation of the NLRP3 inflammasome and IL-1β secretion in endothelial cells[288,292,293].

4.2 Aims and objectives

IL-1β and IL-18 play an important role in the development of multiple inflammatory diseases that are characterised by increased levels of complement components such as toxic shock syndrome or sepsis, rheumatoid arthritis and osteoarthritis, and type II diabetes[176]. As mentioned in chapter 3, IL-1β secretion is tightly regulated by inflammasomes, and blocking IL-1β ameliorates some complement driven-pathologies[295,297,381]. However, the connection between the complement and inflammasome pathways has not been fully explored. Recently, it has been shown that

the complement system not only functions as an adjuvant for the immune system but is also able to initiate cell signalling pathways including the activation of inflammasomes. For example, in combination with TNF, C5a is able to prime the inflammasome in human PBMCs and monocytes activated with cholesterol crystals[382], and potentiates IL-1β secretion in murine LPS-primed peritoneal macrophages exposed to monosodium ureate[312]. Furthermore, serum containing the complement components that form the MAC triggers NLRP3 inflammasome activation in LPS-primed murine dendritic cells, as well as in human epithelial and IFNγ-primed endothelial cells[290,383,292]. Considering that both the inflammasome and the complement system are engaged upon recognition of similar danger signals and that there is evidence for C5a and the MAC to activate the inflammasome in various cell types, the aim of this chapter was to determine whether C5a and the MAC can induce inflammasome activation leading to IL-1β secretion in human macrophages, one of the main sources of this cytokine.

The specific objectives of this chapter were as follows:

1. To determine whether or not C5a can prime the inflammasome in human MDMs.
2. To study if sublytic MAC is able to trigger IL-1β and IL-18 release in human MDMs.
3. To determine if the MAC activates the NLRP3 inflammasome in human macrophages.
4. To establish the role of GSDMD in IL-1β secretion upon stimulation with the MAC in MDMs.
5. To study whether the MAC interacts with the inflammasome speck in human macrophages.

4.3 Results

4.3.1 Establishing whether or not C5a primes the inflammasome in human macrophages

Multiple IL-1β-mediated pro-inflammatory diseases are characterized by high levels of complement deposition. In particular, C5a can potentiate inflammasome priming and activation and engage IL-1β secretion in different cell types, including human monocytes and murine peritoneal macrophages[312,382,384]. Macrophages are one of the primary sources of IL-1β in humans. Thus, we investigated whether C5a primes the inflammasome in human MDMs. Previous studies showed that the use of concentrations in the range of 1 ng/ml to 1 μg/ml engage IL-1β release[312,382]. Thus, we chose an in-between concentration of 100 ng/ml to stimulate MDMs. MDMs were differentiated from monocytes isolated from blood using M-CSF, as described in chapter 3, and stimulated with 100 ng/ml C5a for 4 h followed by 10 μM nigericin in serum-free media for 45 min. MDMs were also treated with 1 μg/ml LPS for 4 h and nigericin for 45 min as a positive control for IL-1β release. Stimulation of MDMs with LPS and nigericin activated the inflammasome as indicated by secretion of IL-1β (Fig 4.1 a) and increased in cell death when compared with untreated cells (Fig 4.1 b). The use of C5a together with nigericin did not significantly increase IL-1β secretion or cell death when compared to unstimulating conditions (Fig 4.1 a and b), being the total concentration of secreted IL-1β 400 ± 746 pg/ml in cells stimulated with C5a and nigericin and 18.3 ± 17.3 pg/ml in untreated cells. Importantly, the standard deviation of the data in cells stimulated with C5a and nigericin was very high, indicating a high variability between donors. Specifically, the MDMs from two of the analysed donors (Fig 4.1 a: green and orange) secreted a higher amount of IL-1β when stimulated with C5a and nigericin when compared to all other donors (Fig 4.1 a). This could indicate that the threshold to respond to C5a stimulation is lower in some donors than in others.

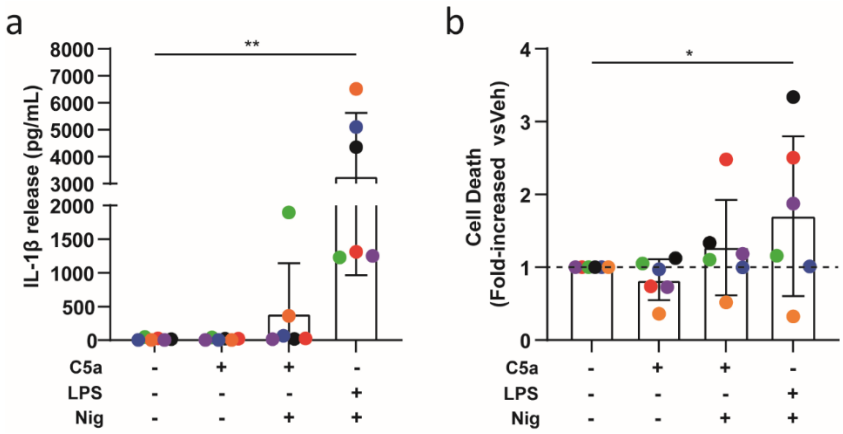

Figure 4.1 C5a stimulation of human MDMs. MDMs were treated with vehicle-only control or primed with 1µg/ml C5a or 1µg/ml LPS for 4 h followed by treatment with 10 µM nigericin (Nig) for 45 min. **a)** IL-1β secretion was measured by ELISA. **b)** LDH release was measured as a proxy for cell death and expressed as fold-increase to unstimulated cells. Data is plotted as mean ± SD, statistical significance was established by Friedman test (*p<0.05 **p<0.01) and each colour represents a matched single donor. Data is representative of 6 independent experiments.

To test whether higher concentrations of C5a could engage IL-1β release in MDMs, concentrations from 10 ng/ml to 2 µg/ml of C5a were used. MDMs were primed with the indicated amount of C5a for 4 h followed by stimulation with 10 µM nigericin for 45 min. Treatment with LPS and nigericin led to a significant increase of IL-1β secretion and cell death (Fig 4.2 a and b), indicating that these MDMs were able to respond to inflammasome activation. However, C5a failed to induce IL-1β release or cell death even when very high concentrations were used (Fig 4.2 a and b). Taking together this data and the previously observed data (Fig 4.1), it was concluded that C5a did not prime the inflammasome in human MDMs.

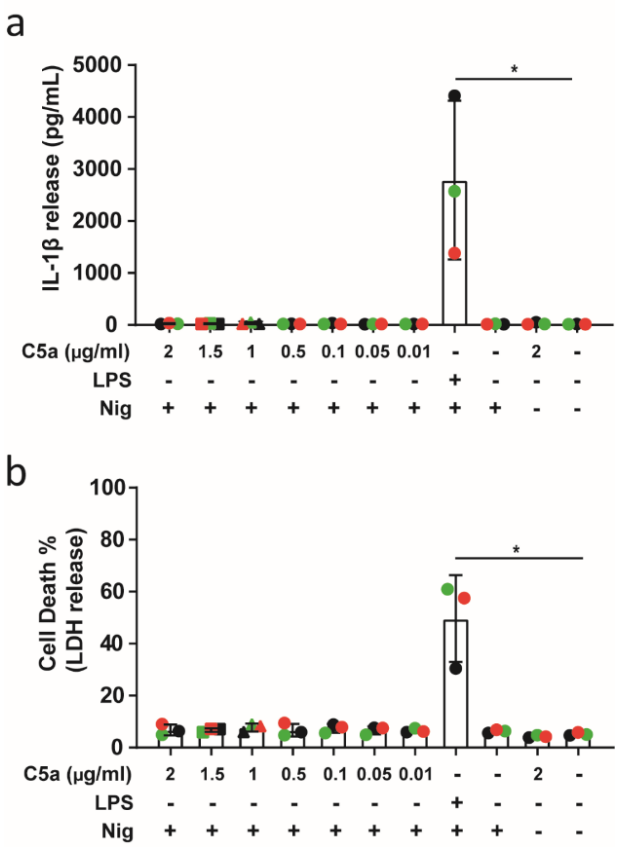

Figure 4.2 C5a titration for stimulation of human MDMs. Cells were treated with vehicle-only controls or primed with the indicated concentrations of C5a or with 1μg/ml LPS for 4 h followed by stimulation with nigericin (Nig) for 45 min. **a)** IL-1β secretion was measured by ELISA. **b)** LDH release was measured as a proxy for cell death. Data is plotted as mean ± SD, statistical significance to untreated cells was established by Friedman test (a) or one-way ANOVA (b) (*p<0.05 **p<0.01 ***p<0.001), each colour represents a matched experiment and data is representative of 3 independent experiments.

4.3.2 The Membrane Attack Complex activates the inflammasome in human MDMs.

In murine cells and human epithelial and endothelial cells, sublytic levels of the MAC, can activate caspase 1 and trigger IL-1β secretion[290,292,383]. However, whether or not the MAC can directly impact inflammasome activation in human myeloid cells, a primary source of IL-1β, is unclear. Understanding this is important because multiple inflammatory diseases are characterized by increased levels of both IL-1β and MAC. For this reason, we next investigate the ability of the MAC to activate the inflammasome in human MDMs. Cells were differentiated from human blood-derived monocytes using M-CSF, as aforementioned (Section 2.1.1). To form the MAC the purified complement components C5b6, C7, C8 and C9 were sequentially added to cells. The receptor CD59

prevents MAC formation in host cells. Nevertheless, this receptor can become exhausted during prolonged inflammation, allowing MAC deposition[274]. To mimic this process, cells were treated with anti-CD59 mAb. To determine the optimal concentrations of purified complement components needed to trigger IL-1β secretion, concentrations from 1 to 20 μg/mL of C5b6, which is the limiting component for MAC formation, were tested (Fig 4.3). MDMs were stimulated with LPS for 3 h followed by the indicated concentration of C5b6 in the presence of 10 μg/ml anti-CD59 mAb in serum-free media for 15 min. Next, cells were treated with 10 μg/ml of C7, C8 and C9 in serum-free media for 3 h. MAC formation and IL-1β release were determined using ELISA assays and cell death was calculated as a percentage of LDH release (Fig 4.3). The amount of MAC detected in cell lysates was enhanced with higher concentrations of C5b6, with a significant increase observed when 2 μg/mL or more of C5b6 were used (Fig 4.3 a). Furthermore, maximum MAC deposition was reached when MDMs were stimulated with 10 μg/mL or 20 μg/mL of C5b6 (Fig 4.3 a). IL-1β secretion was triggered in every condition and maximum release was achieved when cells were stimulated with 10 μg/ml C5b6 (Fig 4.3 b). Cell death remained very low with all concentrations used, suggesting that the effect of the MAC is sublytic (Fig 4.3 b). Considering that the use of 10 μg/ml C5b6 led to maximum IL-1β release and MAC formation, further experiments were carried out using this concentration.

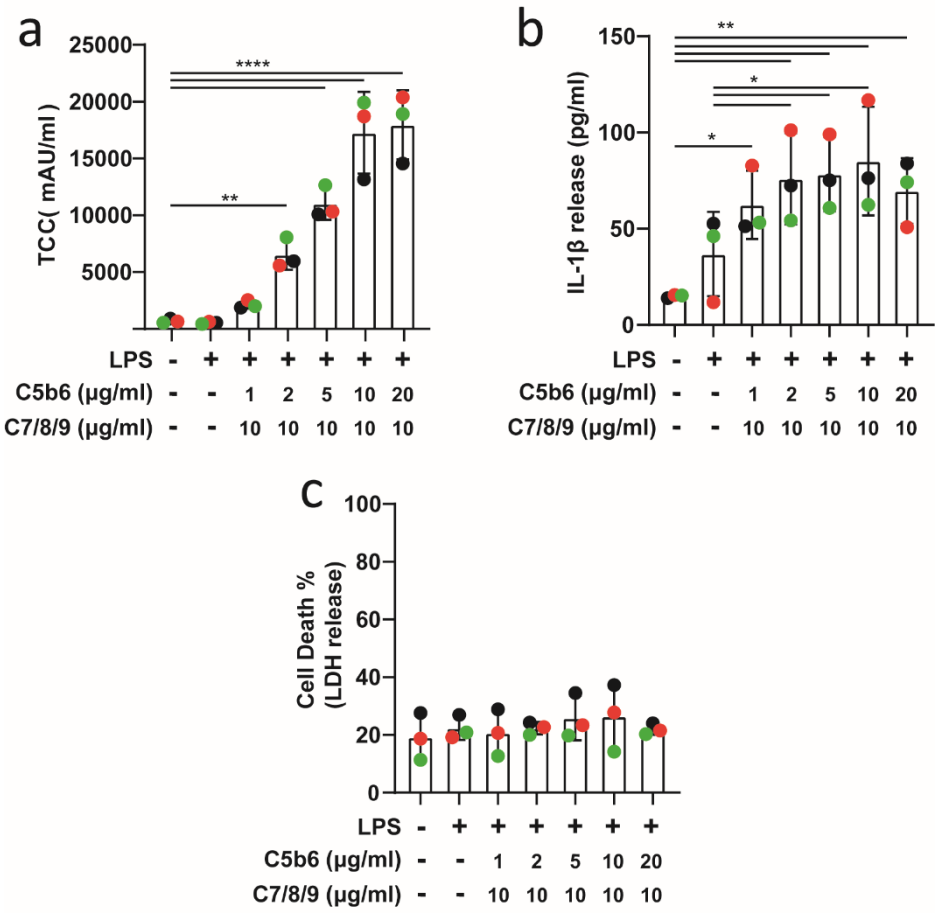

Figure 4.3 C5b6 titration for optimal formation of the MAC and optimal stimulation of IL-1β secretion in human MDMs. Cells were treated with vehicle-only controls or primed with 1 μg/mL LPS for 3 h followed by stimulation with 10 μM nigericin (Nig) for 45 min or with 10 μg/mL anti-CD59 mAb, and the indicated concentration of C5b6, C7, C8 and C9 to form the MAC for 3 h. **a)** TCC (MAC) amount in cell lysates was measured by ELISA. **b)** IL-1β secretion was measured by ELISA. **c)** LDH release was measured as a proxy for cell death. Data is plotted as mean ± SD and is representative of 3 independent experiments, each colour represents a matched donor and statistical significance was measured by one-way ANOVA (*p<0.05 **p<0.01 ****p<0.0001).

The secretion of the cytokine IL-1β is a process tightly regulated by inflammasome complexes. To further investigate MAC-mediated IL-1β secretion in MDMs, events characteristic of inflammasome activation such as cytokine processing, caspase 1 activation and IL-18 release were explored (Fig 4.4). Cells were stimulated with LPS for 3 h followed by stimulation with the MAC for 3 h, or with nigericin for 45min as a positive control. Mature IL-1β and IL-18 release in supernatants was studied using ELISA assays and IL-1β processing was determined by immunoblotting. Caspase 1 activity was assessed using a quantitative luminescence assay and cell death was measured as a percentage of LDH release. As shown in Fig 4.3, stimulation with the MAC

resulted in the secretion of mature IL-1β for cells derived from several different donors, although to a lesser extent than with the positive control nigericin (Fig 4.4 a). In agreement with this, a p17 fragment of IL-1β corresponding with the mature form of this cytokine was detected by immunoblotting in supernatants and cell lysates (Fig 4.4 b and c). Furthermore, a p20 fragment of IL-1β was also released after stimulation with the MAC (Fig 4.4 b). This could indicate a caspase 1-independent cleavage of this cytokine[385]. For this reason, to directly study whether the MAC triggered caspase 1 activation, its activity was measured in supernatants. Caspase 1 activity was significantly increased upon stimulation with the MAC (Fig 4.4 d), as expected for inflammasome activation, suggesting that although other enzymes could be cleaving pro-IL-1β as well, stimulation with the MAC triggers caspase 1 activation in MDMs. Treatment with LPS and the MAC also resulted in the secretion of IL-18 (Fig 4.4 e), further indicating inflammasome activation. As previously observed, MAC formation did not trigger cell death (Fig 4.4 f), confirming that at the concentration used, the MAC has a sublytic effect in MDMs.

Low levels of pro-IL-1β were detected in lysates of cells treated with the MAC alone (Fig 4.4 c), indicating that the MAC could be priming the inflammasome and regulating pro-IL-1β production. In agreement with this, although stimulation with the MAC alone did not result in IL-1β secretion, it resulted in the secretion of IL-18 (Fig 4.4 e), suggesting that the MAC could prime and activate the inflammasome. However, caspase 1 activation was not detected when MDMs were treated with the MAC alone (Fig 4.4 d), indicating that IL-18 processing could have been triggered by other inflammatory caspases in this context.

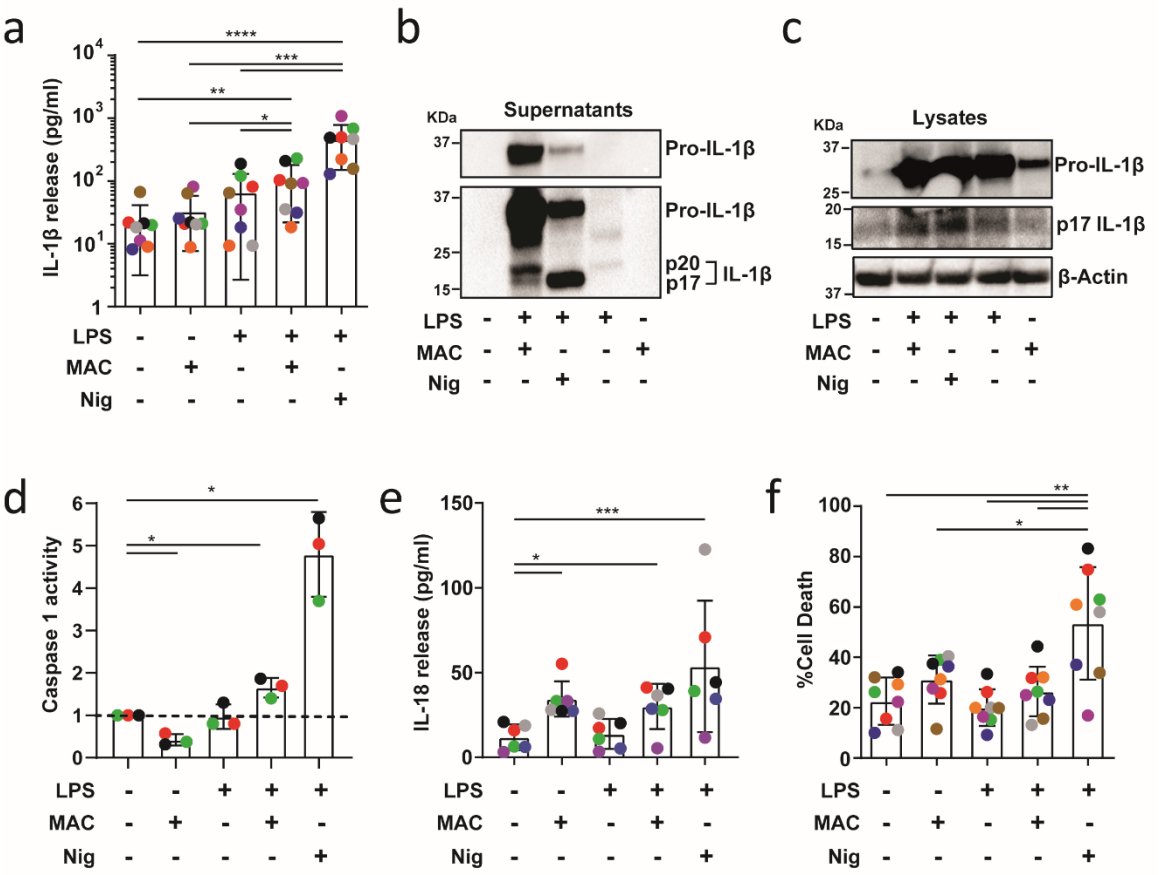

Figure 4.4 The Membrane Attack Complex induces inflammasome activation in human MDMs. Cells were treated with vehicle-only controls or primed with 1 μg/mL LPS for 3 h followed by stimulation with 10 μM nigericin (Nig) for 45 min or with 10 μg/mL anti-CD59 mAb, C5b6, C7, C8 and C9 to form the MAC for 3 h. **a)** IL-1β secretion was measured by ELISA. **b)** IL-1β processing was analysed in cell lysates by immunoblot. **c)** IL-1β processing was analysed in cell supernatants by immunoblot. **d)** Caspase 1 activity was measured in cell supernatants and expressed as fold increase vs untreated cells. **e)** IL-18 secretion was measured by ELISA. **f)** LDH release was measured as a proxy for cell death. In a and d-f data is plotted as mean ± SD, statistical significance was established by Friedman's test (a, e) or one-way ANOVA (d, f) (*p<0.05 **p<0.01 ***p<0.001 ****p<0.0001) and each colour represents a matched single donor. In a and f data is representative of 8, in d of 3, and in e of 6 independent experiments. In b and c blots are representative of 3 independent experiments.

Caspases-4 and 5 can activate caspase 1 leading to inflammasome activation and cytokine secretion[132,133,347]. To further investigate if these caspases have a role in MAC-mediated inflammasome activation, their processing was studied after stimulation with the MAC. MDMs were stimulated for 24 h with LPS alone to induce non-canonical inflammasome activation. As previously shown, treatment with the MAC resulted in IL-1β secretion (Fig 4.5 a) and did not induce cell death (Fig 4.5 b). Furthermore, stimulation with LPS for 24 h led to IL-1β release and cell death (Fig 4.5 a and b), indicating inflammasome activation. Pro-caspase 4 was detected in every condition and treatment

with the MAC alone resulted in caspase 4 processing and activation as evidence by the detection of a p20 fragment corresponding to active caspase 4 in cell lysates (Fig 4.5 c). This p20 fragment became more abundant when cells were primed with LPS before stimulation with the MAC (Fig 4.5 c). On the other hand, pro-caspase-5 was only detected when cells were stimulated with LPS alone or LPS and nigericin, and the MAC did not induce caspase-5 processing (Fig 4.5 d). Importantly, a fragment corresponding to p35 caspase-5 was detected after stimulation with LPS for 24 h, showing that this Ab was able to recognize active/processed caspase-5 (Fig 4.5 d). This treatment did not activate caspase 4 (Fig 4.5 c).

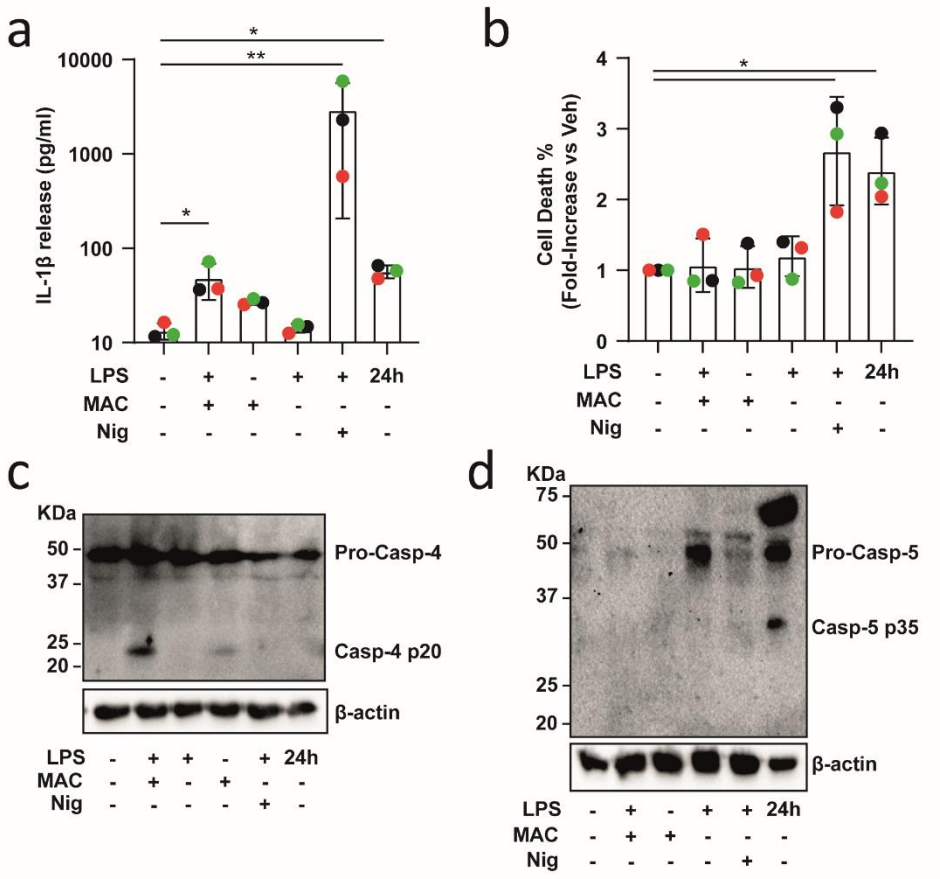

Figure 4.5 The Membrane Attack Complex triggers caspase 4 activation in human MDMs. Cells were treated with vehicle-only controls or primed with 1 μg/mL LPS for 3 h followed by stimulation with 10 μg/mL anti-CD59 mAb, C5b6, C7, C8 and C9 to form the MAC for 3 h or with 1 μg/mL LPS for 24 h. **a)** IL-1β secretion was measured by ELISA. **b)** LDH release was measured as a proxy for cell death. **c)** Caspase 4 processing was analysed in cell lysates by immunoblot. **d)** Caspase 5 processing was analysed in cell lysates by immunoblot. In a and b data is plotted as mean ± SD, statistical significance was established by one-way ANOVA (*p<0.05 **p<0.01) and each colour represents a matched single donor. In a-d data is representative of 3 independent experiments with similar results.

Some Abs can activate the inflammasome by binding Fc receptors and TLR4 in the cell and trigger IL-1β release in human macrophages[386,387]. Thus, the next experiments set out to confirm that the anti-CD59 mAb used together with C5b6 in this project was not driving the observed inflammasome activation in MDMs. Stimulation with anti-CD59 mAb alone did not trigger IL-1β secretion or caspase 1 activation (Fig 4.6 a and b), nor did it induce cell death (Fig 4.6 c). Moreover, stimulation with LPS and the MAC in the absence of anti-CD59 mAb resulted in a small secretion of IL-1β (Fig 4.6 a). LPS priming alone also induced low level secretion of IL-1β (108 ± 42 pg/ml), but to a lesser extent than when combined with the MAC, both in the presence or absence of anti-CD59 mAb (130 ± 54 pg/ml and 180 ± 67 pg/ml, respectively) (Fig 4.6 a). Overall, this indicated that anti-CD59 mAb is not responsible for inflammasome activation, and rather the MAC, in combination with LPS priming, is triggering this process.

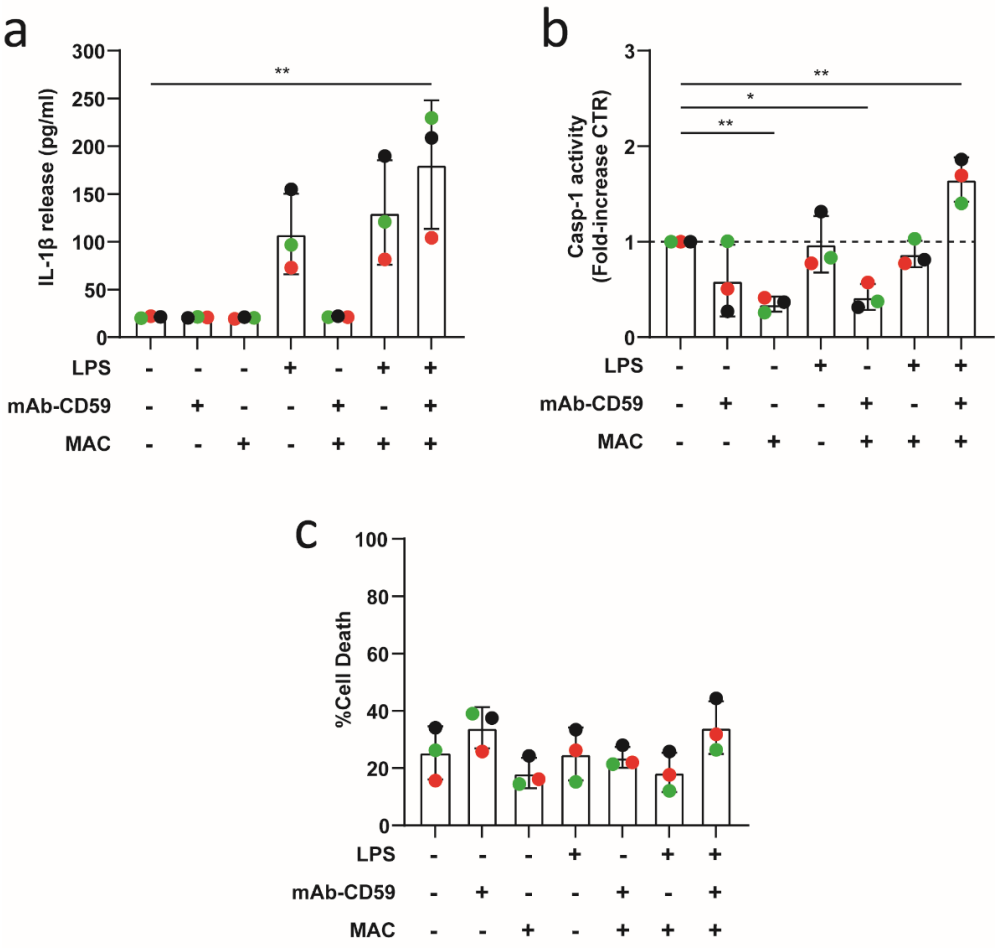

Figure 4.6 Anti-CD59 mAb (BRIC 229) does not induce inflammasome activation in human MDMs. Cells were treated with vehicle-only control or with 1 μg/mL LPS for 3 h followed by stimulation with 10 μg/mL C5b6, C7, C8 and C9 (MAC) or 10 μg/mL anti-CD59 mAb and the MAC or only 10 μg/mL anti-CD59 mAb for 3 h. **a)** IL-1β secretion was measured by ELISA. **b)** Caspase 1 activity was measured in cell supernatants and expressed as fold increase vs untreated cells. **c)** LDH release was measured as a proxy for cell death. In a-c data is plotted as mean ± SD and is representative of 3 independent experiments, each colour represents a matched single donor and statistical significance was measured by one-way ANOVA (*p<0.05 **p<0.01 ***p<0.001).

As previously discussed, the human monocyte-like cell line, THP1 is a common model for inflammasome research in human monocytes and macrophages. Hence, the following experiments investigated whether the MAC triggered inflammasome activation in this cell line. THP1 cells were treated using 50 nM PMA for 16 h to acquire a macrophage-like phenotype. Cells were then rested for 24 h and treated with LPS for 3 h and the MAC, which was formed by sequential addition of C5b6, in the presence of anti-CD59 mAb, C7, C8 and C9 for 3 h. Alternatively, cells were stimulated with LPS followed by nigericin during 45 min as a positive control for NLRP3 inflammasome activation. As expected, treatment with nigericin resulted in IL-1β secretion, LDH release and GSDMD processing, indicative of inflammasome activation (Fig 4.7 a-d). Stimulation with the MAC also triggered IL-1β secretion although to a lesser extent than with nigericin (Fig 4.7 a). In agreement with this, a p17 fragment corresponding with mature IL-1β was detected in cell supernatants by immunoblot (Fig 4.7 b). As in MDMs, the MAC did not induce cell death (Fig 4.7 c), indicating that this complex had a sublytic effect in THP1 cells. Furthermore, the MAC also induced GSDMD processing as evidenced by the detection of a p30 fragment corresponding with the pore-forming NT-GSDMD in cell lysates (Fig 4.7 d). Altogether these data show that the MAC can activate the inflammasome not only in human primary macrophages (MDMs), but also in macrophage-like cell lines (THP1 cells).

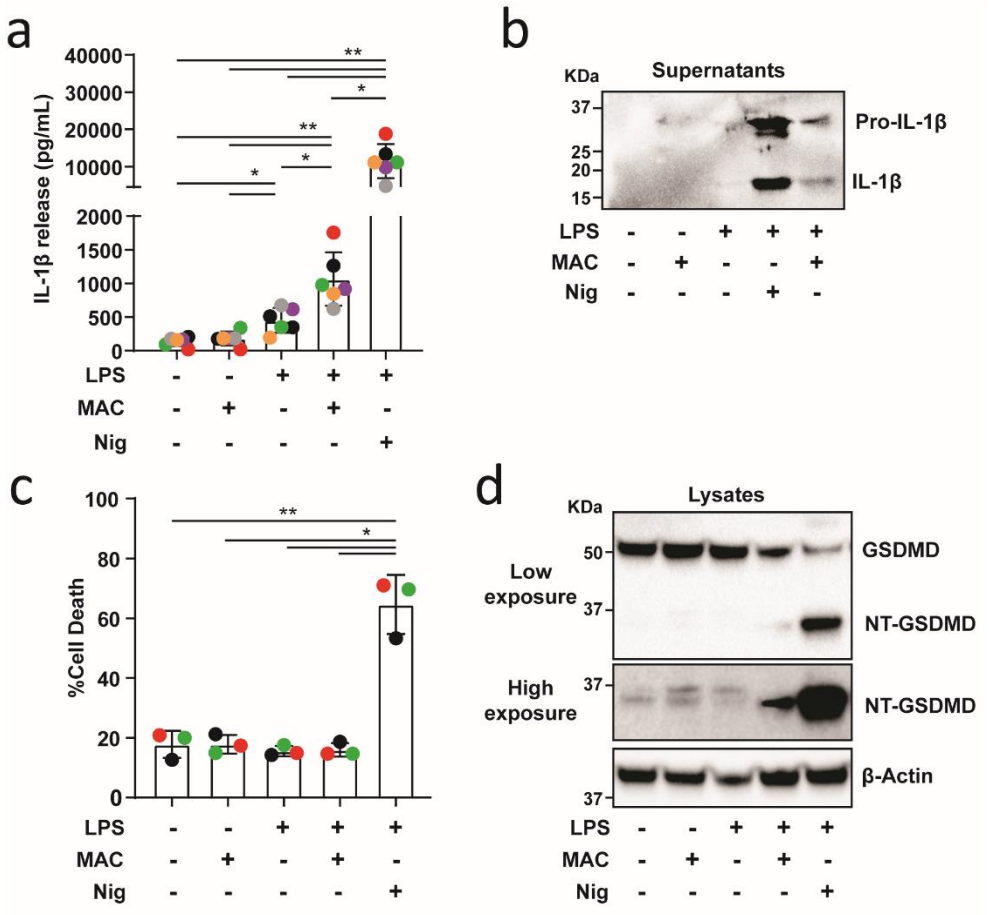

Figure 4.7 The Membrane Attack Complex induces inflammasome activation in THP1 cells. Cells were treated with vehicle-only controls or primed with 1 μg/mL LPS for 3 h followed by stimulation with 10 μM nigericin (Nig) for 45 min or with 10 μg/mL anti-CD59 mAb, C5b6, C7, C8 and C9 to form the MAC for 3 h. **a)** IL-1β secretion was measured by ELISA. **b)** IL-1β processing was analysed in cell supernatants by immunoblot. **c)** LDH release was measured as a proxy for cell death. **d)** GSDMD processing was analysed in cell lysates by immunoblot. In a and c data is plotted as mean ± SD, statistical significance was established by Friedman's test (a, e) or one-way ANOVA (d, f) (*p<0.05 **p<0.01) and each colour represents a repeat. In a data is representative of 6 and in b-d of 3 independent experiments with similar results.

4.3.3 Membrane Attack Complex-mediated IL-1β secretion is dependent on the NLRP3 inflammasome.

Multiple inflammasomes can trigger caspase 1 activation leading to IL-1β and IL-18 secretion[55]. It has been previously decribed that the complement system triggers activation of the NLRP3 inflammasome[284,290,292,383]. Thus, the next set of experiments aimed to determine if this inflammasome mediates IL-1β secretion in MDMs upon stimulation with the MAC. Mutiple NLRP3 activators induce Ca^{2+} or K^+ fluxes that play a role in inflammasome activation[388,389]. Specifically, K^+ efflux is considered to be a crucial

event needed for the activation of the NLRP3 inflammasome with multiple stimuli[114]. Thus, MAC-mediated IL-1β secretion was studied in the prescene of high concentrations of extracellular K^+ to block its efflux. MDMs were primed with LPS for 3 h and stimulated with the MAC for 3 h or nigericin for 45 min in E-total (ET) buffer, or ET buffer supplemented with high K^+ [390]. As previously shown, stimulation with the MAC or nigericin induced IL-1β secretion (Fig 4.8 a) but cell death was only induced by nigericin (Fig 4.8 b). Although not statistically significant, likely due to the high levels of variability among donors, the use of high K^+ considerably reduced IL-1β secretion upon treatment with nigericin from 2210 pg/ml to 84 pg/ml on average (Fig 4.8 a). Moreover, blocking K^+ efflux significantly reduced cell death upon stimulation with nigericin (Fig 4.8 b), suggesting inhibition of the inflammasome. When the MAC was used to stimulate the inflammasome, the amount of IL-1β released when K^+ eflux was blocked was only reduced by half compared to stimulation in ET buffer (96 pg/ml vs 57 pg/ml on average) (Fig 4.8 a). This indicates that MAC-mediated IL-1β secretion may only be partially dependent on K^+ eflux.

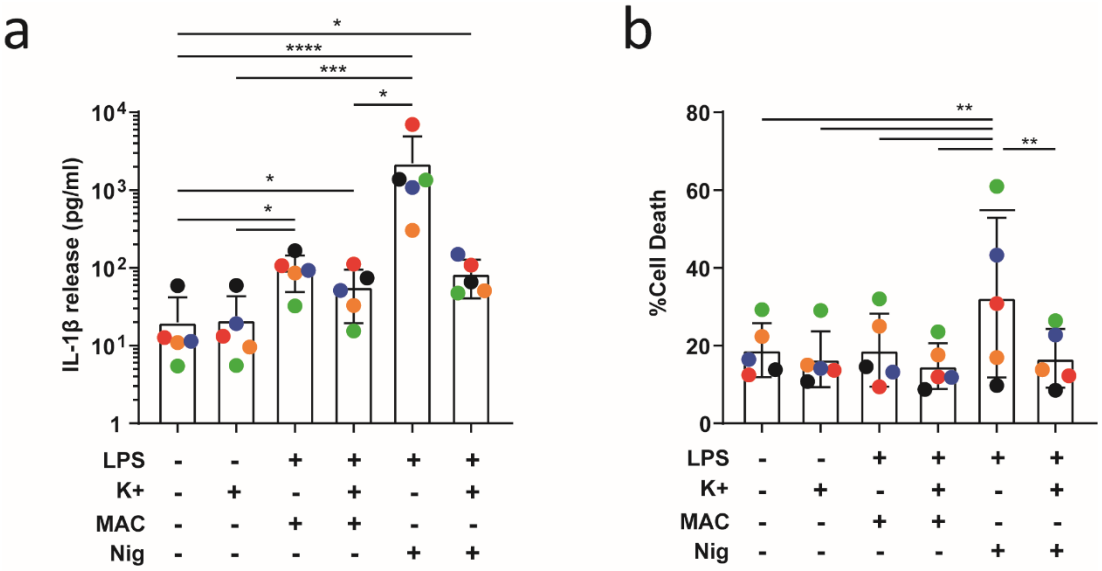

Figure 4.8 K+ efflux inhibition does not block MAC-mediated IL-1β secretion in MDMs. Cells were treated with vehicle-only control or with 1 μg/mL LPS for 3 h followed by stimulation with 10 μg/mL anti-CD59 mAb, C5b6, C7, C8 and C9 (MAC) for 3 h or with nigericin (Nig) for 45 min in the presence or absence of high K+. **a)** IL-1β secretion was measured by ELISA. **b)** LDH release was measured as a proxy for cell death. In a and b data is plotted as mean ± SD and is representative of 5 independent experiments, each colour represents a matched single donor and statistical significance was measured by Friedman's test (a) or one-way ANOVA (b) (*p<0.05 **p<0.01 ***p<0.001 ****p<0.0001).

Potassium efflux is considered one of the upstream events leading to NLRP3 inflammasome activation. However, K^+ efflux-independent mechanisms for NLRP3 inflammasome activation have also been described[117]. For this reason, the NLRP3 inflammasome inhibitor MCC950 was used to directly investigate the involvement of NLRP3 in MAC-mediated IL-1β secretion[391]. MDMs were primed with LPS for 3 h, treated with 10 µM MCC950 for 30 min and activated with the MAC for 3 h, or with nigericin for 45 min as a positive control. As previously reported, the use of MCC950 significantly reduced IL-1β secretion in cells stimulated with nigericin (Fig 4.9 a), showing the efficacy of the inhibitor. Moreover, MAC-mediated IL-1β release was also impaired by MCC950 (Fig 4.9 a), indicating that MAC-mediated inflammasome activation is dependent on NLRP3. In contrast, there was no statistically significant change in LDH release produced by the MAC in the presence of MCC950, establishing that cell death was not altered by addition of this inhibitor (Fig 4.9 b).

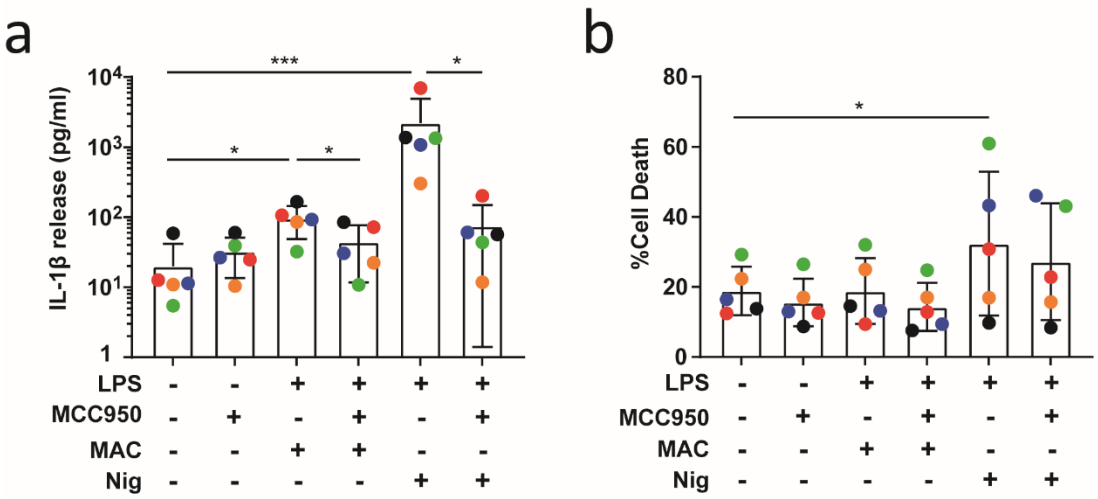

Figure 4.9 MAC-mediated IL-1β secretion is dependent on NLRP3 in MDMs. Cells were treated with vehicle-only control or with 1 µg/mL LPS for 3 h followed by stimulation with 10 µg/mL anti-CD59 mAb, C5b6, C7, C8 and C9 (MAC) for 3 h or with nigericin (Nig) for 45 min in the presence or absence of 10 µM MCC950. **a)** IL-1β secretion was measured by ELISA. **b)** LDH release was measured as a proxy for cell death. In a and b data is plotted as mean ± SD and is representative of 5 independent experiments, each colour represents a matched single donor and statistical significance was measured by one-way ANOVA (*p<0.05 **p<0.01 ***p<0.001).

To investigate whether NLRP3 mediated GSDMD processing and IL-1β release in THP1 cells, a THP1$^{nlrp3-/-}$ cell line was used. These cells were a gift from Prof. Veit Hornung (Gene Centre Munich)[133]. Wild type THP1 cells and THP1$^{nlrp3-/-}$ cells were used in the

following experiments (Fig 4. 10). Cells were differentiated with PMA and treated with LPS for 3 h followed by the MAC for 3 h or nigericin for 45 min as aforementioned. Immunoblotting of NLRP3 in cell lysates from wild type THP1 cells and THP1$^{nlrp3-/-}$ cells verified the lack of NLRP3 expression in the THP1$^{nlrp3-/-}$ cell line (Fig 4. 10 a). Stimulation with LPS and nigericin triggered IL-1β secretion and increased cell death in wild type THP1 cells (Fig 4. 10 b and c). However, these events were impaired in THP1$^{nlrp3-/-}$ cells (Fig 4. 10 b and c), confirming the ablation of NLRP3. Following LPS and MAC treatment, IL-1β secretion was also impaired in THP1$^{nlrp3-/-}$ cells (Fig 4. 10 b). As in wild type THP1 cells, the MAC had a sublytic effect in THP1$^{nlrp3-/-}$ cells, as it did not trigger cell death (Fig 4. 10 c). Thus, NLRP3 is essential for MAC-mediated IL-1β release in human macrophage-like THP1 cells.

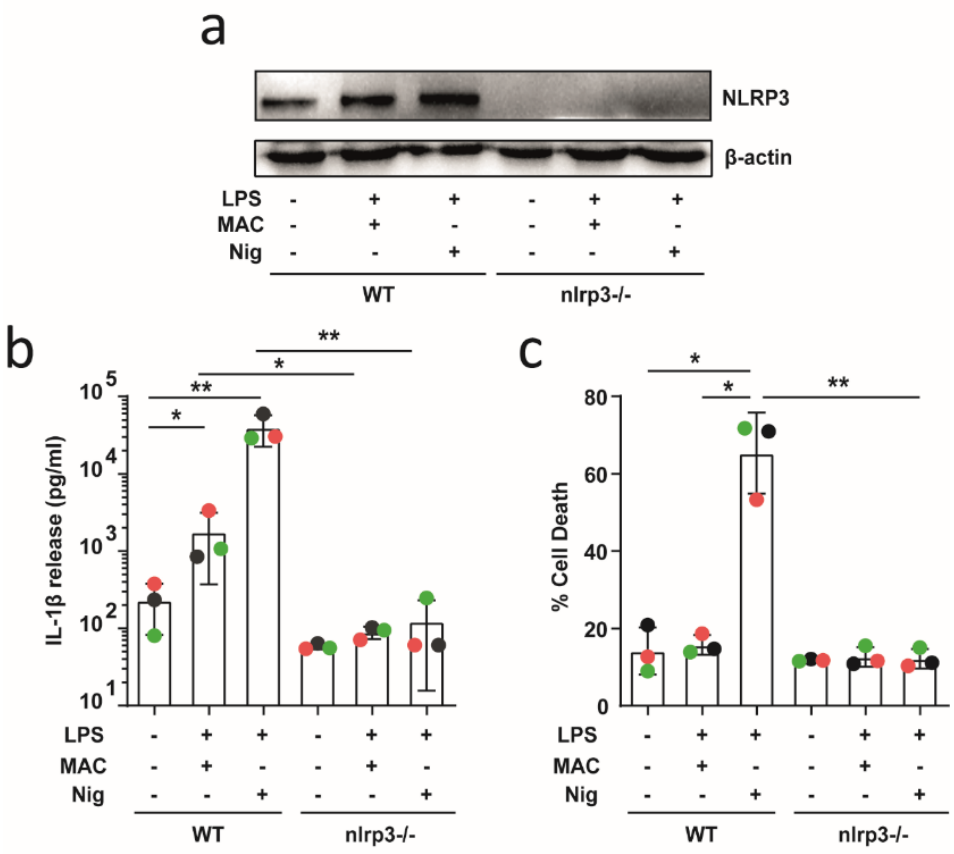

Figure 4.10 MAC-mediated IL-1β secretion is dependent on NLRP3 in THP1 cells. Wild type (WT) or THP1$^{nlrp3-/-}$ cells were treated with vehicle-only controls or primed with 1 μg/mL LPS for 3 h followed by stimulation with 10 μM nigericin (Nig) for 45 min or with 10 μg/mL anti-CD59 mAb, C5b6, C7, C8 and C9 to form the MAC for 3 h. **a)** NLRP3 was analysed in cell lysates by immunoblot. **b)** IL-1β secretion was measured by ELISA. **c)** LDH release was measured as a proxy for cell death. In b and c data is plotted as mean ± SD, statistical significance was established by one-way ANOVA (*p<0.05 **p<0.01) and each colour represents a repeat. In a-c data is representative of 3 independent experiments with similar results.

4.3.4 GSDMD is responsible for Membrane Attack Complex-mediated IL-1β secretion in human MDMs.

The previous chapter established that GSDMD drives IL-1β secretion following canonical NLRP3 inflammasome activation in human macrophages. For this reason, the following experiments investigated whether IL-1β release in MDMs upon stimulation with the MAC is GSDMD-dependent. To test this, MDMs were primed with LPS for 3 h. Then, cells were treated with the GSDMD pore inhibitor necrosulfonamide (NSA) for 30 min[352], and stimulated with the MAC for 3 h, or nigericin for 45 min as a positive control. Akin to cells treated with nigericin, stimulation with the MAC resulted in GSDMD processing as evidenced by the detection of a p30 fragment of GSDMD, corresponding with the pore-forming subunit NT-GSDMD (Fig 4.11 a). As in chapter 3, GSDMD processing was impaired by NSA in MDMs treated with nigericin, evidenced by a lack of NT-GSDMD detection by immunoblotting (Fig 4.11 a). NSA also impaired IL-1β secretion upon nigericin treatment (Fig 4.11 b). Importantly, MAC-mediated GSDMD processing was also blocked by NSA (Fig 4.11 a), and NSA-treated MDMs released significantly less IL-1β upon stimulation with the MAC (Fig 4.11 b). On the other hand, cell death was not significantly affected across conditions (Fig 4.11 c). Altogether, these data suggest that GSDMD processing in MDMs, and consequently pore formation, is important for IL-1β secretion upon stimulation with the MAC.

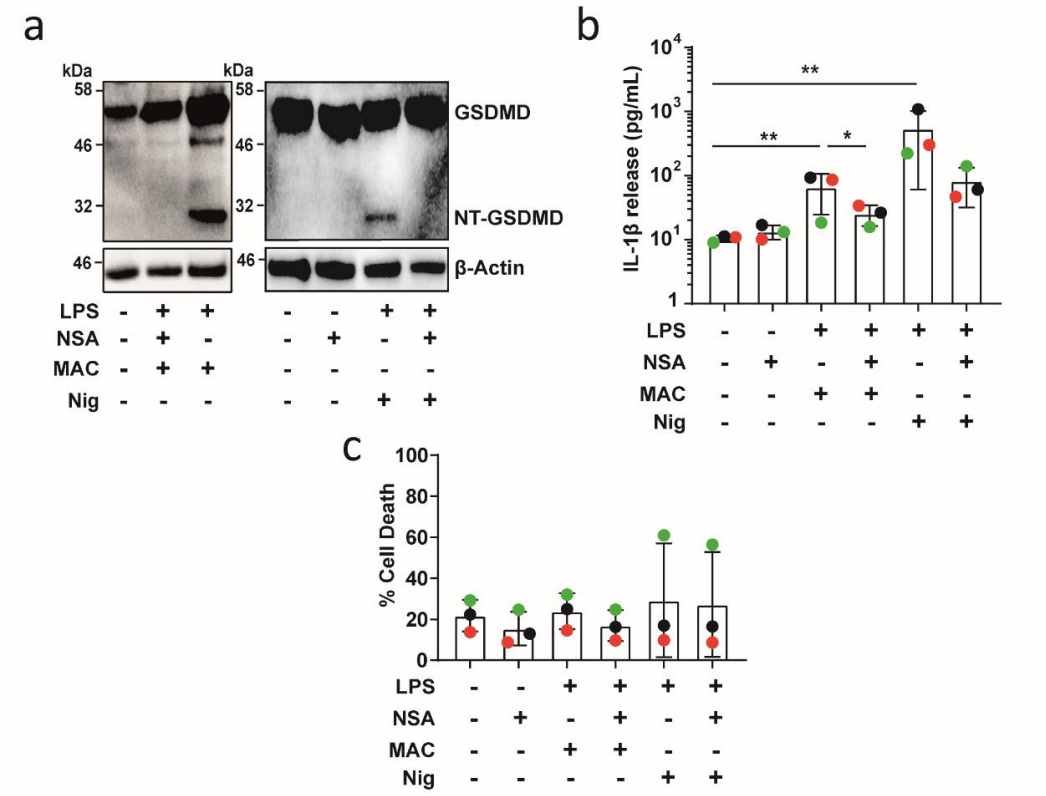

Figure 4.11 MAC-mediated IL-1β secretion is dependent on GSDMD in MDMs. Cells were treated with vehicle-only controls or with 1 μg/mL LPS for 3 h followed by stimulation with 10 μg/mL anti-CD59 mAb, C5b6, C7, C8 and C9 (MAC) for 3 h or with nigericin (Nig) for 45 min in the presence or absence of 10 μM NSA. **a)** GSDMD processing was analysed in cell lysates by immunoblot. **b)** IL-1β secretion was measured by ELISA. **c)** LDH release was measured as a proxy for cell death. In b and c data is plotted as mean ± SD and is representative of 3 independent experiments, each colour represents a matched single donor and statistical significance was measured by one-way ANOVA (*p<0.05 **p<0.01 ***p<0.001).

4.3.5 The Membrane Attack Complex localizes with the NLRP3 inflammasome in human macrophages

Having established that MAC-mediated IL-1β release is dependent on NLRP3 in MDMs (Fig 4.12), to determine whether the MAC interacts with NLPR3, the next set of experiments investigated the localisation of the inflammasome complex and the MAC within cells using confocal microscopy. The MAC is formed by a single subunit of C5b6, C7 and C8 and multiple C9 subunits[256]. For this reason, visualization of this complex was achieved by direct labelling of C9 with the fluorescent dye Janelia Fluor 549 (C9-JF549). An anti-TCC mAb was used to stain samples in order to confirm that the detected C9 was part of the MAC complex, and not an individual subunit. Here, this mAb binds an epitope of the MAC that only appears when C5b6, C7 and C8 are assembled in the complex.

Canonical NLRP3 activation is characterized by the oligomerization of the adaptor protein ASC into a speck[68,83,392]. Thus, cells were stained with an anti-ASC mAb to visualize the inflammasome complex. MDMs were treated with LPS for 3 h and the MAC, using C9-549, for the time indicated. Confocal imaging revealed intracellular C9 30 min after MAC treatment, and the percentage of cells with readily detectable intracellular C9 slightly increased over 3 h (Fig 4.12 a and b). Staining with anti-TCC mAb confirmed these findings (Fig 4.12 a and c). However, the percentage of cells staining with this mAb was lower than the percentage of cells with intracellular C9 (Fig 4.12 b and c). This could suggest that the anti-TCC mAb did not stain all MAC complexes, but also that part of the detected C9 is not bound to C5b6, C7 and C8.

ASC speck formation was detected after 90 min of MAC stimulation, indicative of inflammasome assembly and the percentage of cells with ASC specks increased over 3 h following stimulation (Fig 4.12 a and d). Surprisingly, C9 accumulated in specific regions of the cell and formed structures with a similar appearance to the ASC specks (Fig 4.12 a and e). Furthermore, after 3 h of MAC-stimulation, ASC and C9 colocalised in the majority of cells containing ASC specks (Fig 4.12 a and e). The anti-TCC mAb also marked the regions where both C9 and ASC were detected (Fig 4.12 a and e), establishing that the complete MAC complex is internalized by macrophages and colocalised with the inflammasome speck.

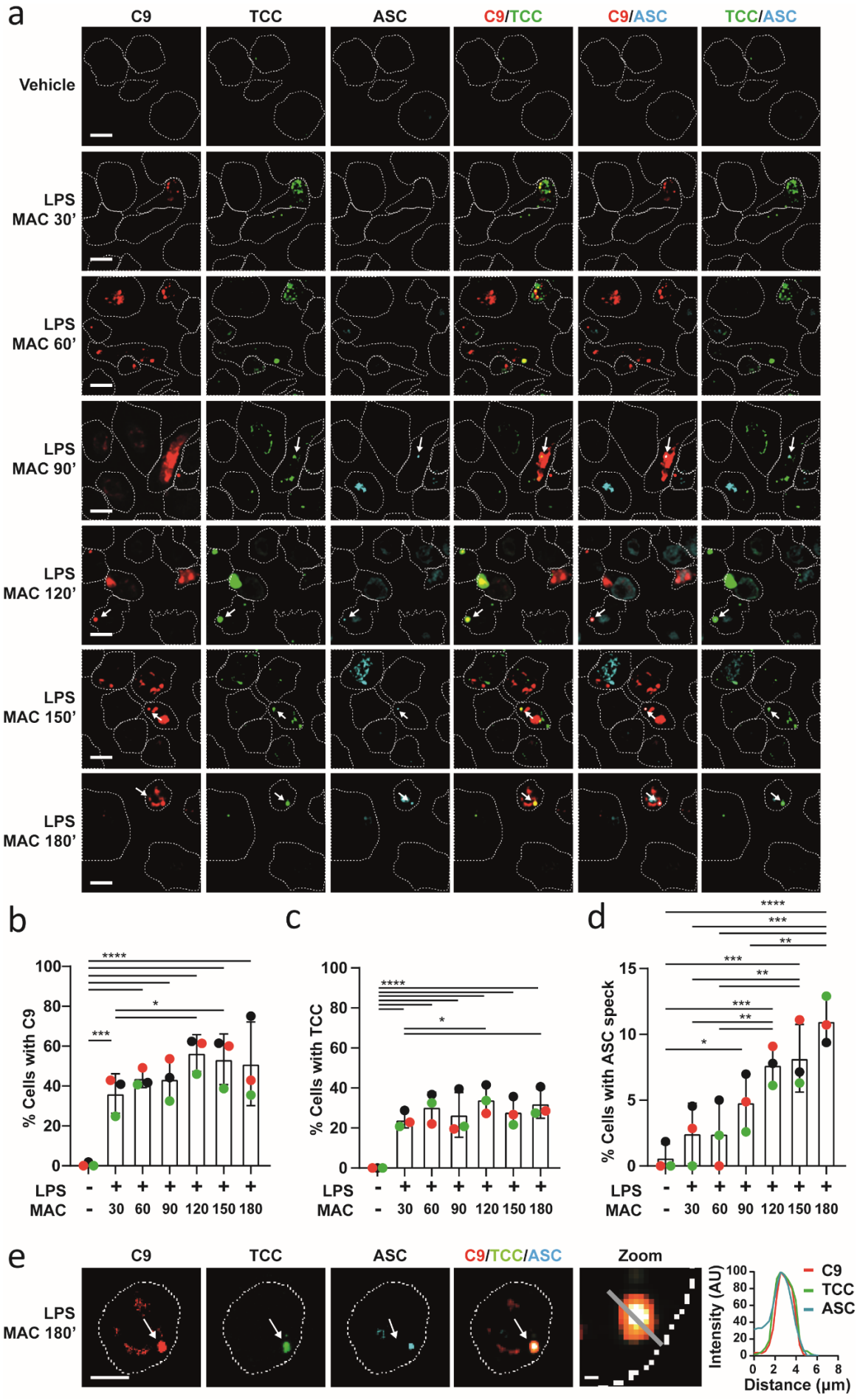
a
C9
TCC
ASC
C9/TCC
C9/ASC
TCC/ASC
Vehicle
LPS MAC 30'
LPS MAC 60'
LPS MAC 90'
LPS MAC 120'
LPS MAC 150'
LPS MAC 180'
b
% Cells with C9
c
% Cells with TCC
d
% Cells with ASC speck
LPS
MAC
- 30 60 90 120 150 180
e
C9/TCC/ASC
Zoom
Intensity (AU)
Distance (µm)

Figure 4.12 The MAC triggers inflammasome assembly and localizes to the ASC speck in MDMs. Cells were treated with vehicle-only controls or with 1 µg/mL LPS for 3 h followed by stimulation with 10 µg/mL anti-CD59 mAb, C5b6, C7, C8 and C9 labelled with JF-549 (MAC) for the indicated time. **a)** Representative confocal images of C9 (red), TCC (green) and ASC (cyan) overtime, scale bars are 20 µm. **b)** Percentage of cells with C9 overtime. **c)** Percentage of cells with TCC overtime. **d)** Percentage of cells with ASC specks overtime. **e)** ROI from panel a, and fluorescence intensity of C9, ASC and TCC along the indicated line profile, scale bars are 5 µm in ROI and 1 µm in Zoom picture. In b-d data is plotted as mean ± SD, each colour represents a matched single donor and statistical significance was measured by one-way ANOVA (*p<0.05 **p<0.01 ***p<0.001 ****p<0.0001). In a and e dashed lines represent the outline of the cell and arrows point to specks. In a-e data is representative of 3 independent experiments and ≥ 117 cells were imaged per condition.

To test whether MAC localisation to the inflammasome speck also happened in THP1 cells, these cells were differentiated using PMA and activated with LPS and the MAC, containing C9-JF549, for 3 h. Cells were then stained with an anti-ASC mAb to identify inflammasome specks. Treatment with LPS and the MAC resulted in ASC speck formation (Fig 4.13 a and b) and C9 accumulation in speck-like puncta (Fig 4.13 a). Furthermore, the majority of cells with an ASC speck also had an accumulation of C9 localized to this site (Fig 4.13 c) indicating that as in MDMs, stimulation with the MAC results in inflammasome assembly and MAC colocalisation with the inflammasome complex in THP1 cells.

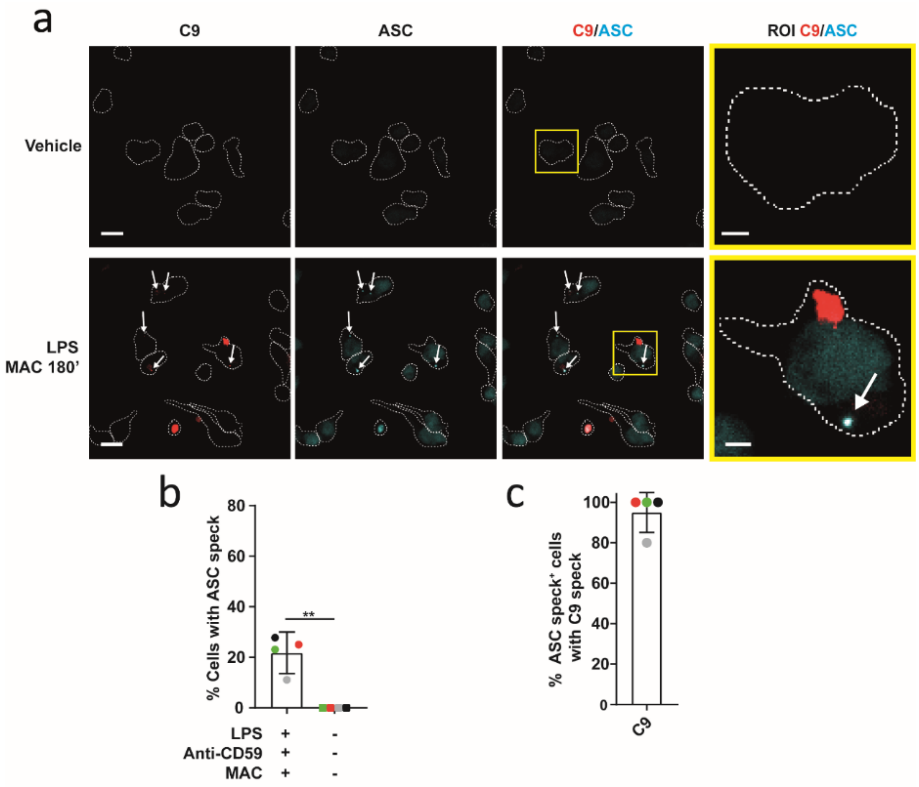

Figure 4.13 The MAC triggers inflammasome assembly and localizes to the ASC speck in THP1 cells. Cells were treated with vehicle-only control or with 1 μg/mL LPS for 3 h followed by stimulation with 10 μg/mL anti-CD59 mAb, C5b6, C7, C8 and C9 labelled with JF-549 (MAC) for 3 h. **a)** Representative confocal images of C9 (red) and ASC (cyan), scale bars are 20 μm and 5 μm in ROI, dashed lines represent the outline of the cell and arrows point to specks. **b)** Percentage of cells with C9. **c)** Percentage of ASC speck positive cells with C9 in the speck. In b and c data is plotted as mean ± SD, each colour represents a matched single donor and statistical significance was measured by un-paired t-test (**p<0.01). In a-c data is representative of 4 independent experiments and ≥ 104 cells were imaged per condition.

To specifically investigate whether the NLRP3 sensor oligomerized upon stimulation with the MAC and localized to the ASC speck, a THP1 cell line that stably expressed eGFP-NLRP3 on an nlrp3$^{-/-}$ background (eGFP-NLRP3-THP1$^{nlrp3-/-}$) was generated as explained in Chapter 2 (Section 2.2.1.1). For this, THP1$^{nlrp3-/-}$ cells were transduced with lentiviral particles containing the vector pLNT-UbC-EGFP-NLRP3. First, the ability of these cells to form an active inflammasome was tested. Stimulation of eGFP-NLRP3-THP1$^{nlrp3-/-}$cells with LPS for 3 h and nigericin for 45 min resulted in IL-18 and IL-1β release (Fig 4. 14 a and b), and caspase 1 activation, as shown by the detection of a p20 fragment corresponding to processed caspase 1 (Fig 4. 14 b). LPS and nigericin treatment also induced cell death (Fig 4. 14 c), and ASC and NLRP3 speck formation (Fig 4. 14 d and e). Furthermore, the use of the NLRP3 inhibitor MCC950 blocked IL-18 secretion, cell death and ASC speck formation (Fig 4.14 a, c and e). Altogether, these results confirmed that transduction of THP1$^{nlrp3-/-}$ cells with eGFP-NLRP3 restored the ability of these cells to form an active inflammasome and that eGFP-NLRP3 is functionally active.

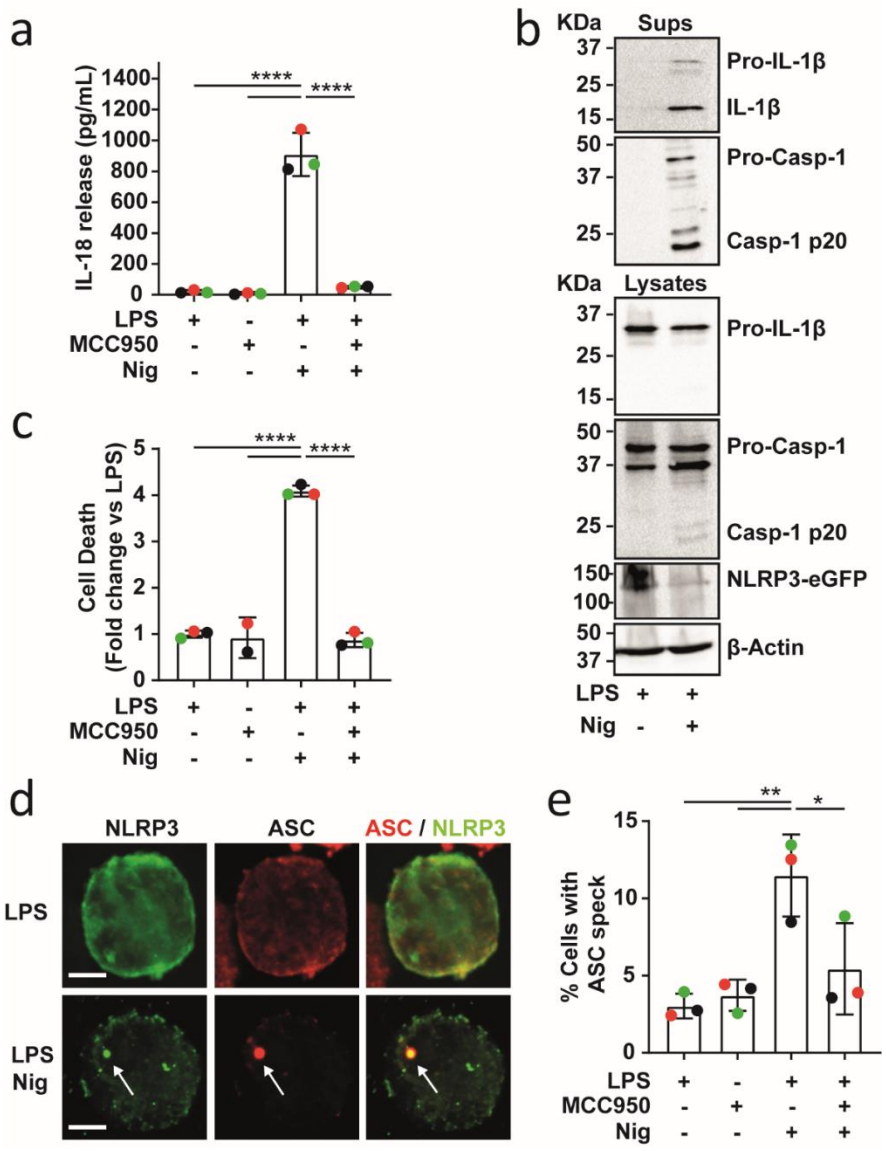

Figure 4.14 EGFP-NLRP3-THP1$^{nlrp3-/-}$ cells exhibit NLRP3 inflammasome activation. THP1$^{nlrp3-/-}$ cells were reconstituted with eGFP-NLRP3, differentiated with 50 nM PMA towards a macrophage-like phenotype and stimulated with vehicle-only controls or 1 µg/mL LPS for 3 h followed by 10 µM (nigericin) Nig for 30 min. **(a, c, e)** Nig treatment took place in the presence or absence of 10µM MCC950**. a)** IL-18 secretion was measured by ELISA. **b)** IL-1β and casp-1 processing was studied in supernatants and cell lysates and eGFP-NLRP3 in lysates by immunoblot. **c)** LDH release was measured as a proxy for cell death and represented as fold change increase vs LPS-treated cells. **d)** Representative confocal images of eGFP-NLRP3 (green) and ASC (red). Arrows point to specks, scale bars are 5 µm and ≥ 97 cells were imaged per condition. **e)** Percentage of cells with ASC specks. In a-c and e data is plotted as mean ± SD and is representative of 3 independent experiments, each colour represents an independent experiment and statistical significance was measured by one-way ANOVA (*p<0.05 **p<0.01 ****p<0.0001). In b immunoblots are representative of 2 independent experiments.

EGFP-NLRP3-THP1$^{nlrp3-/-}$ cells were next used to investigate whether the MAC triggered NLRP3 oligomerization and colocalisation to the ASC speck. These cells were stimulated with LPS and the MAC, with C9-JF549, for 3 h, and then stained with an anti-ASC mAb. As in wild type THP1 cells, the MAC induced ASC speck formation (Fig 4.15 a).

Moreover, it also triggered NLRP3 oligomerization and speck formation (Fig 4.15 a). The percentage of cells with an NLRP3 speck alone was slightly higher than the percentage of cells with an NLRP3 and an ASC speck (30 ±17 % vs 43±20 %), indicating that NLRP3 oligomerization occurred before ASC addition to the inflammasome complex. Importantly, C9 also localized to the ASC speck (Fig 4.15 a and c) and more than 75% of ASC speck positive cells had C9 and NLRP3 in the speck (Fig 4.15 c). Altogether, these data further indicate that the MAC triggers ASC oligomerization, and NLRP3 inflammasome assembly and activation in human macrophages.

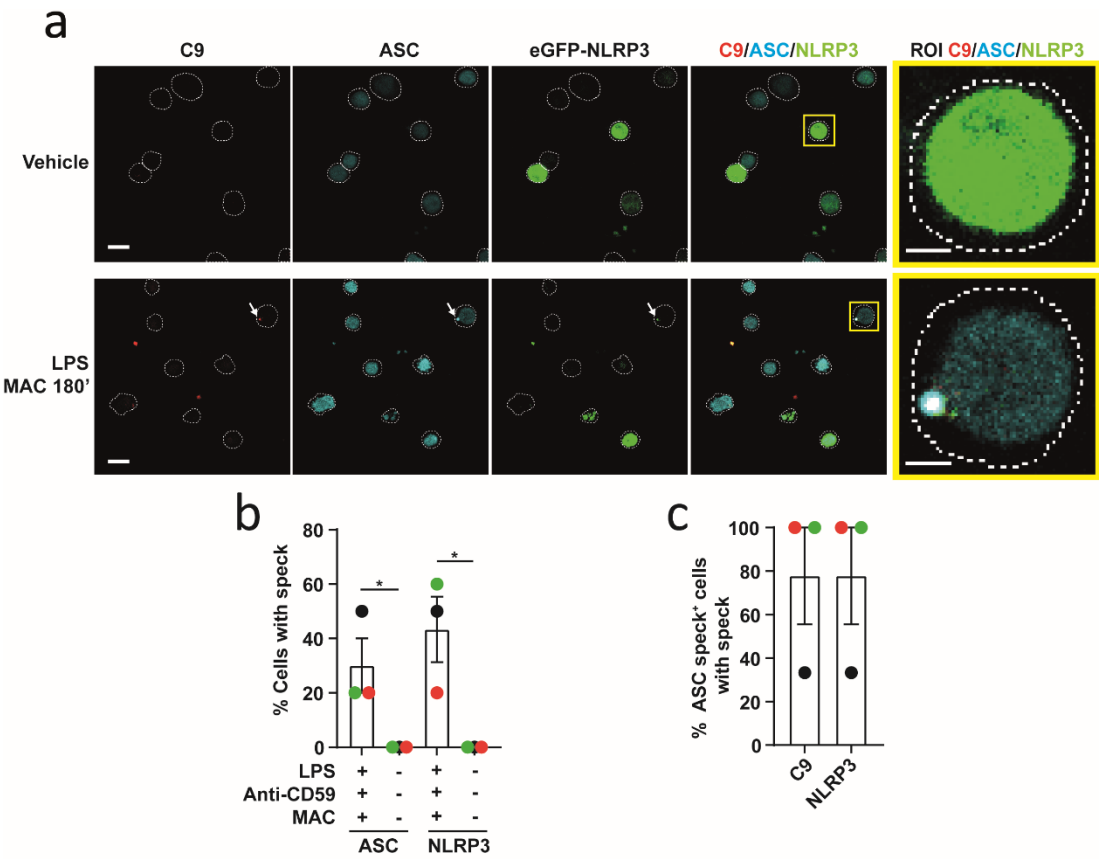

Figure 4.15 The MAC triggers inflammasome assembly and localizes to the ASC-NLRP3 speck in THP1 cells. EGFP-NLRP3-THP1$^{nlrp3-/-}$ cells were treated with vehicle-only controls or with 1 µg/mL LPS for 3 h followed by stimulation with 10 µg/mL anti-CD59 mAb, C5b6, C7, C8 and C9 labelled with JF-549 (MAC) for 3 h. **a)** Representative confocal images of C9 (red), ASC (cyan) and eGFP-NLRP3 (green), scale bars are 20 µm in full pictures and 5 µm in ROIs, dashed lines represent the outline of the cell and arrows point to specks. **b)** Percentage of cells with ASC or with NLRP3 speck. **c)** Percentage of ASC speck$^+$ cells with C9 or NLRP3 in the speck. In b and d data is plotted as mean ± SD, each colour represents a matched single donor. In b statistical significance was measured by un-paired t-test (*p<0.05). In a-c data is representative of 3 independent experiments and ≥ 103 cells were imaged per condition.

4.4 Discussion

4.4.1 Summary of results

The aim of this chapter was to determine whether the complement component 5a (C5a) and the membrane attack complex (MAC) are able to engage inflammasome priming and activation, respectively, leading to IL-1β secretion in human macrophages.

The main findings of this chapter are recapitulated as follows:

1. C5a does not induce IL-1β secretion in combination with nigericin in human MDMs.
2. Sublytic MAC triggers inflammasome activation leading to caspase 1 activation and IL-1β and IL-18 secretion in human MDMs.
3. Sublytic MAC triggers inflammasome activation leading to IL-1β secretion in THP1 cells.
4. MAC-mediated IL-1β release is dependent on NLRP3 and GSDMD in human MDMs.
5. MAC-mediated IL-1β release is dependent on NLRP3 in THP1 cells and MDMs.
6. The MAC colocalises with the inflammasome speck in human MDMs and THP1 cells.

Altogether, these results show that sublytic MAC activates the NLRP3 inflammasome in the absence of cell death in human macrophages, highlighting the ability of this pore to initiate intracellular signalling pathways in these cells (Fig 4.16).

4.4.2 Significance of results

IL-1β and IL-18 are involved in the development of multiple inflammatory diseases characterised by increased levels of the terminal components of the complement system. For example, in serum from patients with bacterial sepsis the amount of C5a and C5b-9, the soluble form of the MAC, are significantly increased[295,296], and IL-1β and IL-18 induce many of the immunopathological characteristics of LPS-induced septic shock[393,394]. C5b-9 is also increased in the synovial fluid and the plasma of patients with rheumatoid arthritis and osteoarthritis[297–299]. Moreover, IL-1β expression in myeloid cells and IL-1β-driven pathways, such as TLR signalling and cytokine production, are also

increased in synovial tissues from these patients[395]. There is a growing body of evidence showing that both the final components of the complement system and the cytokines IL-1β and IL-18 are mediators of multiple inflammatory diseases. However, whether C5a and the MAC play a direct role in the release of these cytokines in human macrophages, one of the main sources of these cytokines, has not been studied. For this reason, this chapter focused on understanding whether C5a and the MAC could trigger inflammasome activation in these cells.

4.4.2.1 C5a as a stimulus for inflammasome activation

C5a can promote inflammasome priming in various cell types. In human monocytes, in combination with TNFα, C5a stimulates pro-IL-1β expression, resulting in IL-1β secretion after the use of cholesterol crystals as a second signal for inflammasome activation[382]. In retinal pigment epithelial cells, C5a upregulates the expression of pro-IL-18 and induces the secretion of IL-18, indicating a role for C5a in inflammasome priming and activation[396]. However, in the experiments performed in this thesis cytokine secretion was not achieved in human MDMs stimulated with C5a and the potent inflammasome activator nigericin. This suggests that C5a does not prime the inflammasome in these cells. However, C5a could be priming the inflammasome but inhibiting the effects of nigericin at the same time and therefore, blocking inflammasome activation and IL-1β release. To confirm whether C5a is able to prime the NLRP3 inflammasome, the expression of pro-IL-1β and of NLRP3 upon treatment with C5a could have been studied using immunoblotting or PCR techniques. Moreover, the role of C5a in the context of inflammasome activation differs in monocytes and macrophages. For instance, treatment with C5a promotes LPS-induced NLRP3 and pro-IL-1β expression in murine monocytes[310]. However, the same treatment inhibits LPS-induced NLRP3, caspase 1 and pro-IL-1β expression, resulting in a reduction in IL-1β secretion, in murine macrophages[310]. Additionally, the expression of C5aR is lower in macrophages than in monocytes[308]. These findings could therefore help to explain why C5a failed to induce IL-1β secretion in human MDMs.

Previous studies showed that C5a modulates the effects of LPS in inflammasome activation, but they did not investigate whether C5a alone could prime the inflammasome in myeloid cells[310]. Therefore, C5a may only function as a modulator for

inflammasome activation and IL-1β secretion and not as a trigger for inflammasome priming in immune cells. On the other hand, C5a could fail to prime pro-IL-1β production whilst still priming the NLRP3 inflammasome. However, further research is needed to establish this.

4.4.2.2 Sublytic MAC and the release of IL-1β

The ability of the MAC to trigger inflammasome activation leading to cytokine secretion has been previously described[290,292,383]. Stimulation of LPS-primed murine dendritic cells with rabbit complement induces caspase 1 activation and IL-1β release, with the release of this cytokine reduced when anti-C6 and anti-C9 blocking Abs are used[383]. This indicates a role for the MAC in activating the inflammasome in murine myeloid cells. On the other hand, human serum that contains the complement components needed to form the MAC also triggers IL-1β secretion in lung epithelial cells and in IFNγ-primed endothelial cells[290,292], indicating that the MAC can trigger inflammasome activation in human non-myeloid cells. However, the role of the MAC in human myeloid cells in the context of inflammasome activation has not been studied. The results of this chapter show that formation of the MAC by sequential addition of C5b6, C7, C8 and C9 in serum-free media induced NLRP3 inflammasome assembly in human macrophages. Indeed, this also resulted in IL-1β and IL-18 secretion, demonstrating that the MAC triggers inflammasome activation in human myeloid cells – a group of cells that represent an important source of IL-1β and IL-18 in the human body. Prior studies not only used different cell types but also used serum as a source of complement. Growth factors such as fibroblast growth factor and other bioactive molecules like complement component 3a that activate the NLRP3 inflammasome are present in serum[308,397], and could enhance the observed inflammasome responses mediated by the MAC in previous studies. Hence, the findings of this chapter clarify that the MAC can induce inflammasome activation independently of other serum components.

In human macrophages, phagocytosis of inulin that has been opsonized by complement-containing serum triggers IL-1β secretion[284]. Our results indicate that MAC deposition induces caspase 1 activation and GSDMD processing leading to IL-1β release independently of phagocytosis. This shows a broader role for the MAC in mediating

proinflammatory responses including during sterile inflammation. In this context, IL-18 secretion mediated by the MAC alone could promote these responses. In addition, IL-1β secretion could drive inflammation when pro-IL-1β production is induced by endogenous DAMPs such as amyloid aggregates and cholesterol crystals[91].

In general, inflammasome activation is associated with triggering a specific type of cell death called pyroptosis. However, as mentioned in chapter 3, inflammasome activation can lead to cytokine release in the absence of pyroptosis. This activation state is known as "hyperactive"[398]. Our observation that the MAC induces IL-1β release in the absence of cell death, suggests that the MAC is driving macrophages into a state of hyperactivation. In this thesis, cell death is inferred from the absence of LDH in cell supernatant. LDH is a molecule whose release indicates loss of membrane integrity and, generally, pyroptosis. However, the MAC could be triggering other types of cell death that do not involve LDH release and have not been investigated in this thesis. To further determine this, other cell death detection methods could be used, including flow cytometry-based Annexin V assays to determine whether membrane integrity was lost, the measurement of mitochondrial depolarization to analyse mitochondrial damage, or the determination of morphological changes characteristic of cell death (e.g. membrane blebbing, nuclear fragmentation) using microscopy[57].

Pyroptotic macrophages release more IL-1β than hyperactive macrophages[201]. This correlates with the findings of this chapter that show that MAC-mediated cytokine secretion occurs to a lesser extent than in cells treated with nigericin. Of note, low concentrations of IL-1β can trigger downstream signalling pathways in target cells [390,399–403]. For example, concentrations of 100 pg/mL IL-1β can promote nerve growth factor expression and secretion from articular chondrocytes, and 10 pg/ml IL-1β induces phosphorylation of Src kinase in hippocampal neurons[401,403]. Thus, the levels of inflammasome activation and cytokine release observed in human macrophages after stimulation with the MAC can be biologically relevant.

GSDMD pores are responsible for pyroptosis. However, whether a minimum number of pores are required to trigger this type of cell death is unknown. The amount of cleaved GSDMD, and consequently GSDMD pore formation, detected upon MAC-mediated inflammasome activation is considerably lower than in nigericin-treated cells.

Thus, if there is a threshold in the number of GSDMD pores needed to trigger membrane rupture and cell death, it could be possible that, upon stimulation with the MAC, or under hyperactivation conditions, the number of GSDMD pores in the cell membrane is not enough to trigger cell death. Apart from this, myeloid cells prevent membrane rupture induced by pore-forming proteins, including the MAC, through mechanisms such as endocytosis or exocytosis[404]. These mechanisms could play a role in repairing the membrane not only from MAC pores but also from GSDMD pores, explaining the observed lack of cell death in human macrophages stimulated with this terminal complement complex. Furthermore, it has recently been discovered that GSDMD pores are dynamically active and can open and close, suggesting that in hyperactive cells, GSDMD pores could open to release IL-1β and IL-18 and then close to avoid osmolysis[405]. This could explain why MAC mediated inflammasome activation results in the release of low amounts of these cytokines in the absence of cell death. Of note, the ability to release low amounts of pro-inflammatory cytokines in the absence of cell death could contribute to a sustained but more controlled pro-inflammatory response, preventing overstimulation of the immune system and its potentially fatal consequences.

There is no evidence indicating that pro-IL-1β is biologically active. Nevertheless, pro-IL-1β can be processed into bioactive IL-1β independently of inflammatory caspases by multiple proteins including proteases, elastases and granzymes[406–408]. Specifically, neutrophil-derived serine proteases can cleave pro-IL-1β into active molecules, and processing of pro-IL-1β by proteinase 3 has been demonstrated in a murine model of acute arthritis[406]. As previously mentioned, MAC deposition is increased in patients with arthritis[297–299] meaning that the observed levels of pro-IL-1β secretion induced by the MAC could be important during sterile inflammation. Additionally, proteases from pathogens such as *Candida albicans* and *Staphylococcus aureus* also process pro-IL-1β into active IL-1β[409,410]. Gram-positive bacteria and yeast can activate the lectin pathway of the complement system leading to MAC formation[410]. This suggests that during infection, pro-IL-1β released after stimulation with the MAC could be cleaved by pathogen-derived proteases into mature IL-1β leading to the activation of proinflammatory responses.

4.4.2.3 Caspase 4 in MAC-mediated inflammasome activation and cytokine release

Non-canonical NLRP3 inflammasome activation is mediated by caspases 4 and/or 5. These caspases can be activated by intracellular PAMPs and DAMPs, and in turn they activate the NLRP3 inflammasome. It has recently been shown that non-pathogenic stimuli can activate caspase 4. In human podocytes, high levels of glucose drive caspase 4 activation leading to IL-1β secretion[411]. In addition, heme groups that are released upon erythrocyte destruction and endocytosed by macrophages trigger caspase 4 activation in human MDMs[411], showing that caspase 4 can be activated by sterile stimuli. Thus, our observation that caspase 4 is processed upon treatment with the MAC alone is relevant in the context of sterile inflammation, and could indicate that MAC-mediated NLRP3 inflammasome activation is initiated by caspase 4. Specific inhibitors for caspase 4 are not commercially available. Therefore, studying whether MAC-mediated IL-18 and IL-1β secretion is dependent on caspase 4 is challenging. Although technically difficult in human primary cells, an approach using siRNA against this caspase to block its expression in MDMs could be tested to determine the role of this enzyme in MAC-mediated inflammasome activation. On the other hand, intracellular LPS is the most studied activator for caspases 4 and 5[131,347]. Although a washing step to remove LPS before MAC stimulation was performed in our experiments, residual levels of LPS could have potentially entered cells through MAC pores, contributing to caspase 4 activation. This could explain why the MAC induced a higher processing of caspase 4 in LPS-primed MDMs. To confirm that caspase 4 and NLRP3 inflammasome activation in this context is independent of intracellular LPS, other NLRP3 priming stimuli such as Pam3CSK4, Poly(I:C) or flagellin could be used to stimulate MDMs before treatment with the MAC. Importantly, the complement cascade can be activated by LPS from gram-negative bacteria[412,413]. Consequently, it would be important to determine whether the entrance of LPS through MAC pores could result in the activation of caspase 4 and downstream signalling pathways in the context of infection.

Caspase 4 can cleave pro-IL-1β into mature IL-1β[414]. Caspases 4 and 1 are both cysteine-aspartate proteases and pro-IL-1β and pro-IL-18 are cleaved at a similar site by caspase 1, an aspartate followed by a polar amino acid[72,73,82]. Therefore, if caspase 4 is able to process pro-IL-1β, it should also be able to cleave pro-IL-18. As such, the release

of mature IL-18 induced by the MAC alone in the absence of caspase 1 activation could be mediated by caspase 4. However, further investigation is needed to confirm this hypothesis. Unlike pro-IL-1β, pro-IL-18 is constitutively expressed meaning that a priming signal to induce its production is not required. This would explain why only the secretion of IL-18 and not IL-1β is observed after stimulation with the MAC alone if caspase 4 is able to cleave pro-IL-18.

4.4.2.4 K^+ efflux in MAC-mediated inflammasome activation

Several stimuli activate the NLRP3 inflammasome, and the intracellular pathways and proteins involved in NLRP3 inflammasome activation are context-dependent. Thus, it is difficult to identify a common cellular event responsible for NLRP3 activation. K^+ efflux is widely accepted as a common event upstream of NLRP3 inflammasome activation for a wide variety of stimuli[114]. However, K^+ efflux-independent mechanisms for inflammasome activation have also been described[117]. Formation of the MAC pore in the cell membrane induces ion fluxes, including K^+ efflux, that could induce the observed MAC-mediated NLRP3 inflammasome activation in human MDMs. Nevertheless, inhibition of K^+ efflux did not fully impair MAC-mediated IL-1β secretion, indicating that this process may not be completely dependent on K^+ efflux in these cells. The observed variability between donors in the levels of IL-1β secreted made it difficult to fully determine whether MAC-mediated inflammasome activation is dependent on K^+ efflux. To confirm this, the experiments carried out in this chapter could be performed using the macrophage-like cell line THP1. On the other hand, the observation that the MAC colocalises with the inflammasome speck may indicate a more direct mechanism for this complex to activate the NLRP3 inflammasome. Nonetheless, further investigation is required to determine whether MAC pore formation in the cell membrane leading to ion fluxes is required for MAC-mediated inflammasome activation.

4.4.3 Conclusion and future directions

This chapter demonstrates that the MAC triggers IL-1β and IL-18 release in human macrophages providing a direct connection between the inflammasome and the terminal pathway of the complement system in these cells (Fig 4.16). Next steps should

focus in understanding the mechanism by which the MAC activates the NLRP3 inflammasome.

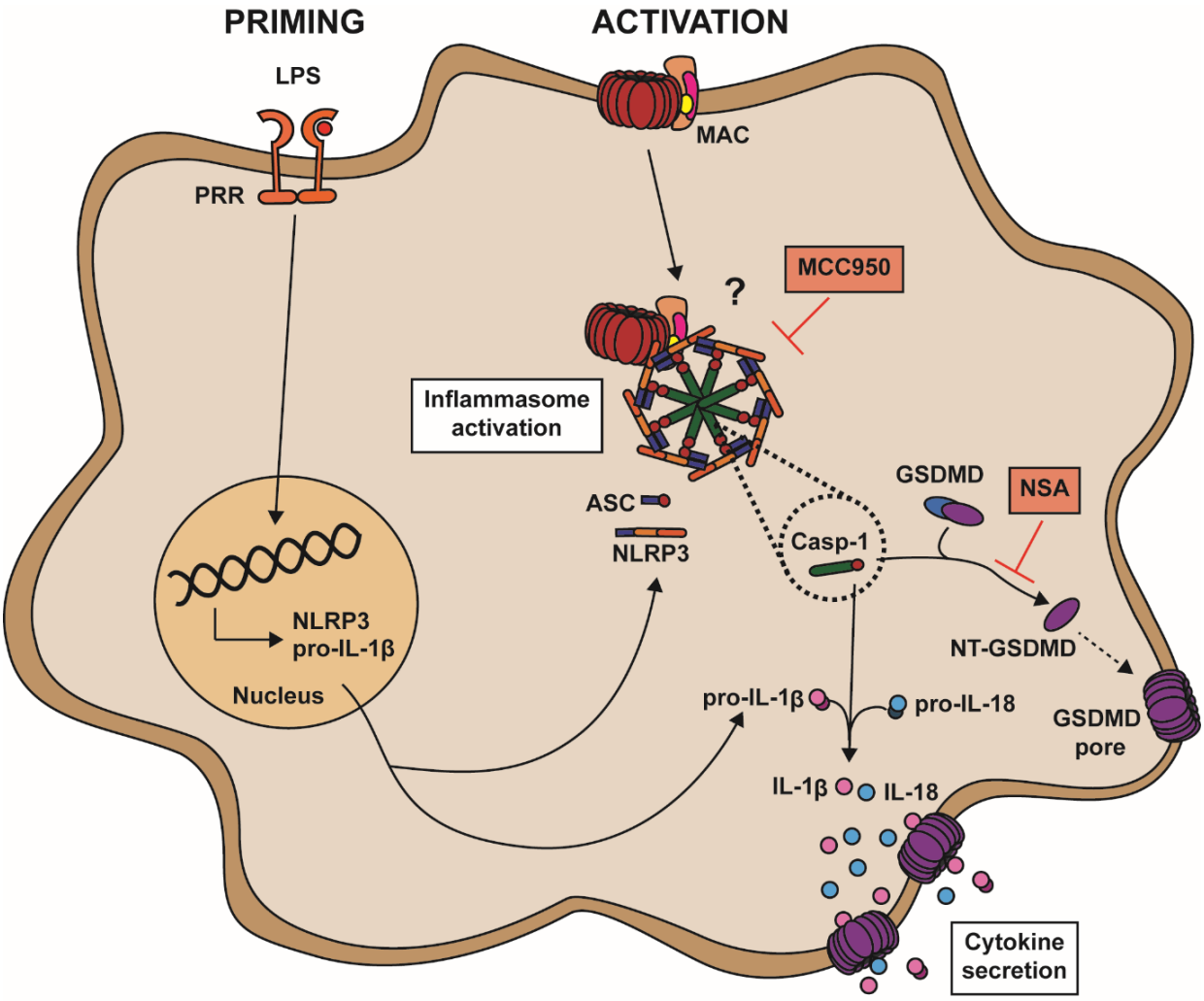

Figure 4.16 MAC-mediated NLRP3 inflammasome activation in human macrophages. Formation of the MAC in the cell of LPS-primed human macrophages triggers NLRP3 inflammasome assembly and activation. This results in the activation of caspase 1 that cleaves GSDMD into its pore forming subunit NT-GSDMD, and processed pro-IL-1β and pro-IL-18 into their mature forms to be released to the extracellular milieu in a GSDMD-dependent manner. MAC-mediated NLRP3 inflammasome activation and cytokine release are inhibited by the NLRP3 inhibitor MCC950 and the GSDMD inhibitor NSA.

Multiple pore-forming toxins, including nigericin, induce ion fluxes that trigger NLRP3 inflammasome activation, with K^+ efflux shown to be the main driver of NLRP3 inflammasome activation in this context[389]. However, inhibition of K^+ efflux did not completely impair MAC-mediated IL-1β secretion in human macrophages, suggesting that although MACs form pores in the cell membrane, direct induction of K^+ efflux by

these pores may not be the mechanism for inflammasome activation. Moreover, in human macrophages the MAC is observed inside the cell soon after deposition at the cell membrane. Therefore, studying how the MAC is internalized and whether this process is necessary for inflammasome activation is key to further understanding MAC-mediated inflammasome activation. Likewise, the MAC is observed at the NLRP3 inflammasome speck at later time points, which indicates that the MAC could interact with inflammasome components or proteins that mediate inflammasome assembly to trigger inflammasome activation. In line with this, multiple cellular localizations for NLRP3 inflammasome assembly have been described, which link to different mechanisms of inflammasome activation[92,102,142,143,146,147]. Therefore, determining the intracellular compartment where the MAC and NLRP3 colocalize together could help to determine how the MAC, and potentially other pore-forming proteins, trigger inflammasome activation.

Chapter 5 Internalization of the Membrane Attack Complex is required for IL-1β secretion in human macrophages

5.1 Introduction

The membrane attack complex has the ability to form membrane pores in pathogens and defective cells leading to osmotic lysis and cell death[221]. As mentioned before, nucleated cells have developed mechanisms to diminish the cytolytic effect of the MAC, one of them being the removal of MAC membrane pores through internalization of MAC complexes to prevent osmotic lysis[221]. Specifically, in K562 cells, the MAC is internalized within 5-10 min of MAC deposition at the cell membrane and in human neutrophils, membrane-associated C9 is internalized and partially degraded after 60 min of stimulation with human serum[275,278]. In addition, internalization of the MAC is required for NLRP3 inflammasome engagement in response to Ab-mediated complement activation in endothelial cells[292]. Particularly, this involves the recruitment of NLRP3 to early endosomes in a process mediated by NF-κB inducing kinase (NIK)[292]. Of note, to activate the NLRP3 inflammasome, various pathogenic and non-pathogenic stimuli need to be internalized, including bacterial toxins such as Group A streptococcal M protein and particulate matter such as monosodium urate crystals, alum or indium tin oxide nanoparticles[124,389,415,416].

A common cellular event responsible for the activation of the NLRP3 inflammasome upon stimulation with every NLRP3 activator is yet to be discovered. Nonetheless, some of the main described events preceding the assembly of this inflammasome are: mitochondrial DNA (mtDNA) release and ROS production, dispersion of the trans-Golgi network (TGN) and lysosomal disruption[92,102,109,125,417–419]. Specifically, in murine ASC-deficient macrophages, NLRP3 localises to the dispersed TGN (dTGN) upon treatment with multiple NLRP3 inflammasome stimuli[417]. Moreover, when NLRP3 recruitment to the dTGN is impaired in murine macrophages stimulated with K^+-dependent and K^+-independent NLRP3 activators, caspase 1 activation and IL-1β

secretion is inhibited, indicating that the dispersion of the TGN is important for NLRP3 inflammasome activation upon treatment with a wide variety of stimuli[417].

In unstimulated cells, the NLRP3 sensor is located in the endoplasmic reticulum (ER) in THP1 cells or in the cytosol in murine macrophages[92,140]. On the other hand, during resting conditions ASC has been reported to be at the mitochondria and the nucleus in murine macrophages, in the nucleus in human macrophages and at the cytosol in macrophage-like THP1 cells[70,141–143]. However, after treatment with NLRP3 activators, the NLRP3-ASC speck has been found in different cell compartments including, but not only, the centrosome in murine macrophages and THP1 cells, and at the mitochondria-associated ER membranes (MAMs) or the autophagosome in murine and human macrophages[142,143,146,147]. This variation in the localisation of the inflammasome speck may indicate that the cell compartment where NLRP3 inflammasome assembly occurs is not unique and may vary among cell types and depending on the NLRP3 activator.

5.2 Aims and objectives

In chapter 4, it was determined that in human macrophages the membrane attack complex (MAC) can trigger NLRP3 inflammasome assembly which in turn activated caspase 1 leading to the release of IL-1β and IL-18 through GSDMD pores. Importantly, the MAC was detected intracellularly and localised to the inflammasome speck. As previously described, to diminish the lytic effects of the MAC, multiple cells remove MAC pores from the cell membrane through endocytosis. Therefore, considering that the MAC did not lyse human macrophages and that it was detected inside the cell, the main objective of this chapter was to understand if internalization of the MAC was required for inflammasome activation and if this process initiated downstream events leading to IL-1β secretion in these cells. Additionally, the observation of the MAC in the inflammasome speck made important to investigate in which intracellular compartment the MAC and the inflammasome localised together.

The specific objectives of this chapter were as follows:

1. To establish how the MAC is internalized by human monocyte-derived macrophages (MDMs).
2. To determine whether endocytosis of the MAC is required for MAC-mediated inflammasome activation in MDMs.
3. To study whether NF-κB inducing kinase plays a role in MAC-mediated inflammasome activation in MDMs.
4. To investigate which cellular event occurs upstream of NLRP3 inflammasome activation and downstream of MAC internalization in MDMs.
5. To examine in which cellular compartment the MAC colocalises to the NLRP3/ASC speck.

5.3 Results

5.3.1 The Membrane attack complex is internalized in EEA1^{+} endosomes upon deposition on the cell membrane

Formation of the MAC in cell membranes is a quick process that occurs within minutes[420]. Importantly, in the previous results chapter, intracellular MAC was observed in MDMs from 30 min after stimulation with C5b6, C7, C8 and C9 (Fig 4.12). To understand the dynamics of MAC deposition in the cell membrane and how this complex is taken up by human macrophages, the next experiments investigated the process of MAC internalization in MDMs. To this end, MDMs were stimulated with 1 µg/mL LPS for 3 h followed by C5b6 in the presence of anti-CD59 mAb, C7, C8 and C9 labelled with AF647 (C9-AF647) to visualize the complex for the indicated time. Cells were then fixed and analysed by confocal microscopy. The amount of C9 at the cell surface was compared with intracellular C9 levels. This was expressed as a ratio between the amount of C9 fluorescence at the cell surface divided by the amount of C9 fluorescence inside the cell (Fig 5.1 a). Here, the cell surface was defined from the cell outline to 2 µm inside the cell (Fig 5.1 a). After 5 min of stimulation with the MAC, C9 was mainly observed at the cell periphery indicating localisation in the cell membrane (Fig 5.1 a and b). Localisation in the membrane was maintained after 10 min of MAC stimulation but after 30 min, the amount of C9 inside the cell increased (Fig 5.1 a and b). By 90 min, C9 was mainly detected intracellularly indicating that upon deposition in the cell membrane, the MAC is internalized by the macrophage.

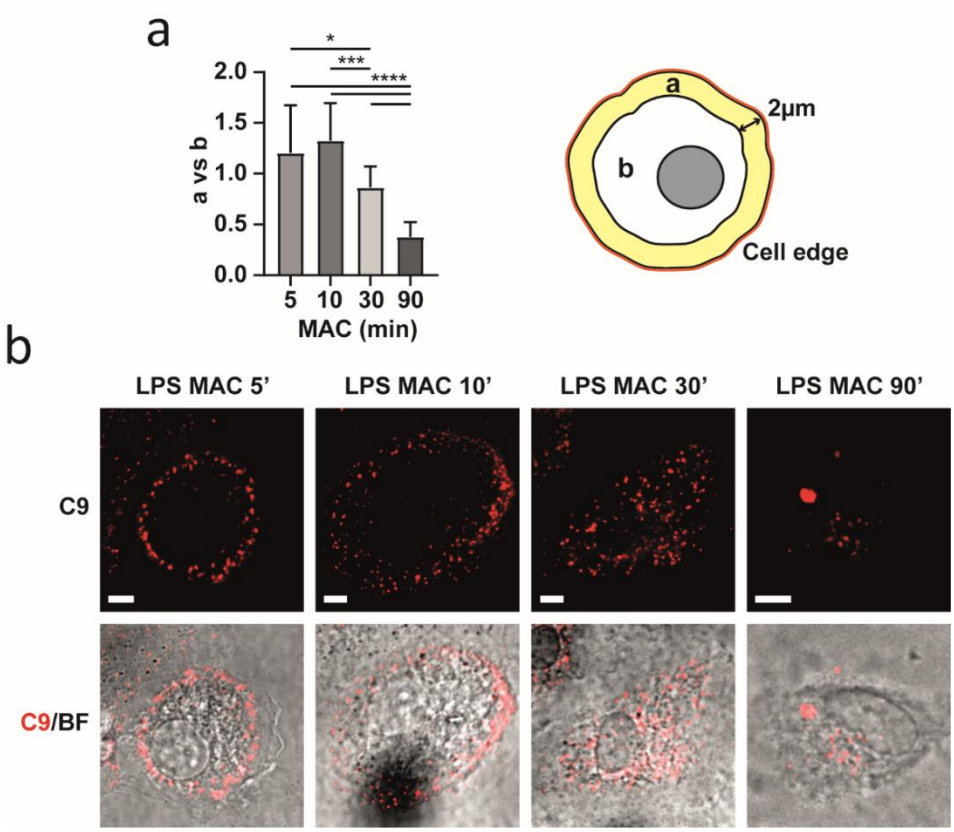

Figure 5.1 The MAC is deposited in the cell membrane before internalization. Human MDMs were treated with 1 µg/mL LPS for 3 h followed by stimulation with 10 µg/mL anti-CD59 mAb and 10 µg/mL C5b6, C7, C8 and C9-AF647 to form the MAC for the indicated time (in min). **a)** Ratio between mean fluorescence intensity of membrane C9 (a) vs intracellular C9 (b). **b)** Representative confocal images of C9-AF647 (red) and brightfield (gray). Scale bars are 5 µm and ≥ 15 cells were imaged per condition in each experiment. Data is plotted as mean ± SD and is representative of 2 independent experiments and statistical significance was measured by Kruskal-Wallis test (*p<0.05 ***p<0.001 ****p<0.0001).

To further investigate MAC internalization in MDMs, cells were primed with 1 µg/mL LPS and treated with C5b6, C7, C8 and C9-AF647 to form the MAC for 30, 90 or 180 min. Then cells were fixed and stained with an Ab against EEA1 to visualize early endosomes. As previously seen (Figure 5.1 c), upon 30 min of MAC treatment, multiple C9 puncta were homogeneously distributed inside the cell (Fig 5.2 a). Importantly, these C9 puncta were encircled by the early endosomal marker EEA1 (Fig 5.2 a). This was confirmed by the fluorescence pattern observed in line profiles across EEA1 endosomes, in which a peak of C9 fluorescence was confined between two peaks of EEA1 fluorescence (Fig 5.2 b). These findings suggest that C9 is internalized via $EEA1^+$ endosomes. At later time points, colocalisation of C9 and EEA1 was reduced (Fig 5.2 c). In agreement with this, after 180 min of stimulation with the MAC, C9 accumulated in larger puncta resembling the structure of inflammasome specks (Fig 5.2 a). Thus, these

results show that the MAC is firstly internalized into EEA1^{+} early endosomes and then colocalises with the inflammasome complex.

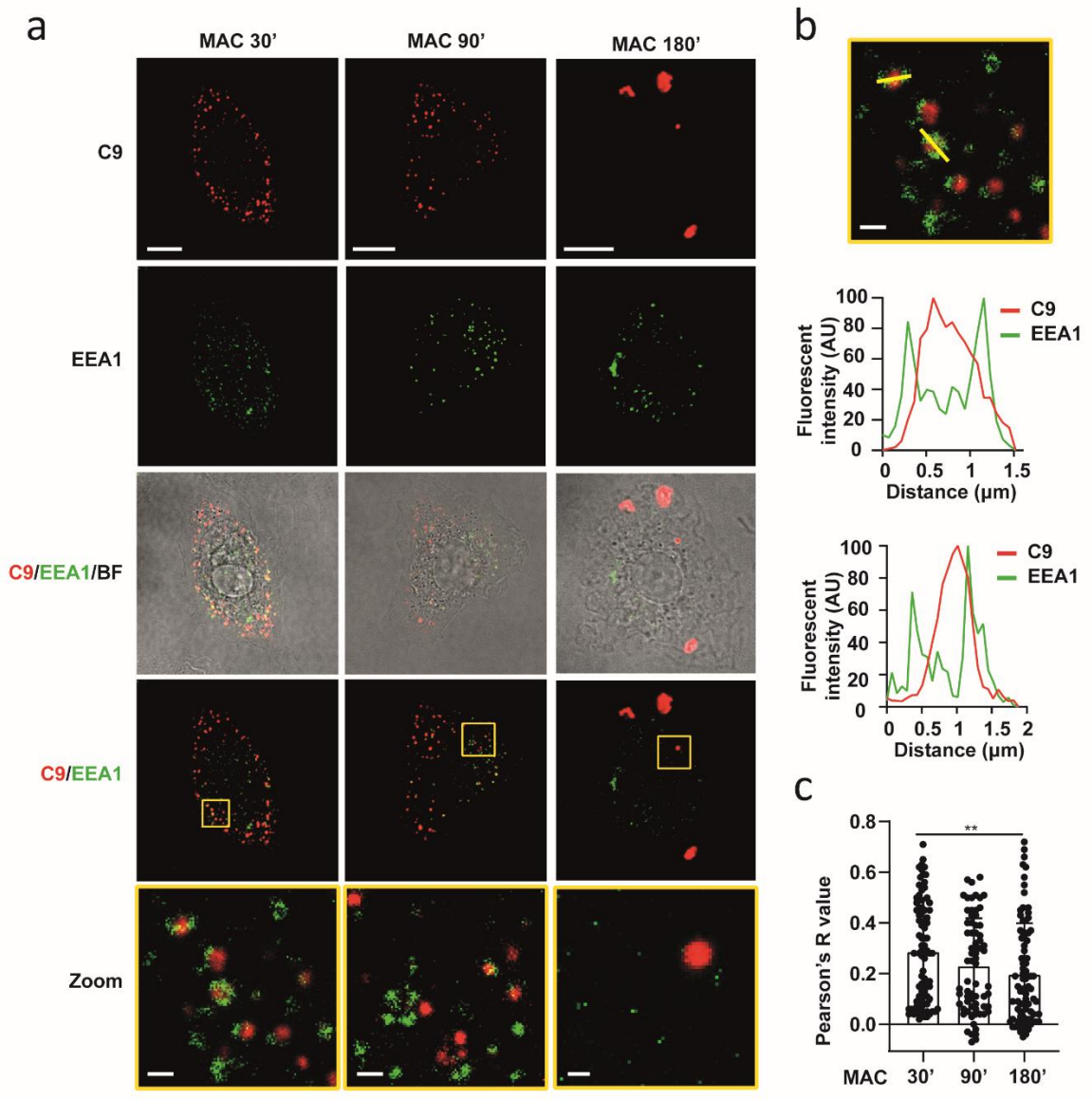

Figure 5.2 The MAC is internalized in EEA1^{+} endosomes. Human MDMs were treated with 1 μg/mL LPS for 3 h followed by stimulation with 10 μg/mL anti-CD59 mAb and 10 μg/mL C5b6, C7, C8 and C9-AF647 to form the MAC for the indicated time (in min). **a)** Representative confocal images of C9-AF647 (red) and EEA1 (green). Yellow squares represent zoom regions and scale bars are 10 μm in full pictures and 1 μm in zoom regions. **b)** Fluorescence intensity of C9 and EEA1 along the indicated line profiles. **c)** Pearson's correlation coefficient of C9 compared to EEA1. In c data is plotted as mean ± SD, and statistical significance was measured by Kruskal-Wallis test (**p<0.01). In a-c data is representative of 3 independent experiments and ≥ 15 cells were imaged per condition in each experiment.

5.3.2 IL-1β secretion is dependent on MAC internalization

Pore formation in the cell membrane can trigger ion fluxes that induce NLRP3 inflammasome activation[121]. The MAC is a pore-forming complex, and its formation in the cell membrane of lung epithelial cells initiates ion fluxes leading to IL-1β secretion[290]. On the other hand, in endothelial cells treated with human serum, the MAC needs to be endocytosed to mediate the secretion of this cytokine[292]. Therefore, the following experiments set out to investigate whether MAC formation in the cell membrane, leading to ion fluxes, was sufficient to activate the inflammasome, or if internalization of the complex was required to engage this process in human macrophages. Previous studies showed that internalization of the MAC can be mediated by caveolin-1, dynamin-2 and lipid rafts in K562 cells, and by clathrin in endothelial cells[279,288]. Moreover, actin is key in the dynamics of caveolae and clathrin-coated vesicles[421,422]. Thus, three endocytosis inhibitors that specifically block the aforementioned processes were chosen: nystatin (Nys) a caveolae and lipid-mediated endocytosis inhibitor, dynasore (Dyn), a dynamin inhibitor, and cytochalasin D (Cyt), an actin-polymerization inhibitor[423–425]. The concentrations used of these compounds to inhibit endocytosis in the experiments were chosen based on previous publications[426,427]. Specifically for Dyn, it has been shown in K562 cells that MAC endocytosis is inhibited by concentrations of 40-100 µM Dyn[279]. However, high concentrations of Dyn have also been shown to activate the inflammasome in murine macrophages and macrophage-like THP1 cells[428,429]. Thus, it was first investigated whether high concentrations of this endocytosis inhibitor triggered IL-1β secretion by itself in LPS-primed MDMs. To do so, cells were treated with 1 µg/mL LPS for 3 h followed by 10-160 µM Dyn, or nigericin as a positive control, for 45 min. IL-1β and LDH release were measured in cell supernatants to assess inflammasome activation and cell death, respectively. Treatment with 40-160 µM Dyn induced IL-1β secretion but did not trigger cell death (Fig 5.3 a and b). In contrast, 10-20 µM Dyn did not trigger IL-1β secretion by itself, nor did it induce cell death (Fig 5.3 a and b). For this reason, concentrations of 10-40 µM Dyn were used in further experiments. Here, 40 µM served as the minimum concentration for Dyn to trigger cytokine release.

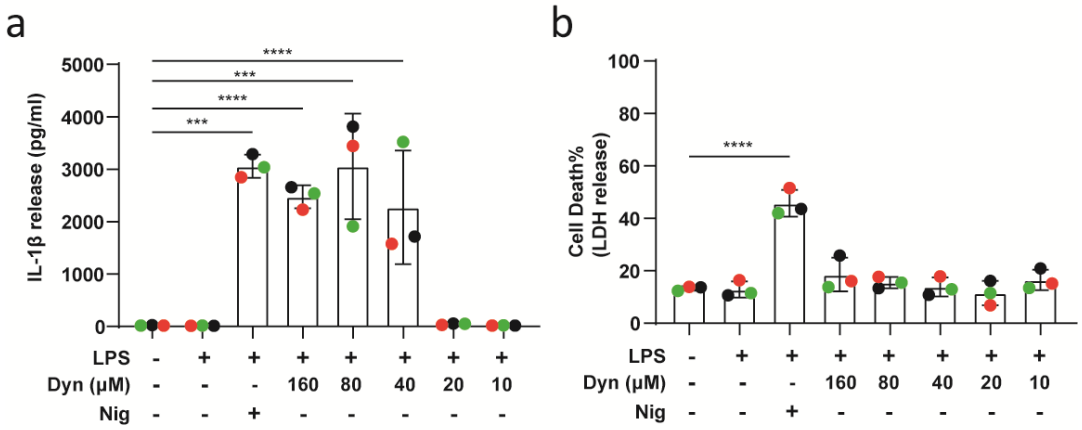

Figure 5.3 High concentrations of dynasore trigger IL-1β release in LPS-primed MDMs. Human MDMs were treated with 1 μg/mL LPS for 3 h followed by stimulation with the indicated concentration of dynasore (Dyn) or 10 μM nigericin (Nig) for 45min. **a)** IL-1β secretion was measured by ELISA. **b)** LDH release was measured as a proxy for cell death. Data is plotted as mean ± SD and is representative of 3 independent experiments. Each colour represents a matched single donor and statistical significance was measured by one-way ANOVA (***p<0.001 ****p<0.0001).

To investigate whether or not MAC internalization is necessary for inflammasome activation, MDMS were stimulated with 1 μg/mL LPS for 3 h and with the MAC for 3 h, as previously explained, in the presence or absence of 0.1-10 μg/mL Nys, 5-20 μM Cyt and 10-40 μM Dyn. IL-1β release in supernatants was studied using ELISA assays, LDH release was measured as a proxy for cell death and GSDMD processing was analysed by immunoblotting. All concentrations of Nys and Cyt significantly reduced MAC-mediated IL-1β secretion (Fig 5.4 a and b). Moreover, IL-1β released was also significantly reduced when 10-20 μM Dyn, concentrations that do not trigger IL-1β secretion by itself (Fig 5.3 a), were used (Fig 5.4 c). This indicates that endocytosis of the MAC is required to trigger inflammasome activation. The highest reduction of IL-1β secretion was achieved when 0.1 μg/ml Nys, 10 μM Cyt or 10 μM Dyn were used (Fig 5.4 a, b and c). At these concentrations, these inhibitors impaired IL-1β release and did not induce cell death (Fig 5.4 d and e). Moreover, GSDMD cleavage, indicated by the detection of the p30 NT-GSDMD fragment in cell lysates, was only seen when MDMs were treated with 1 μg/mL LPS and the MAC in the absence of endocytosis inhibitors (Fig 5.4 f), showing that inhibition of MAC endocytosis impaired downstream caspase 1 activity and prevented processing of GSDMD.

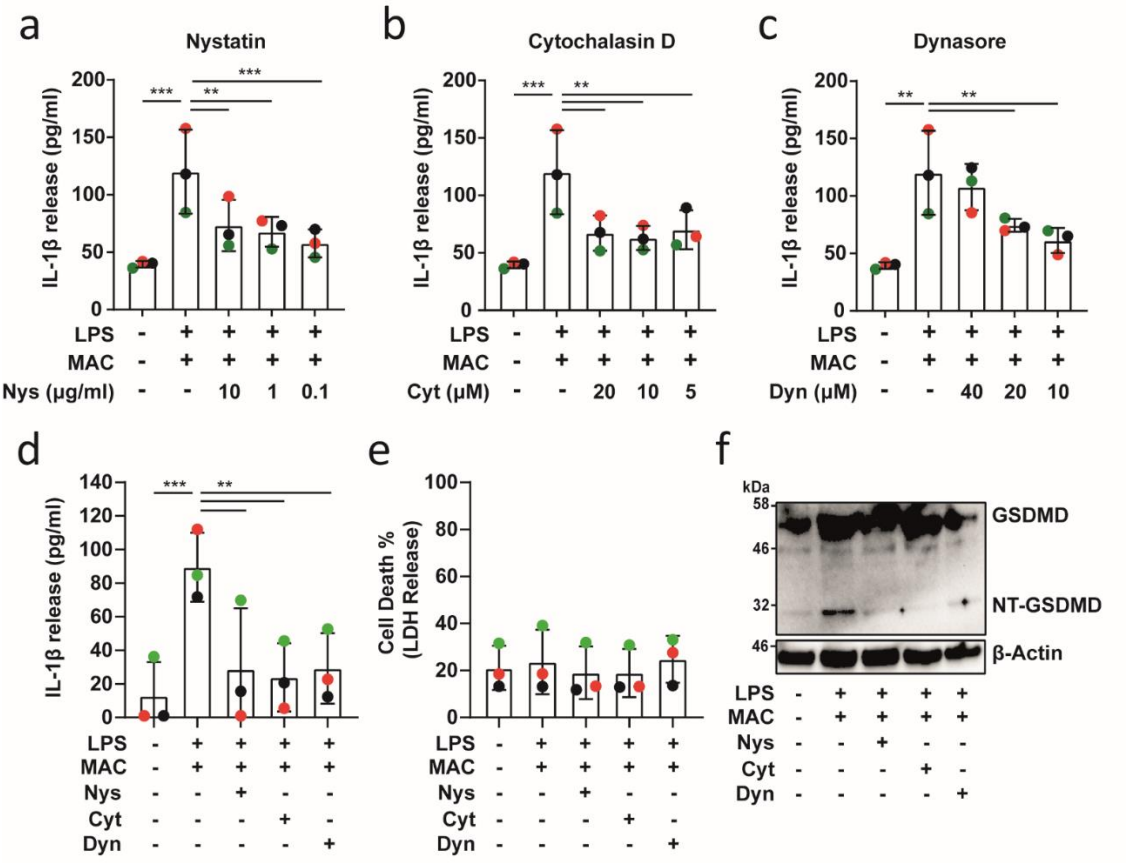

Figure 5.4 Internalization of the MAC is required for inflammasome activation. Human MDMs were treated with 1 μg/mL LPS for 3 h followed by stimulation with 10 μg/mL anti-CD59 mAb and 10 μg/mL C5b6, C7, C8 and C9 to form the MAC for 3 h in the presence or absence of the indicated concentration of nystatin (Nys), cytochalasyn D (Cyt) or dynasore (Dyna). In **d-f** 0.1 μg/ml Nys, 10 μM Cyt or 10 μM Dyn were used. **a-d)** IL-1β secretion was measured by ELISA. **e)** LDH release was measured as a proxy for cell death. **f)** GSDMD processing was analysed by immunoblot. In a-e data is plotted as mean ± SD, and statistical significance was measured by one-way ANOVA (*p<0.05, **p<0.01, ***p<0.001). In a-f data is representative of 3 independent experiments.

To investigate if endocytosis inhibitors impaired inflammasome activation in general, MDMs were primed with 1 μg/mL LPS for 3 h and stimulated with nigericin in the presence or absence of 0.1 μg/ml Nys, 10 μM Cyt or 10 μM Dyn. Neither IL-1β release nor cell death were affected by these endocytosis inhibitors when cells were stimulated with nigericin (Fig 5.5 a and b). Therefore, in MDMs, MAC-mediated inflammasome activation and IL-1β release are specifically dependent on endocytosis of the MAC.

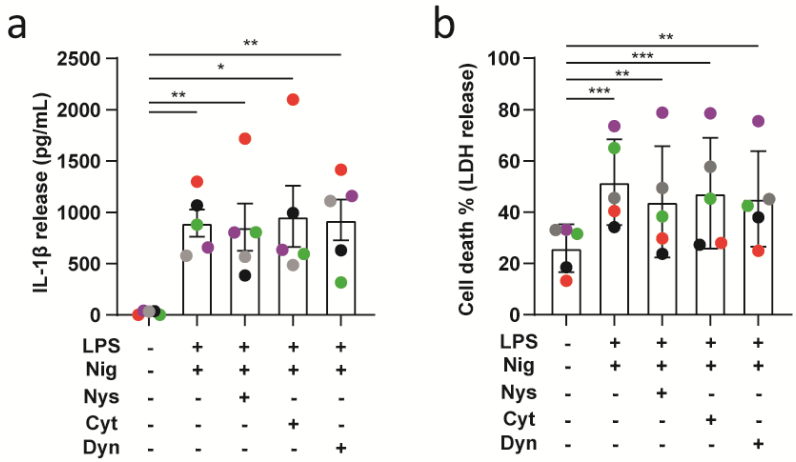

Figure 5.5 Endocytosis inhibition does not impair nigericin-mediated inflammasome activation. Human MDMs were treated with 1 µg/mL LPS for 3 h followed by stimulation with 10 µM nigericin (Nig) for 45min in the presence or absence of 0.1 µg/ml nystatin (Nys), 10 µM cytochalasin D (Cyt) or 10 µM dynasore (Dyn). **a)** IL-1β secretion was measured by ELISA. **b)** LDH release was measured as a proxy for cell death. Data is plotted as mean ± SD and is representative of 5 independent experiments. Each colour represents a matched single donor and statistical significance was measured by Friedman's test (a) or one-way ANOVA (b) (*p<0.05 **p<0.01 ***p<0.001 ****p<0.0001).

5.3.3 Does NF-κB-inducing kinase play a role in MAC-mediated IL-1β secretion in MDMs?

In endothelial cells treated with sera from transplant patients with high titre of Abs against the received tissue (alloantibodies), NF-κB-inducing kinase (NIK) is stabilized in MAC+ early endosomes leading to NLRP3 recruitment and activation[288,292,293]. Considering that MAC is internalized in early endosomes in MDMs, and that internalization is required for IL-1β secretion, the next experiments aimed to investigate whether NIK plays a role in MAC-mediated NLRP3 inflammasome activation in human macrophages. To address this, the potent NIK small-molecule inhibitor-1 (NIK SMI-1) was used [430,431]. Previous studies used this inhibitor for 24 h and at concentrations from 1 nM to 10 µM, being concentrations in the µM range more efficient[430,431]. For this reason, MDMs were pre-incubated with the 0.1-10 µM NIK SMI-1 or vehicle-only control overnight and treated with 1 µg/mL LPS for 3 h and the MAC for 3 h or nigericin for 45 min in the presence or absence of NIK SMI-1. Surprisingly, in the absence of MAC or nigericin stimulation, the use of NIK SMI-1 in LPS-primed MDMs resulted in a dose-dependent increase of IL-1β secretion and cell death - up to a 3-fold increase compared to cells treated with vehicle-only controls (Fig 5.6 a and b). Thus, treatment of LPS-

primed cells with NIK SMI-1 alone activated the inflammasome. Stimulation of LPS-primed MDMs treated with NIK SMI-1 and the MAC also led to a dose-dependent increase of IL-1β secretion (Fig 5.6 a), but this result is difficult to interpret given the effect of the inhibitor alone. NIK-SMI-1 did not have any effect in IL-1β secretion or cell death in MDMs treated with LPS and nigericin (Fig 5.6 a and b).

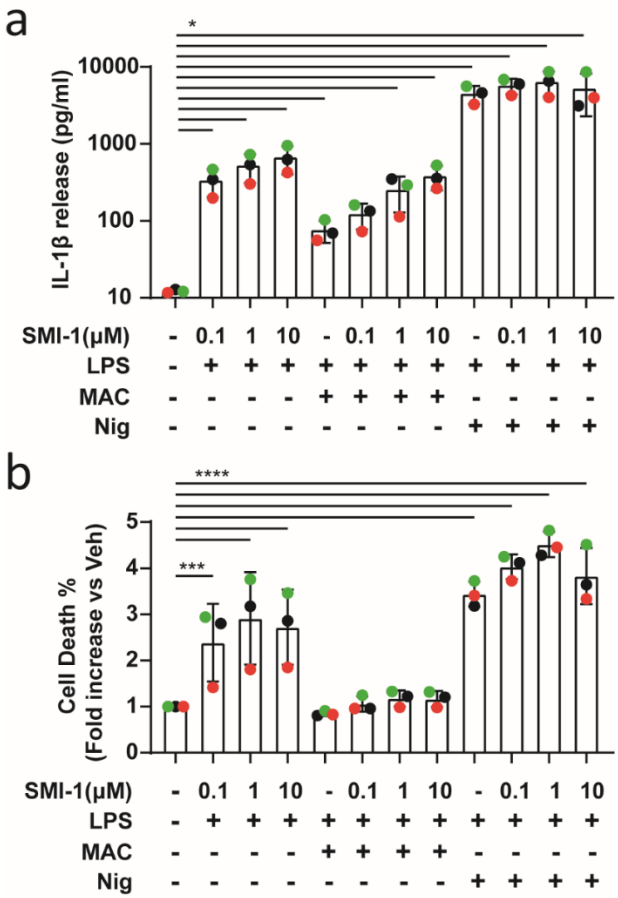

Figure 5.6 Effect of NF-κB-inducing kinase small molecule inhibitor 1 (SMI-1) in MDMs. Human MDMs were treated with vehicle-only controls or the indicated concentration of SMI-1 overnight and stimulated with 1 μg/mL LPS for 3 h followed by stimulation with 10 μg/mL anti-CD59 mAb, C5b6, C7, C8 and C9 (MAC) for 3 h or 10 μM nigericin (Nig) for 45min in the presence or absence of SMI-1. **a)** IL-1β secretion was measured by ELISA. **b)** LDH release was measured as a proxy for cell death. Data is plotted as mean ± SD and is representative of 3 independent experiments. Each colour represents a matched single donor and statistical significance was measured by one-way ANOVA (*p<0.05 **p<0.01 ***p<0.001 ****p<0.0001).

LPS can trigger the non-canonical NF-kB pathway, and therefore NIK activation, in various cell types[432,433]. Thus, to investigate whether the previously seen effects of NIK SMI-1 were due to long exposure to this compound and interference with the inflammasome priming step, NIK SMI-1 was used after LPS treatment. MDMs were

primed with 1 µg/mL LPS for 3 h and then treated with 1 µM NIK SMI-1 for 30 min followed by stimulation with the MAC for 3 h or 10 µM nigericin for 45 min in the presence or absence of NIK SMI-1. This inhibitor had no effect in IL-1β secretion or cell death after stimulation with the MAC or nigericin (Fig 5.7 a and b). However, the use of NIK SMI-1 after stimulation with LPS only, triggered IL-1β release in MDMs (Fig 5.7 a), making difficult to interpret these results.

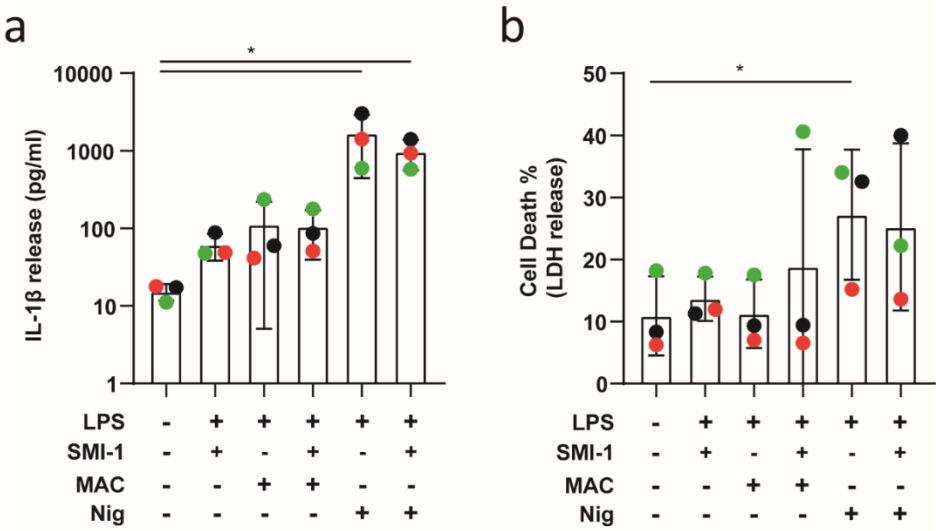

Figure 5.7 Inhibition of NF-κB-inducing kinase does not impair inflammasome activation in MDMs. Human MDMs were treated with vehicle-only controls or with 1 µg/mL LPS for 3 h followed by treatment with 1 µM SMI-1 for 30 min and stimulation with 10 µg/mL anti-CD59 mAb, C5b6, C7, C8 and C9 (MAC) for 3 h or 10 µM nigericin (Nig) for 45min in the presence or absence of SMI-1. **a)** IL-1β secretion was measured by ELISA. **b)** LDH release was measured as a proxy for cell death. Data is plotted as mean ± SD and is representative of 3 independent experiments. Each colour represents a matched single donor and statistical significance was measured by one-way ANOVA (*p<0.05).

To further investigate whether NIK plays a role in MAC-mediated inflammasome activation in MDMs, these cells were treated with 1 µg/mL LPS and 10 µg/mL C5b6, anti-CD59 mAb, C7, C8 and C9-AF647 to form the MAC for different times. Then, cells were fixed, stained for NIK and studied using confocal microscopy. This revealed a dynamism in localisation of NIK after treatment with the MAC (Fig 5.8 a and b). Specifically, NIK moved from the nucleus to the cytoplasm over 30 min following stimulation with the MAC and then re-localised to the nucleus after 90 min (Fig 5.8 a and b). However, NIK did not colocalise with C9 at any tested time point (Fig 5.8 c), including at time points when C9 is localised to early endosomes (Fig 5.2 a). Altogether, this suggest that NIK may not interact with MAC+ endosomes and may not be involved in NLRP3

inflammasome assembly in MDMs. However, this is likely to be a dynamic process and the interaction between NIK and MAC+ endosomes may be transient.

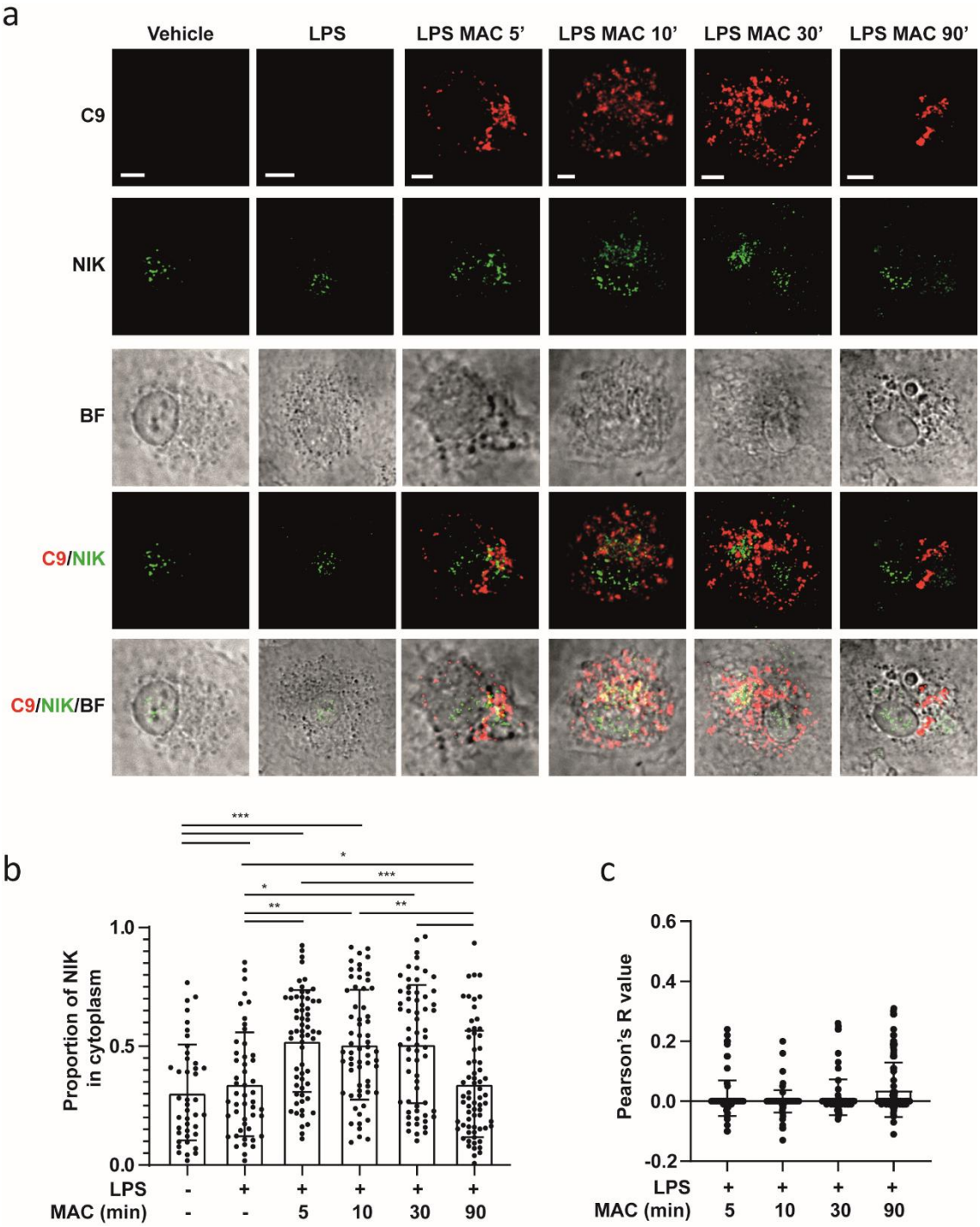

Figure 5.8 NF-κB inducing kinase (NIK) localised to the cytoplasm upon stimulation with the MAC. Human MDMs were treated with vehicle-only controls or 1 µg/mL LPS for 3 h followed by stimulation with 10 µg/mL anti-CD59 mAb, C5b6, C7, C8 and C9-AF647 (MAC) for the indicated time. **a)** Representative confocal images of C9-AF647 (red), NIK (green) and brightfield (gray). Scale bars are 5 µm. **b)** Proportion of NIK within the cytoplasm. **c)** Pearson's correlation coefficient of C9 compared to NIK overtime. In b and c data is plotted as mean ± SD and statistical significance was measured by Kruskal-Wallis test (*p<0.05 **p<0.01 ***p<0.001). In a-c data is representative of 2 independent experiments with similar results and ≥ 20 cells were imaged per condition in each experiment.

The non-canonical NF-kB pathway is characterized by the activation of NIK which in turn induces downstream events, leading to the activation of NF-κB p52/ RelB complex and its recruitment to the cell nucleus[36]. To study whether the MAC induces NIK activation, we next investigated the dynamics of NF-κB p52 and RelB. To this end, MDMs were primed with 1 µg/mL LPS for 3 h and treated with 10 µg/mL C5b6, anti-CD59 mAb, C7, C8 and C9-AF647 to form the MAC for the indicated time. Alternatively, cells were treated with vehicle-only controls or with 1 µg/mL LPS and 10 µM nigericin for 45 min. Next, cells were fixed, stained for p52 and RelB and imaged using confocal microscopy. The proportion of p52 and RelB in the nucleus significantly increased after LPS treatment (Fig 5.9 a, b and c). Interestingly, stimulation with nigericin did not change the localisation of p52 and RelB (Fig 5.9 a, b and c). However, the proportion of p52 and RelB in the nucleus was significantly reduced after treatment with the MAC, regardless of the length of the stimulation (Fig 5.9 a, b and c). The Pearson's R value used to analyse the colocalisation of p52 and RelB was very similar across conditions: 0.49 ± 0.1 in vehicle-only treated cells, 0.57 ± 0.1 in cells treated with LPS only, 0.56 ± 0.05, 0.49± 0.07 and 0.41 ± 0.09 in LPS-primed cells treated with the MAC for 10, 30 and 90 min, respectively, and 0.48 ± 0.06 in cells stimulated with LPS and nigericin (Fig 5.9 d). This suggests that the interaction between these proteins did not vary upon any treatment. Importantly, all the Pearson's R values were close or above 0.5 indicating colocalisation between both proteins (Fig 5.9 d). In contrast, the level of colocalisation of p52 or RelB with C9 was very low (Fig 5.9 e and f), suggesting no interaction between these proteins and the MAC. Of note, the dynamics of p52 and RelB were similar to those observed for NIK during the first 30 min of stimulation with the MAC. Specifically, NIK, p52 and RelB were predominantly in the nucleus after stimulation with LPS and re-localised to the cytoplasm upon treatment with the MAC (Fig 5.8 b and Fig 5.9 b and c).

Altogether, this suggests that the MAC triggers a change in localisation of NIK and its downstream proteins p52 and RelB, which may indicate stimulation of the non-canonical NF-kB pathway. However, these proteins did not colocalise with C9, showing that they do not directly interact with the MAC in human MDMs.

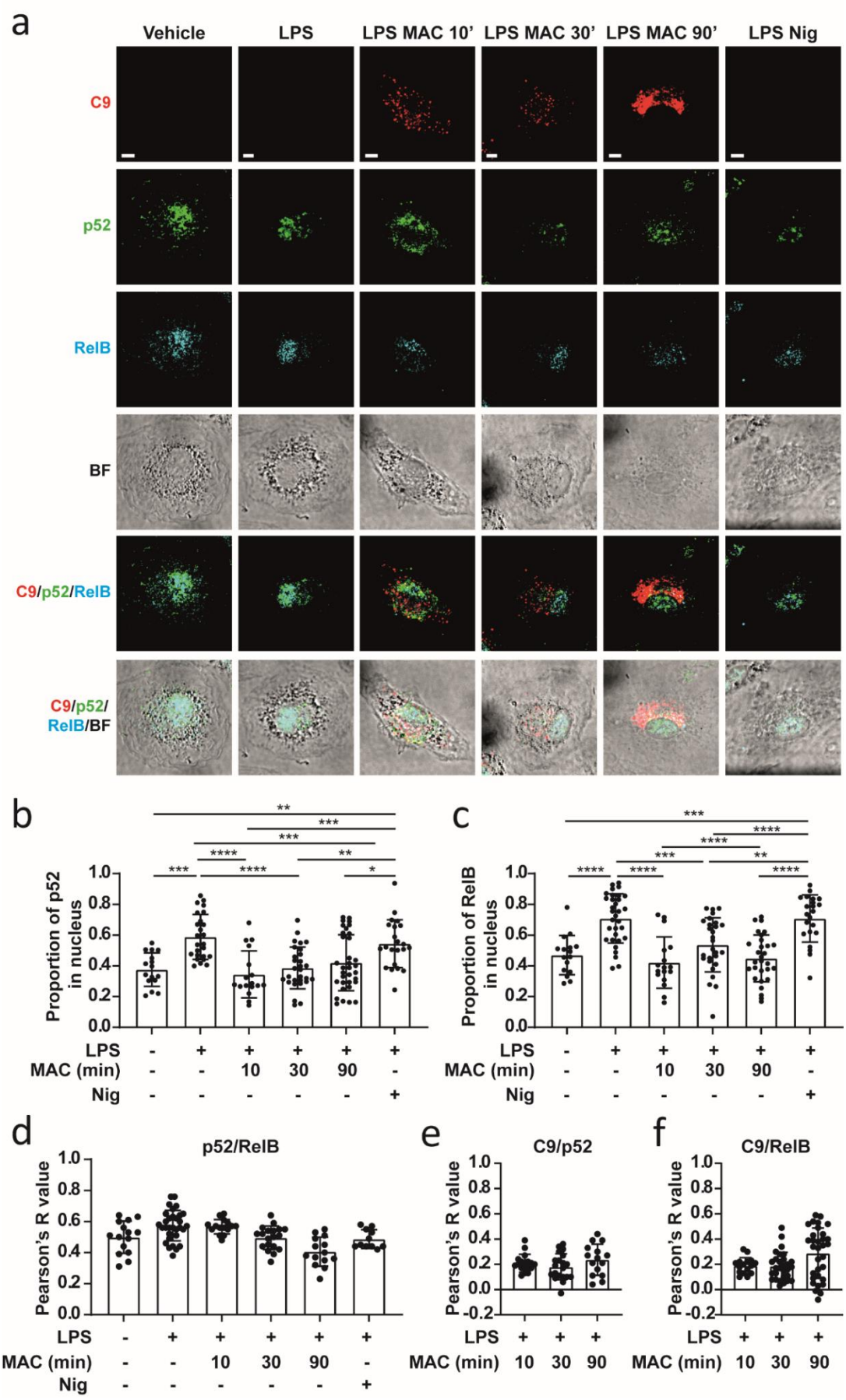
a
Vehicle
LPS
LPS MAC 10'
LPS MAC 30'
LPS MAC 90'
LPS Nig
C9
p52
RelB
BF
C9/p52/RelB
C9/p52/
RelB/BF
b
Proportion of p52 in nucleus
LPS
MAC (min)
Nig
c
Proportion of RelB in nucleus
LPS
MAC (min)
Nig
d
p52/RelB
Pearson's R value
LPS
MAC (min)
Nig
e
C9/p52
Pearson's R value
LPS
MAC (min)
f
C9/RelB
Pearson's R value
LPS
MAC (min)

Figure 5.9 NF-κB p52 and RelB localise to the cytoplasm upon stimulation with the MAC. Human MDMs were treated with vehicle-only controls or 1 µg/mL LPS for 3 h followed by stimulation with 10 µg/mL anti-CD59 mAb, C5b6, C7, C8 and C9-AF647 (MAC) for the indicated time. **a)** Representative confocal images of C9-AF647 (red), p52 (green), RelB (cyan) and brightfield (gray). Scale bars are 5 µm. **b)** Proportion of p52 within the nucleus. **c)** Proportion of RelB within the nucleus. **d)** Pearson's correlation coefficient of p52 compared to RelB. **e)** Pearson's correlation coefficient of C9 compared to p52. **f)** Pearson's correlation coefficient of C9 compared to RelB. In b-f data is plotted as mean ± SD and statistical significance was measured by Kruskal-Wallis test (*p<0.05 **p<0.01 ***p<0.001). In a-f data is representative of 3 independent experiments with similar results and ≥ 15 cells were imaged per condition.

5.3.4 Internalization of the Membrane Attack Complex induces the dispersion of the trans-Golgi network

Multiple inflammasome activators, including nigericin, trigger the dispersion of the trans-Golgi network (TGN) upstream of NLRP3 inflammasome activation. The dispersion of the TGN results in the recruitment of NLRP3 leading to inflammasome assembly and activation[417]. Therefore, the next experiments set out to investigate whether the MAC triggers TGN dispersion in MDMs. First, cells were treated with 1 µg/mL LPS for 3 h followed by the MAC using C9-AF647 for 30, 90 or 180 min, or nigericin for 45 min. Then, cells were fixed and stained with an Ab against TGN46, a resident membrane protein of the TGN. Confocal imaging revealed different conformations of the TGN and for this reason, cells were classified as exhibiting one of three specific TGN structures: an intact TGN (iTGN), characterized by a compact single structure; a fragmented TGN (fTGN), characterized by various stranded structures; or a dispersed TGN (dTGN), characterized by multiple granular-like dispersed formations (Fig 5.10).

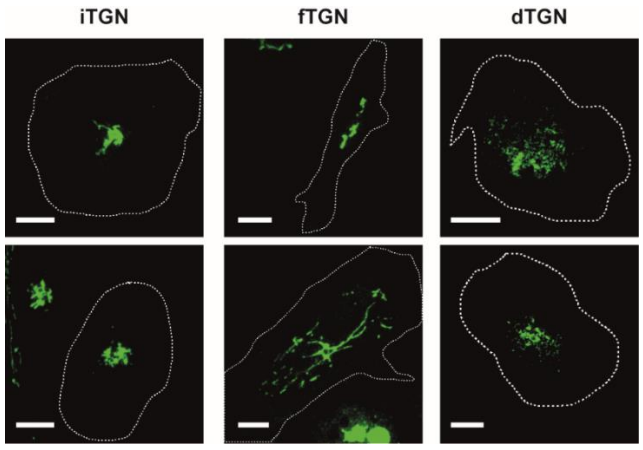

Figure 5.10 Conformations of the trans-Golgi network. Representative confocal images of the different trans-Golgi network (TGN) conformations: intact TGN (iTGN), fragmented TGN (fTGN) and dispersed TGN (dTGN).

Dispersion of the TGN was only observed in LPS-primed MDMs stimulated with the MAC or nigericin (Fig 5.11 a). On the other hand, MDMs unstimulated or only primed with LPS had mainly iTGN or fTGN (Fig 5.11 a and b). This indicates that as multiple inflammasome activators[417], the MAC induces dispersion of the TGN, providing further evidence of the MAC's ability to trigger NLRP3 inflammasome activation in MDMs. With the exception of nigericin-stimulated cells which mainly exhibited dTGN, the percentage of cells with fTGN was similar across conditions (Fig 5.11 c), suggesting that fTGN was not specifically triggered by inflammasome activators. The percentage of cell with dTGN was significantly increased after 30 min of stimulation with the MAC and this remained similar after 90 min of MAC stimulation (Fig 5.11 c). However, 180 min after MAC stimulation the percentage of cells with dTGN was slightly reduced (25.5 ± 9 % at 30 min, 25.8 ± 18.9 % at 90 min and 18.7± 7.3% at 180 min) (Fig 5.11 c). This indicates that dispersion of the TGN happened soon after endocytosis of the MAC, suggesting that this complex is able to rapidly trigger this intracellular process.

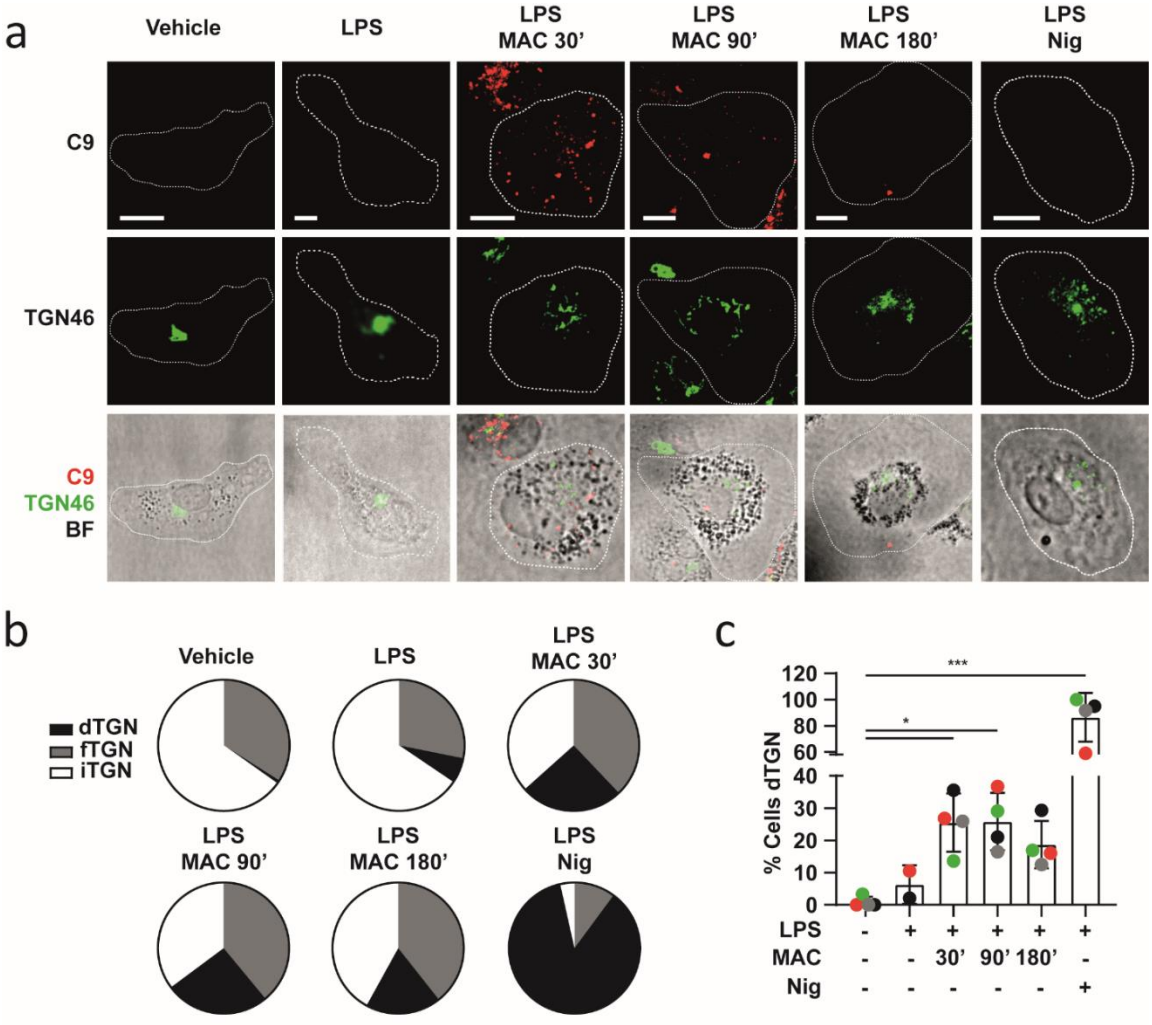

Figure 5.11 The MAC triggers disruption of the TGN. Human MDMs were primed with 1 μg/mL LPS for 3 h followed by stimulation with 10 μg/mL anti-CD59 mAb, C5b6, C7, C8 and C9 labelled with AF-647 (MAC) for the indicated time or nigericin (Nig) for 45 min. **a)** Representative confocal images of C9-AF647 (red), TGN46 (green) and brightfield (grey), dashed lines represent cell outlines and scale bars are 10 μm. **b)** Percentage of cells with intact TGN (iTGN), fragmented TGN (fTGN) and dispersed TGN (dTGN). **c)** Percentage of cells with dTGN. In c, data is plotted as mean ± SD, each colour represents a matched donor and statistical significance was measured by Friedman's test (*p<0.05 **p<0.01 ***p<0.001). In a-c data is representative of 4 independent experiments and ≥ 132 cells were imaged per condition.

Considering that MAC internalization is required for IL-1β secretion (Fig 5.3), the following experiments aimed to understand whether internalization of the MAC was important for triggering the dispersion of the TGN. Consequently, MDMs were stimulated with 1 μg/mL LPS for 3 h and the MAC or nigericin for 3 h and 45 min, respectively, in the presence or absence of Nys. Inhibition of MAC endocytosis using Nys reduced the dispersion of the TGN to similar levels to untreated cells or cells treated

only with LPS (Figure 5.12 a and b), indicating that internalization of the MAC precedes dispersion of the TGN. Moreover, Nys did not impair TGN dispersion upon stimulation with nigericin (Figure 5.12 a and b). As for IL-1β secretion, this shows that MAC-mediated dispersion of the TGN is specifically dependent on endocytosis of this complex.

To investigate whether dispersion of the TGN occurs upstream of NLRP3 inflammasome assembly, MDMs were treated with 1µg/mL LPS and the MAC or nigericin in the presence or absence the NLRP3 inhibitor MCC950. The use of MCC950 did not reduce MAC-mediated TGN dispersion (Fig 5.13 a and b), indicating that NLRP3 inflammasome assembly occurs downstream of treatment with the MAC and is independent of inflammasome assembly. Altogether, the performed experiments showed that, in MDMs, dispersion of the TGN following stimulation with the MAC occurs downstream of endocytosis of the MAC and upstream of NLRP3 inflammasome assembly.

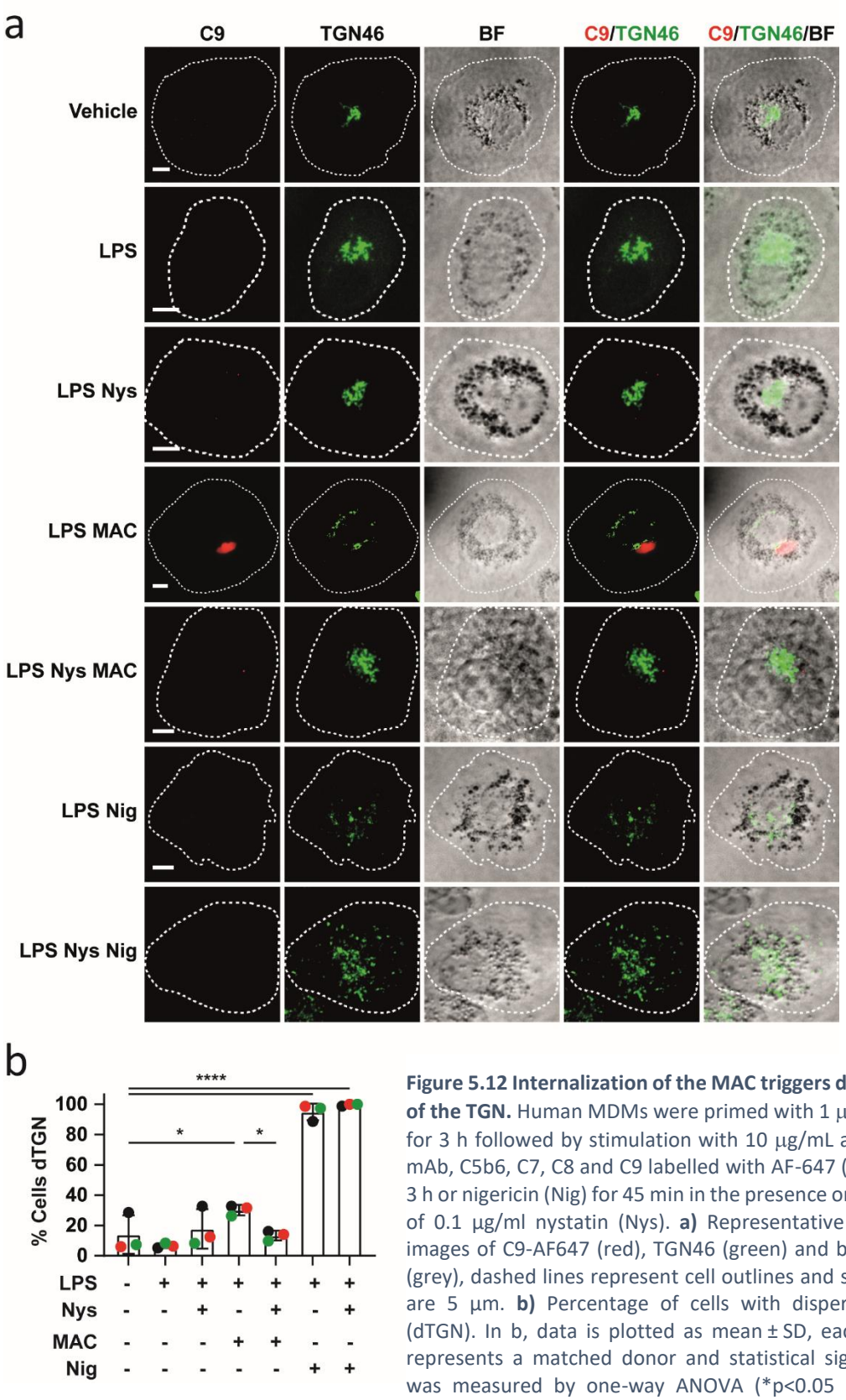

Figure 5.12 Internalization of the MAC triggers disruption of the TGN. Human MDMs were primed with 1 μg/mL LPS for 3 h followed by stimulation with 10 μg/mL anti-CD59 mAb, C5b6, C7, C8 and C9 labelled with AF-647 (MAC) for 3 h or nigericin (Nig) for 45 min in the presence or absence of 0.1 μg/ml nystatin (Nys). **a)** Representative confocal images of C9-AF647 (red), TGN46 (green) and brightfield (grey), dashed lines represent cell outlines and scale bars are 5 μm. **b)** Percentage of cells with dispersed TGN (dTGN). In b, data is plotted as mean ± SD, each colour represents a matched donor and statistical significance was measured by one-way ANOVA (*p<0.05 **p<0.01 ***p<0.001). In a and b data is representative of 3 independent experiments and ≥ 453 cells were imaged per condition.

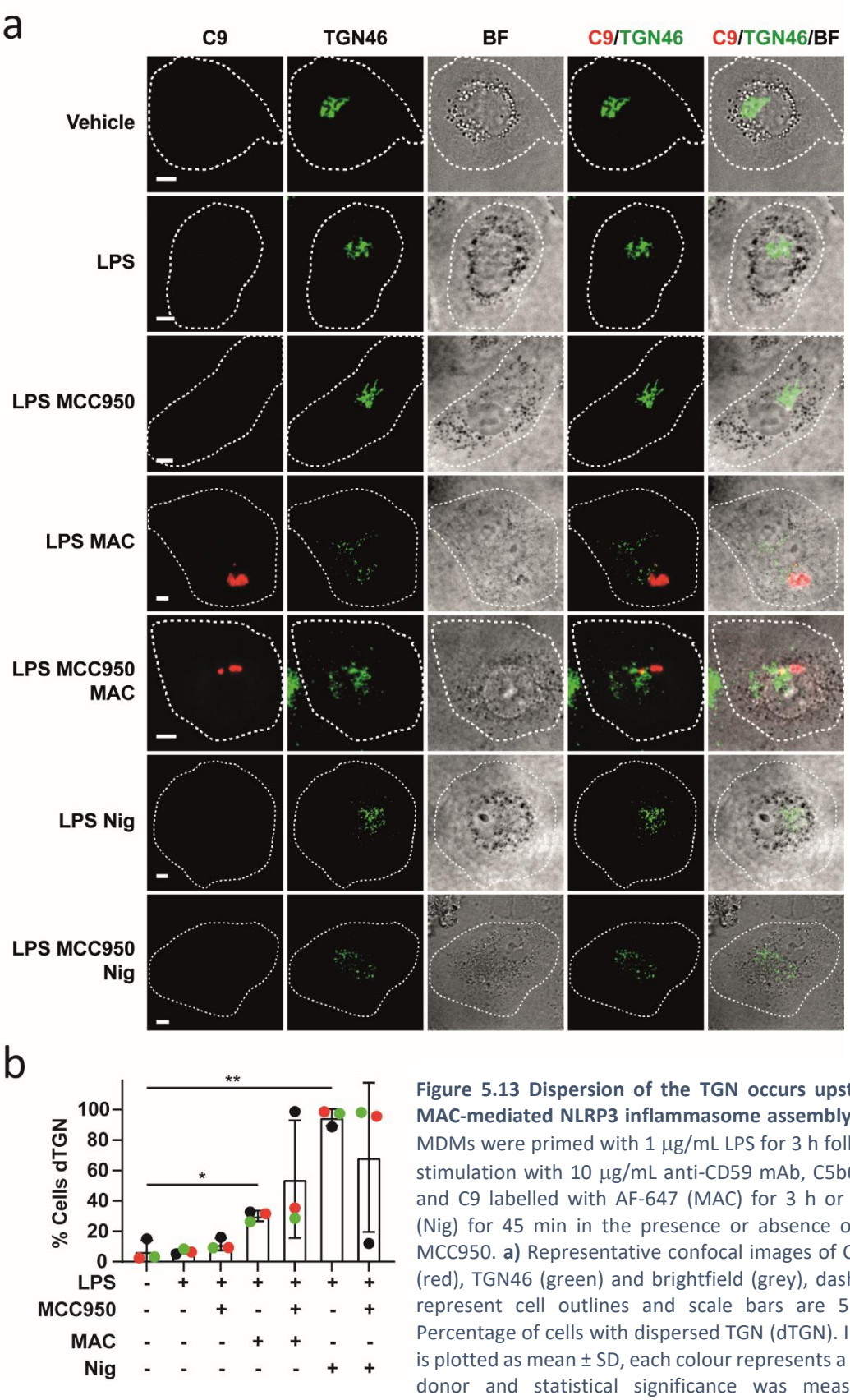

Figure 5.13 Dispersion of the TGN occurs upstream of MAC-mediated NLRP3 inflammasome assembly. Human MDMs were primed with 1 μg/mL LPS for 3 h followed by stimulation with 10 μg/mL anti-CD59 mAb, C5b6, C7, C8 and C9 labelled with AF-647 (MAC) for 3 h or nigericin (Nig) for 45 min in the presence or absence of 10 μM MCC950. **a)** Representative confocal images of C9-AF647 (red), TGN46 (green) and brightfield (grey), dashed lines represent cell outlines and scale bars are 5 μm. **b)** Percentage of cells with dispersed TGN (dTGN). In b, data is plotted as mean ± SD, each colour represents a matched donor and statistical significance was measured by Friedman's test (*p<0.05 **p<0.01). In a and b data is representative of 3 independent experiments and ≥ 384 cells were imaged per condition.

5.3.5 Where do the MAC and the inflammasome speck colocalise in MDMs?

In chapter 4, it was determined that from 90 min after stimulation with the MAC, this complex colocalised with the inflammasome speck in human macrophages (Fig 4.12). However, it remains unclear where the MAC and the inflammasome speck were detected together inside the cell. Thus, the following experiments aimed to investigate in which intracellular compartment the MAC and the ASC speck colocalise. In podocytes and retinal epithelial cells, the MAC is internalized and targeted for degradation through the autophagic-lysosomal pathway[434], with the expression of the autophagy marker LC3 enhanced during this process[435]. In LPS-primed human macrophage-like THP1 cells, NLRP3 colocalises with LC3 and ASC colocalises with LC3B after stimulation with ATP or monosodium urate crystals, respectively[146,147]. This suggests a crosslink between the autophagic pathway in the NLRP3 and the MAC signalling cascades. For this reason, the following experiments investigated whether the MAC interacts with the autophagosome in MDMs. To this end, MDMs were primed with 1 µg/mL LPS for 3 h and stimulated with 10 µg/mL C5b6, anti-CD59 mAb, C7, C8 and C9-AF647 to form the MAC for the indicated time or with 10 µM nigericin for 45 min. Alternatively, cells were treated with vehicle-only controls. Then, cells were fixed, stained with an anti-ASC Ab and an anti-LC3B Ab and studied using confocal microscopy. As previously shown, ASC specks were detected after 90 min of stimulation with the MAC and an accumulation of C9 was observed in the ASC speck (Fig 5.14 a). Of note, stimulation with nigericin also resulted in ASC speck formation (Fig 5.14 a). The fluorescence intensity of LC3B increased over 90 min of stimulation with the MAC and was reduced after 180 min (Fig 5.14 b). An increase in LC3B expression can reflect the enhance of autophagy. Thus, our findings could indicate that the MAC stimulates the process of autophagy in MDMs. However, the Pearson's R values used to analyse the colocalisation of C9 and LC3B were low (0.07 ± 0.17 after 30 min, 0.02 ± 0.1 after 90 min and 0.16 ± 0.26 after 180 min) (Fig 5.14 a and c), indicating that LC3B and C9 did not interact at the studied time points. Altogether, the lack of interaction between C9 and LC3B shows that the MAC and the inflammasome speck are not in the autophagosome when they colocalise together.

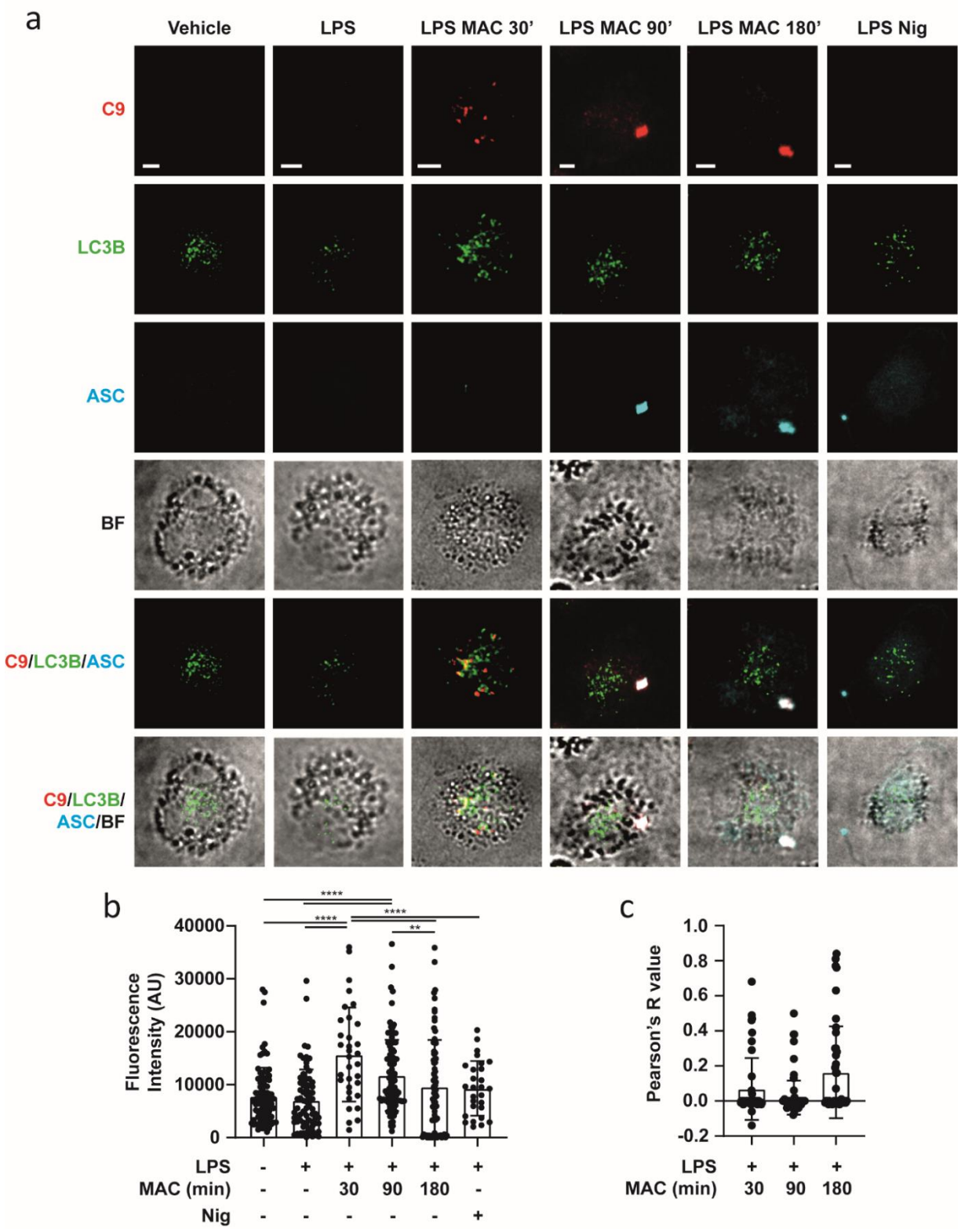

Figure 5.14 Spatial localisation of LC3B upon inflammasome activation in MDMs. Human MDMs were treated with vehicle-only controls or 1 µg/mL LPS for 3 h followed by stimulation with 10 µg/mL anti-CD59 mAb, C5b6, C7, C8 and C9-AF647 (MAC) for the indicated time. **a)** Representative confocal images of C9-AF647 (red), LC3B (green), ASC (cyan) and brightfield (gray). Scale bars are 5 µm. **b)** Fluorescence intensity of LC3B. **c)** Pearson's correlation coefficient of C9 compared to LC3B. In b and c data is plotted as mean ± SD and statistical significance was measured by Kruskal-Wallis test (*p<0.05 **p<0.01 ***p<0.001). In a-c data is representative of 3 independent experiments and ≥ 40 cells were imaged per condition.

It has recently been shown in immortalized bone-marrow derived murine macrophages and in THP1 cells treated with LPS and various NLRP3 inflammasome activators that the NLRP3 and ASC speck localises to the centrosome[146]. Thus, we next investigated if the MAC also localises to the centrosome in MDMs. MDMs were treated with vehicle-only controls or primed with 1 µg/mL LPS for 3 h and stimulated with 10 µg/mL anti-CD59 mAb, C5b6, C7, C8 and C9-AF647 to form the MAC for 3 h or with 10 µM nigericin for 45 min. Pericentrin (PCN) is one of the integral components of the centrosome[436]. Therefore, MDMs were stained with an anti-PCN Ab to visualize this cellular compartment (Fig 5.15 a). Confocal imaging showed two foci of PCN in every cell, regardless of the treatment used. This is in agreement with the centrosome being formed by two centrioles[437]. Nevertheless, after 3 h, the MAC was not localised to the centrosome, as indicated by a lack of colocalisation of C9 and PCN (Fig 5.15 a and b). This suggests that the inflammasome speck and the MAC are not in the centrosome when they localised together.

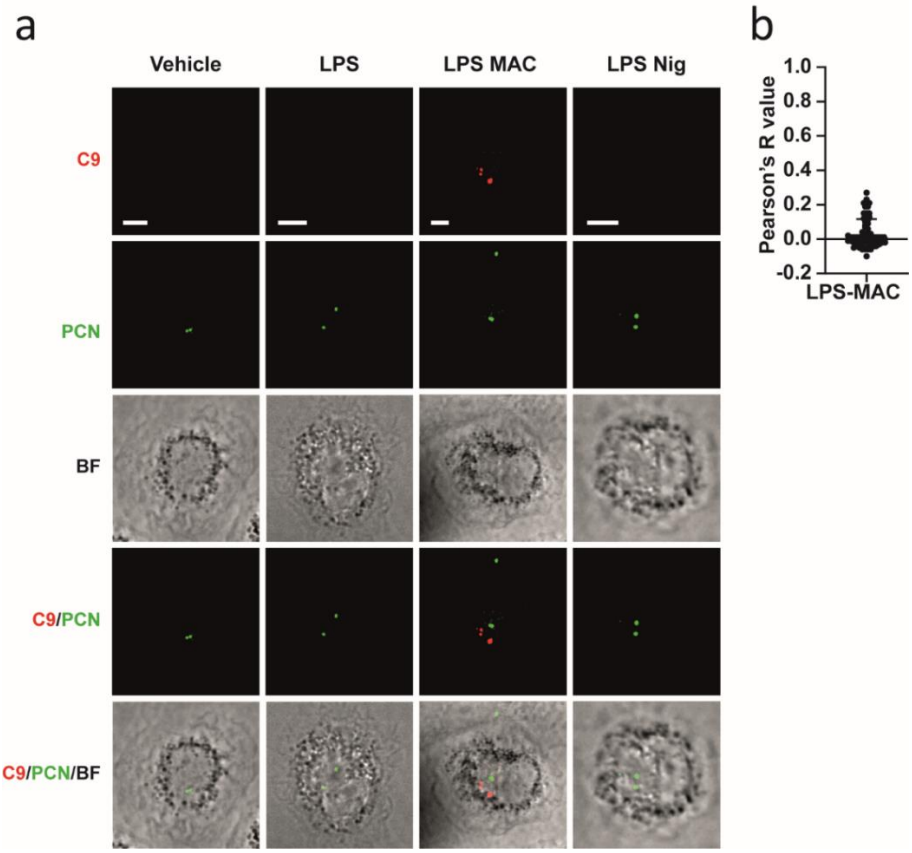

Figure 5.15 Spatial localization of pericentrin upon inflammasome activation in MDMs. Human MDMs were treated with vehicle-only controls or 1 µg/mL LPS for 3 h followed by stimulation with 10 µg/mL anti-CD59 mAb, C5b6, C7, C8 and C9-AF647 (MAC) for 3 h. **a)** Representative confocal images of C9-AF647 (red), pericentrin (PCN, green) and brightfield (gray). Scale bars are 5 µm. **b)** Pearson's correlation coefficient of C9 compared to PCN. Data is plotted as mean ± SD and statistical significance was measured by Kruskal-Wallis test (*p<0.05 **p<0.01 ***p<0.001). In a and b data is representative of 3 independent experiments and ≥ 60 cells were imaged per condition.

5.4 Discussion

5.4.1 Summary of results

The aim of this chapter was to investigate how the membrane attack complex (MAC) activate the NLRP3 inflammasome and trigger IL-1β release in human macrophages. The main discoveries made in human MDMs in this chapter are summarised as follows:

1. The MAC is internalized in $EEA1^+$ endosomes.
2. MAC-mediated IL-1β secretion is dependent on endocytosis.
3. Internalization of the MAC triggers dispersion of the trans-Golgi network.
4. NF-κB-inducing kinase and their downstream proteins p52 and RelB do not interact with the MAC.
5. The MAC is not in the autophagosome when it colocalises with the ASC speck.
6. The MAC does not localise to the centrosome at a time point when it localises to the inflammasome speck.

These results indicates that internalization of the MAC induces downstream signalling events leading to NLRP3 inflammasome activation and IL-1β secretion, being the cell compartment where the MAC and the inflammasome speck colocalise together still further to determine (Fig 5.16).

5.4.2 Significance of results

5.4.2.1 Internalization of the MAC and NLRP3 inflammasome activation

The mechanisms by which the complement proteins induce cell activation are complex and differ by cell type. In human epithelial cells, human serum containing the proteins that form the MAC can trigger inflammasome activation and IL-1β secretion. It has been proposed that an increase in cytosolic Ca^{2+} and a reduction of mitochondrial membrane potential triggered by MAC pore formation in the cell membrane are responsible for NLRP3 inflammasome activation in these cells[290]. This chapter showed that the MAC is internalized by human MDMs from early time points being the internalization of the complex required for inflammasome activation and IL-1β release. Moreover, in chapter 4, it was established that inhibition of K^+ efflux was not sufficient

to impair MAC-mediated inflammasome activation in human MDMs. Ion fluxes are known to play an important role in regulating endocytic trafficking[438]. Therefore, ion fluxes produced by MAC formation in the cell membrane may not be sufficient for triggering the activation of the inflammasome in human macrophages but may be key for initiating the internalization of the complex leading to inflammasome activation. In agreement with this, dispersion of the TGN, an event that occurs upstream of NLRP3 inflammasome assembly[417], was only induced after endocytosis of the MAC.

Multiple pore-forming toxins can induce NLRP3 inflammasome activation. For instance, α-haemolysin from *Staphylococcus aureus* and streptolysin O from *Streptococcus pyogenes* trigger caspase 1 activation and IL-1β secretion in murine monocytes and monocyte-like THP1 cells and in murine macrophages and macrophage-like THP1 cells[439–441], respectively. Cells have developed different mechanisms to remove these pore-forming toxins from the cell membrane, including endocytosis of the toxin[404]. Therefore, internalization of a pore-forming toxin may, in general, be able to induce activation of the inflammasome.

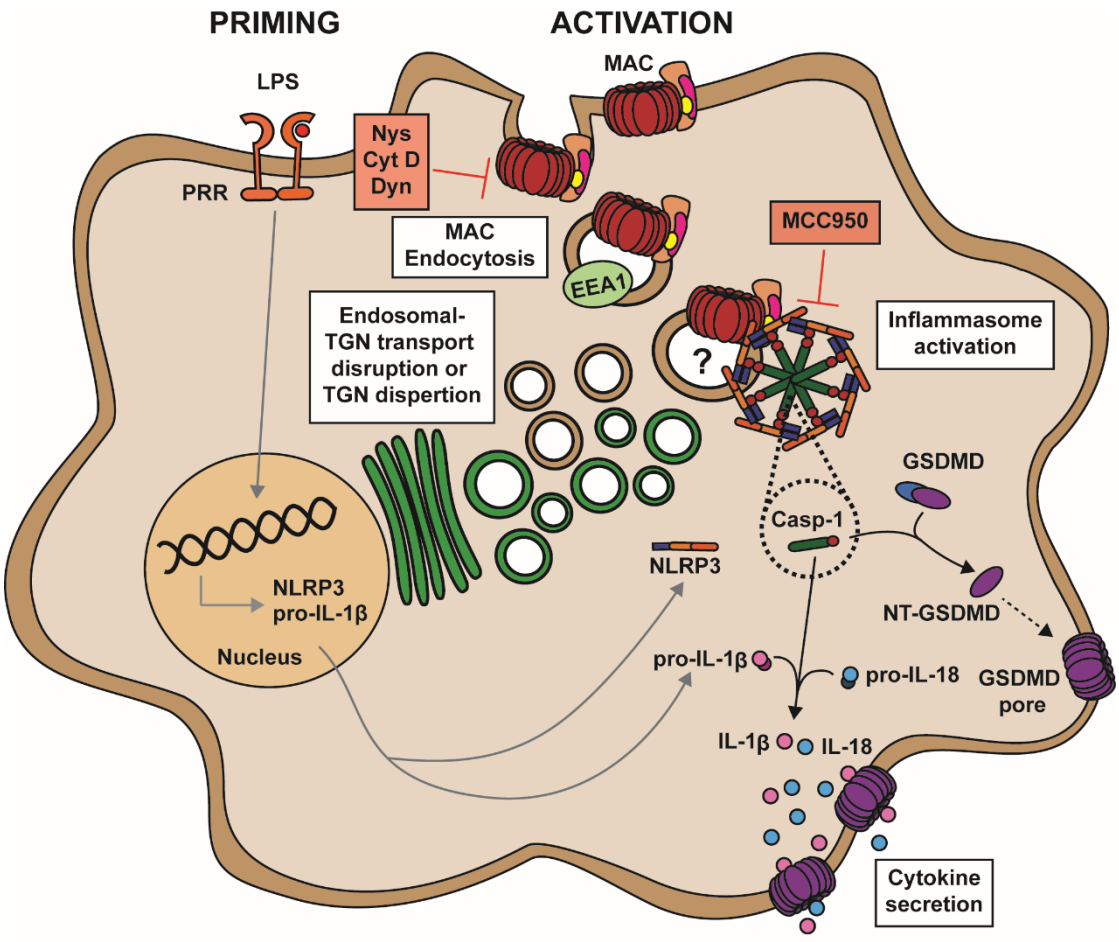

Figure 5.16 Internalization of the MAC triggers NLRP3 inflammasome activation in human macrophages. Formation of the MAC in LPS-primed human macrophages results in its internalization in EEA1+ endosomes. Endocytosis of this complex possibly results in the dispersion of the trans-Golgi network leading to NLRP3 inflammasome assembly and activation. In the NLRP3 inflammasome complex, caspase 1 (Casp-1) becomes active and cleaves GSDMD into its pore forming subunit NT-GSDMD and processed pro-IL-1β and pro-IL-18 into their mature forms to be released through GSDMD pores. MAC-mediated NLRP3 inflammasome activation and cytokine release are inhibited by the NLRP3 inhibitor MCC950, and the endocytosis inhibitors dynosore (Dyn), cytochalasin D (Cyt D) and nystatin (Nys) all inhibit the events downstream of MAC internalization, indicating that this complex needs to be endocytosed to trigger the NLRP3 inflammasome signalling pathway.

5.4.2.2 The role of NIK in MAC-mediated inflammasome activation

Previous research has described a role for NF-κB-inducing kinase (NIK) and its accessory proteins in complement-mediated inflammasome activation in endothelial cells[292]. Upon treatment with serum containing reactive Abs from transplant patients, these cells endocytose the MAC in $Rab5^+$ and $EEA1^+$ early endosomes. This results in the stabilization of the MAC-induced Rab5 effector ZFYVE21 on the endosome and the recruitment of activated Akt[293]. Then, Akt phosphorylates and activates NIK leading to non-canonical activation of the NF-κB signalling pathway[288,293]. Furthermore, when endothelial cells are primed with IFNγ, internalization of the MAC and association of NIK with early endosomes triggers NLRP3 recruitment and inflammasome assembly leading to IL-1β secretion[292]. Moreover, this research showed one example of NIK and its downstream protein RelB colocalising with the ASC speck[292]. In contrast to this, colocalisation of RelB with the ASC speck or of NIK with C9 was not observed at time points when C9 localises to the inflammasome speck upon stimulation with the MAC in human MDMs. This could suggest that the mechanism by which the MAC triggers inflammasome activation and IL-1β release in human MDMs varies from the one observed in endothelial cells.

In general, the non-canonical activation of NIK results in the processing of NF-κB p100 into NF-κB p52 and RelB and their recruitment to the cell nucleus to activate downstream signalling[36]. As previously mentioned, LPS can induce the non-canonical NF-κB pathway meaning that can activate NIK[432,433]. In agreement with this, we observed a translocation from the cytoplasm to the nucleus of p52 and RelB in MDMs treated only with LPS. However, LPS-primed MDMs treatment with the MAC restored the localisation of p52 and RelB to the cell cytoplasm possibly indicating the loss of NIK activity. Of note,

stimulation with nigericin did not restore p52 and RelB localisation to the cytoplasm suggesting that this event was particularly triggered by the MAC. Whilst NIK localisation clearly changed overtime, colocalisation with C9 was not detected, implying that the MAC and NIK may not directly associate. Nonetheless, NIK and C9 localisation was always studied by visualizing fixed cells at specific time points upon stimulation with the MAC. If the interaction between the MAC and NIK is transient, this method may not have detected it. Therefore, in order to confirm whether NIK and the MAC interact, live imaging or immunoprecipitation of one of the proteins and immunoblotting against the other could have been used.

5.4.2.3 Trans-Golgi network and the endocytic pathway

The mechanism by which the MAC triggers NLRP3 inflammasome activation in human macrophages is still unclear. Perhaps, dispersion of the TGN plays a role in this process. The endosomal compartment continuously interact with the TGN to exchange cargo[442]. Moreover, in NLRP3 and TGN38-expressing HeLa cells, EEA1 and TGN38, the rat homolog to human TGN46, stimulated with NLRP3 activators, NLRP3 and EEA1 colocalise with TGN38 in the dispersed TGN, showing the interaction between NLRP3, early endosomes, and the dispersed TGN. Moreover, it has been shown that NLRP3 is recruited to the TGN by direct binding with phosphatidylinositol-4-phosphate (PtdIns4P) that gets exposed when the TGN is dispersed[417]. Considering that our findings indicates that dispersion of the TGN occurs before inflammasome activation, endocytosis of the MAC and the recruitment of MAC-containing $EEA1^+$ endosomes to the TGN could induce dispersion of this cell compartment leading to NLRP3 recruitment, inflammasome assembly and activation, and IL-1β secretion in human macrophages (Fig 5.16).

Very recently, two pre-prints have linked disruption of endosomal trafficking or endosome-TGN transport to NLRP3 inflammasome activation[443,444]. Specifically, these studies show that $EEA1^+$ and TGN46/38 colocalisation increased in COS7 cells or in LPS-primed BMDMs stimulated with inflammasome activators like nigericin or imiquimoid, and that EGFP-NLRP3 is transported to mApple-$Rab5^+$ endosomes that also expressed TGN46 in HeLa cells treated with nigericin[443,444]. Moreover, in COS7 cells NLRP3-m-Venus partially colocalised with EEA1, TGN46 and LAMP1, a lysosomal marker, when cells were stimulated with NLRP3 inflammasome activators[443]. These findings suggest

that endosomes or endolysosomes could constitute a platform for NLRP3 inflammasome activation and assembly. Moreover, they also show that chemical or genetic disruption of the endosomal or endosome-TGN trafficking potentiate NLRP3 inflammasome activation, indicating that endosomal disruption may be important for NLRP3 inflammasome activation[443,444]. Importantly, these pre-prints showed that TGN38 or TGN46 can be localised to EEA1+ and Rab5+ endosomes when the endosome-TGN transport is perturbed, and that PtdIns4P is enriched in early endosomes upon treatment with NLRP3 stimuli[443,444]. This could indicate that the previously observed dispersion of the TGN upon stimulation with NLRP3 activators, the localisation of NLRP3 to the dTGN (based on the study of TGN38 or TGN46), and the interaction of NLRP3 with PtdIns4P in this compartment could have been misinterpreted. If this is the case, NLRP3 could interact with PtdIns4P in early endosomes rather than in the TGN and what was previously described as dTGN could represent multiple endosomes containing TGN38 or TGN46. Of note, one of these pre-prints showed that disturbance of endosomal-TGN transport increases IL-1β secretion without triggering cell death in LPS-primed murine macrophages[444]. This is in agreement with the findings of this thesis indicating that MAC-mediated inflammasome activation in human macrophages occurs in the absence of cell death. Based on this, endocytosis of the MAC and the presence of MAC pores in early endosomes could result in exposure of PtdIns4P in these intracellular vesicles and in the disturbance of the endosomal-TGN transport leading to NLRP3 recruitment and the initiation of NLRP3 inflammasome activation in human macrophages (Fig 5.16).

5.4.2.4 The autophagosome and lysosomes as hubs for NLRP3 inflammasome assembly

Upon treatment with NLRP3 activators, the NLRP3 inflammasome can localise to different cellular compartments. For example, in THP1 cells the ASC speck is targeted for degradation and together with NLRP3 localises to the autophagosome upon stimulation with ATP[445]. Podocytes and retinal epithelial cells reduce the lytic effects of the MAC by internalization of the complex in early endosomes and by targeting it for degradation through the autophagosome and lysosomal pathway[57,434]. Specifically, internalization of the MAC induces an increase in expression of the autophagosomal markers LC3 and p62 showing that the MAC activates the process of autophagy in these cells[434,435]. Furthermore, upon inflammasome activation, LC3, p62 and ASC localise together in

THP1 cells[146,147], indicating an interplay between the autophagic pathway in the NLRP3 and the MAC signalling cascades. Despite this, we showed that stimulation of human macrophages with the MAC did not trigger colocalisation of ASC with the autophagosome. In addition, we did not detect colocalisation of C9 and LC3B in MDMs. Nevertheless, the observed increase in LC3B expression may indicate the activation of the autophagic pathway. Thus, considering that the detected amount of intracellular C9 decreased over time, autophagy could play a role in the degradation of the MAC in human macrophages. In agreement with this, in podocytes internalization of the MAC induces an increase in the number of autophagosomes but inhibits the lysosomal degradation pathway by triggering lysosomal membrane permeabilitation[435]. Importantly, phagosomal and lysosomal disruption are responsible for the activation of the NLRP3 inflammasome in human PBMCs and murine macrophages upon treatment with particulate matter[124,446] (Fig 5.16). Thus, internalization of the MAC could result in lysosomal membrane damage leading to inflammasome activation and IL-1β release in MDMs.

5.4.2.5 The NLRP3 inflammasome and its interaction with the centrosome

The centrosome serves as the main microtubule organizing centre of the cell[447]. Importantly, NEK7 is a centrosomal kinase that is key for NLRP3 inflammasome assembly, and it has been described that the NLRP3 inflammasome can localise to the centrosome[117,145,146]. Specifically, in murine macrophages and macrophage-like THP1 cells, stimulation of the NLRP3 sensor results in the recruitment of mitochondria-associated endoplasmic reticulum membranes (MAMs) to the Golgi[92,142]. Here, NLRP3 is activated by phosphorylation, and released from the MAMs for transport to the centrosome where, after recruitment of ASC and caspase 1, the inflammasome complex is assembled[146]. This phenomenon is observed with multiple NLRP3 inflammasome activators including particulate matter such us monosodium urate and alum which are known to be endocytosed by the cell and targeted for degradation[92]. Our findings show that the MAC is internalized upon deposition in the cell membrane and possibly targeted for degradation as a reduction in the amount of intracellular C9 was observed overtime. However, although colocalisation of the MAC to the ASC speck was detected, C9 did not colocalised with pericentrin indicating that the inflammasome speck is not in the

centrosome when it colocalised with the MAC. Of note, previous research has described localisation of the NLRP3 inflammasome speck to multiple cellular compartments[142,143,146,147]. Therefore, further investigation is needed to determine precisely where the MAC and the inflammasome speck are localised together in human macrophages.

5.4.3 Significance in disease

The details about how intracellular MAC activates the inflammasome in human macrophages discovered in this thesis are important because multiple pro-inflammatory diseases characterised by increased levels of complement proteins, including the MAC, are mediated by IL-1β and IL-18[293,295,297,302,381]. Two examples are arthritis and sepsis and its related pathologies such as septic shock syndrome.

5.4.3.1 Arthritis

During arthritis, IL-1β and IL-18 are found at the joint interface, and they are responsible for driving pro-inflammatory responses leading to this pathology. Amongst other functions, IL-1β mediates the degradation of proteoglycans[167], which represent one of the main components of cartilage. Moreover, IL-1β also regulates the production of metalloproteases that are responsible for degrading collagen[167]. Thus, as collagen is a major component of cartilage and bones, an increase in IL-1β at the joint results in the destruction of these tissues, which is characteristic of arthritis. IL-1β also triggers complement synthesis by chondrocytes and synoviocytes[448], two cell types that are abundant at joints. In rheumatoid arthritis (RA), IL-18 secreted by macrophages in the synovium strongly induces the production of pro-inflammatory mediators such us TNFα and IFNγ, by synovial macrophages and infiltrated T-cells[449–451]. These cytokines trigger a positive loop of activation in the cells localised at the joint, including macrophages and synovial fibroblasts, that result in the destruction of tissue[168].

The complement pathway is significantly activated in various types of arthritis. Specifically, the levels of C5b-9 (MAC) are enhanced in synovial fluid and plasma from patients with RA and osteoarthritis (OA)[297–299]. During RA, the MAC promotes hypercitrullination of proteins, one of the first signs of the disease[452]. Moreover, in

murine models of both RA and OA, depletion or pharmacological inhibition of C5 or C6, and consequently impairment of MAC formation, protects against the development of these diseases[453], indicating a major role for the MAC in the progress of these pathologies.

At the inflamed joint, IL-1β and IL-18 are mainly produced by infiltrating monocytes, infiltrating macrophages and synovial macrophages[169,170]. This is supported by the fact that the amount of IL-1β in OA synovial cell cultures is significantly reduced when macrophages are depleted[171]. Nonetheless, how the production of these cytokines is triggered in macrophages during arthritis is not fully understood. Based on the results of this thesis and considering that complement levels are increased at the arthritic joint, MAC-mediated inflammasome activation in human macrophages could induce the secretion of IL-1β and IL-18 release. This may contribute to the onset of the pathology and feed the observed pro-inflammatory loop that induces damage of the joint.

3.1.1.1 Sepsis

It has been long known that IL-1β plays a major role in the pathogenesis of sepsis and similar diseases such as septic shock syndrome. In these pathologies, IL-1β promotes the recruitment and/or activation of multiple immune cells including myeloid cells, neutrophils and B and T cells[454]. This results in the over-production of pro-inflammatory mediators, which is characteristic of the early stages of these pathologies. Moreover, IL-1β also plays a role in vascular tone dysfunction involved in organ injury and failure during late stages of sepsis[455,456]. The processes that IL-18 mediates during sepsis are not fully explored. However, in murine models of LPS-induce endotoxemia, sustained levels of IL-18 leading to IFNγ production are lethal[457]. Furthermore, mice lacking caspase 1, but not IL-1β$^{-/-}$ mice, are resistant to lethal endotoxemia suggesting that IL-18 plays a major role in LPS-induced lethality[458]. Importantly, the role of both IL-1β and IL-18 in mediating sepsis and related diseases is supported by the fact that depletion or pharmacological inhibition of these cytokines or their receptors ameliorate these diseases in animal models and in human patients, and by the fact that high levels of these cytokines correlate with a poor prognosis for these diseases[459].

The terminal pathway of the complement system is also involved in the development of sepsis. For instance, C5a contributes to the activation of phagocytes leading to the release of pro-inflammatory mediators including histones[460,461]. Histones are prothrombotic and trigger inflammasome activation and cell cytotoxicity, playing a major role in organ dysfunction during sepsis[462]. On the other hand, although the role of the MAC during sepsis is not well understood, the MAC is able to activate intracellular pro-inflammatory cascades leading, not only to IL-1β and IL-18 secretion as described in this thesis, but also to the production and release of multiple pro-inflammatory cytokines including IL-6, TNFα and IL-8[290,291,383,463,464]. Therefore, the secretion of these cytokines induced by the MAC could contribute to the development of sepsis and septic shock. Moreover, deletion of C9, and consequently MAC formation inhibition, attenuates LPS-induced septic shock in mice[302], and high levels of C5b-9 in plasma are associated with a worse prognosis of this disease in humans[295,465], indicating a role for the MAC in this pathology.

Similar to arthritis, IL-1β and IL-18 secretion by macrophages is detrimental during sepsis. Indeed, this is evidenced by the fact that Macrophage Activation Syndrome, in which IL-1β and IL-18 play a major role, prompts death in septic patients[168]. Therefore, the increase in the activation of the complement cascade described by others during sepsis could result in deposition of the MAC in human macrophages, leading to inflammasome activation and cytokine release, contributing to the physiopathology of this disease.

3.1.1.2 Disease treatment

Several drugs that directly or indirectly block IL-1β or IL-18 have been used in the treatment of various complement-driven inflammatory diseases[176]. Unfortunately, this approach is not always efficient and varies among diseases and patients[176]. Considering that IL-1β and IL-18 release can be triggered by the MAC in human macrophages, one of the primary sources of these cytokines, and that the complement system is involved in the development of IL-1β and IL-18-driven diseases, future therapies for such diseases could contemplate targeting the upstream events that induce cytokine secretion.

5.4.4 Conclusion and future directions

Several mechanisms have been described for the activation of the NLRP3 inflammasome pathway downstream of inflammasome stimuli (Fig 5.18). This thesis defines the MAC as a new activator of the NLRP3 inflammasome in human macrophages and establishes that internalization of the MAC, resulting in the dispersion of the TGN and/or disruption of the endosomal-TGN transport, triggers NLRP3 inflammasome assembly and activation in these cells (Fig 5.17).

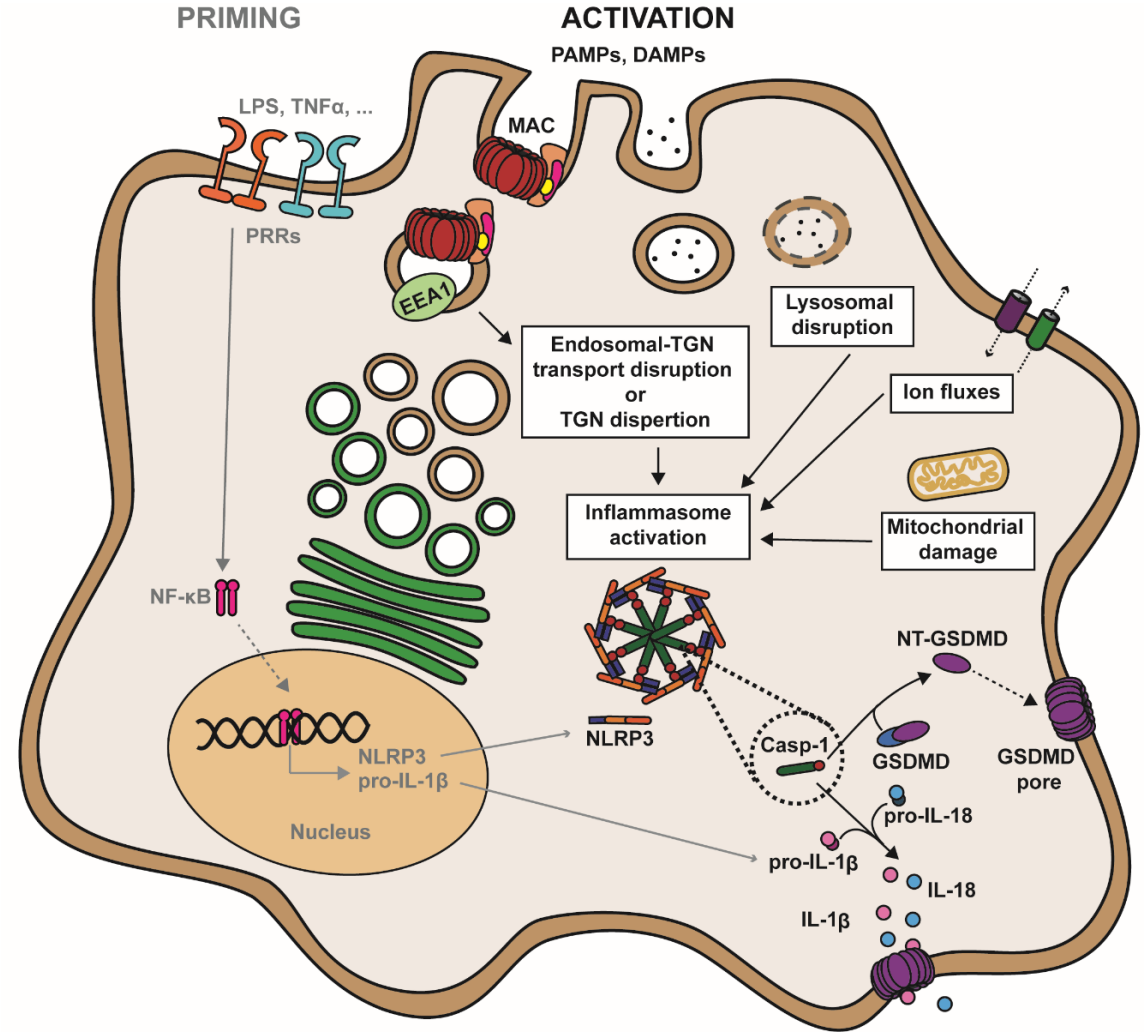

Figure 5.17 Graphical summary of canonical NLRP3 inflammasome activation incorporating existing models and the findings of this thesis. NLRP3 canonical activation requires two steps: a priming step, activated by stimuli such as LPS, that engages PRRs signalling pathways leading to NF-κB activation and production of NLRP3 and pro-IL-1B, and an activation step that leads to inflammasome assembly. Multiple stimuli trigger inflammasome assembly by inducing ion fluxes, lysosomal disruption, mitochondrial damage, dispersion of the trans-Golgi network (TGN) or disruption of the transport between endosomes and the TGN. The findings of this thesis suggest that internalization of the membrane attack complex (MAC) in early endosomes (EEA1+) leads to disruption of the TGN or of the transport between the TGN and the endosomal compartment, resulting in NLRP3 inflammasome assembly. NLRP3 inflammasome assembly, in general, triggers activation of caspase 1, leading to GSDMD pore formation and IL-1β and IL-18 maturation and release.

There are still open questions regarding the mechanism or mechanisms by which intracellular MAC activates the NLRP3 inflammasome in macrophages. Although in this thesis various intracellular compartments have been discarded, it remains important to determine where in the cell the MAC and the NLRP3/ASC speck are colocalised. Previous research has shown the MAC colocalising with cathepsin D in retinal epithelial cells, which could indicate its localisation to lysosomes[434]. Moreover, in lung epithelial cells stimulated with human serum, NLRP3 and ASC colocalise with mitotracker, indicating that the MAC and the inflammasome components could be located in the mitochondria[290]. Furthermore, considering that NLRP3 inflammasome activation is a dynamic and plastic process, localisation of the inflammasome components might change with time or intensity of stimuli. Therefore, the MAC could colocalise with NLRP3 at different cell compartments at different time points, with this process altered by the amount of MAC used to stimulate cells. To determine where the MAC and the NLRP3 inflammasome colocalise together in human macrophages, an approach using specific cell compartment markers or Abs against specific cell compartments and fluorescent microscopy could be used.

This thesis has established that the MAC localises to the NLRP3 inflammasome speck in human macrophages. However, whether the MAC physically interacts with the NLRP3 sensor in this context needs to be determined. In epithelial cells, the NLRP3 sensor is detected when Rab5 is immunoprecipitated, and the MAC is detected in Rab5 endosomes[288,292]. Despite this, it has never been shown that the MAC directly interacts with NLRP3 or other inflammasome components. Thus, defining if and how these proteins interact may help to further dissect the mechanism by which the MAC induces IL-1β and IL-18 secretion. To determine whether these complexes interact, the presence of NLRP3 could be studied in samples of immunoprecipitated C9 or vice versa. However, this may be difficult if this interaction is transient. If this is the case, strategies using proximity ligation or live-imaging with tagged-NLRP3 could be used.

On the other hand, other NLRP3 activators do not need to physically interact with the NLRP3 sensor to activate this inflammasome. Instead, these activators normally induce intracellular events leading to the activation of the NLRP3 sensor and assembly of the inflammasome. This thesis has established that the MAC induces dispersion of the

TGN or of the endosomal-TGN transport, events that precede inflammasome assembly upon stimulation with multiple other NLRP3 activators[417,443,444]. Therefore, addressing whether this is also fundamental for MAC-mediated IL-1β release could help to uncover the mechanism by which this complement complex mediates NLRP3 inflammasome activation.

Previous studies determined that the MAC activates the inflammasome in murine myeloid cells and in human epithelial and endothelial cells[283,284,290,292]. However, how the NLRP3 inflammasome is activated is known to vary between species and cell types. Thus, future work should study if MAC-mediated inflammasome activation is restricted to macrophages in humans, or if internalization of the MAC also triggers IL-1β and IL-18 release in other human myeloid cells.

Overall, the findings of this thesis begin to provide mechanistic evidence of how the MAC mediates inflammation through engagement of the inflammasome. Thus, this could establish a broader application of anti-MAC therapies in the treatment of pro-inflammatory pathologies mediated by the complement system and IL-1β or IL-18, including both pathogen-mediated and sterile inflammatory diseases.

Chapter 6 Final remarks

Multiple proinflammatory diseases develop as a result of the incorrect resolution of the immune response upon activation by danger stimuli, or due to an overstimulation of this response. Proinflammatory mediators play a major role in the development of these immune responses, with IL-1β and IL-18 as two such mediators that are important therapeutic targets for proinflammatory disorders. These cytokines are mainly produced by innate immune cells, with macrophages being one of their main sources in humans. Therefore, understanding how the production of IL-1β and IL-18 is triggered and how they are secreted to the extracellular milieu from this cell type is key for the design of strategies to treat pathologies mediated by these cytokines. Gasdermin D (GSDMD) pores have been shown to be required for the secretion of IL-1β and IL-18 from liposomes, murine cells, and human macrophage-like cell lines. This thesis now shows that GSDMD processing is required for cytokine release in human primary macrophages, indicating that this protein could represent a druggable target in human diseases. Another important component of the innate immune response is the complement system. This comprises a group of proteins, the activation of which results in the formation of the membrane attack complex (MAC). The overstimulation of this system also contributes to the development of several proinflammatory pathologies. However, although dysregulation of both the terminal pathway of the complement system and the production of IL-1β and/or IL-18 are detrimental for some diseases, whether the complement system could trigger the release of this cytokines in human myeloid cells was unknown. This thesis establishes that, indeed, the MAC can induce IL-1β and IL-18 secretion in human macrophages, paving the way for broader application of therapies targeting the complement cascade.

In summary, the main discoveries of this thesis are:

1. In human macrophages, canonical activation of the NLRP3 inflammasome results in the processing of GSDMD, leading to the transport of NT-GSDMD to the cell membrane to oligomerize and form pores. GSDMD processing, and therefore, pore formation, results in IL-1β and IL-18 secretion independently of membrane

rupture, most likely indicating that in human macrophages IL-1β and IL-18 secretion takes place through GSDMD pores.

2. In human macrophages, formation of the MAC by sequential addition of its purified complement components triggers NLRP3 activation leading to the formation of an ASC and an NLRP3 speck, the activation of caspase 1 and processing of pro-IL-1β and pro-IL-18 into their mature forms to be released in a GSDMD-dependent manner. This demonstrates for the first time that the terminal complex of the complement cascade induces inflammasome activation in human myeloid cells, indicating that the complement system could be targeted to reduce inflammasome activation in certain pro-inflammatory diseases.

3. In human macrophages, deposition of the MAC in the cell membrane is not sufficient to activate the NLRP3 inflammasome. The MAC needs to be internalized for this purpose. Internalization of this complex results in the dispersion of the trans-Golgi network and the production and release of IL-1β. Contrary to previous findings in epithelial cells treated with human serum, the MAC does not interact with NF-κB inducing kinase, indicating that the MAC may be able to activate the inflammasome through different pathways.

Altogether, this thesis shows that in human macrophages GSDMD is fundamental for IL-1β and IL-18 secretion upon NLRP3 inflammasome activation and that the MAC can engage the production and release of these cytokines. This highlights GSDMD, the MAC, and the events upstream of MAC assembly, as druggable targets for proinflammatory diseases mediated by excessive production of IL-1β and IL-18 and/or overstimulation of the complement system. Since activation of the complement system and inflammation are intricately connected, MAC-mediated inflammasome activation could therefore be implicated in a variety of acute and chronic inflammatory diseases. As such, future research should focus on understanding if this mechanism is responsible for, or involved in, the onset of IL-1β and IL-18-mediated pathologies.

References

1. Lazzaro, B. P. & Rolff, J. Danger, microbes, and homeostasis. *Science* **332**, 43–44 (2011).
2. Netea, M. G. *et al.* A guiding map for inflammation. *Nat. Immunol.* **18**, 826–831 (2017).
3. Stuart E. Turvey, MB BS, DPhil and David H. Broide, M. C. CHAPTER 2 Innate Immunity. *Immunology* **125**, 1–4 (2006).
4. Rock, Kenneth L; Kono, H. The Inflammatory Response to Cell Death. *Annu. Rev. Pathol. Dis.* **3**, 67–97 (2008).
5. Fujiwara, N. & Kobayashi, K. Macrophages in inflammation. *Curr. Drug Targets. Inflamm. Allergy* **4**, 281–6 (2005).
6. Ariel, A., Maridonneau-Parini, I., Rovere-Querini, P., Levine, J. S. & Mühl, H. Macrophages in inflammation and its resolution. *Front. Immunol.* **3**, 2–3 (2012).
7. Murray, P. J. & Wynn, T. A. Protective and pathogenic functions of macrophage subsets. *Nat. Rev. Immunol.* **11**, 723–737 (2011).
8. Gordon, S. Phagocytosis: The Legacy of Metchnikoff. *Cell* **166**, 1065–1068 (2016).
9. Koh, T. J. & DiPietro, L. A. Inflammation and wound healing: the role of the macrophage. *Expert Rev. Mol. Med.* **13**, e23 (2011).
10. Wynn, T. A., Chawla, A. & Pollard, J. W. Macrophage biology in development, homeostasis and disease. *Nature* **496**, 445–455 (2013).
11. Gordon, S. & Taylor, P. R. Monocyte and macrophage heterogeneity. *Nat. Rev. Immunol.* **5**, 953–964 (2005).
12. Gautier, E. L. *et al.* Gene-expression profiles and transcriptional regulatory pathways that underlie the identity and diversity of mouse tissue macrophages. *Nat. Immunol.* **13**, 1118–1128 (2012).
13. Italiani, P. & Boraschi, D. From Monocytes to M1/M2 Macrophages: Phenotypical vs. Functional Differentiation. *Front. Immunol.* **5**, 514 (2014).
14. Hoeffel, G. *et al.* Adult Langerhans cells derive predominantly from embryonic fetal liver monocytes with a minor contribution of yolk sac–derived macrophages. *J. Exp. Med.* **209**, 1167–81 (2012).
15. Ginhoux, F. *et al.* Fate Mapping Analysis Reveals That Adult Microglia Derive from Primitive Macrophages. *Science* **330**, 841–5 (2010).
16. Martinez, F. O. & Gordon, S. The M1 and M2 paradigm of macrophage activation: Time for reassessment. *F1000Prime Rep.* **6**, (2014).
17. Gordon, S. Alternative activation of macrophages. *Nat. Rev. Immunol.* **3**, 23–35 (2003).
18. Erblich, B., Zhu, L., Etgen, A. M., Dobrenis, K. & Pollard, J. W. Absence of Colony Stimulation Factor-1 Receptor Results in Loss of Microglia, Disrupted Brain Development and Olfactory Deficits. *PLoS One* **6**, e26317 (2011).
19. Hercus, T. R. *et al.* The granulocyte-macrophage colony-stimulating factor receptor: linking its structure to cell signaling and its role in disease. *Blood* **114**, 1289–98 (2009).
20. Bertani, F. R. *et al.* Classification of M1/M2-polarized human macrophages by label-free hyperspectral reflectance confocal microscopy and multivariate analysis. *Sci. Reports 2017 71* **7**, 1–9 (2017).

21. Dominguez-Gutierrez, P. R., Kusmartsev, S., Canales, B. K. & Khan, S. R. Calcium Oxalate Differentiates Human Monocytes Into Inflammatory M1 Macrophages. *Front. Immunol.* **9**, 1863 (2018).

22. Verreck, F. A. W., de Boer, T., Langenberg, D. M. L., van der Zanden, L. & Ottenhoff, T. H. M. Phenotypic and functional profiling of human proinflammatory type-1 and anti-inflammatory type-2 macrophages in response to microbial antigens and IFN-γ- and CD40L-mediated costimulation. *J. Leukoc. Biol.* **79**, 285–293 (2006).

23. Takeuchi, O. & Akira, S. Pattern Recognition Receptors and Inflammation. *Cell* **140**, 805–820 (2010).

24. Atri, C., Guerfali, F. Z. & Laouini, D. Role of human macrophage polarization in inflammation during infectious diseases. *International Journal of Molecular Sciences* **19**, (2018).

25. Brown, G. D., Willment, J. A. & Whitehead, L. C-type lectins in immunity and homeostasis. *Nat. Rev. Immunol. 2018 186* **18**, 374–389 (2018).

26. Sharma, B. R., Karki, R. & Kanneganti, T. D. Role of AIM2 inflammasome in inflammatory diseases, cancer and infection. *Eur. J. Immunol.* **49**, 1998–2011 (2019).

27. Rehwinkel, J. & Gack, M. U. RIG-I-like receptors: their regulation and roles in RNA sensing. *Nat. Rev. Immunol. 2020 209* **20**, 537–551 (2020).

28. Janssens, S., Burns, K., Tschopp, J. & Beyaert, R. Regulation of Interleukin-1- and Lipopolysaccharide-Induced NF-κB Activation by Alternative Splicing of MyD88. *Curr. Biol.* **12**, 467–471 (2002).

29. Medzhitov, R. *et al.* MyD88 Is an Adaptor Protein in the hToll/IL-1 Receptor Family Signaling Pathways. *Mol. Cell* **2**, 253–258 (1998).

30. Wesche, H., Henzel, W. J., Shillinglaw, W., Li, S. & Cao, Z. MyD88: An Adapter That Recruits IRAK to the IL-1 Receptor Complex. *Immunity* **7**, 837–847 (1997).

31. Gangloff, M. Different dimerisation mode for TLR4 upon endosomal acidification? *Trends Biochem. Sci.* **37**, 92–8 (2012).

32. Xia, Z.-P. *et al.* Direct Activation of Protein Kinases by Unanchored Polyubiquitin Chains. *Nature* **461**, 114 (2009).

33. Jenkins, K. A. & Mansell, A. TIR-containing adaptors in Toll-like receptor signalling. *Cytokine* **49**, 237–244 (2010).

34. Cargnello, M. & Roux, P. P. Activation and function of the MAPKs and their substrates, the MAPK-activated protein kinases. *Microbiol. Mol. Biol. Rev.* **75**, 50–83 (2011).

35. Lawrence, T. The nuclear factor NF-kappaB pathway in inflammation. *Cold Spring Harb. Perspect. Biol.* **1**, a001651 (2009).

36. Sun, S.-C. Non-canonical NF-κB signaling pathway. *Cell Res.* **21**, 71 (2011).

37. Xiao, G., Harhaj, E. W. & Sun, S.-C. NF-κB-Inducing Kinase Regulates the Processing of NF-κB2 p100. *Mol. Cell* **7**, 401–409 (2001).

38. Distefano, M. D. Macrophage activation by endogenous danger signals. **214**, 161–178 (2008).

39. O'Garra, A. & Vieira, P. TH1 cells control themselves by producing interleukin-10. *Nat. Rev. Immunol.* **7**, 425–428 (2007).

40. Shen, H.-M. & Pervaiz, S. TNF receptor superfamily-induced cell death: redox-

dependent execution. *FASEB J.* **20**, 1589–98 (2006).

41. Huynh, M.-L. N., Fadok, V. A. & Henson, P. M. Phosphatidylserine-dependent ingestion of apoptotic cells promotes TGF-beta1 secretion and the resolution of inflammation. *J. Clin. Invest.* **109**, 41–50 (2002).

42. Pahl, J. H. H. *et al.* Macrophages inhibit human osteosarcoma cell growth after activation with the bacterial cell wall derivative liposomal muramyl tripeptide in combination with interferon-γ. *J. Exp. Clin. Cancer Res.* **33**, 27 (2014).

43. Ingman, W. V., Wyckoff, J., Gouon-Evans, V., Condeelis, J. & Pollard, J. W. Macrophages promote collagen fibrillogenesis around terminal end buds of the developing mammary gland. *Dev. Dyn.* **235**, 3222–3229 (2006).

44. Boyle, W. J., Simonet, W. S. & Lacey, D. L. Osteoclast differentiation and activation. *Nature* **423**, 337–342 (2003).

45. Perry, V. H. & O'Connor, V. The role of microglia in synaptic stripping and synaptic degeneration: a revised perspective. *ASN Neuro* **2**, 281–291 (2010).

46. K, B. & G, K. Displacement of synaptic terminals from regenerating motoneurons by microglial cells. *Z. Zellforsch. Mikrosk. Anat.* **85**, 145–157 (1968).

47. Mosser, D. M. & Edwards, J. P. Exploring the full spectrum of macrophage activation. *Nature Reviews Immunology* **8**, 958–969 (2008).

48. Kawane, K. *et al.* Chronic polyarthritis caused by mammalian DNA that escapes from degradation in macrophages. *Nature* **443**, 998–1002 (2006).

49. Smith, A. M. *et al.* Disordered macrophage cytokine secretion underlies impaired acute inflammation and bacterial clearance in Crohn's disease. *J. Exp. Med.* **206**, 1883–97 (2009).

50. Murphy, C. A. *et al.* Divergent pro- and antiinflammatory roles for IL-23 and IL-12 in joint autoimmune inflammation. *J. Exp. Med.* **198**, 1951–7 (2003).

51. Qian, B.-Z. & Pollard, J. W. Macrophage Diversity Enhances Tumor Progression and Metastasis. *Cell* **141**, 39–51 (2010).

52. Martinon, F., Burns, K. & Tschopp, J. The Inflammasome: A Molecular Platform Triggering Activation of Inflammatory Caspases and Processing of proIL-β. *Mol. Cell* **10**, 417–426 (2002).

53. Schroder, K. & Tschopp, J. The Inflammasomes. *Cell* **140**, 821–832 (2010).

54. Guo, H., Callaway, J. B. & Ting, J. P.-Y. Inflammasomes: mechanism of action, role in disease, and therapeutics. *Nat. Med.* **21**, 677–687 (2015).

55. Broz, P. & Dixit, V. M. Inflammasomes: Mechanism of assembly, regulation and signalling. *Nature Reviews Immunology* **16**, 407–420 (2016).

56. Latz, E., Xiao, T. & Stutz, A. Activation and regulation of the inflammasomes. **13**, 23702978 (2013).

57. Xing Liu and Judy Lieberman. A Mechanistic Understanding of Pyroptosis: The Fiery Death Triggered by Invasive Infection. (2017). doi:10.1016/BS.AI.2017.02.002

58. Henao-Mejia, J., Elinav, E., Strowig, T. & Flavell, R. A. Inflammasomes: far beyond inflammation. *Nat. Immunol.* **13**, 321–324 (2012).

59. Miao, E. A., Rajan, J. V. & Aderem, A. Caspase-1 induced pyroptotic cell death. *Immunol. Rev.* **243**, 206 (2011).

60. Downs, K. P., Nguyen, H., Dorfleutner, A. & Stehlik, C. An overview of the non-canonical inflammasome. *Molecular Aspects of Medicine* **76**, 100924 (2020).

61. Kayagaki, N. *et al.* Non-canonical inflammasome activation targets caspase-11. *Nature* **479**, 117–121 (2011).

62. Yi, Y. S. Caspase-11 non-canonical inflammasome: a critical sensor of intracellular lipopolysaccharide in macrophage-mediated inflammatory responses. *Immunology* **152**, 207–217 (2017).

63. Kayagaki, N. *et al.* Caspase-11 cleaves gasdermin D for non-canonical inflammasome signalling. *Nature* **526**, 666–671 (2015).

64. Rathinam, V. A. K. *et al.* The AIM2 inflammasome is essential for host defense against cytosolic bacteria and DNA viruses. *Nat. Immunol.* **11**, 395–402 (2010).

65. Spranger, J. *et al.* Inflammatory Cytokines and the Risk to Develop Type 2 DiabetesResults of the Prospective Population-Based European Prospective Investigation into Cancer and Nutrition (EPIC)-Potsdam Study. *Diabetes* **52**, 812–817 (2003).

66. Masumoto, J. *et al.* ASC, a Novel 22-kDa Protein, Aggregates during Apoptosis of Human Promyelocytic Leukemia HL-60 Cells *. *J. Biol. Chem.* **274**, 33835–33838 (1999).

67. Alba, E. de. Structure and Interdomain Dynamics of Apoptosis-associated Speck-like Protein Containing a CARD (ASC). *J. Biol. Chem.* **284**, 32932 (2009).

68. Fernandes-Alnemri, T. *et al.* The pyroptosome: A supramolecular assembly of ASC dimers mediating inflammatory cell death via caspase-1 activation. *Cell Death Differ.* **14**, 1590–1604 (2007).

69. Srinivasula, S. M. *et al.* The PYRIN-CARD Protein ASC Is an Activating Adaptor for Caspase-1 *. *J. Biol. Chem.* **277**, 21119–21122 (2002).

70. Bryan, N. B., Dorfleutner, A., Rojanasakul, Y. & Stehlik, C. Activation of inflammasomes requires intracellular redistribution of the apoptotic speck-like protein containing a caspase recruitment domain (ASC). *J. Immunol.* **182**, 3173 (2009).

71. Fukami, K. A novel heterodimeric cysteinprotease is required for interleukin-1beta processing in monocytes. **359**, 150–152 (1992).

72. Ghayur, T. *et al.* Caspase-1 processes IFN-γ-inducing factor and regulates LPS-induced IFN- γ production. *Nat. 1997 3866625* **386**, 619–623 (1997).

73. Gu, Y. *et al.* Activation of Interferon-γ Inducing Factor Mediated by Interleukin-1β Converting Enzyme. *Science (80-.).* **275**, 206–209 (1997).

74. Mariathasan, S. *et al.* Differential activation of the inflammasome by caspase-1 adaptors ASC and Ipaf. *Nature* **430**, 213–218 (2004).

75. Bergsbaken, T., Fink, S. L. & Cookson, B. T. Pyroptosis: Host cell death and inflammation. *Nature Reviews Microbiology* **7**, 99–109 (2009).

76. Kaplanski, G. Interleukin-18: Biological properties and role in disease pathogenesis. *Immunol. Rev.* **281**, 138–153 (2018).

77. Garlanda, C., Dinarello, C. A. A. & Mantovani, A. The Interleukin-1 Family: Back to the Future. *Immunity* **39**, 1003–1018 (2013).

78. He, W. *et al.* Gasdermin D is an executor of pyroptosis and required for interleukin-1β secretion. *Cell Res.* **25**, 1285–1298 (2015).

79. Ding, J. *et al.* Pore-forming activity and structural autoinhibition of the gasdermin family. *Nature* **535**, 111–116 (2016).

80. Aglietti, R. A. *et al.* GsdmD p30 elicited by caspase-11 during pyroptosis forms pores in membranes. *Proc. Natl. Acad. Sci. U. S. A.* **113**, 7858–63 (2016).

81. Liu, X. *et al.* Inflammasome-activated gasdermin D causes pyroptosis by forming membrane pores. *Nature* **535**, 153–158 (2016).

82. Howard, A. D. *et al.* Probing the role of interleukin-1β convertase in interleukin-1β secretion. in *Agents and Actions* **35**, 77–83 (1991).

83. Broz, P. *et al.* Differential Requirement for Caspase-1 Autoproteolysis in Pathogen-Induced Cell Death and Cytokine Processing. *Cell Host Microbe* **8**, 471–483 (2010).

84. Thornberry, N. A. *et al.* A novel heterodimeric cysteine protease is required for interleukin-1βprocessing in monocytes. *Nature* **356**, 768–774 (1992).

85. Boucher, D. *et al.* Caspase-1 self-cleavage is an intrinsic mechanism to terminate inflammasome activity. *J. Exp. Med.* **215**, 827–840 (2018).

86. Kelley, N., Jeltema, D., Duan, Y. & He, Y. The NLRP3 inflammasome: An overview of mechanisms of activation and regulation. *International Journal of Molecular Sciences* **20**, 3328 (2019).

87. Kingsbury, S. R., Conaghan, P. G. & McDermott, M. F. The role of the NLRP3 inflammasome in gout. *J. Inflamm. Res.* **4**, 39 (2011).

88. Li, Z., Guo, J. & Bi, L. Role of the NLRP3 inflammasome in autoimmune diseases. *Biomed. Pharmacother.* **130**, 110542 (2020).

89. Booshehri, L. M. & Hoffman, H. M. CAPS and NLRP3. *Journal of Clinical Immunology* **39**, 277–286 (2019).

90. Paik, S., Kim, J. K., Silwal, P., Sasakawa, C. & Jo, E.-K. An update on the regulatory mechanisms of NLRP3 inflammasome activation. *Cell. Mol. Immunol.* **18**, 1141–1160 (2021).

91. Patel, M. N. *et al.* Inflammasome Priming in Sterile Inflammatory Disease. *Trends in Molecular Medicine* **23**, 165–180 (2017).

92. Zhou, R., Yazdi, A. S., Menu, P. & Tschopp, J. A role for mitochondria in NLRP3 inflammasome activation. *Nat. 2010 4697329* **469**, 221–225 (2010).

93. Bauernfeind, F. G. *et al.* Cutting Edge: NF-κB Activating Pattern Recognition and Cytokine Receptors License NLRP3 Inflammasome Activation by Regulating NLRP3 Expression. *J. Immunol.* **183**, 787–791 (2009).

94. Guarda, G. *et al.* Differential Expression of NLRP3 among Hematopoietic Cells. *J. Immunol.* **186**, 2529–2534 (2011).

95. Ayala, J. M. *et al.* IL-1 beta-converting enzyme is present in monocytic cells as an inactive 45-kDa precursor. *J. Immunol.* **153**, (1994).

96. Miller, D. K. *et al.* Purification and characterization of active human interleukin-1 beta-converting enzyme from THP.1 monocytic cells. *J. Biol. Chem.* **268**, 18062–18069 (1993).

97. Puren, A. J., Fantuzzi, G. & Dinarello, C. A. Gene expression, synthesis, and secretion of interleukin 18 and interleukin 1β are differentially regulated in human blood mononuclear cells and mouse spleen cells. *Proc. Natl. Acad. Sci.* **96**, 2256–2261 (1999).

98. Awad, F. *et al.* Impact of human monocyte and macrophage polarization on NLR

expression and NLRP3 inflammasome activation. *PLoS One* **12**, 1–18 (2017).

99. Masumoto, J. *et al.* Expression of Apoptosis-associated Speck-like Protein Containing a Caspase Recruitment Domain, a Pyrin N-terminal Homology Domain-containing Protein, in Normal Human Tissues: *http://dx.doi.org/10.1177/002215540104901009* **49**, 1269–1275 (2016).

100. Py, B. F., Kim, M. S., Vakifahmetoglu-Norberg, H. & Yuan, J. Deubiquitination of NLRP3 by BRCC3 Critically Regulates Inflammasome Activity. *Mol. Cell* **49**, 331–338 (2013).

101. Song, N. *et al.* NLRP3 Phosphorylation Is an Essential Priming Event for Inflammasome Activation. *Mol. Cell* **68**, 185-197.e6 (2017).

102. Zhang, Z. *et al.* Protein kinase D at the Golgi controls NLRP3 inflammasome activation. *J. Exp. Med.* **214**, 2671–2693 (2017).

103. Fischer, F. A. *et al.* TBK1 and IKKε act like an off switch to limit NLRP3 inflammasome pathway activation. *Proc. Natl. Acad. Sci. U. S. A.* **118**, (2021).

104. Labbé, K., McIntire, C. R., Doiron, K., Leblanc, P. M. & Saleh, M. Cellular inhibitors of apoptosis proteins cIAP1 and cIAP2 are required for efficient caspase-1 activation by the inflammasome. *Immunity* **35**, 897–907 (2011).

105. Xing, Y. *et al.* Cutting Edge: TRAF6 Mediates TLR/IL-1R Signaling–Induced Nontranscriptional Priming of the NLRP3 Inflammasome. *J. Immunol.* **199**, 1561–1566 (2017).

106. Solle, M. *et al.* Altered Cytokine Production in Mice Lacking P2X7Receptors *. *J. Biol. Chem.* **276**, 125–132 (2001).

107. Le Feuvre, R. A., Brough, D., Iwakura, Y., Takeda, K. & Rothwell, N. J. Priming of macrophages with lipopolysaccharide potentiates P2X7-mediated cell death via a caspase-1-dependent mechanism, independently of cytokine production. *J. Biol. Chem.* **277**, 3210–3218 (2002).

108. Halle, A. *et al.* The NALP3 inflammasome is involved in the innate immune response to amyloid-β. **9**, (2008).

109. Hornung, V. *et al.* Silica crystals and aluminum salts activate the NALP3 inflammasome through phagosomal destabilization. *Nat. Immunol.* **9**, 847–856 (2008).

110. Duewell, P. *et al.* NLRP3 inflammasomes are required for atherogenesis and activated by cholesterol crystals. *Nature* **464**, 1357–1361 (2010).

111. Martinon, F., Pétrilli, V., Mayor, A., Tardivel, A. & Tschopp, J. Gout-associated uric acid crystals activate the NALP3 inflammasome. *Nat. 2006 4407081* **440**, 237–241 (2006).

112. Mariathasan, S. *et al.* Cryopyrin activates the inflammasome in response to toxins and ATP. (2006). doi:10.1038/nature04515

113. Seoane, P. I. *et al.* The NLRP3-inflammasome as a sensor of organelle dysfunction. *J. Cell Biol.* **219**, (2020).

114. Rivers-Auty, J. & Brough, D. Potassium efflux fires the canon: Potassium efflux as a common trigger for canonical and noncanonical NLRP3 pathways. *Eur. J. Immunol.* **45**, 2758–2761 (2015).

115. Pétrilli, V. *et al.* Activation of the NALP3 inflammasome is triggered by low intracellular potassium concentration. *Cell Death Differ. 2007 149* **14**, 1583–1589 (2007).

116. Perregaux, D. & Gabel, C. A. Interleukin-1 beta maturation and release in response to ATP and nigericin. Evidence that potassium depletion mediated by these agents is a

necessary and common feature of their activity. *J. Biol. Chem.* **269**, 15195–15203 (1994).

117. Groß, C. J. J. *et al.* K+ Efflux-Independent NLRP3 Inflammasome Activation by Small Molecules Targeting Mitochondria. *Immunity* **45**, 761–773 (2016).

118. Brough, D. *et al.* Ca2+ Stores and Ca2+ Entry Differentially Contribute to the Release of IL-1β and IL-1α from Murine Macrophages. *J. Immunol.* **170**, 3029–3036 (2003).

119. Murakami, T. *et al.* Critical role for calcium mobilization in activation of the NLRP3 inflammasome. *Proc. Natl. Acad. Sci.* **109**, 11282–11287 (2012).

120. Katsnelson, M. A., Rucker, L. G., Russo, H. M. & Dubyak, G. R. K+ Efflux Agonists Induce NLRP3 Inflammasome Activation Independently of Ca2+ Signaling. *J. Immunol.* **194**, 3937–3952 (2015).

121. Gong, T., Yang, Y., Jin, T., Jiang, W. & Zhou, R. Orchestration of NLRP3 Inflammasome Activation by Ion Fluxes. *Trends in Immunology* **39**, 393–406 (2018).

122. Nakahira, K. *et al.* Autophagy proteins regulate innate immune response by inhibiting NALP3 inflammasome-mediated mitochondrial DNA release. *Nat. Immunol.* **12**, 222 (2011).

123. Yaron, J. R. *et al.* K+ regulates Ca2+ to drive inflammasome signaling: Dynamic visualization of ion flux in live cells. *Cell Death Dis.* **6**, 1–11 (2015).

124. Hornung, V. *et al.* Silica crystals and aluminum salts mediate NALP-3 inflammasome activation via phagosomal destabilization. *Nat. Immunol.* **9**, 847 (2008).

125. Dostert, C. *et al.* Innate Immune Activation Through Nalp3 Inflammasome Sensing of Asbestos and Silica. *Science* **320**, 674 (2008).

126. Duewell, P. *et al.* NLRP3 inflamasomes are required for atherogenesis and activated by cholesterol crystals that form early in disease. *Nature* **464**, 1357 (2010).

127. Cassel, S. L. *et al.* The Nalp3 inflammasome is essential for the development of silicosis. *Proc. Natl. Acad. Sci. U. S. A.* **105**, 9035 (2008).

128. Kool, M. *et al.* Cutting Edge: Alum Adjuvant Stimulates Inflammatory Dendritic Cells through Activation of the NALP3 Inflammasome. *J. Immunol.* **181**, 3755–3759 (2008).

129. C, S. *et al.* Sodium overload and water influx activate the NALP3 inflammasome. *J. Biol. Chem.* **286**, 35–41 (2011).

130. Kayagaki, N. *et al.* Noncanonical inflammasome activation by intracellular LPS independent of TLR4. *Science (80-.).* **341**, 1246–1249 (2013).

131. Shi, J. *et al.* Inflammatory caspases are innate immune receptors for intracellular LPS. *Nat. 2014 5147521* **514**, 187–192 (2014).

132. Viganò, E. *et al.* Human caspase-4 and caspase-5 regulate the one-step non-canonical inflammasome activation in monocytes. *Nat. Commun.* **6**, 8761 (2015).

133. Schmid-Burgk, J. L. *et al.* Caspase-4 mediates non-canonical activation of the NLRP3 inflammasome in human myeloid cells. *Eur. J. Immunol.* **45**, 2911–2917 (2015).

134. Santos, J. C. *et al.* LPS targets host guanylate-binding proteins to the bacterial outer membrane for non-canonical inflammasome activation. *EMBO J.* **37**, (2018).

135. Meunier, E. *et al.* Caspase-11 activation requires lysis of pathogen-containing vacuoles by IFN-induced GTPases. *Nat. 2014 5097500* **509**, 366–370 (2014).

136. Fisch, D. *et al.* Human GBP1 Differentially Targets Salmonella and Toxoplasma to

License Recognition of Microbial Ligands and Caspase-Mediated Death. *Cell Rep.* **32**, 108008 (2020).

137. Pilla, D. M. *et al.* Guanylate binding proteins promote caspase-11-dependent pyroptosis in response to cytoplasmic LPS. *Proc. Natl. Acad. Sci. U. S. A.* **111**, 6046–6051 (2014).

138. Kayagaki, N. *et al.* Caspase-11 cleaves gasdermin D for non-canonical inflammasome signalling. doi:10.1038/nature15541

139. Hamilton, C. & Anand, P. K. Right place, right time: localisation and assembly of the NLRP3 inflammasome. *F1000Research* **8**, (2019).

140. Subramanian, N., Natarajan, K., Clatworthy, M. R., Wang, Z. & Germain, R. N. The Adaptor MAVS Promotes NLRP3 Mitochondrial Localization and Inflammasome Activation. *Cell* **153**, 348–361 (2013).

141. Zhou, Y. *et al.* Virulent Mycobacterium bovis Beijing Strain Activates the NLRP7 Inflammasome in THP-1 Macrophages. *PLoS One* **11**, e0152853 (2016).

142. Misawa, T. *et al.* Microtubule-driven spatial arrangement of mitochondria promotes activation of the NLRP3 inflammasome. *Nat. Immunol.* **14**, 454–460 (2013).

143. Li, X. *et al.* MARK4 regulates NLRP3 positioning and inflammasome activation through a microtubule-dependent mechanism. *Nat. Commun. 2017 81* **8**, 1–13 (2017).

144. Iyer, S. S. *et al.* Mitochondrial cardiolipin is required for Nlrp3 inflammasome activation. *Immunity* **39**, 311–323 (2013).

145. He, Y., Zeng, M. Y., Yang, D., Motro, B. & Núñez, G. NEK7 is an essential mediator of NLRP3 activation downstream of potassium efflux. *Nature* **530**, 354 (2016).

146. Magupalli, V. G. *et al.* HDAC6 mediates an aggresome-like mechanism for NLRP3 and pyrin inflammasome activation. *Science (80-.).* **369**, (2020).

147. Shi, C. S. *et al.* Activation of autophagy by inflammatory signals limits IL-1β production by targeting ubiquitinated inflammasomes for destruction. *Nat. Immunol.* **13**, 255–263 (2012).

148. Harris, J. *et al.* Autophagy controls IL-1β secretion by targeting Pro-IL-1β for degradation. *J. Biol. Chem.* **286**, 9587–9597 (2011).

149. Wallach, D. & Kang, T. B. Programmed Cell Death in Immune Defense: Knowledge and Presumptions. *Immunity* **49**, 19–32 (2018).

150. Yang, Y., Jiang, G., Zhang, P. & Fan, J. Programmed cell death and its role in inflammation. *Mil. Med. Res.* **2**, (2015).

151. Aglietti, R. A. & Dueber, E. C. Recent Insights into the Molecular Mechanisms Underlying Pyroptosis and Gasdermin Family Functions. *Trends Immunol.* **38**, 261–271 (2017).

152. Miao, E. A. *et al.* Caspase-1-induced pyroptosis is an innate immune effector mechanism against intracellular bacteria. *Nat. Immunol.* **11**, 1136–1142 (2010).

153. Aziz, M., Jacob, A. & Wang, P. Revisiting caspases in sepsis. *Cell Death Dis.* **5**, e1526 (2014).

154. Aziz, M., Jacob, A., Yang, W.-L., Matsuda, A. & Wang, P. Current trends in inflammatory and immunomodulatory mediators in sepsis. *J. Leukoc. Biol.* **93**, 329–42 (2013).

155. Cookson, B. T. & Brennan, M. A. Pro-inflammatory programmed cell death. *Trends Microbiol.* **9**, 113–114 (2001).

156. Shi, J. *et al.* Cleavage of GSDMD by inflammatory caspases determines pyroptotic cell death. *Nature* **526**, 660–665 (2015).

157. Kayagaki, N. *et al.* NINJ1 mediates plasma membrane rupture during lytic cell death A forward-genetic screen identifies NINJ1. *Nature* **591**, (2021).

158. Danielski, L. G., Giustina, A. Della, Bonfante, S., Barichello, T. & Petronilho, F. The NLRP3 Inflammasome and Its Role in Sepsis Development. *Inflammation* **43**, 24–31 (2020).

159. Zhou, R., Tardivel, A., Thorens, B., Choi, I. & Tschopp, J. Thioredoxin-interacting protein links oxidative stress to inflammasome activation. *Nat. Immunol. 2009 112* **11**, 136–140 (2009).

160. Maedler, K., Dharmadhikari, G., Schumann, D. M. & Størling, J. Interleukin-1 beta targeted therapy for type 2 diabetes. *http://dx.doi.org/10.1517/14712590903136688* **9**, 1177–1188 (2009).

161. Larsen, C. M. *et al.* Interleukin-1–Receptor Antagonist in Type 2 Diabetes Mellitus. *N. Engl. J. Med.* **356**, 1517–1526 (2007).

162. Larsen, C. M. *et al.* Sustained Effects of Interleukin-1 Receptor Antagonist Treatment in Type 2 Diabetes. *Diabetes Care* **32**, 1663–1668 (2009).

163. Talbott, J. H. Serum urate in relatives of gouty patients. *J. Clin. Invest.* **19**, 645–648 (1940).

164. Terkeltaub, R. *et al.* The interleukin 1 inhibitor rilonacept in treatment of chronic gouty arthritis: results of a placebo-controlled, monosequence crossover, non-randomised, single-blind pilot study. *Ann. Rheum. Dis.* **68**, 1613–1617 (2009).

165. So, A., De Smedt, T., Revaz, S. & Tschopp, J. A pilot study of IL-1 inhibition by anakinra in acute gout. *Arthritis Res. Ther.* **9**, 1–6 (2007).

166. McGonagle, D., Tan, A. L., Madden, J., Emery, P. & McDermott, M. F. Successful treatment of resistant pseudogout with anakinra. *Arthritis Rheum.* **58**, 631–633 (2008).

167. Beekman, B., Verzijl, N., De Roos, J. A. D. M. & TeKoppele, J. M. Matrix degradation by chondrocytes cultured in alginate: IL-1β induces proteoglycan degradation and proMMP synthesis but does not result in collagen degradation. *Osteoarthr. Cartil.* **6**, 330–340 (1998).

168. Fattahi, F. & Ward, P. A. Understanding Immunosuppression after Sepsis. *Immunity* **47**, 3–5 (2017).

169. Bondeson, J. *et al.* The role of synovial macrophages and macrophage-produced mediators in driving inflammatory and destructive responses in osteoarthritis. *Arthritis Rheum.* **62**, 647–657 (2010).

170. Kinne, R. W., Stuhlmüller, B. & Burmester, G.-R. Cells of the synovium in rheumatoid arthritis. Macrophages. *Arthritis Res. Ther.* **9**, 224 (2007).

171. Bondeson, J., Wainwright, S. D., Lauder, S., Amos, N. & Hughes, C. E. The role of synovial macrophages and macrophage-produced cytokines in driving aggrecanases, matrix metalloproteinases, and other destructive and inflammatory responses in osteoarthritis. *Arthritis Res. Ther. 2006 86* **8**, 1–12 (2006).

172. Guo, C. *et al.* NLRP3 inflammasome activation contributes to the pathogenesis of rheumatoid arthritis. *Clin. Exp. Immunol.* **194**, 231–243 (2018).

173. Ni, B. *et al.* MCC950, the NLRP3 Inhibitor, Protects against Cartilage Degradation in a Mouse Model of Osteoarthritis. *Oxid. Med. Cell. Longev.* **2021**, 1–14 (2021).

174. Fusco, R., Siracusa, R., Genovese, T., Cuzzocrea, S. & Paola, R. Di. Focus on the Role of NLRP3 Inflammasome in Diseases. *Int. J. Mol. Sci.* **21**, 1–25 (2020).

175. Dinarello, C. A. Overview of the IL-1 family in innate inflammation and acquired immunity. *Immunol. Rev.* **281**, 8–27 (2018).

176. Dinarello, C. A., Simon, A. & Van Der Meer, J. W. M. Treating inflammation by blocking interleukin-1 in a broad spectrum of diseases. *Nature Reviews Drug Discovery* **11**, 633–652 (2012).

177. Dinarello, C. A. Immunological and Inflammatory Functions of the Interleukin-1 Family. *Annu. Rev. Immunol.* **27**, 519–550 (2009).

178. Dinarello, C. A., Simon, A. & van der Mee, J. W. M. Treating inflammation by blocking interleukin-1 in a broad. *Nat Rev Drug Discov.* **193**, 118–125 (2011).

179. Dinarello, C. A. The IL-1 family of cytokines and receptors in rheumatic diseases. *Nature Reviews Rheumatology* **15**, 612–632 (2019).

180. Ren, K. & Torres, R. Role of interleukin-1beta during pain and inflammation. *Brain Res. Rev.* **60**, 57–64 (2009).

181. Coeshott, C. *et al.* Converting enzyme-independent release of tumor necrosis factor α and IL-1β from a stimulated human monocytic cell line in the presence of activated neutrophils or purified proteinase 3. *Proc. Natl. Acad. Sci.* **96**, 6261–6266 (1999).

182. Sugawara, S. *et al.* Neutrophil Proteinase 3-Mediated Induction of Bioactive IL-18 Secretion by Human Oral Epithelial Cells. *J. Immunol.* **167**, 6568–6575 (2001).

183. Boraschi, D. et al. The family of the interleukin- 1 receptors. *Immunol. Rev.* **281**, 2014 (2018).

184. Korn, T., Bettelli, E., Oukka, M. & Kuchroo, V. K. IL-17 and Th17 Cells. *Annu. Rev. Immunol.* **27**, 485–517 (2009).

185. Risbud, M. V. & Shapiro, I. M. Role of cytokines in intervertebral disc degeneration: Pain and disc content. *Nat. Rev. Rheumatol.* **10**, 44–56 (2014).

186. Brikos, C., Wait, R., Begum, S., O'Neill, L. A. J. & Saklatvala, J. Mass Spectrometric Analysis of the Endogenous Type I Interleukin-1 (IL-1) Receptor Signaling Complex Formed after IL-1 Binding Identifies IL-1RAcP, MyD88, and IRAK-4 as the Stable Components. *Mol. Cell. Proteomics* **6**, 1551–1559 (2007).

187. Nakamura, K., Okamura, H., Wada, M., Nagata, K. & Tamura, T. Endotoxin-induced serum factor that stimulates gamma interferon production. *Infect. Immun.* **57**, 590–595 (1989).

188. Kohka, H. *et al.* Interleukin-18/interferon-gamma-inducing factor, a novel cytokine, up-regulates ICAM-1 (CD54) expression in KG-1 cells. *J. Leukoc. Biol.* **64**, 519–27 (1998).

189. Morel, J. C., Park, C. C., Woods, J. M. & Koch, A. E. A novel role for interleukin-18 in adhesion molecule induction through NF kappa B and phosphatidylinositol (PI) 3-kinase-dependent signal transduction pathways. *J. Biol. Chem.* **276**, 37069–75 (2001).

190. Lopez-Castejon, G. & Brough, D. Understanding the mechanism of IL-1β secretion. *Cytokine Growth Factor Rev.* **22**, 189 (2011).

191. Okamura, H. *et al.* Cloning of a new cytokine that induces IFN-γ production by T cells. *Nat. 1995 3786552* **378**, 88–91 (1995).

192. Auron, P. E. *et al.* Nucleotide sequence of human monocyte interleukin 1 precursor cDNA. **81**, 7907–7911 (1984).

193. Stevenson, F. T., Torrano, F., Locksley, R. M. & Lovett, D. H. Interleukin 1: The patterns of translation and intracellular distribution support alternative secretory mechanisms. *J. Cell. Physiol.* **152**, 223–231 (1992).

194. Singer, I. I. *et al.* Interleukin 1 beta is localized in the cytoplasmic ground substance but is largely absent from the Golgi apparatus and plasma membranes of stimulated human monocytes. *J. Exp. Med.* **167**, 389–407 (1988).

195. Rubartelli, A., Cozzolino, F., Talio, M. & Sitia, R. A novel secretory pathway for interleukin-1 beta, a protein lacking a signal sequence. **9**, (1990).

196. Lopez-Castejon, G. & Brough, D. Understanding the mechanism of IL-1B secretion. *Cytokine Growth Factor Rev.* **22**, 189–195 (2011).

197. Andrei, C. *et al.* The secretory route of the leaderless protein interleukin 1beta involves exocytosis of endolysosome-related vesicles. *Mol. Biol. Cell* **10**, 1463–75 (1999).

198. Harris, J. *et al.* Autophagy controls IL-1beta secretion by targeting pro-IL-1beta for degradation. *J. Biol. Chem.* **286**, 9587–97 (2011).

199. MacKenzie, A. *et al.* Rapid Secretion of Interleukin-1β by Microvesicle Shedding. *Immunity* **15**, 825–835 (2001).

200. Ghonime, M. G. *et al.* Inflammasome Priming by Lipopolysaccharide Is Dependent upon ERK Signaling and Proteasome Function. *J. Immunol.* **192**, 3881–3888 (2014).

201. Evavold, C. L. *et al.* The Pore-Forming Protein Gasdermin D Regulates Interleukin-1 Secretion from Living Macrophages. *Immunity* **48**, 1–10 (2017).

202. Rathkey, J. K. *et al.* Live-cell visualization of gasdermin D-driven pyroptotic cell death. *J. Biol. Chem.* **292**, 14649–14658 (2017).

203. Gaidt, M. M. & Hornung, V. Pore formation by GSDMD is the effector mechanism of pyroptosis. *EMBO J.* **35**, 2167–2169 (2016).

204. Shi, J., Gao, W. & Shao, F. Pyroptosis: Gasdermin-Mediated Programmed Necrotic Cell Death. *Trends Biochem. Sci.* **42**, 245–254 (2017).

205. Broz, P., Pelegrín, P. & Shao, F. The gasdermins, a protein family executing cell death and inflammation. doi:10.1038/s41577

206. Saeki, N. & Sasaki, H. Gasdermin Superfamily : A Novel Gene Family Functioning in Epithelial Cells. *Endothel. Ep.* 193–211 (2012).

207. Laer, L. Van *et al.* Nonsyndromic hearing impairment is associated with a mutation in DFNA5. *Nat. Genet.* **20**, 194–197 (1998).

208. Delmaghani, S. *et al.* Mutations in the gene encoding pejvakin, a newly identified protein of the afferent auditory pathway, cause DFNB59 auditory neuropathy. *Nat. Genet.* **38**, 770–778 (2006).

209. Chen, X. *et al.* Pyroptosis is driven by non-selective gasdermin-D pore and its morphology is different from MLKL channel-mediated necroptosis. *Cell Res.* **26**, 1007–1020 (2016).

210. Sborgi, L. *et al.* GSDMD membrane pore formation constitutes the mechanism of pyroptotic cell death. *EMBO J.* **35**, 1766–78 (2016).

211. Platnich, J. M. *et al.* Shiga Toxin/Lipopolysaccharide Activates Caspase-4 and Gasdermin D to Trigger Mitochondrial Reactive Oxygen Species Upstream of the NLRP3 Inflammasome . (2018). doi:10.1016/j.celrep.2018.09.071

212. Huang, L. S. *et al.* mtDNA Activates cGAS Signaling and Suppresses the YAP-Mediated Endothelial Cell Proliferation Program to Promote Inflammatory Injury. *Immunity* **52**, 475-486.e5 (2020).

213. Kovacs, S. B. & Miao, E. A. Gasdermins: Effectors of Pyroptosis. *Trends Cell Biol.* **27**, 673–684 (2017).

214. Liu, Z. *et al.* Crystal Structures of the Full-Length Murine and Human Gasdermin D Reveal Mechanisms of Autoinhibition, Lipid Binding, and Oligomerization. *Immunity* (2019). doi:10.1016/J.IMMUNI.2019.04.017

215. Liu, Z. *et al.* Structures of the Gasdermin D C-Terminal Domains Reveal Mechanisms of Autoinhibition. *Structure* **0**, 1–7 (2018).

216. Kuang, S. *et al.* Structure insight of GSDMD reveals the basis of GSDMD autoinhibition in cell pyroptosis. *Proc. Natl. Acad. Sci.* **114**, 201708194 (2017).

217. de Beeck, K. O. *et al.* The DFNA5 gene, responsible for hearing loss and involved in cancer, encodes a novel apoptosis-inducing protein. *Eur. J. Hum. Genet.* **19**, 965–973 (2011).

218. Van Laer, L. *et al.* DFNA5: hearing impairment exon instead of hearing impairment gene? *J. Med. Genet.* **41**, 401–6 (2004).

219. Xia, S. *et al.* Gasdermin D pore structure reveals preferential release of mature interleukin-1. *Nature* **593**, 607–611 (2021).

220. Graves, B. J. *et al.* Structure of Interleukin lα at 2.7-Å Resolution. *Biochemistry* **29**, 2679–2684 (1990).

221. Janeway, CA; Travers, P; Walport, M. The complement system and innate immunity - Immunobiology - NCBI Bookshelf. *Immunobiol. Immune Syst. Heal. Dis.* **5th Editio**, 1–13 (2001).

222. Dunkelberger, J. R. & Song, W. C. Complement and its role in innate and adaptive immune responses. *Cell Res.* **20**, 34–50 (2010).

223. Navratil, J. S., Watkins, S. C., Wisnieski, J. J. & Ahearn, J. M. The Globular Heads of C1q Specifically Recognize Surface Blebs of Apoptotic Vascular Endothelial Cells. *J. Immunol.* **166**, 3231–3239 (2001).

224. Korb, L. C. & Ahearn, J. M. C1q binds directly and specifically to surface blebs of apoptotic human keratinocytes: complement deficiency and systemic lupus erythematosus revisited. *J. Immunol.* **158**, (1997).

225. Peng, Q., Li, K., Sacks, S. & Zhou, W. The Role of Anaphylatoxins C3a and C5a in Regulating Innate and Adaptive Immune Responses. *Inflamm. Allergy - Drug Targets* **8**, 236–246 (2009).

226. Xie, C. B., Jane-Wit, D. & Pober, J. S. Complement Membrane Attack Complex: New Roles, Mechanisms of Action, and Therapeutic Targets. *Am. J. Pathol.* **190**, 1138–1150 (2020).

227. Ghebrehiwet, B. The complement system: An evolution in progress. *F1000Research* **5**, (2016).

228. Huber-Lang, M. *et al.* Generation of C5a by Phagocytic Cells. *Am. J. Pathol.* **161**, 1849 (2002).

229. W, V. Cleavage of the fifth component of complement and generation of a functionally active C5b6-like complex by human leukocyte elastase. *Immunobiology* **201**, 470–477

(2000).

230. Shin, H. S., Snyderman, R., Friedman, E., Mellors, A. & Mayer, M. M. Chemotactic and anaphylatoxic fragment cleaved from the fifth component of guinea pig complement. *Science (80-.).* **162**, 361–363 (1968).

231. Manthey, H. D., Woodruff, T. M., Taylor, S. M. & Monk, P. N. Complement component 5a (C5a). *International Journal of Biochemistry and Cell Biology* **41**, 2114–2117 (2009).

232. El-Lati, S. G., Dahinden, C. A. & Church, M. K. Complement Peptides C3a- and C5a-Induced Mediator Release from Dissociated Human Skin Mast Cells. *J. Invest. Dermatol.* **102**, 803–806 (1994).

233. Becker, E. L. *et al.* The inhibition of neutrophil granule enzyme secretion and chemotaxis by pertussis toxin. *J. Cell Biol.* **100**, 1641–1646 (1985).

234. S, T., K, T., K, I. & CA, D. Degranulation from human eosinophils stimulated with C3a and C5a. *Int. Arch. Allergy Immunol.* **104 Suppl 1**, 27–29 (1994).

235. Marder, S. R., Chenoweth, D. E., Goldstein, I. M. & Perez, H. D. Chemotactic responses of human peripheral blood monocytes to the complement-derived peptides C5a and C5a des Arg. *J. Immunol.* **134**, 3325–31 (1985).

236. Hartmann, K. *et al.* C3a and C5a Stimulate Chemotaxis of Human Mast Cells. *Blood* **89**, 2863–2870 (1997).

237. Gallin, E. & Gallin, J. Interaction of chemotactic factors with human macrophages: induction of transmembrane potential changes. *J. Cell Biol.* **75**, 277–289 (1977).

238. Ehrengruber, M. U., Geiser, T. & Deranleau, D. A. Activation of human neutrophils by C3a and C5A Comparison of the effects on shape changes, chemotaxis, secretion, and respiratory burst. *FEBS Lett.* **346**, 181–184 (1994).

239. Seow, V. *et al.* Inflammatory Responses Induced by Lipopolysaccharide Are Amplified in Primary Human Monocytes but Suppressed in Macrophages by Complement Protein C5a. *J. Immunol.* **191**, 4308–4316 (2013).

240. Nataf, S., Davoust, N., Ames, R. S. & Barnum, S. R. Human T cells express the C5a receptor and are chemoattracted to C5a. *J. Immunol.* **162**, 4018–23 (1999).

241. P, C. *et al.* Immune cell-derived C3a and C5a costimulate human T cell alloimmunity. *Am. J. Transplant* **13**, 2530–2539 (2013).

242. Tsuji, R. F. *et al.* Early Local Generation of C5a Initiates the Elicitation of Contact Sensitivity by Leading to Early T Cell Recruitment. *J. Immunol.* **165**, 1588–1598 (2000).

243. Okinaga, S. *et al.* C5L2, a Nonsignaling C5A Binding Protein †. (2003). doi:10.1021/bi034489v

244. Wetsel, R. A. Structure, function and cellular expression of complement anaphylatoxin receptors. *Curr. Opin. Immunol.* **7**, 48–53 (1995).

245. Gerard, C. & Gerard, N. P. C5a anaphylatoxin and its seven transmembrane-segment receptor. *Annual Review of Immunology* **12**, 775–808 (1994).

246. Li, R., Coulthard, L. G., Wu, M. C. L., Taylor, S. M. & Woodruff, T. M. C5L2: A controversial receptor of complement anaphylatoxin, C5a. *FASEB J.* **27**, 855–864 (2013).

247. Bamberg, C. E. *et al.* The C5a Receptor (C5aR) C5L2 Is a Modulator of C5aR-mediated Signal Transduction *. *J. Biol. Chem.* **285**, 7633–7644 (2010).

248. Zaal, A., van Ham, S. M. & ten Brinke, A. Differential effects of anaphylatoxin C5a on

antigen presenting cells, roles for C5aR1 and C5aR2. *Immunol. Lett.* **209**, 45–52 (2019).

249. Bosmann, M. *et al.* Complement activation product C5a is a selective suppressor of TLR4-induced, but not TLR3-induced, production of IL-27(p28) from macrophages. *J. Immunol.* **188**, 5086 (2012).

250. Bosmann, M., Sarma, J. V., Atefi, G., Zetoune, F. S. & Ward, P. A. Evidence for anti-inflammatory effects of C5a on the innate IL-17A/IL-23 axis. *FASEB J.* **26**, 1640 (2012).

251. Sala, A. la, Gadina, M. & Kelsall, B. L. Gi-Protein-Dependent Inhibition of IL-12 Production Is Mediated by Activation of the Phosphatidylinositol 3-Kinase-Protein 3 Kinase B/Akt Pathway and JNK. *J. Immunol.* **175**, 2994–2999 (2005).

252. Pan, Z. K. Anaphylatoxins C5a and C3a induce nuclear factor κB activation in human peripheral blood monocytes. *Biochim. Biophys. Acta - Gene Struct. Expr.* **1443**, 90–98 (1998).

253. Braun, L., Christophe, T. & Boulay, F. Phosphorylation of Key Serine Residues Is Required for Internalization of the Complement 5a (C5a) Anaphylatoxin Receptor via a β-Arrestin, Dynamin, and Clathrin-dependent Pathway. *J. Biol. Chem.* **278**, 4277–4285 (2003).

254. Christophe, T., Rabiet, M. J., Tardif, M., Milcent, M. D. & Boulay, F. Human complement 5a (C5a) anaphylatoxin receptor (CD88) phosphorylation sites and their specific role in receptor phosphorylation and attenuation of G protein-mediated responses. *J. Biol. Chem.* **275**, 1656–1664 (2000).

255. Li, X. X., Lee, J. D., Kemper, C. & Woodruff, T. M. The Complement Receptor C5aR2: A Powerful Modulator of Innate and Adaptive Immunity. *J. Immunol.* **202**, 3339–3348 (2019).

256. Serna, M., Giles, J. L., Morgan, B. P. & Bubeck, D. Structural basis of complement membrane attack complex formation. *Nat. Commun.* **7**, 10587 (2016).

257. Discipio, R. G., Smith, C. A., Muller-Eberhards, H. J. & Hugli, T. E. The Activation of Human Complement Component C 5 by a Fluid Phase C5 Convertase*. *J. Biol. Chem.* **258**, 10629–10636 (1983).

258. Menny, A. *et al.* CryoEM reveals how the complement membrane attack complex ruptures lipid bilayers. *Nat. Commun.* **9**, 5316 (2018).

259. Dudkina, N. V. *et al.* Structure of the poly-C9 component of the complement membrane attack complex. *Nat. Commun.* **7**, 10588 (2016).

260. Sharp, T. H., Koster, A. J. & Gros, P. Heterogeneous MAC Initiator and Pore Structures in a Lipid Bilayer by Phase-Plate Cryo-electron Tomography. *Cell Rep.* **15**, 1–8 (2016).

261. Tomlinson, S., Taylor, P. W., Paul Morgan$, I. B. & Luzio, J. P. Killing of Gram-negative bacteria by complement Fractionation of cell membranes after complement C5b-9 deposition on to the surface of Salmonella minnesota Re595. *Biochem. J* **263**, 505–511 (1989).

262. Nakamura, M. *et al.* Quantification of the CD55 and CD59, Membrane Inhibitors of Complement on HIV-1 Particles as a Function of Complement-Mediated Virolysis. *Microbiol. Immunol.* **40**, 561–567 (1996).

263. Hoover, D. L., Berger, M., Nacy, C. A., Hockmeyer, W. T. & Meltzer, M. S. Killing of Leishmania tropica amastigotes by factors in normal human serum. *J. Immunol.* **132**, 893–7 (1984).

264. McNamara, L. A. *et al.* High Risk for Invasive Meningococcal Disease Among Patients Receiving Eculizumab (Soliris) Despite Receipt of Meningococcal Vaccine. *MMWR. Morb. Mortal. Wkly. Rep.* **66**, 734 (2017).

265. Turley, A. J. *et al.* Spectrum and Management of Complement Immunodeficiencies (Excluding Hereditary Angioedema) Across Europe. *J. Clin. Immunol. 2015 352* **35**, 199–205 (2015).

266. Ram, S., Lewis, L. A. & Rice, P. A. Infections of People with Complement Deficiencies and Patients Who Have Undergone Splenectomy. *Clin. Microbiol. Rev.* **23**, 740 (2010).

267. Barilla-LaBarca, M. L., Liszewski, M. K., Lambris, J. D., Hourcade, D. & Atkinson, J. P. Role of Membrane Cofactor Protein (CD46) in Regulation of C4b and C3b Deposited on Cells. *J. Immunol.* **168**, 6298–6304 (2002).

268. Oglesby, T. J., Allen, C. J., Liszewski, M. K., White, D. J. G. & Atkinson, J. P. Membrane cofactor protein (CD46) protects cells from complement- mediated attack by an intrinsic mechanism. *J. Exp. Med.* **175**, 1547 (1992).

269. Devaux, P., Christiansen, D., Fontaine, M. & Gerlier, D. Control of C3b and C5b deposition by CD46 (membrane cofactor protein) after alternative but not classical complement activation. *Eur. J. Immunol.* **29**, 815–822 (1999).

270. Brodbeck, W. G., Kuttner-Kondo, L., Mold, C. & Medof, M. E. Structure/function studies of human decay-accelerating factor. *Immunology* **101**, 104 (2000).

271. Ninomiya, H. & Sims, P. J. The human complement regulatory protein CD59 binds to the α-chain of C8 and to the 'b' domain of C9. *J. Biol. Chem.* **267**, 13675–13680 (1992).

272. Farkas, I. *et al.* CD59 blocks not only the insertion of C9 into MAC but inhibits ion channel formation by homologous C5b-8 as well as C5b-9. *J. Physiol.* **539**, 537–545 (2002).

273. Meri, S. *et al.* Human protectin (CD59), an 18,000-20,000 MW complement lysis restricting factor, inhibits C5b-8 catalysed insertion of C9 into lipid bilayers. *Immunology* **71**, 1–9 (1990).

274. Morgan, B. P. The membrane attack complex as an inflammatory trigger. *Immunobiology* **221**, 747–751 (2016).

275. Moskovich, O. & Fishelson, Z. Live cell imaging of outward and inward vesiculation induced by the complement C5b-9 complex. *J. Biol. Chem.* **282**, 29977–29986 (2007).

276. Scolding, N. J. *et al.* Vesicular removal by oligodendrocytes of membrane attack complexes formed by activated complement. **339**, 620–622 (1989).

277. Kerjaschki, D. *et al.* Transcellular transport and membrane insertion of the C5b-9 membrane attack complex of complement by glomerular epithelial cells in experimental membranous nephropathy. *J. Immunol.* **143**, 546–52 (1989).

278. Morgan, B. P., Dankert, J. R. & Esser, A. F. Recovery of human neutrophils from complement attack: removal of the membrane attack complex by endocytosis and exocytosis. *J. Immunol.* **138**, 246–53 (1987).

279. Moskovich, O., Herzog, L.-O. O., Ehrlich, M. & Fishelson, Z. Caveolin-1 and Dynamin-2 Are Essential for Removal of the Complement C5b-9 Complex via Endocytosis. *J. Biol. Chem.* **287**, 19904–19915 (2012).

280. Halperin, J. A., Taratuska, A. & Nicholson-Weller, A. Terminal complement complex C5b-9 stimulates mitogenesis in 3T3 cells. *J. Clin. Invest.* **91**, 1974 (1993).

281. Niculescu, F., Badea, T. & Rus, H. Sublytic C5b-9 induces proliferation of human aortic smooth muscle cells: Role of mitogen activated protein kinase and phosphatidylinositol 3-kinase. *Atherosclerosis* **142**, 47–56 (1999).

282. Kumar, B., Cashman, S. M. & Kumar-Singh, R. Complement-Mediated Activation of the NLRP3 Inflammasome and Its Inhibition by AAV-Mediated Delivery of CD59 in a Model of Uveitis. *Mol. Ther.* **26**, 1568–1580 (2018).

283. Laudisi, F. *et al.* Cutting Edge: The NLRP3 Inflammasome Links Complement-Mediated Inflammation and IL-1β Release. *J. Immunol.* **191**, 1006–1010 (2013).

284. Suresh, R., Chandrasekaran, P., Sutterwala, F. S. & Mosser, D. M. Complement-mediated 'bystander' damage initiates host NLRP3 inflammasome activation. *J Cell Sci* **129**, 1928–1939 (2016).

285. Kilgore, K. S. *et al.* Sublytic concentrations of the membrane attack complex of complement induce endothelial interleukin-8 and monocyte chemoattractant protein-1 through nuclear factor-kappa B activation. *Am. J. Pathol.* **150**, 2019 (1997).

286. Tedesco, F. *et al.* The cytolytically inactive terminal complement complex activates endothelial cells to express adhesion molecules and tissue factor procoagulant activity. *J. Exp. Med.* **185**, 1619–1627 (1997).

287. Kilgore, K. S., Shen, J. P., Miller, B. F., Ward, P. A. & Warren, J. S. Enhancement by the complement membrane attack complex of tumor necrosis factor-alpha-induced endothelial cell expression of E-selectin and ICAM-1. *J. Immunol.* **155**, 1434–41 (1995).

288. Jane-wit, D. *et al.* Complement membrane attack complexes activate noncanonical NF-κB by forming an Akt+NIK+ signalosome on Rab5+ endosomes. *Proc. Natl. Acad. Sci. U. S. A.* **112**, 9686–9691 (2015).

289. Hänsch, G. M., Seitz, M. & Betz, M. Effect of the late complement components C5b-9 on human monocytes: Release of prostanoids, oxygen radicals and of a factor inducing cell proliferation. *Int. Arch. Allergy Immunol.* **82**, 317–320 (1987).

290. Triantafilou, K., Hughes, T. R., Triantafilou, M. & Morgan, B. P. . The complement membrane attack complex triggers intracellular Ca2+ fluxes leading to NLRP3 inflammasome activation. *J. Cell Sci.* **126**, 2903–2913 (2013).

291. Lueck, K. *et al.* Sub-lytic C5b-9 induces functional changes in retinal pigment epithelial cells consistent with age-related macular degeneration. *Eye 2011 258* **25**, 1074–1082 (2011).

292. Xie, C. B. *et al.* Complement Membrane Attack Complexes Assemble NLRP3 Inflammasomes Triggering IL-1 Activation of IFN-γ–Primed Human Endothelium. *Circ. Res.* **124**, 1747–1759 (2019).

293. Fang, C. *et al.* ZFYVE21 is a complement-induced Rab5 effector that activates non-canonical NF-κB via phosphoinosotide remodeling of endosomes. *Nat. Commun.* **10**, (2019).

294. Jane-wit, D. *et al.* Alloantibody and Complement Promote T Cell-Mediated Cardiac Allograft Vasculopathy through Non-Canonical NF-κB Signaling in Endothelial Cells. *Circulation* **128**, 2504–2516 (2013).

295. Furebring, M., Håkansson, L. D., Venge, P., Nilsson, B. & Sjölin, J. Expression of the C5a receptor (CD88) on granulocytes and monocytes in patients with severe sepsis. *Crit. Care* **6**, 363–370 (2002).

296. Vollrath, J. T., Marzi, I., Herminghaus, A., Lustenberger, T. & Relja, B. Post-Traumatic

Sepsis Is Associated with Increased C5a and Decreased TAFI Levels. *J. Clin. Med.* **9**, 1230 (2020).

297. Bemis, E. A. *et al.* Complement and its environmental determinants in the progression of human rheumatoid arthritis. *Mol. Immunol.* **112**, 256–265 (2019).

298. Morgan, B. P., Daniels, R. H., Williams, B. D., Daniels & Williams. Measurement of terminal complement complexes in rheumatoid arthritis. *Clin. Exp. Immunol.* **73**, 473 (1988).

299. Struglics, A. *et al.* The complement system is activated in synovial fluid from subjects with knee injury and from patients with osteoarthritis. *Arthritis Res. Ther.* **18**, 1–11 (2016).

300. Wang, Y. *et al.* A Role for Complement in Antibody-Mediated Inflammation: C5-Deficient DBA/1 Mice Are Resistant to Collagen-Induced Arthritis. *J. Immunol.* **164**, 4340–4347 (2000).

301. Ji, H. *et al.* Genetic Influences on the End-Stage Effector Phase of Arthritis. *J. Exp. Med.* **194**, 321–330 (2001).

302. Fu, X. *et al.* Target deletion of complement component 9 attenuates antibody-mediated hemolysis and lipopolysaccharide (LPS)-induced acute shock in mice. *Sci. Rep.* **6**, 1–12 (2016).

303. Grafals, M. & Thurman, J. M. The Role of Complement in Organ Transplantation. *Front. Immunol.* **10**, 2380 (2019).

304. Kremlitzka, M. *et al.* Functional analyses of rare genetic variants in complement component C9 identified in patients with age-related macular degeneration. *Hum. Mol. Genet.* **27**, 2678–2688 (2018).

305. Nishizaka, H. *et al.* Molecular bases for inherited human complement component C6 deficiency in two unrelated individuals. *J. Immunol.* **156**, (1996).

306. Nishizaka, H., Horiuchi, T., Zhu, Z.-B., Fukumori, Y. & Volanakist, J. E. Genetic Bases of Human Complement C7 Deficiency'. *J. Immunol.* **157**, 4239–4243 (1996).

307. Carney, D. F., Lang, T. J. & Shin, M. L. Multiple signal messengers generated by terminal complement complexes and their role in terminal complement complex elimination. *J. Immunol.* **145**, 623–9 (1990).

308. Asgari, E. *et al.* C3a modulates IL-1b secretion in human monocytes by regulating ATP efflux and subsequent NLRP3 inflammasome activation. *Blood* **122**, 3473–81 (2013).

309. Arbore, G. *et al.* T helper 1 immunity requires complement-driven NLRP3 inflammasome activity in $CD4^+$ T cells. *Science* **352**, aad1210 (2016).

310. Haggadone, M. D., Grailer, J. J., Fattahi, F., Zetoune, F. S. & Ward, P. A. Bidirectional crosstalk between C5a receptors and the NLRP3 inflammasome in macrophages and monocytes. *Mediators Inflamm.* **2016**, (2016).

311. Yu, S. *et al.* The complement receptor C5aR2 promotes protein kinase R expression and contributes to NLRP3 inflammasome activation and HMGB1 release from macrophages. *J. Biol. Chem.* **294**, 8384–8394 (2019).

312. Khameneh, H. J. *et al.* C5a Regulates IL-1β Production and Leukocyte Recruitment in a Murine Model of Monosodium Urate Crystal-Induced Peritonitis. *Front. Pharmacol.* **8**, (2017).

313. Pan, Z. K., Chen, L.-Y., Cochrane, C. G. & Zuraw, B. L. fMet-Leu-Phe Stimulates

Proinflammatory Cytokine Gene Expression in Human Peripheral Blood Monocytes: The Role of Phosphatidylinositol 3-Kinase 1. *J. Immunol.* **164**, 404–411 (2000).

314. Gupta, K., Subramanian, H., Klos, A. & Ali, H. Phosphorylation of C3a Receptor at Multiple Sites Mediates Desensitization, β-Arrestin-2 Recruitment and Inhibition of NF-κB Activity in Mast Cells. *PLoS One* **7**, e46369 (2012).

315. Kastl, S. P. *et al.* The complement component C5a induces the expression of plasminogen activator inhibitor-1 in human macrophages via NF-κB activation. *J. Thromb. Haemost.* **4**, 1790–1797 (2006).

316. Shutov, L. P. *et al.* The Complement System Component C5a Produces Thermal Hyperalgesia via Macrophage-to-Nociceptor Signaling That Requires NGF and TRPV1. *J. Neurosci.* **36**, 5055–5070 (2016).

317. Möller, T., Nolte, C., Burger, R., Verkhratsky, A. & Kettenmann, H. Mechanisms of C5a and C3a Complement Fragment-Induced [Ca2+]i Signaling in Mouse Microglia. *J. Neurosci.* **17**, 615 (1997).

318. Elsner, J. *et al.* C3a activates reactive oxygen radical species production and intracellular calcium transients in human eosinophils. *Eur. J. Immunol.* **24**, 518–522 (1994).

319. Norgauer, J. *et al.* Complement fragment C3a stimulates Ca2+ influx in neutrophils via a pertussis-toxin-sensitive G protein. *Eur. J. Biochem.* **217**, 289–294 (1993).

320. Gombault, A., Baron, L. & Couillin, I. ATP release and purinergic signaling in NLRP3 inflammasome activation. *Frontiers in Immunology* **3**, 414 (2012).

321. Lichtman, J. W. & Conchello, J. A. Fluorescence microscopy. *Nat. Methods* **2**, 910–919 (2005).

322. Sheppard, C. J. R. Resolution and super-resolution. *Microsc. Res. Tech.* **80**, 590–598 (2017).

323. Tam, J. & Merino, D. Stochastic optical reconstruction microscopy (STORM) in comparison with stimulated emission depletion (STED) and other imaging methods. *J. Neurochem.* **135**, 643–658 (2015).

324. Fish, K. N. Total internal reflection fluorescence (TIRF) microscopy. *Curr. Protoc. Cytom.* **Chapter 12**, Unit12.18 (2009).

325. Semwogerere, D. & Weeks, E. R. Confocal Microscopy. *Encycl. Biomater. Biomed. Eng.* 1–10 (2005).

326. Sydor, A. M., Czymmek, K. J., Puchner, E. M. & Mennella, V. Super-Resolution Microscopy: From Single Molecules to Supramolecular Assemblies. *Trends Cell Biol.* **25**, 730–748 (2015).

327. Sahl, S. J., Hell, S. W. & Jakobs, S. Fluorescence nanoscopy in cell biology. *Nat. Rev. Mol. Cell Biol.* **18**, 685–701 (2017).

328. Tapia, V. S. *et al.* The three cytokines IL-1β, IL-18, and IL-1α share related but distinct secretory routes. *J. Biol. Chem.* **294**, 8325–8335 (2019).

329. Palazón-Riquelme, P. *et al.* USP7 and USP47 deubiquitinases regulate NLRP3 inflammasome activation. *EMBO Rep.* **19**, e44766 (2018).

330. Lopes, F. B. *et al.* Membrane nanoclusters of FcγRI segregate from inhibitory SIRPα upon activation of human macrophages. *J. Cell Biol.* **216**, 1123–1141 (2017).

331. Landy, A. Dynamic, Strucutral, and regulatory aspects of lambda site-speficic recombination. *Annu. Rev. Biochem.* **58**, 913–949 (1989).

332. Hartley, J. L., Temple, G. F. & Brasch, M. A. DNA Cloning Using In Vitro Site-Specific Recombination. *Genome Res.* **10**, 1788–1795 (2000).

333. Bagnall, J. *et al.* Quantitative dynamic imaging of immune cell signalling using lentiviral gene transfer. *Integr. Biol.* **7**, 713–725 (2015).

334. Ran, F. A. *et al.* Genome engineering using the CRISPR-Cas9 system. *Nat. Protoc.* **8**, 2281 (2013).

335. Platnich, J. M. *et al.* Shiga Toxin/Lipopolysaccharide Activates Caspase-4 and Gasdermin D to Trigger Mitochondrial Reactive Oxygen Species Upstream of the NLRP3 Inflammasome. *Cell Rep.* **25**, 1525-1536.e7 (2018).

336. Schneider, C. A., Rasband, W. S. & Eliceiri, K. W. NIH Image to ImageJ: 25 years of image analysis. *Nature Methods* **9**, 671–675 (2012).

337. Ovesný, M., Křížek, P., Borkovec, J., Švindrych, Z. & Hagen, G. M. ThunderSTORM: A comprehensive ImageJ plug-in for PALM and STORM data analysis and super-resolution imaging. *Bioinformatics* **30**, 2389–2390 (2014).

338. Smith, C. S., Joseph, N., Rieger, B. & Lidke, K. A. Fast, single-molecule localization that achieves theoretically minimum uncertainty. *Nat. Methods 2010 75* **7**, 373–375 (2010).

339. Stallinga, S. & Rieger, B. Accuracy of the Gaussian Point Spread Function model in 2D localization microscopy. *Opt. Express* **18**, 24461 (2010).

340. Thompson, R. E., Larson, D. R. & Webb, W. W. Precise Nanometer Localization Analysis for Individual Fluorescent Probes. *Biophys. J.* **82**, 2775–2783 (2002).

341. Brough, D. & Rothwell, N. J. Caspase-1-dependent processing of pro-interleukin-1beta is cytosolic and precedes cell death. *J. Cell Sci.* **120**, 772–781 (2007).

342. Baroja-Mazo, A. *et al.* The NLRP3 inflammasome is released as a particulate danger signal that amplifies the inflammatory response. *Nat. Immunol.* **15**, 738–748 (2014).

343. Yeap, W. H. *et al.* CD16 is indispensable for antibodydependent cellular cytotoxicity by human monocytes. *Sci. Rep.* **6**, 1–22 (2016).

344. Perussia, B. & Ravetch, J. V. FcγRIII (CD16) on human macrophages is a functional product of the FcγRIII-2 gene. *Eur. J. Immunol.* **21**, 425–429 (1991).

345. Azad, A. K., Rajaram, M. V. S. & Schlesinger, L. S. Exploitation of the Macrophage Mannose Receptor (CD206) in Infectious Disease Diagnostics and Therapeutics. *J. Cytol. Mol. Biol.* **1**, (2014).

346. Gritsenko, A. *et al.* Priming Is Dispensable for NLRP3 Inflammasome Activation in Human Monocytes In Vitro. *Front. Immunol.* **11**, 1 (2020).

347. Casson, C. N. *et al.* Human caspase-4 mediates noncanonical inflammasome activation against gram-negative bacterial pathogens. *Proc. Natl. Acad. Sci.* **112**, 6688–6693 (2015).

348. Ziegler, U. Morphological Features of Cell Death. *News Physiol. Sci.* **19**, 124–128 (2004).

349. Conos, S. A. *et al.* Active MLKL triggers the NLRP3 inflammasome in a cell-intrinsic manner. *Proc. Natl. Acad. Sci. U. S. A.* **114**, E961–E969 (2017).

350. Loomis, W. P., den Hartigh, A. B., Cookson, B. T. & Fink, S. L. Diverse small molecules prevent macrophage lysis during pyroptosis. *Cell Death Dis.* **10**, 326 (2019).

351. Fink, S. L. & Cookson, B. T. Caspase-1-dependent pore formation during pyroptosis leads to osmotic lysis of infected host macrophages. *Cell. Microbiol.* **8**, 1812–1825

(2006).

352. Rathkey, J. K. *et al.* Chemical disruption of the pyroptotic pore-forming protein gasdermin D inhibits inflammatory cell death and sepsis. *Sci. Immunol.* **3**, eaat2738 (2018).

353. Sims, J. E. & Smith, D. E. The IL-1 family: regulators of immunity. *Nat. Rev. Immunol.* **10**, 89–102 (2010).

354. Heilig, R. *et al.* The Gasdermin-D pore acts as a conduit for IL-1β secretion in mice. *Eur. J. Immunol.* **48**, 1–9 (2017).

355. Bayliss, M. K. & Skett, P. Isolation and culture of human hepatocytes. *Methods Mol. Med.* **2**, 369–389 (1996).

356. Vogel, D. Y. S. *et al.* Macrophages in inflammatory multiple sclerosis lesions have an intermediate activation status. *J. Neuroinflammation* **10**, 1–12 (2013).

357. Jaguin, M., Houlbert, N., Fardel, O. & Lecureur, V. Polarization profiles of human M-CSF-generated macrophages and comparison of M1-markers in classically activated macrophages from GM-CSF and M-CSF origin. *Cell. Immunol.* **281**, 51–61 (2013).

358. Tarique, A. A. *et al.* Phenotypic,functional,and plasticity features of classical and alternatively activated human macrophages. *Am. J. Respir. Cell Mol. Biol.* **53**, 676–688 (2015).

359. Martinez, F. O., Gordon, S., Locati, M. & Mantovani, A. Transcriptional Profiling of the Human Monocyte-to-Macrophage Differentiation and Polarization: New Molecules and Patterns of Gene Expression. *J. Immunol.* **177**, 7303–7311 (2006).

360. Schlaepfer, E., Rochat, M.-A., Duo, L. & Speck, R. F. Triggering TLR2, -3, -4, -5, and -8 Reinforces the Restrictive Nature of M1- and M2-Polarized Macrophages to HIV. *J. Virol.* **88**, 9769–9781 (2014).

361. Semino, C., Carta, S., Gattorno, M., Sitia, R. & Rubartelli, A. Progressive waves of IL-1β release by primary human monocytes via sequential activation of vesicular and gasdermin D-mediated secretory pathways. *Cell Death Dis.* **9**, 1088 (2018).

362. Qu, Y., Franchi, L., Nunez, G. & Dubyak, G. R. Nonclassical IL-1 Secretion Stimulated by P2X7 Receptors Is Dependent on Inflammasome Activation and Correlated with Exosome Release in Murine Macrophages. *J. Immunol.* **179**, 1913–1925 (2007).

363. Mulvihill, E. *et al.* Mechanism of membrane pore formation by human gasdermin-D. *EMBO J.* **37**, e98321 (2018).

364. Monteleone, M. *et al.* Interleukin-1β Maturation Triggers Its Relocation to the Plasma Membrane for Gasdermin-D-Dependent and -Independent Secretion. *Cell Rep.* **24**, (2018).

365. Liu, Y. *et al.* Visualization of perforin/gasdermin/complement-formed pores in real cell membranes using atomic force microscopy. *Cell. Mol. Immunol.* **16**, 1 (2018).

366. Fernandes-Alnemri, T., Yu, J.-W., Datta, P., Wu, J. & Alnemri, E. S. AIM2 activates the inflammasome and cell death in response to cytoplasmic DNA. *Nature* **458**, 509–513 (2009).

367. Girardin, S. E. *et al.* Nod2 is a general sensor of peptidoglycan through muramyl dipeptide (MDP) detection. *J. Biol. Chem.* **278**, 8869–72 (2003).

368. Zhao, Y. *et al.* The NLRC4 inflammasome receptors for bacterial flagellin and type III secretion apparatus. *Nature* **477**, 596–600 (2011).

369. Ricklin, D., Hajishengallis, G., Yang, K. & Lambris, J. D. Complement: a key system for immune surveillance and homeostasis. *Nat. Immunol. 2010 119* **11**, 785–797 (2010).

370. Morrison, D. C. & Kline, L. F. Activation of the classical and properdin pathways of complement by bacterial lipopolysaccharides (LPS). *J. Immunol.* **118**, 362–368 (1977).

371. Sonnen, A. F.-P. & Henneke, P. Structural biology of the membrane attack complex. *Subcell. Biochem.* **80**, 83–116 (2014).

372. Qu, Z. *et al.* Hepatitis B virus sensitizes hepatocytes to complement-dependent cytotoxicity through downregulating CD59. *Mol. Immunol.* **47**, 283–289 (2009).

373. Marinho, C. F. *et al.* Down-Regulation of Complement Receptors on the Surface of Host Monocyte Even as In Vitro Complement Pathway Blocking Interferes in Dengue Infection. *PLoS One* **9**, e102014 (2014).

374. Yang, L. B., Li, R., Meri, S., Rogers, J. & Shen, Y. Deficiency of complement defense protein CD59 may contribute to neurodegeneration in Alzheimer's disease. *J. Neurosci.* **20**, 7505–7509 (2000).

375. Michielsen, L. A. *et al.* Reduced expression of membrane complement regulatory protein CD59 on leukocytes following lung transplantation. *Front. Immunol.* **8**, 2008 (2018).

376. Ehrlenbach, S. *et al.* Shiga toxin 2 reduces complement inhibitor CD59 expression on human renal tubular epithelial and glomerular endothelial cells. *Infect. Immun.* **81**, 2678–2685 (2013).

377. Kraus, S. & Fishelson, Z. Cell desensitization by sublytic C5b-9 complexes and calcium ionophores depends on activation of protein kinase C. *Eur. J. Immunol.* **30**, 1272–1280 (2000).

378. Lusthaus, M., Mazkereth, N., Donin, N. & Fishelson, Z. Receptor-interacting protein kinases 1 and 3, and mixed lineage kinase domain-like protein are activated by sublytic complement and participate in complement-dependent cytotoxicity. *Front. Immunol.* **9**, 306 (2018).

379. Ziporen, L., Donin, N., Shmushkovich, T., Gross, A. & Fishelson, Z. Programmed Necrotic Cell Death Induced by Complement Involves a Bid-Dependent Pathway. *J. Immunol.* **182**, 515–521 (2009).

380. Hänsch, G. M. *et al.* Macrophages release arachidonic acid, prostaglandin E2, and thromboxane in response to late complement components. *J. Immunol.* **133**, (1984).

381. Unnewehr, H. *et al.* Changes and Regulation of the C5a Receptor on Neutrophils during Septic Shock in Humans. *J. Immunol.* **190**, 4215–4225 (2013).

382. Samstad, E. O. *et al.* Cholesterol crystals induce complement-dependent inflammasome activation and cytokine release. *J. Immunol.* **192**, 2837–45 (2014).

383. Laudisi, F. *et al.* Cutting edge: the NLRP3 inflammasome links complement-mediated inflammation and IL-1β release. *J. Immunol.* **191**, 1006–10 (2013).

384. Brandstetter, C., Holz, F. G. & Krohne, T. U. Complement component c5a primes retinal pigment epithelial cells for inflammasome activation by lipofuscin-mediated photooxidative damage. *J. Biol. Chem.* **290**, 31189–31198 (2015).

385. Edye, M. E., Lopez-Castejon, G., Allan, S. M. & Brough, D. Acidosis drives damage-associated molecular pattern (DAMP)-induced interleukin-1 secretion via a caspase-1-independent pathway. *J. Biol. Chem.* **288**, 30485–30494 (2013).

386. Labzin, L. I. *et al.* Antibody and DNA sensing pathways converge to activate the inflammasome during primary human macrophage infection. *EMBO J.* **38**, (2019).

387. Zhang, H. *et al.* Anti-dsDNA antibodies bind to TLR4 and activate NLRP3 inflammasome in lupus monocytes/macrophages. *J. Transl. Med. 2016 141* **14**, 1–12 (2016).

388. Lee, G.-S. *et al.* The calcium-sensing receptor regulates the NLRP3 inflammasome through Ca2+ and cAMP. *Nat. 2012 4927427* **492**, 123–127 (2012).

389. Muñoz-Planillo, R. *et al.* K+ Efflux Is the Common Trigger of NLRP3 Inflammasome Activation by Bacterial Toxins and Particulate Matter. *Immunity* **38**, 1142–1153 (2013).

390. Friedman, W. W. J., Thakur, S., Seidman, L. & Rabson, A. B. A. Regulation of Nerve Growth Factor mRNA by Interleukin-1 in Rat Hippocampal Astrocytes Is Mediated by NFkB. *J. Biol. Chem.* **271**, 31115–31120 (1996).

391. Coll, R. C. *et al.* A small molecule inhibitior of the NLRP3 inflammasome is a potential therapeutic for inflammatory diseases. **21**, 248–255 (2015).

392. Broz, P. *et al.* Redundant roles for inflammasome receptors NLRP3 and NLRC4 in host defense against Salmonella. *J. Exp. Med.* **207**, 1745–1755 (2010).

393. Dinarello, C. A. Proinflammatory and Anti-inflammatory Cytokines as Mediators in the Pathogenesis of Septic Shock. *Chest* **112**, 321S-329S (1997).

394. Cohen, J. The immunopathogenesis of sepsis. *Nature* **420**, 885–891 (2002).

395. Zhang, F. *et al.* Defining inflammatory cell states in rheumatoid arthritis joint synovial tissues by integrating single-cell transcriptomics and mass cytometry. *Nat. Immunol. 2019 207* **20**, 928–942 (2019).

396. Cao, S. *et al.* CFH Y402H polymorphism and the complement activation product C5a: Effects on NF-κB activation and inflammasome gene regulation. *Br. J. Ophthalmol.* **100**, 713–718 (2016).

397. ZhuGe, D. L., Javaid, H. M. A., Sahar, N. E., Zhao, Y. Z. & Huh, J. Y. Fibroblast growth factor 2 exacerbates inflammation in adipocytes through NLRP3 inflammasome activation. *Arch. Pharm. Res.* **43**, 1311–1324 (2020).

398. Zanoni, I. *et al.* An endogenous caspase-11 ligand elicits interleukin-1 release from living dendritic cells. *Science (80-.).* **352**, 1232–1236 (2016).

399. Silva, I., Peccerella, T., Mueller, S. & Rausch, V. IL-1 beta-mediated macrophage-hepatocyte crosstalk upregulates hepcidin under physiological low oxygen levels. *Redox Biol.* **24**, 101209 (2019).

400. Andersen, P. A. K. *et al.* Proinflammatory Cytokines Perturb Mouse and Human Pancreatic Islet Circadian Rhythmicity and Induce Uncoordinated β-Cell Clock Gene Expression via Nitric Oxide, Lysine Deacetylases, and Immunoproteasomal Activity. *Int. J. Mol. Sci.* **22**, 1–25 (2021).

401. Huang, Y., Smith, D. E., Ibáñez-Sandoval, O., Sims, J. E. & Friedman, W. J. Neuron-Specific Effects of Interleukin-1β Are Mediated by a Novel Isoform of the IL-1 Receptor Accessory Protein. *J. Neurosci.* **31**, 18048–18059 (2011).

402. McNulty, A. L., Rothfusz, N. E., Leddy, H. A. & Guilak, F. Synovial Fluid Concentrations and Relative Potency of Interleukin-1 alpha and beta in Cartilage and Meniscus Degradation. *J. Orthop. Res.* **31**, 1039 (2013).

403. E, P. *et al.* Induction of nerve growth factor expression and release by mechanical and inflammatory stimuli in chondrocytes: possible involvement in osteoarthritis pain.

Arthritis Res. Ther. **16**, (2014).

404. Husmann, M. *et al.* Elimination of a bacterial pore-forming toxin by sequential endocytosis and exocytosis. *FEBS Lett.* **583**, 337–344 (2009).

405. Beatriz, A., Garcia, S. C., Schnur, K. P., Malik, A. B. & Mo, G. C. H. Gasdermin D pores are dynamically regulated by local phosphoinositide circuitry. *Nat. Commun. 2022 131* **13**, 1–11 (2022).

406. Joosten, L. A. B. *et al.* Inflammatory arthritis in caspase-1 gene deficient mice: Contribution of proteinase 3 for caspase-1-independent production of bioactive IL-1β. *Arthritis Rheum.* **60**, 3651 (2009).

407. Irmler, M. *et al.* Granzyme A is an interleukin 1β-converting enzyme. *J. Exp. Med.* **181**, 1917–1922 (1995).

408. Black, R. A. *et al.* Generation of biologically active interleukin-1β by proteolytic cleavage of the inactive precursor. *J. Biol. Chem.* **263**, 9437–9442 (1988).

409. Beauséjour, A., Grenier, D., Goulet, J.-P. & Deslauriers, N. Proteolytic Activation of the Interleukin-1β Precursor by Candida albicans. *Infect. Immun.* **66**, 676 (1998).

410. Black, R. A., Kronheim, S. R. & Sleath, P. R. Activation of interleukin- 1β by a co-induced protease. *FEBS Lett.* **247**, 386–390 (1989).

411. Bolívar, B. E. *et al.* Noncanonical Roles of Caspase-4 and Caspase-5 in Heme-Driven IL-1β Release and Cell Death. *J. Immunol.* **206**, 1878–1889 (2021).

412. Brandtzaeg, P., Hagåsen, K., Kierulf, P. & Mollnes, T. E. The Excessive Complement Activation in Fulminant Meningococcal Septicemia Is Predominantly Caused by Alternative Pathway Activation. *J. Infect. Dis.* **173**, 647–655 (1996).

413. Hsueh, W., Sun, X., Rioja, L. N. & Gonzalez-Crussi, F. The role of the complement system in shock and tissue injury induced by tumour necrosis factor and endotoxin. *Immunology* **70**, 309 (1990).

414. Fassy, F. *et al.* Enzymatic activity of two caspases related to interleukin-1β-converting enzyme. *Eur. J. Biochem.* **253**, 76–83 (1998).

415. JA, V. *et al.* Group A streptococcal M protein activates the NLRP3 inflammasome. *Nat. Microbiol.* **2**, 1425–1434 (2017).

416. Naji, A. *et al.* Endocytosis of indium-tin-oxide nanoparticles by macrophages provokes pyroptosis requiring NLRP3-ASC-Caspase1 axis that can be prevented by mesenchymal stem cells. *Sci. Rep.* **6**, (2016).

417. Chen, J. & Chen, Z. J. PtdIns4P on dispersed trans-Golgi network mediates NLRP3 inflammasome activation. *Nature* **564**, 71–76 (2018).

418. Shimada, K. *et al.* Oxidized Mitochondrial DNA Activates the NLRP3 Inflammasome during Apoptosis. *Immunity* **36**, 401–414 (2012).

419. Weber, K. & Schilling, J. D. Lysosomes Integrate Metabolic-Inflammatory Cross-talk in Primary Macrophage Inflammasome Activation. *J. Biol. Chem.* **289**, 9158 (2014).

420. Parsons, E. S. *et al.* Single-molecule kinetics of pore assembly by the membrane attack complex. *Nat. Commun.* **10**, 2066 (2019).

421. Kaksonen, M., Toret, C. P. & Drubin, D. G. Harnessing actin dynamics for clathrin-mediated endocytosis. *Nat. Rev. Mol. Cell Biol. 2006 76* **7**, 404–414 (2006).

422. DI, M., T, M., YS, Y., RG, A. & GS, B. Dual control of caveolar membrane traffic by

microtubules and the actin cytoskeleton. *J. Cell Sci.* **115**, 4327–4339 (2002).

423. Macia, E. *et al.* Dynasore, a Cell-Permeable Inhibitor of Dynamin. *Dev. Cell* **10**, 839–850 (2006).

424. Payne, C. K., Jones, S. A., Chen, C. & Zhuang, X. Internalization and Trafficking of Cell Surface Proteoglycans and Proteoglycan-Binding Ligands. *Traffic* **8**, 389–401 (2007).

425. Casella, J. F., Flanagan, M. D. & Lin, S. Cytochalasin D inhibits actin polymerization and induces depolymerization of actin filaments formed during platelet shape change. *Nat. 1981 2935830* **293**, 302–305 (1981).

426. Tang, X., Basavarajappa, D., Haeggström, J. Z. & Wan, M. P2X 7 Receptor Regulates Internalization of Antimicrobial Peptide LL-37 by Human Macrophages That Promotes Intracellular Pathogen Clearance. *J. Immunol.* **195**, 1191–1201 (2015).

427. Kim, S. & Choi, I.-H. Phagocytosis and Endocytosis of Silver Nanoparticles Induce Interleukin-8 Production in Human Macrophages. *Yonsei Med. J.* **53**, 654 (2012).

428. Seil, M., El Ouaaliti, M. & Dehaye, J. P. Secretion of IL-1β triggered by dynasore in murine peritoneal macrophages. *Innate Immun.* **18**, 241–249 (2012).

429. Hongbin Wang, E. P., Mao, L. & Meng, G. The NLRP3 Inflammasome activation in human or mouse cells, sensitivity causes puzzle. *Protein Cell* **4**, 565–568 (2013).

430. Wang, J., Wang, B., Lv, X. & Wang, L. NIK inhibitor impairs chronic periodontitis via suppressing non-canonical NF-κB and osteoclastogenesis. *Pathog. Dis.* **78**, 45 (2020).

431. Brightbill, H. D. *et al.* NF-κB inducing kinase is a therapeutic target for systemic lupus erythematosus. *Nat. Commun. 2018 91* **9**, 1–14 (2018).

432. Mordmüller, B., Krappmann, D., Esen, M., Wegener, E. & Scheidereit, C. Lymphotoxin and lipopolysaccharide induce NF-κB-p52 generation by a co-translational mechanism. *EMBO Rep.* **4**, 82–87 (2003).

433. Bhattacharyya, S., Borthakur, A., Dudeja, P. K. & Tobacman, J. K. Lipopolysaccharide-induced activation of NF-κB non-canonical pathway requires BCL10 serine 138 and NIK phosphorylations. *Exp. Cell Res.* **316**, 3317–3327 (2010).

434. Georgiannakis, A. *et al.* Retinal Pigment Epithelial Cells Mitigate the Effects of Complement Attack by Endocytosis of C5b-9. *J. Immunol.* **195**, 3382–3389 (2015).

435. Liu, W. J. *et al.* Blockage of the lysosome-dependent autophagic pathway contributes to complement membrane attack complex-induced podocyte injury in idiopathic membranous nephropathy. *Sci. Rep.* **7**, 1–18 (2017).

436. Doxsey, S. J., Stein, P., Evans, L., Calarco, P. D. & Kirschner, M. Pericentrin, a highly conserved centrosome protein involved in microtubule organization. *Cell* **76**, 639–650 (1994).

437. Kloc, M., Kubiak, J. Z., Li, X. C. & Ghobrial, R. M. The newly found functions of MTOC in immunological response. *J. Leukoc. Biol.* **95**, 417–430 (2014).

438. Chadwick, S. R., Grinstein, S. & Freeman, S. A. From the inside out: Ion fluxes at the centre of endocytic traffic. *Curr. Opin. Cell Biol.* **71**, 77–86 (2021).

439. Craven, R. R. *et al.* Staphylococcus aureus α-Hemolysin Activates the NLRP3-Inflammasome in Human and Mouse Monocytic Cells. *PLoS One* **4**, (2009).

440. Harder, J. *et al.* Activation of the Nlrp3 Inflammasome by Streptococcus pyogenes Requires Streptolysin O and NF-κB Activation but Proceeds Independently of TLR Signaling and P2X7 Receptor . *J. Immunol.* **183**, 5823–5829 (2009).

441. Alcantara, C. A. T. & Okumura, C. Y. M. SLO and Steady: Role of Streptolysin O during Inflammasome Activation in Group A Streptococcus-infected THP-1 Macrophages. *FASEB J.* **34**, 1–1 (2020).

442. Tu, Y., Zhao, L., Billadeau, D. D. & Jia, D. Endosome-to-TGN Trafficking: Organelle-Vesicle and Organelle-Organelle Interactions. *Frontiers in Cell and Developmental Biology* **8**, 163 (2020).

443. Lee, B. *et al.* NLRP3 activation in response to disrupted endocytic traffic. *bioRxiv* 2021.09.15.460426 (2021).

444. Zhang, Z. *et al.* Defective endosome-TGN retrograde transport promotes NLRP3 inflammasome activation. *bioRxiv* 2021.09.14.460331 (2021).

445. Sun, Q., Fan, J., Billiar, T. R. & Scott, M. J. Inflammasome and autophagy regulation: A two-way street. *Mol. Med.* **23**, 188–195 (2017).

446. PA, K., R, R., WM, Y., JE, H. & RD, S. Reduction of streptolysin O (SLO) pore-forming activity enhances inflammasome activation. *Toxins (Basel).* **5**, 1105–1118 (2013).

447. Conduit, P. T., Wainman, A. & Raff, J. W. Centrosome function and assembly in animal cells. *Nat. Rev. Mol. Cell Biol. 2015 1610* **16**, 611–624 (2015).

448. Assirelli, E. *et al.* Complement factor expression in osteoarthritis joint compartments. *Osteoarthr. Cartil.* **24**, S383–S384 (2016).

449. JA, G. *et al.* A proinflammatory role for IL-18 in rheumatoid arthritis. *J. Clin. Invest.* **104**, 1393–1401 (1999).

450. Joosten, L. A. B. *et al.* Association of interleukin-18 expression with enhanced levels of both interleukin-1β and tumor necrosis factor α in knee synovial tissue of patients with rheumatoid arthritis. *Arthritis Rheum.* **48**, 339–347 (2003).

451. Yamamura, M. *et al.* Interferon-Inducing Activity of Interleukin-18 in the Joint With Rheumatoid Arthritis. *ARTHRITIS Rheum.* **44**, 275–285 (2001).

452. Romero, V. *et al.* Immune-mediated pore-forming pathways induce cellular hypercitrullination and generate citrullinated autoantigens in rheumatoid arthritis. *Sci. Transl. Med.* **5**, (2013).

453. Q, W. *et al.* Identification of a central role for complement in osteoarthritis. *Nat. Med.* **17**, 1674–1679 (2011).

454. Pruitt, J. H., Copeland, E. M. I. & Moldawer, L. L. Interleukin-1 and interleukin-1 antagonism in sepsis, systemic inflammatory response syndrome, and septic shock. *Shock* **3**, 235–251 (1995).

455. JL, L., GM, Y., T, L. & LM, L. Effects of interleukin-1β on vascular reactivity after lipopolysaccharide-induced endotoxic shock in rabbits and its relationship with PKC and Rho kinase. *J. Cardiovasc. Pharmacol.* **62**, 84–89 (2013).

456. Astiz, M. E., Tilly, E., Rackow, E. D. & Weil, M. H. Peripheral Vascular Tone in Sepsis. *Chest* **99**, 1072–1075 (1991).

457. Joshi, V. D., Kalvakolanu, D. V., Hasday, J. D., Hebel, R. J. & Cross, A. S. IL-18 Levels and the Outcome of Innate Immune Response to Lipopolysaccharide: Importance of a Positive Feedback Loop with Caspase-1 in IL-18 Expression. *J. Immunol.* **169**, 2536–2544 (2002).

458. MG, N. *et al.* Neutralization of IL-18 reduces neutrophil tissue accumulation and protects mice against lethal Escherichia coli and Salmonella typhimurium endotoxemia.

J. Immunol. **164**, 2644–2649 (2000).

459. Ge, Y., Huang, M. & Yao, Y. ming. Recent advances in the biology of IL-1 family cytokines and their potential roles in development of sepsis. *Cytokine and Growth Factor Reviews* **45**, 24–34 (2019).

460. Kalbitz, M. *et al.* Role of extracellular histones in the cardiomyopathy of sepsis. *FASEB J.* **29**, 2185 (2015).

461. Bosmann, M. *et al.* Extracellular histones are essential effectors of C5aR- and C5L2-mediated tissue damage and inflammation in acute lung injury. *FASEB J.* **27**, 5010 (2013).

462. Li, Y. *et al.* Circulating Histones in Sepsis: Potential Outcome Predictors and Therapeutic Targets. *Frontiers in Immunology* **12**, 972 (2021).

463. M, S., R, D., G, R., K, R. & GM, H. Induction of mediator release from human glomerular mesangial cells by the terminal complement components C5b-9. *Int. Arch. Allergy Appl. Immunol.* **96**, 331–337 (1991).

464. Zwaka, T. P. *et al.* Complement and Dilated Cardiomyopathy: A Role of Sublytic Terminal Complement Complex-Induced Tumor Necrosis Factor-α Synthesis in Cardiac Myocytes. *Am. J. Pathol.* **161**, 449 (2002).

465. Abe, T. *et al.* Complement Activation in Human Sepsis is Related to Sepsis-Induced Disseminated Intravascular Coagulation. *Shock* **54**, 198–204 (2020).